Rac1 dependent Polarization triggers Contact Inhibition of Locomotion during Epithelial-to-Mesenchymal Transition

Elena Scarpa

Submitted in partial fulfilment of the requirements for the degree of Doctor of Philosophy at University College London

April 2015

I declare that the work presented in this thesis is my own, unless otherwise indicated

Elena Scarpa

Abstract

Contact inhibition of locomotion (CIL) was discovered more than 60 years ago, but has only recently been shown to regulate developmental migration and cell invasion in vivo. CIL is the process through which cells move away from each other after cell-cell contact. However, many cells do not exhibit CIL and instead remain in contact after cell collision and in some cases form stable junctions. To investigate what determines this behaviour, here I study neural crest (NC) cells, a migratory stem cell population whose invasive behaviour has been likened to cancer metastasis. I show that NC cells acquire CIL at the same time that they activate their Epithelial-to-Mesenchymal (EMT) program and start migrating. By comparing pre-migratory and migratory NC cells, I show that switching E- to N-cadherin during EMT is essential for CIL. I demonstrate that, before EMT, E-Cadherin exerts an inhibitory effect of on contact-dependent cell polarity via p120 and Rac1. The main function of the cadherin switch is to lift this inhibition. As a consequence, cell-cell junction breakdown observed during CIL is caused by high forces resulting from cell re-polarisation. These data provide insight into the balance of adhesion signalling that contributes to CIL in cells in vivo.

Acknowledgements

First, I would like to acknowledge who contributed to this work. I would like to thank Professor Roberto Mayor for careful supervision and great science discussions during these three years. In addition, I would like to thank Dr Maddy Parsons and Dr Eric Theveneau for our fruitful collaborative interactions, which gave an important contribution to the development of this project. Concerning experimental contributions : Dr.Maddy Parson performed imaging and analysis of the FRET experiments; Dr Andras Szabò performed curve fitting of the FRAP experiments and analysis of traction force microscopy and of focal adhesion dynamics; Dr Eric Theveneau performed grafts experiments of E-Cadherin neural crest cells in *Xenopus* embryos and helped with presentation of the movies and statistical analysis, and Anne Bibonne helped me with *in situs* of E-Cadherin mutants. In addition, I would like to thank Dr Xiaobo Wang for assistance while setting-up the photoactivation conditions, Dr Kris Vleminckx and Dr C.P. Heisenberg for sharing the XE-Cadh 750AAA and 753AAA constructs and the PA-Rac and DN-PA-Rac plasmids, respectively, and Dr Masa Tada for sharing the MRLC2-GFP plasmid. Special thanks go to the members of the Mayor lab from 2011 to 2015, who provided constant help and support and excellent discussions.

On a more personal note, I would like to thank my family for long-distance support, patience and encouragement, Maria, David, Elias, Isabel, Libero, Eleni, Kristina, Miguel and Scott for their friendship, the fun and the existential discussions during these PhD years at UCL. Finally, I would like to thank Francesco for everything.

Table of Contents

List of Figures and Tables

List of Supplemental Movies

Supplemental Movie S1. An example of Mig-NC collisions in which cells undergo CIL (left) and of Premig-NC, cells forming a stable contact (right). Magenta: nuclear-mCherry. Green: membrane GFP. Frame delay: 5 minutes. Magnification 20X.

Supplemental Movie S2. An example of Mig-NC explant overlap assay in which explants undergo CIL and do not overlap(left) and of Premig-NC, in which explants overlap and cells intermingle (right). Magenta: Rhodamine Dextran. Green: Fluorescein-Dextran. Frame delay: 5 minutes. Magnification 10X.

Supplemental Movie S3. Dispersion assay. Mig-NC explants undergo EMT and disperse (left) while Premig-NC do not disperse (right). Magenta: nuclear-mCherry. Green: membrane GFP. Frame delay: 5 minutes. Magnification 10X.

Supplemental Movie S4. Protrusion analysis. Mig-NC are strongly polarised and produce protrusions directed outwards (arrow, left panel) while Premig-NC protrusions are not polarised(arrow, right) and produce protrusions at cell cell contact sites (arrowhead). Magenta: nuclear-mCherry. Green: membrane GFP. Frame delay: 10 seconds. Magnification 60X.

Supplemental Movie S5. Lifeact-GFP. Mig-NC are strongly polarised and produce actin-rich protrusions directed outwards (arrow, left panel) while Premig-NC protrusions are not polarised(arrow, right) and produce actin-rich protrusions at cell cell contacts (arrowhead). Frame delay: 10 seconds. Magnification 60X.

Supplemental Movie S6. An example of Mig-NC collisions in which cells undergo CIL (left) and of Premig-NC, cells forming a stable junction (right).

Magenta: nuclear-mCherry. Green: p120-GFP. Frame delay: 20 seconds. Magnification 60X.

Supplemental Movie S7. An example of Mig-NC collisions in which cells undergo CIL (left) and of Premig-NC, cells forming a stable junction (right). Magenta: nuclear-mCherry. Green: α-catenin-GFP. Frame delay: 20 seconds. Magnification 60X.

Supplemental Movie S8. An example of Mig-NC collisions in which cells undergo CIL (left) and of Mig-NC expressing E-Cadherin forming a stable contact (right). Magenta: nuclear-mCherry. Green: membrane GFP. Frame delay: 5 minutes. Magnification 20X.

Supplemental Movie S9. Dispersion assay. Mig-NC explants undergo EMT and disperse (left) while Mig-NC expressing E-Cadherin remain in a more compact cluster (right). Magenta: nuclear-mCherry. Green: membrane GFP. Frame delay: 5 minutes. Magnification 10X.

Supplemental Movie S10. Protrusion analysis. Mig-NC (left) are strongly polarised and produce protrusions directed outwards (arrow) while in E-Cadherin expressing Mig-NC (right) protrusions are not polarised(arrow) and produce protrusions at cell cell contact sites (arrowhead). Magenta: nuclear-mCherry. Green: membrane GFP. Frame delay: 10 seconds. Magnification 60X.

Supplemental Movie S11. Protrusion Analysis. Mig-NC (top left) or Mig-NC +p120 MO (top right) are polarised and produce protrusions directed outwards (arrow) while in E-Cadherin expressing Mig-NC protrusions are not polarised(arrow, bottom left). P120 knockdown restores normal protrusion polarity in E-Cadherin expressing NC (arrow, bottom right). Magenta: nuclear-mCherry. Green: membrane GFP. Frame delay: 10 seconds. Magnification 60X.

Supplemental Movie S12. Mig-NC cell-cell collision. p120-GFP (green) and lifeact-mCherry (magenta) in left panel, Rac1 FRET (heatmap) in right panel. Protrusions formation (arrow, left) and Rac1 activation (arrow, right) at the free edge correlate with the disassembly of the p120-GFP positive cell-cell junction (arrowhead, left). Frame delay: 1 minute. Magnification 60X.

Supplemental Movie S13. Cell confinement inhibits CIL. An example of Mig-NC collisions in unconstrained (open) Fn, cells undergoing CIL (left) and of Mig-NC confined on a H shaped (middle) or disc shaped micropattern (right). Magenta: nuclear-mCherry. Green: membrane GFP. Frame delay: 5 minutes. Magnification 60X.

Supplemental Movie S14. Cell confinement stabilises NC-NC junctions. N-Cadherin-mCherry, p120-GFP or α-catenin-GFP injected NC. An example of Mig-NC unconstrained (open) Fn, cells undergoing CIL (left) and of Mig-NC confined on a disc micropattern, cells forming a stable junction (right). Frame delay: 3 minutes. Magnification 60X.

Supplemental Movie S15. Actomyosin dynamics during migratory neural crest collisions (left) and in confined conditions (right). Myosin regulatory Light Chain-GFP: green Lifeact-Cherry : Red. Magnification 60X.

Supplemental Movie S16. PA-Rac promotes protrusion formation in single NC cells. The boxed area was illuminated with 45 seconds pulses of 514 nm control laser light (left) or with 458 nm wavelength (right). Red: PA-Rac-mCherry Grey: transmitted light. Frame delay: 1 minute. Magnification 60X.

Supplemental Movie S17. DN-PA-Rac promotes protrusion collapse in single NC cells. The boxed area was illuminated with 45 seconds pulses of 514 nm

control laser light (left) or with 458 nm wavelength (right). Red: DN-PA-Rac-mCherry Grey: transmitted light. Frame delay: 1 minute. Magnification 60X.

Supplemental Movie S18. DN-PA-Rac inhibits cell dissociation in Mig-NC doublets. The boxed areas were illuminated with 45 seconds pulses of 514 nm control laser light (left) or with 458 nm wavelength (right). Red: PA-Rac-mCherry Green: membrane-GFP. Frame delay: 1 minute. Magnification 60X.

Supplemental Movie S19. PA-Rac promotes cell dissociation in E-Cadherin expressing NC doublets. The boxed areas were illuminated with 45 seconds pulses of 514 nm control laser light (left) or with 458 nm wavelength (right). Red: PA-Rac-mCherry Green: E-Cadherin-GFP. Frame delay: 1 minute. Magnification 60X.

Supplemental Movie S20. PA-Rac activation by illumination does not affect E-cadherin junctional recruitment. E-Cadherin-GFP injected Mig-NC cells. The boxed areas were illuminated with 45 seconds pulses of 514 nm control laser light (left) or with 458 nm wavelength (right). Frame delay: 1 minute. Magnification 60X.

I. Introduction

1. Epithelial Cells and Mesenchymal Cells

Epithelial Cells

Epithelia are the most ancient building blocks of tissues and organs: they are found in primitive organisms such as the non-metazoan social amoeba *Dictyostelium Discoideum* (Dickinson et al., 2011). They constitute a tissue structure capable of segregating their internal compartment from the outside environment. Epithelial tissue organization varies according to its function: epithelia can be simple, stratified or glandular (Figure 1.1A, see (Rodriguez-Boulan and Macara, 2014)). An epithelial cell sheet consists of uniformly polarized cells, the basolateral surface of which is in contact with a basal lamina while the apical domain is equipped with specialised structures that separate their internal compartment from the external environment. These are formed asymmetrically at the apical region and are constituted of three major adhesive complexes: adherens junctions, tight junctions and desmosomes (St Johnston and Ahringer, 2010). Adherens junctions are formed of calcium-dependent cell adhesion molecules of the cadherin superfamily, which maintain the sheet of cells cohesive by linking the plasma membrane with the actin cytoskeleton. Organization of cadherin and actin cytoskeleton in a supercellular actin belt makes epithelia suitable for cell shape changes and tissue remodelling events which occur during morphogenesis (St Johnston and Ahringer, 2010). As cadherin-dependent cell-cell adhesion is one of the main topics investigated in this thesis, an exhaustive description of cadherins junctions will be discussed in the third chapter of this introduction. Tight junctions segregate the apical from

the basolateral domain of the plasma membrane and regulate the differential paracellular permeability of apical and basolateral domains for ions and small molecules. They are constituted of four pass transmembrane proteins claudin and occludins and by their cytoplasmic interactors ZO1 and ZO3 (Furuse and Tsukita, 2006). Desmosomes are formed of transmembrane desmocollins and desmogleins, which anchor intermediate filaments such as keratins or vimentin to the cell membranes via interaction with proteins called desmoplakins, plakoglobins and plakophilins (Franke, 2009; Thomason et al., 2010). Desmosomes and adherens junctions cooperate during junctional assembly and their coordinate maturation contributes to integrity of epithelial cell sheets (Huen et al., 2002; Vasioukhin et al., 2001). In addition, epithelia have a polarized trafficking machinery composed of membrane organelles such as Golgi, endoplasmic reticulum and endosomes which is required for the generation and for the maintenance of the polarized distribution of plasma membrane proteins (Rodriguez-Boulan and Macara, 2014) (Figure 1.1B).

Mesenchymal Cells

During embryonic development, cells often originate far away from their final destination, which they will reach through long distance migration. To acquire migratory and invasive properties, epithelial cells undergo a process of conversion into a mesenchymal phenotype known as epithelial-to-mesenchymal transition (EMT, reviewed in (Nieto, 2011)).

During EMT, epithelial cells lose apicobasal polarity and acquire front-rear polarity. The properties of a fully mesenchymal cell include loss of cell-cell adhesion and ability to form only transitory junctions when interacting with

other mesenchymal cells (Trelstad et al., 1967); in addition, a typical mesenchymal cell is polarized for cell locomotion, with a trailing pseudopodium and an actin-rich leading edge which contains the Golgi apparatus (Hay, 2005). Mesenchymal cells often express matrix metalloproteinases which facilitate EMT by digesting basal laminas (Lochter et al., 1997) and promote invasion of the extracellular matrix (Egeblad and Werb, 2002). Mesenchymal cell types in the adult include fibroblasts and chondrocytes (Figure 1.1 C,D,E).

Epithelial-to-Mesenchymal Transition

Epithelial-to-Mesenchymal transition was first observed by Betty Hay in 1968 and defined as *"[E]pithelial cells exhibit apico-basal polarity, and during the transformation of epithelium to mesenchyme, the transforming cells produce filopodia on their basal side followed by a new leading pseudopodium that is pushed out into the [extracellular matrix]. A mesenchymal cell has front end–back end polarity and forms only transient contacts with its neighbors"* (Hay, 1995). Adult tissues and organs arise through a series of conversions of epithelial embryonic tissues into mesenchymal cells. These are able to reach their distant destinations in the embryo, and can subsequently reconvert into epithelia, a process defined as mesenchymal-to-epithelial transition (MET).

For this reason, epithelial-to-mesenchymal transitions are of fundamental importance for several morphogenetic processes during both invertebrate and vertebrate development. EMT is required for gastrulation among metazoans. Gastrulation is the process through which the body plan is established, the key steps of which include changes in cell shape, internalization of mesendoderm, convergence to the midline and extension along the anteroposterior axis of the

embryo. A crucial structure is the region where cells ingress. Although the nature of the organiser varies among different animal models, the key factors inducing EMT are conserved: the transcription factors Snail and Twist are required for delamination of primary mesenchymal cells in sea urchin (Wu et al., 2007; Wu et al., 2008) and for ventral furrow formation and apical constriction during *Drosophila* gastrulation (Grosshans and Wieschaus, 2000; Kolsch et al., 2007; Martin et al., 2009; Oda et al., 1998). In addition, Snail1 and Snail2 (SNAI family) are required for gastrulation in vertebrates (Carver et al., 2001; Nieto et al., 1994).

In vertebrates, after gastrulation the territories of neural plate and epidermis are specified, and at their interface a transient migratory population, called neural crest, is induced through a complex gene regulatory network (reviewed in (Sauka-Spengler and Bronner-Fraser, 2008)). Neural crest delaminates from the dorsal neuroepithelium, undergoes EMT and migrates extensively through the cranial and trunk regions to colonise distant targets. Similar to gastrulation, neural crest EMT requires activation of the SNAI (Snail1 and Snail 2) family and Twist transcription factors (Betancur et al., 2010; Taneyhill et al., 2007). Because neural crest is the model I used in the experimental work described in this thesis, neural crest cell EMT will be treated in detail in chapter 5.

Increasing evidence suggests that the EMT process is important for carcinoma progression. The EMT programme correlates with poor prognosis in patients and confers cancer cells the ability to invade the adjacent stroma, to form distant metastasis, resist drug treatments and acquire cancer stem cell phenotypes [reviewed in (Polyak and Weinberg, 2009)]. Activation of the EMT program in malignant cells can be promoted by signals they receive in their

microenvironment, including TGF- β (Massague, 2008), hypoxic conditions (Gort et al., 2008), and by tumour-stroma interactions(Franci et al., 2006; Sheehan et al., 2008). As for developmental EMT, the signalling pathways promoting EMT in cancer converge on activation of the SNAI (Snail1 and Snail2), Zeb1/2 and Twist transcription factors (Bolos et al., 2003; Moreno-Bueno et al., 2008; Peinado et al., 2004b).

EMT inducers

The Epithelial –to –Mesenchymal transition leads to loss of cell-cell adhesion and apicobasal polarity and acquisition of motile and invasive features. A key event in this process is the downregulation of the levels of the epithelial cell-cell adhesion molecule E-Cadherin. The SNAI, Zeb1/2 and bHLH transcription factors such as Twist favour this process by repressing directly or indirectly the expression of the epithelial cell-cell adhesion molecule E-Cadherin and a plethora of other cell-adhesion and polarity factors, which will be discussed in the next section. In particular, SNAI and Zeb1/2 factors repress E-Cadherin transcription directly by binding to E-Boxes in the E-Cadherin promoter (Batlle et al., 2000; Cano et al., 2000; Comijn et al., 2001; Eger et al., 2005) and promotes local alterations of the chromatin structure by recruiting its co-repressor SIN3a and the histone deacetylases HDAC1 and 2 (Peinado et al., 2004a). On the other hand, Twist represses E-Cadherin (Yang et al., 2004) acting cooperatively with the Polycomb group protein Bmi1 (Yang et al., 2010).

In addition, E-Cadherin function can be downregulated at the post-transcriptional level during EMT. In mouse gastrulation, E-Cadherin protein levels are controlled by the P38 interacting protein (IP), p38-MAP Kinase and by

the FERM domain protein EPB4.1L5 (Hirano et al., 2008; Zohn et al., 2006).

EMT inducing transcription factors are not only essential for control of junctional proteins levels. Indeed, they drive a complex rewiring of gene expression that involves upregulation of genes controlling extracellular matrix remodelling, cytoskeletal reorganization, acquisition of cell motility (Barrallo-Gimeno and Nieto, 2005), cell survival (Escriva et al., 2008) and invasion of the extracellular matrix (Jorda et al., 2005; Yokoyama et al., 2003). However, the mechanisms through which these transcription factors upregulate motility and survival genes are poorly understood and probably involve indirect gene regulation (Grotegut et al., 2006; Jorda et al., 2005; Vega et al., 2004).

2. Cell Polarity

Apicobasal Polarity in Epithelial Cells

Epithelial tissues need to be correctly polarized to exert their functions. The basolateral domain interacts with a basal lamina constituted by ECM , while the apical domain contains polarity factors that are required to correctly localise junctional complexes (tight junctions, adherens junctions and desmosomes) at the interface between the apical and basolateral domains of the epithelial cell membrane. Here we discuss how such polarity is established and how can be disrupted by the EMT program.

Key players of the Epithelial Polarity Program

Several protein complexes as well as lipids have been involved in the establishment and maintenance of the epithelial polarity program. These include Par complex proteins, which are expressed ubiquitously and mediate several different functions, including polarity, proliferation and differentiation; Crumbs and Scribble complexes, the expression of which is restricted to epithelial cell types; small GTPases of the Rho family and phosphoinositides.

PAR Complex

The PAR proteins were first identified in *C. Elegans*, where they are required for correct anteroposterior sorting of cytoplasmic components in the early embryo (Kemphues et al., 1988). The protein kinases PAR1 and PAR4, the 14-3-3-like cytoplasmic protein PAR5, the PDZ-domain containing scaffold proteins PAR3 and PAR6, the kinase aPKC and the small GTPase Cdc42 are considered to be part of the complex. The PAR complex has a key role in formation and

maintenance of two distinct apical and basolateral membrane domains: Par3 and Par6 interact with tight junctions and localise to cell-cell contacts (Macara, 2004), but are also required for apical delivery of aPKC (Morais-de-Sa et al., 2010). The latter localises to the apical cortex, where it excludes basolateral proteins: protein residues phosphorylated by aPKC attract PAR5, which detaches them from the cell cortex (Benton and St Johnston, 2003; Macara, 2004). Conversely, PAR1 is normally considered to antagonise the rest of the complex and is recruited at the basolateral cortex, where it excludes apical proteins (Benton and St Johnston, 2003).

Crumbs and Scribble complexes

The Crumbs and Scribble complexes were discovered in *Drosophila* and consist in additional polarity components, which are specific for epithelial cells. The Crumbs complex consists of the transmembrane protein CRB and the scaffold proteins PALS1 and PATJ and it confers apical identity to the apical membrane (Tepass, 2012). The Crumbs complex interacts with the PAR proteins: the localization of the PAR complex to the apical domain is stabilised by the Crumbs complex, and their distribution is reciprocally interdependent (Bilder et al., 2003). The Scribble complex contains discs-large homologue (DLG), lethal giant larvae (LGL) and Scribble, localises basolaterally (Bilder et al., 2000) and functions as an antagonist of the PAR complex. LGL proteins compete with PAR3 for binding to the PAR complex and sequester the active PAR complex away from the apical junction domain. On the other hand, when LGL is phosphorylated by aPKC it inactivates the Scribble complex (Assemat et al., 2008; Lee and Vasioukhin, 2008).

Small GTPases

Small GTPases of the Rho family are molecular switches, which cycle between a GTP-bound, active state, and a GDP-bound inactive state. The GDP/GTP exchange can be favoured by Guanine Exchange Factors (GEFs), which promote small GTPase activation, while GTPase Activating Proteins (GAPs) and Guanine Dissociation Inhibitors (GDIs) can promote inactivation of the GTPases either by activating their GTPase activity or maintaining them in a GDP-bound state (reviewed in (Jaffe and Hall, 2005). They were first discovered as master cytoskeleton regulators in migrating cells: RhoA promotes stress fibers and actomyosin contractility, while Rac1 is involved in lamellipodia formation and actin branched network organization and Cdc42 is important for filopodia formation (reviewed in (Ridley, 2001)). Importantly, the Cdc42-GEFs Tuba and DBL3 generate active Cdc42-GTP at the apical cortex of epithelial cells, thereby promoting its interaction with PAR6 and recruitment of the PAR complex to the apical domain and aPKC activity (Qin et al., 2010; Zihni et al., 2014) . In addition, there is strong evidence in favour of a role for Rac1 activity in the establishment of apicobasal polarization. The interaction between the Rac GEF Tiam-1 and Par3 couples activation of Rac1 to the activation of aPKC and to tight junction assembly (Chen and Macara, 2005), in addition, loss of Tiam1 leads to impairment of tight junction formation in keratinocytes (Mertens et al., 2005). Moreover, Rac1 is required for the reorientation of apicobasal polarity induced by the extracellular matrix in three-dimensional cultures of epithelial cysts acting via PI3K and aPKC (Liu et al., 2007; O'Brien et al., 2001). Regarding RhoA, live imaging of epithelial junction formation reveals that RhoA is excluded from the cell-cell contacts at early stages of cell-cell contact establishment, however,

RhoA activity and actomyosin contractility seem to be required for junctional maturation and maintenance in epithelial cells, as will be discussed in closer detail in chapter 3 (Yamada and Nelson, 2007). In addition, assembly of a contractile actomyosin ring during apicobasal polarization is required for tight junction assembly (Ivanov et al., 2005).

Inositol Phospholipids

Phosphoinositides are also involved in establishment and maintainance of apicobasal polarity in epithelia. They constitute only a small fraction (1%) of the total membrane lipids but they exert several important physiological roles as precursors of second lipid messengers and as membrane docking sites for protein effectors of several signalling cascades. There are different inositol phospholipids isoforms, which differ in the number and position of phosphorylations in the inositol ring. They are spatiotemporally regulated by kinases and phosphatases specific for different organelles. Because multiple phosphoinositide-binding protein domains have been discovered, phosphoinositides can fine-tune the composition of the membrane-cytoplasm interface (reviewed by (Di Paolo and De Camilli, 2006)). In particular, phosphatidylilinositol-3,4,5-triphosphate (PIP_3) is involved in basolateral plasma membrane identity (Gassama-Diagne et al., 2006), while phosphatidyilinositol-4,5-triphosphate (PIP_2) is responsible for apical plasma membrane identity by controlling the apical localization of Cdc42 (Martin-Belmonte et al., 2007). In addition, PTEN, a protein phosphatase which generates PIP_2 by dephosphorylating PIP_3 is localised apically in fly embryonic epithelia (von Stein et al., 2005).

Establishment of a polarized epithelium

The epithelial phenotype is established early in development: during mammalian embryogenesis the zygote undergoes a series of cleavage divisions that generate the blastula epithelium through compaction, cavitation and transport of fluids as soon as the 8-16 cell stage(Ziomek and Johnson, 1980).

In addition, organogenesis in vertebrates requires a series of transitions from epithelial state to mesenchymal state to generate migratory precursors which colonise distant sites in the embryos and give rise to new organs via Mesenchymal-to-Epithelial transitions (MET), which provide excellent models to understand establishment of epithelial apicobasal polarity (Nelson, 2009).

The *de novo* organization of apicobasal polarity in an epithelium requires the clustering of cells through specific cell-cell interactions. Cells need to distinguish between adhesive surfaces, which are formed by interactions between cells and interactions with the extracellular matrix and will give rise to basolateral membrane domains. On the other hand, non–adhesive surfaces will become the apical domains.

The open surface of two-dimensional tissue culture conditions and the outside surface of the preimplantation mammalian embryo are immediately evident nonadhesive surfaces. However, the formation of a non-adhesive surface (lumen) in cell aggregates is more complex and may require a) selective apoptosis of cells located in the centre of the cluster; b) insertion of apical proteins as Crumbs from intracellular stores into the cell-cell junction and exclusion of E-Cadherin and basolateral proteins from that site; c) vectorial fluid secretion into the luminal space (reviewed in (Nelson, 2009).

The initiation of epithelial cell-cell contacts requires cell-cell adhesion mediated by the epithelial cadherin molecule E-Cadherin (Gumbiner and Simons, 1987).

First, cell adhesion molecules of the Nectin family, Ig-like proteins which are involved in Ca^{2+} independent cell-cell adhesion, engage in heterophilic binding at nascent contacts of epithelial cells (Takai and Nakanishi, 2003). Nectin adhesions form a scaffold for E-Cadherin trans- and cis- homophilic binding. In addition, several tight junction proteins are pre-enriched at contacting filopodia and lamellipodia (Ebnet, 2008). Nectin and E-Cadherin clustering leads to activation of the small GTPases Rac1 and Cdc42 (Fukuhara et al., 2004; Kawakatsu et al., 2002; Kim et al., 2000b; Nakagawa et al., 2001). The primordial adhesions formed in these early steps are often called “punctate adhesions” and their maturation into linear apicobasally polarised adhesions with discrete adherens and tight junction domains requires crosstalk between small GTPases and the PAR complex. As previously discussed, the interaction between the Rac GEF Tiam-1 and Par3 couples activation of Rac1 to the activation of aPKC and to tight junction assembly (Chen and Macara, 2005). Maturation of cadherin adhesions from “punctate” to linear junctions also underlies extensive reorganization of the actin cytoskeleton at the cadherin-actin interface (Brieher and Yap, 2013), which will be treated in detail in the next chapter of this Introduction.

In addition to establishment of polarized cell-cell adhesions, interactions with the extracellular matrix (ECM) help establishing basolateral identity: in three dimensional MDCK epithelial cysts, Rac1 dependent adhesion of integrins to laminin, a component of the ECM, orientates apicobasal polarity in a PI3K and aPKC dependent manner (Liu et al., 2007; O'Brien et al., 2001).

Finally, as previously mentioned, apically and basolaterally localised phosphoinositides contribute to apical localization of Cdc42 and reinforce maturation of a correct apicobasal polarity (Martin-Belmonte et al., 2007). Establishment of epithelial polarity is summarised in (Figure 2.1A)

As the newly formed epithelium generates its apicobasal polarity, the exocytic and endocytic pathways organise into a polarized trafficking machinery that controls correct sorting of plasma membrane proteins that carry out vectorial transport functions into the appropriate apical or basolateral domain (reviewed in (Rodriguez-Boulan and Macara, 2014)).

Loss of epithelial polarity during EMT

Cell-cell adhesion and polarity in epithelia relies on assembly of E-Cadherin dependent adherens junctions, which cooperate with the activity of cell polarity complexes and extracellular matrix signalling in establishing and maintaining a functional, polarized epithelial tissue. During EMT, apicobasal polarity is lost. Cells acquire instead front-rear polarity, the ability to degrade the extracellular matrix and migratory capabilities. Both during embryonic development and in pathological conditions such as cancer, activation of the EMT program by extracellular and microenvironmental signals converges on posttranscriptional and transcriptional downregulation of E-Cadherin and apicobasal polarity components. Indeed, SNAI factors directly repress several components of tight junctions by directly binding to E-boxes in the promoters of occludin, claudin and claudin-7 (Ikenouchi et al., 2003; Martinez-Estrada et al., 2006).

In addition, recent reports show that several members of the Crumbs and Scribble polarity complexes can be directly repressed by Zeb and SNAI

transcription factors. In breast and colorectal carcinoma cells, Zeb1 knockdown results in upregulation of CRB3, PATJ and LGL2 and restoration of cell polarity, and chromatin immunoprecipitation assays show that their promoters can be bound directly by Zeb1 (Aigner et al., 2007); SNAI transcription factors also repress CRB3 and LGL2 transcription by direct binding to E-boxes in their promoter (Whiteman et al., 2008).

EMT transcription factors could influence cell polarity by acting on additional players of the epithelial polarity machinery: indeed, Snail1 has been shown to directly repress PTEN transcription (Escriva et al., 2008). Because PTEN has been proposed to play an important role in apical localization of PIP_2 in epithelial cells (Martin-Belmonte et al., 2007) it is likely that Snail1 mediated repression of PTEN provides an indirect mechanism to induce loss of cell polarity during EMT.

Concerning Twist, its ability to regulate expression of polarity factors is unclear (Moreno-Bueno et al., 2008).

PAR polarity complexes have not emerged so far as direct targets of EMT inducers; however, there is evidence that they can be regulated in response to microenvironmental signals: in normal mammary cells Par6 forms a complex with TGF-βRI at the tight junction. Upon exposure to TGF-β, the TGF-βRII is recruited to the complex where it phosphorylates Par6, which can then recruit the E3-ubiquitin ligase Smurf3 and in turn trigger degradation of the small GTPase RhoA, thus causing loss of the apical actomyosin ring, loss of apicobasal polarity and, eventually, EMT (Ozdamar et al., 2005). Loss of apicobasal polarity during EMT is summarised in figure 2.1B.

Front-Rear Polarity in Mesenchymal Cells

Epithelial cells undergoing EMT progressively loosen their cell-cell adhesion and disassemble their apicobasal polarity machinery. Mesenchymal cells derived from the transition acquire a front-rear polarity, which allows efficient migration.

Front-rear polarized migratory cells display a leading edge, where branched actin polymerization occurs and filopodia and lamellipodia are formed and large focal adhesions are assembled providing attachment to exert traction on the substrate. At the back of the cell actomyosin contractility is predominant and leads to focal adhesion disassembly and retraction of the tail. In addition, microtubules are polarized, their plus ends being localized at the leading edge, and the microtubule organizing centre (MTOC) being located in front of the nucleus (reviewed in (Ridley et al., 2003) .

The very key players involved in polarizing epithelial cells are also responsible, through different molecular pathways, for establishment of front rear-polarity in migratory cells.

Small GTPases and control of the cytoskeleton

Small GTPases of the Rho family are master regulators of the cytoskeleton and their activity needs to be tightly regulated to orchestrate the complex actin and microtubule cytoskeletal machinery that is required for efficient cell migration (Ridley, 2001).

In front-rear polarized migrating cells, Cdc42 and Rac1 are activated at the leading edge of the cell. The molecular mechanisms underlying localised activation of Cdc42 and Rac1 at the leading edge impinge at least partially on the

activity of the apicobasal polarity complexes and will be discussed in the next section. Cdc42 is a master regulator of cell polarity, it is active at the front of migrating cells and it is important to promote formation of a single, long lived leading edge (Srinivasan et al., 2003). Furthermore, together with members of the PAR, Crumbs and Scribble complex, it has been involved in correct positioning of the MTOC in migrating cells (Etienne-Manneville and Hall, 2001, 2003; Etienne-Manneville et al., 2005).

An important function of Cdc42 in migrating cells is defining the location where Rac1 can be active (Srinivasan et al., 2003). Rac1 in turn promotes activation of the WASP/WAVE complex, which stimulates branched actin network polymerization via the Arp2/3 complex: Arp2/3 binds to the side of a pre-existing actin filament and promotes nucleation of a new one. The protrusion event *per se*, pushing of the plasma membrane, occurs by an "elastic Brownian ratchet" mechanism: thermal energy bends the nascent short filaments, therefore storing elastic energy. Elongation of these nascent filaments leads to their unbending against the leading edge membrane, therefore providing the driving force for protrusion (Pollard and Borisy, 2003).

In addition, Rac1 can be activated and targeted to the membrane by integrins at the leading edge of the cell (del Pozo et al., 2000; Etienne-Manneville and Hall, 2001). Newly formed adhesions in turn activate Rac, which is able to induce recruitment and clustering of additional activated integrins to the lamellipodium (Kiosses et al., 2001; Schwartz and Shattil, 2000).

Active RhoA is involved in retracting the trailing edge of the cells via ROCK I and assembly of actomyosin contractile structures. Inhibition of RhoA in several cell types leads to the formation of an extended tail at the trailing edge (Ridley et al.,

2003). Importantly, RhoA is involved in stabilization of microtubules at the trailing edge of the cell, which in turn promotes focal adhesion disassembly (Small and Kaverina, 2003; Srinivasan et al., 2003). In addition, RhoA and Rac have been shown to mutually antagonise each other: in migrating monocytes, inhibition of Rho A leads to formation of multiple, multipolar protrusions which impair efficient migration (Worthylake and Burridge, 2003; Xu et al., 2003). Finally, it has recently been shown that front-rear polarity can be sustained by increased membrane tension at the leading edge of the cell, normaly induced by actin polymerization: applying tension to the membrane with a micropipette or by osmotic shock is sufficient to promote Rac1 activation and "frontness", while inhibiting "backness" identity (Houk et al., 2012).

Polarity complexes

The polarity complexes Scribble, Crumbs and PAR have been shown to be able to locally activate the small GTPases Cdc42 and Rac1 at the leading edge of migrating cells.

Scribble is able to form a complex with the Cdc42/Rac-GEF β-Pix and to its partner GIT-1 and promote Cdc42 activation at the leading edge of PC-12 cells (Audebert et al., 2004). Knockdown of Scribble also induces a decrease in Rac1 activation, suggesting that the scribble complex could also indirectly or directly promote Rac1 activity (Zhan et al., 2008).

In addition, PATJ, a component of the Crumbs complex, has been found to localize at the leading edge of migrating cells during wound healing assays. PATJ recruits PAR3 and aPKC to the leading edge, and knockdown of PATJ results in mislocalization of the microtubule organizing centre (MTOC) in a PAR3-aPKC

dependent manner (Shin et al., 2007). Between the substrates of aPKC is the kinase GSK3β. aPKCs is able to phosphorylate and inactivate GSK3β, therefore allowing its substrate, APC, to bind and stabilise microtubule plus ends at the plasma membrane (Zumbrunn et al., 2001). An additional substrate of aPKC is the Rac1-GEF TIAM1, which localises with PAR3 and aPKC at the leading edge of keratinocytes and together with PAR3 is required for their directional migration in a microtubule dependent manner (Pegtel et al., 2007).

Furthermore, the aPKC-PAR6 complex localises at the leading edge of wounded astrocyte monolayers as a consequence of integrin-dependent Cdc42 activation (Etienne-Manneville and Hall, 2001). Here, it promotes protrusion formation by recruiting Rac1 (Etienne-Manneville and Hall, 2001) and controls centrosome positioning via inhibition of GSK3β (Etienne-Manneville and Hall, 2003) or by recruiting Dlg1 to the leading edge and therefore inducing the association of APC with microtubule plus ends (Etienne-Manneville et al., 2005).

Inositol Phospholipids

As discussed for establishment of epithelial apicobasal polarity, inositol phospholipids are important polarity determinants also in front-rear polarized migrating cells. In migrating neutrophils, "frontness" is established by PIP_3 localized accumulation downstream of G_i proteins (Xu et al., 2003) and PI3K (Wang et al., 2002), while PIP_2 localises at the trailing edge and confers "backness" identity. Correspondingly, the activity of the phosphatase PTEN is also localised at the cell trailing edge (Funamoto et al., 2002).

An overview of mesenchymal front-rear polarity is depicted in Figure 2.2.

Contact-dependent cell polarity

More than fifty years ago, Abercrombie and Heaysman discovered that the direction of migration of chick heart fibroblasts cultured in vitro was modified by their interaction with other cells (Abercrombie and Heaysman, 1953). The process was defined as contact inhibition of locomotion (CIL) and was proposed as the main force driving epithelial wound healing (Abercrombie, 1979; Abercrombie and Ambrose, 1962).

CIL is defined as the ability of a cell to change the direction of its movement after contact with another cell. It consists of a stereotyped sequence of steps: (i) cell–cell contact, (ii) inhibition of membrane protrusions at the site of contact, (iii) repolarization through generation of a new protrusion away from the site of cell contact and (iv) migration in the direction of the new protrusion (Mayor and Carmona-Fontaine, 2010).

Historically, the importance of this behaviour emerged when it was observed that malignant mesenchymal cells showed a reduced CIL response, being able to invade fibroblast cultures in what was compared to invasive metastasis (Abercrombie, 1979; Abercrombie and Ambrose, 1962; Abercrombie and Heaysman, 1954). More recently, Eph-Ephrin signaling was shown to regulate the invasiveness of prostate malignant cells towards stromal fibroblast via an inhibition of the CIL response in the cancer cells (Astin et al., 2010a). PC3 prostate cancer cells display CIL towards one another, but have an impaired CIL response towards stromal fibroblasts and are able to continuing migrating directionally when they interact with one of them, thus raising the possibility that this differential contact inhibition response may drive cancer cell invasion (Astin et al., 2010a). Furthermore, the fundamental relevance of CIL in guiding

complex migratory processes during embryonic development has been demonstrated *in vivo* for collective migration of Neural Crest (NC) cells as well as for dispersion of macrophages and of Cajal-Retzius neurons (Carmona-Fontaine et al., 2008; Stramer et al., 2010a; Villar-Cervino et al., 2013).

The molecular pathways underlying CIL remained poorly understood for decades. However, in prostate cancer cells, in neurons and in *Xenopus* neural crest cells the CIL response seems to dependent on cell-cell contact dependent signalling. In particular, Eph-Ephrin signalling, which mediates repulsive cell-cell interactions [reviewed in (Lisabeth et al., 2013)], has been found to be responsible for CIL in cancer cells (Astin et al., 2010b) as well as in neurons (Villar-Cervino et al., 2013). On the other hand, upon cell-cell contact neural crest cells activate a Wnt-PCP pathway which leads to recruitment of Dishevelled to the cell-cell contacts via Wnt11 and its receptor Fz7 and, eventually, to activation of RhoA-ROCK signalling. In particular, RhoA is activated at the site of cell-cell contact, and RhoA/ROCK activity is required for cell repolarization upon cell-cell interactions (Carmona-Fontaine et al., 2008).

In addition, microtubule remodelling appears to be important for an efficient CIL response. During development of *Drosophila* immune system, macrophages display a CIL response towards one another. Alignment of microtubule bundles between the two colliding cells precedes cell separation (Davis et al., 2012), however, it is unclear whether cell-cell contact dependent signalling occurs in this context. In addition, destabilization of dynamic microtubules has been shown to be required for CIL downstream of the polarity protein PAR3 in neural crest cells and PAR3 is recruited at cell-cell contact sites during cell-cell collisions (Moore et al., 2013).

Furthermore, it has been suggested that cadherin-dependent cell-cell adhesion is required for CIL. In particular, mesenchymal cadherins such as Cadherin11 and N-Cadherin, are required for CIL (Becker et al., 2013; Theveneau et al., 2010; Theveneau et al., 2013). During *Xenopus* homotypic Neural Crest-Neural Crest and heterotypic Neural Crest-Placode cell-cell interactions N-Cadherin is functionally required for CIL and a classical cell adhesion complex including the cadherin binding partners α-catenin, β-catenin and p120 is transiently assembled, but eventually broken down (Theveneau et al., 2010; Theveneau et al., 2013). How junction disassembly occurs during CIL is currently unclear.

Work in neural crest cells has demonstrated that, in a group of cells migrating as a collective, CIL prevents the formation of protrusions between cells. Therefore, when cells are in high density conditions only the cells with a free edge can produce large lamellipodia whereas cells surrounded by other cells can only generate smaller transient protrusions. Such behaviour is defined as contact-dependent cell polarity (Mayor and Carmona-Fontaine, 2010; Theveneau et al., 2010). As a consequence, cells exhibiting CIL do not crawl over their neighbours leading to monolayer formation in groups and eventually, as cell density decreases as a consequence of monolayering, to scattering to single cells (Mayor and Carmona-Fontaine, 2010). Furthermore, when two cell clusters exhibiting CIL-like behavior are juxtaposed, they will remain separated rather than invading into each other (Carmona-Fontaine et al., 2008).

Contact-dependent cell polarity observed in cell populations which exhibit CIL promotes collective, directional migration by orientating and polarizing protrusive activity at the edge of the group via formation of transient cell-cell interactions. Components of the epithelial polarity machinery such as Par3 and

cell-cell adhesion molecules such as N-Cadherin are involved in the establishment of such contact-dependent polarity by controlling the spatial activation of the small GTPase Rac. Rac1-GTP is localized at the leading edge of migrating neural crest cells, creating a polarized gradient of activity (Theveneau et al., 2010). Perturbation of N-Cadherin activity or Par3 levels results in loss of Rac1 polarity (Moore et al., 2013; Theveneau et al., 2010) and results in impaired collective migration of neural crest. Rac-GEF Trio controls the polarized distribution of active Rac1 downstream of Par3 (Moore et al., 2013). However, whether Par3 and N-Cadherin regulates Rac1 distribution via the same pathway or whether additional Rac-GAPs are involved in hampering Rac1 activity at the cell-cell junction is currently unknown.

3. Cadherins

Cadherin family proteins, types and subtypes

Cadherins are Ca^{2+} dependent cell adhesion molecules. They were first identified as glycoproteins responsible for as Ca^{2+} dependent homophilic cell-cell adhesion in compaction of the morula during preimplantation development of the mouse embryo and in early chick embryo development (Gallin et al., 1983; Peyrieras et al., 1983; Yoshida and Takeichi, 1982). The function of cadherins is not limited to cell-cell adhesion, but they exert a variety of functions during development and tissue morphogenesis including cell sorting, maintenance of boundaries and maintenance of tissue polarity (reviewed in (Halbleib and Nelson, 2006)).

Since their discovery three decades ago, more than 100 cadherin family members have been identified in vertebrates. They are subdivided in three main types: classical cadherins, protocadherins and atypical cadherins involved in planar cell polarity (PCP).

Classical cadherins are the best characterized cadherin type. They are localised at adherens junctions in a variety of cell types and mediate dynamic interactions with the actin cytoskeleton. They are single pass transmembrane proteins, characterized by five Ca^{2+} binding Ig-like globular domains of about 110 aminoacids (EC domains) on their extracellular portion, a single pass transmembrane domain and a short cytoplasmic domain which contains sites for the direct binding partners p120-catenin and β-catenin. Classical cadherins are subdivided in type I and type II. Type I cadherins such as E- and N-Cadherin mediate strong cell-cell adhesion, while type II classical cadherins such as VE-Cadherin and Cadherin 11 mediate weaker cell-cell adhesion. The molecular

characteristics of the classical cadherins extracellular and cytoplasmic domain will be discussed in closer detail in the next section of this Chapter.

Protocadherins are the largest cadherin subfamily, with more than 60 family members. They are mainly expressed in the nervous system (Wu and Maniatis, 1999). Compared to classical cadherins, their functions are still poorly understood. They also are single pass transmembrane proteins, but their extracellular domain has six to seven EC repeats and lacks sequence elements conserved in classical cadherins (Junghans et al., 2005). Furthermore, the cytoplasmic domain of protocadherins is very diverse across family members and little is known about their binding partners. The adhesive properties of protocadherins in aggregation assays are poor (Chen and Gumbiner, 2006), but stronger adhesion can be obtained by replacing protocadherin cytoplasmic domains with the E-Cadherin one (Obata et al., 1995), thus suggesting that their EC domains may retain adhesive properties but their cytoplasmic domains are mainly required for signal transduction. Among the cytoplasmic partners of protocadherins are the actin bundling protein fascin (Triana-Baltzer and Blank, 2006) and the Src family kinase Fyn, both of which can interact with Pcdh-α (Kohmura et al., 1998).

The third cadherin category is that of atypical cadherins: Fat, Dachsous and Flamingo. These are much larger molecules, Fat and Dachsous showing 27 and 34 EC repeats respectively. Their intracellular domains show homology to the β-catenin binding domain of the classical cadherins, although interaction with β-catenin has not been demonstrated for either of the two (Clark et al., 1995; Mahoney et al., 1991). Flamingo is a unique member of the cadherin family. It has a large extracellular region which contains nine ECs and seven transmembrane

domains and its cytoplasmic domain binds to the actin cytoskeleton regulator Ena/VASP (Tanoue and Takeichi, 2004). Atypical cadherins functionally and physically interact with members of the Wnt-PCP planar cell polarity pathway both in mammals and in *Drosophila* (reviewed in (Halbleib and Nelson, 2006).

Classical Cadherins

Classical cadherins are the main components of vertebrate adherens junctions. They mediate homophilic cell-cell interactions through their extracellular adhesive domain and interact dynamically with the actin cytoskeleton via their cytoplasmic domain. Here, I will review their molecular structure, oligomerization dynamics, cytoplasmic binding partners and their ability to modulate Rho GTPases activity and actin cytoskeleton organization.

Molecular Structure

Classical cadherins consist of an extracellular domain characterized by five EC repeats, in which linker regions between each EC domain are stabilized by 3 Ca^{2+} ions. These domains are defined EC1-EC5, where EC1 corresponds to the most distal and EC5 to the most proximal to the plasma membrane. Classical cadherins are single pass transmembrane domain and display a highly conserved cytoplasmic domain which binds to the intracellular partners p120-catenin and β-catenin.

Extracellular homophilic binding

Recent studies suggest that the ectodomains of classical cadherins, uncoupled from their cytoplasmic regions, are sufficient to initiate assembly of adherens junctions, a process that is mediated by *trans* interactions of cadherin ectodomains on the membrane of opposing cells as well by *cis* interactions

between cadherins expressed on the membrane of the same cell. Indeed, a cadherin mutant deleted not only for p120 and β-catenin binding site, but also lacking a crucial clathrin adapter binding motif, so that cadherin endocytosis dynamics are slowed down, can be incorporated into cell-cell junctions in E-Cadherin expressing A431 cells and can assemble into adherens junction-like structures in cadherin-deficient A431-D cells (Hong et al., 2010).

In addition, expression of cadherin ectodomains in cell-free liposome systems followed by cryo-electromicroscopy shows that both E-Cadherin (Harrison et al., 2011) and VE-Cadherin (Taveau et al., 2008) extracellular domains are able to self-assemble into "artificial adherens junctions" characterized by flattening of the juxtaposed membranes and cadherin lateral clustering. These results suggest that the cytoplasmic domain is dispensable for the initial assembly of the adherens junction.

The crystal structure of the extracellular domain of several type I and type II cadherin has been resolved, and several studies provide a good understanding of cadherin dimerization and oligomerization dynamics. The ectodomains of cadherin molecules protruding from opposing cell membranes interact in trans via their most distal EC1 domain. All classical cadherins share a common binding mechanism in which the the most N-terminal portion of the EC1, called the A* strand, is swapped between the EC1 domains of the two opposing cadherins. In type I cadherins, the tryptophan residue at position 2 (Trp2) docks into a conserved hydrophobic pocket in the EC1 domain of the partner cadherin (Boggon et al., 2002; Harrison et al., 2011; Shapiro et al., 1995). This mechanism has been defined as strand-swapping (Figure 3.1A). Comparison of the EC1 domain, which undergoes swapping, with the non-swapping EC2-EC5 domains

reveals that the first has a shorter N-terminal β strand, and that in the others Trp2 is substituted with a phenylalanine (Phe). A glutamate residue in position 11 (Glu11) coordinates Ca^{2+} docking and introduces strain in the EC1 domain, which is shorter, thus favouring the strand swapping, which releases this strain (Vendome et al., 2011). Indeed, introducing point mutations that decrease the strain in the EC1 domain such a W2F mutation (Trp to Phe) relieves the strain in the N-terminal strand and decrease the dimerization affinity constant (K_A)(Vendome et al., 2011).

Analytical Ultra Centrifugation (AUC) measures the dimerization affinities of soluble macromolecules, such as classical cadherin extracellular domains. Such measurements show that the E-Cad EC1 domain K_A is about four-fold lower than N-Cadherin K_A (Katsamba et al., 2009). A conserved Pro5-Pro6 motif is responsible for the difference in dimerization affinity: when the diproline motif is mutated to alanine in E- and N- cadherins, the affinity of dimers is increased and the affinity of N- and E-Cadherin, as measured by AUC, become indistinguishable (Vendome et al., 2011). The diproline motif seems to be a structural element that account for affinity differences between E- and N-cadherin *trans* homophilic binding.

It is currently unclear whether the strength of E- and N-Cadherin based junctions is different. Indeed, while *in vitro* studies of analytical ultra centrifugation show that the homophilic binding affinity of N-Cadherin extracellular domain is fourfold higher than for E-Cadherin (Katsamba et al., 2009), dual pipette separation studies performed in living cells in suspension suggest the E-Cadherin junction to be stronger than the N-Cadherin one (Chu et al., 2004).

In addition to *trans* interactions between molecules on opposing membranes, type I cadherins are able to undergo *cis* lateral clustering. A lateral interaction site has been observed in the crystal structure of full-length ectodomains of C- (Boggon et al., 2002), N- and E- Cadherins (Harrison et al., 2011). Indeed, all three structures reveal a lateral interface formed between the base of the EC1 domain of one molecule and a region at the top of EC2 of the adjacent molecule. The portion of EC1 involved in the *cis* interaction is opposite to the site of strand swapping, therefore *cis* and *trans* interactions can form at the same time, which results, in crystallized protein complexes, in a continuous two dimensional lattice which size is close to that of the adherens junction (Figure 3.1C).

Concerning Type II Cadherins, which mediate weaker cell-cell interactions, the strand-swapping EC1 homophilic binding is mediated by two tryptophan residues, Trp2 and Trp4, and the dimer interface in the EC1 domain extends along its whole face, involving conserved hydrophobic residues at position 8, 10 and 13 (Patel et al., 2006). (Figure 3.1C) In addition, type II cadherins have not been reported to form *cis* lateral interactions (Brasch et al., 2011; Patel et al., 2006), which may account for the diminished strength of cell-cell adhesion mediated by type II cadherins.

The Cadherin-Catenin Complex

Classical cadherins are single pass transmembrane protein. While mediating *trans* and *cis* homophilic interactions via their EC domains, they are also able to modulate small GTPase activity and interact with the actin and microtubule cytoskeleton via their highly conserved cytoplasmic domain. Direct interactors of the cadherin intracellular tail are Armadillo (ARM) domain proteins of the

catenin family. In particular, p120 catenin interacts with the juxtamembrane domain of classical cadherins, while β-catenin interacts with their most C-terminal domain and links cadherins to the actin cytoskeleton via the vinculin homolog α-catenin (Nelson, 2008). A diagram of the cadherin-catenin complex is shown in Figure 4.1.

p120-Catenin

p120-Ctn (p120 hereafter) was first identified in a screening for tyrosine-phosphorylated substrates of oncogenic v-Src (Reynolds et al., 1989). It contains four ARM repeats, a 42 aminoacids repeated motif that occurs in β-catenin and in the desmosome associated protein plakoglobin (Reynolds et al., 1992). p120 was found to localise at E-Cadherin junctions (Reynolds et al., 1994) and to interact with E-Cadherin but not with β-catenin or α-catenin (Daniel and Reynolds, 1995). E-Cadherin interacts with p120 via its juxtamembrane region in the cytoplasmic domain (aa 758-785 in mouse E-Cadherin) (Thoreson et al., 2000). In particular, alanine substitutions of a conserved triple glycine repeat of the E-Cadherin JMD (^{761}GGG^{763}→AAA) or of the following acidic triplet (^{764}EED^{766}→AAA) (^{750}GGG^{752}→AAA; ^{753}EED^{755}→AAA in *Xenopus laevis* (Ciesiolka et al., 2004)) abolish the interaction with p120 catenin (Thoreson et al., 2000). Concerning p120, its central ARM domain is required for the interaction with cadherins (Daniel and Reynolds, 1995; Ishiyama et al., 2010). The crystal structure of the E-Cadherin juxtamembrane domain (JMD) bound to p120 has been resolved (Ishiyama et al., 2010). Importantly, the interaction between the JMD core region and the central ARM domain of p120 requires electrostatic interactions between the N-terminal acidic region of the E-Cadherin JMD and the

p120 basic ARM domain. Several salt bridges are formed between the acidic residues of the cadherin and basic residues of the ARM domain of p120 (i.e. Lys 401). In addition, the conserved triple glycine motif of the cadherin juxtamembrane core forms a turn that fits into a trough formed by Phe437, Trp477 and Asn478 of p120. The core mutations of E-Cadherin JMD used by (Thoreson et al., 2000) prevent the formation of salt bridges between p120 basic ARM repeats and the E-Cadh JMD (Ishiyama et al., 2010). Importantly, functional experiments as well as sequence conservation of the p120 binding site suggest that the biochemical interaction between E-Cadherin or N-Cadherin with p120 is equivalent (Ishiyama et al., 2010).

Cadherin-dependent regulation of small GTPases: the role of p120

p120 has been shown to regulate cell-cell adhesion by controlling small GTPase activity. Early studies have shown that p120 exerts a strong RhoA inhibitory activity by acting as a Rho-GDI: in vitro pull down assays show that p120 can interact and inhibit RhoA directly, and that it preferentially binds to the GDP-bound form of RhoA (Anastasiadis et al., 2000). Ectopic expression of p120 in fibroblasts results in a branching phenotype due to accumulation of p120 in the cytoplasm that can by rescued by constitutively active RhoA (Anastasiadis et al., 2000). Interestingly, cytoplasmic p120 can prevent maturation of focal adhesions, an effect that can be rescued by expression of constitutively active RhoA (Grosheva et al., 2001). Further studies have shown that p120 is not only able to inhibit RhoA directly, but that it is required for recruitment of p190RhoGAP, which antagonises RhoA activation, at the adherens junction. Importantly, p190-p120 interaction is required for junction formation

(Wildenberg et al., 2006). Moreover, p120 has been found to interact with the RhoA effector Rock at adherens junctions (Smith et al., 2012).

Conversely to its negative regulation on RhoA, p120 has been shown to promote Rac1 activity via activation of the Rac GEF Vav2 (Noren et al., 2000). The dendritic phenotype induced by p120 overexpression can be rescued by expression of full-length C-Cadherin, but not by p120-uncoupled C-Cadherin mutants, thus indicating a cross-talk between junction and cytoplasm domains. Furthermore, the branching phenotype can be rescued by dominant negative Rac1 or Cdc42, and p120 is able to increase Rac1 and Cdc42 activities in the cytoplasm via Vav2 (Noren et al., 2000).

Consistent with the notion that p120 positively regulates Rac1 activity, E-Cadherin ligation leads to activation of Rac1, and expression of p120 uncoupled cadherin mutants abrogates cadherin-dependent Rac1 activation (Goodwin et al., 2003). Cadherin ligation can also activate Rac independently of p120 via a c-Src-C3G-Rap1-PI3K-Vav2 dependent pathway (Fukuyama et al., 2006). It is worth noting that other Rac GEFs such as Tiam1 have been reported to be activated upon cadherin ligation (Sander et al., 1998), although other authors suggest that E-Cadherin ligation triggers Rac1 activation and Arp2/3 dependent actin assembly independently of Tiam1 (Kraemer et al., 2007). It is clear that p120-E-Cadherin interaction leads to activation of Rac1 (Goodwin et al., 2003) and inhibition of RhoA (Wildenberg et al., 2006) at the cell-cell adhesion, and that it is required for adherens junction stabilization (Ireton et al., 2002; Thoreson et al., 2000; Yap et al., 1998). In addition, a recent report suggests a role for p120 in regulating early steps of adhesion formation, namely spreading and extension of the cell-cell adhesion area, in a Rac1 dependent manner (Oas et al., 2013).

Nevertheless, although several studies have suggested the requirement for p120-Vav2 interaction for Rac1 activation (Noren et al., 2000) (Valls et al., 2012), there is no direct evidence for p120-dependent Vav2 recruitment upon cadherin ligation. In conclusion, several reports highlight a function for p120 in activating Rac1 at the cell-cell contact as well as the cytoplasm, but how exactly p120 induces Rac1 activation at junctions upon cadherin ligation still remains elusive.

In metastatic cancer cells MDA-MB-231 and URM3, characterized by loss of E-Cadherin expression, p120 interaction with mesenchymal cadherins such as Cadherin11 and N-Cadherin leads to cadherin-dependent Rac1 activation and cadherin-independent inhibition of RhoA, both of which are required to confer migratory properties to the cells. Restoration of E-Cadherin expression leads to a decrease of mesenchymal cadherin levels and repression of migration (Yanagisawa and Anastasiadis, 2006). In addition, it has also been reported that in PDGF-stimulated fibroblast, p120 negatively regulates Rac1 activity in the proximity of the N-Cadherin junction indirectly, via modulation of integrin activation (Ouyang et al., 2013), and therefore polarizes Rac1 activity opposite to the cell-cell junction. Consistently, N-Cadherin has been found to inhibit Rac1 activity at the cell-cell junction, leading to polarized activity of Rac1 towards the cell leading edge in *Xenopus* neural crest cells (Theveneau et al., 2010), although the requirement for p120 in mediating such polarization has not yet been tested. Overall, these reports suggest a context-dependent and cadherin-isoform dependent function for small-GTPase activity downstream of p120, and raise the possibility that p120 may play a different role in polarizing Rac1 activity at or away from the cell cell junction in epithelial or in mesenchymal cell types.

p120 : cadherin stability and trafficking

In addition to regulating small GTPase activity, p120 plays key roles in controlling cadherin stability at the plasma membrane and cadherin trafficking. In SW48 cells, which carry a mutation for p120, the cadherin adhesion system is impaired as a direct consequence of p120 mutation. Indeed, restoring p120 expression in these cells restores cell-cell adhesion and E-Cadherin expression. Importantly, in SW48 cells lacking or re-expressing p120 E-Cadherin mRNA levels are unchanged, thus suggesting that p120 controls E-Cadherin protein stability. Furthermore, expression of p120 uncoupled E-Cadherin mutants promotes formation of adherens junctions and restores an epithelial morphology in SW48 cells (Ireton et al., 2002). Additional reports have shown that p120 acts as a rheostat for control of cadherin protein stability. Expression of dominant negative cadherins causes downregulation of endogenous cadherin levels, and this depends on competition between endogenous and mutant cadherins for binding to p120 (Xiao et al., 2003). Upon expression of mutant cadherins, the endogenous VE-Cadherin, but not β-catenin or p120, are internalized into lysosomal compartments (Davis et al., 2003; Xiao et al., 2003). Knockdown of p120 results in downregulation of endogenous cadherin expression, and this holds true for several classical cadherins including E-, N-, P- and VE-Cadherin, as well as for α- and β- catenin (Davis et al., 2003). This report suggests that upon p120 RNA interference knockdown, internalised cadherins are subject to lysosomal and proteasomal degradation, as treatment with cloroquine or lactacystine repectively restores cadherin expression. (Davis et al., 2003). Taken together, these findings suggest that p120 acts as a setpoint to control the total levels of expression of cadherins at the plasma membrane. It is worth noting that

p120 is dispensable for post-Golgi trafficking of E-Cadherin, but it is strictly necessary to control E-Cadherin levels at the membrane (Davis et al., 2003). It has been suggested that the interaction of p120 with the cadherin juxtamembrane domain may mask binding sites for the endocytosis machinery (Ishiyama et al., 2010) or for targeted destruction. Indeed, the c-Cbl related ubiquitin ligase Hakai competes with p120 for binding to the E-Cadherin juxtamembrane domain upon Src tyrosine phosphorylation (Fujita et al., 2002). Hakai targets specifically E-Cadherin, but not other cadherins, for endocytosis and proteasomal degradation (Fujita et al., 2002). Recent work has added molecular insight in how the endocytotic machinery may compete with p120 binding to the cadherin juxtamembrane domain. Nanes and colleagues identified a conserved acidic motif within the core p120 binding region of VE-Cadherin juxtamembrane domain (^{646}DEE^{648}) which, if mutated, can completely abrogate VE-Cadherin endocytosis. Importantly, the ^{646}DEE^{648} →AAA mutant is stable at the plasma membrane upon p120 knockdown, thus further supporting the requirement of this motif for endocytotic internalization (Nanes et al., 2012). Cadherin endocytosis has been reported to occur both via clathrin–dependent and clathrin independent pathways. Indeed, upon chelation of Ca^{2+} from the extracellular environment, the whole cadherin apical complex including E-Cadherin and p120 is internalised in a clathrin-dependent manner into a syntaxin-4 positive compartment, from where it can be recycled back to the plasma membrane (Ivanov et al., 2004). In addition, cadherin recycling has been reported to occur during epithelial to mesenchymal transition. Indeed, stimulation of MDCK cells with the pro-migratory growth factor HGF leads to activation of ARF6 downstream of the HGF receptor c-Met and to internalization

of E-Cadherin in a clathrin and dynamin dependent manner (Palacios et al., 2001). In addition, N-Cadherin recycling via Rab5 downstream of the LPA-receptor Edg4 is required for EMT and in vivo migration of *Xenopus* neural crest cells (Kuriyama et al., 2014). Concerning clathrin-independent recycling, E-Cadherin internalization through caveolin vesicles has also been reported (Lu et al., 2003), and in CHO and MCF-7 cells E-Cadherin can be recycled by ARF6 dependent but clathrin- independent pathway (Paterson et al., 2003). Thus, the modalities of cadherin internalization downstream of p120 seem to be varied and context-dependent.

Finally, it is worth mentioning that p120 may play a differential role in cadherin biogenesis depending on the cadherin isoform. Indeed, while p120 is required for E-Cadherin stability at the plasma membrane (Davis et al., 2003), but not for earlier steps of its biogenesis, it associates with proN-Cadherin in the endoplasmic reticulum or at the Golgi before being transported to the plasma membrane (Wahl et al., 2003). In addition, p120 can interact with microtubules directly (Franz and Ridley, 2004) or via kinesin (Chen et al., 2003; Yanagisawa et al., 2004), and can promote kinesin dependent transport of N-Cadherin to the adherens junction (Chen et al., 2003).

β-Catenin

β-Catenin is a conserved protein containing 12 ARM repeats which interacts directly with the most C-term domain of cadherins cytoplasmic tail. The catenin binding site has been mapped to the last 56 C-terminal aminoacids of E-Cadherin (Ozawa et al., 1990). Early studies used recombinant cadherin cytoplasmic tail and purified catenins to show that β-Catenin directly binds to cadherin

cytoplasmic tail and links α-catenin to cadherin (Aberle et al., 1994; Jou et al., 1995). Importantly, deletion of the cadherin C-terminal tail or of its catenin binding site abolishes cadherin-mediated cellular aggregation (Ozawa, Ringwald et al. 1990) (Nagafuchi and Takeichi, 1988). β-Catenin is required for cell-cell adhesion mainly because it mediates recruitment of α-catenin to the cadherin tail: β-Catenin binds to the cadherin C-terminal domain via its ARM domain (Hulsken et al., 1994b), and α-catenin in turn binds to β-Catenin via its N-terminal domain. (Aberle et al., 1994; Hulsken et al., 1994a). In fact, β-Catenin appears to be dispensable for cell-cell adhesion, as a chimaeric protein in which E-Cadherin is fused to α-catenin can mediate normal adhesion (Nagafuchi et al., 1994). Nevertheless, E-Cadherin/β-Catenin can be modulated by intracellular signalling. Phosphorylation of E-Cadherin by Casein Kinase II has been reported to promote affinity for β-Catenin and junction stability (Lickert et al., 2000; Serres et al., 2000) and signalling from the extracellular matrix can impair cell-cell adhesion via tyrosine phosphorylation of β-Catenin: in pancreatic cancer cell lines, collagen-I induces disruption of E-Cadherin junctional complexes because of FAK-mediated tyrosine phosphorylation of β-Catenin (Koenig et al., 2006). Finally, β-Catenin is also a key component of the Wnt signalling pathway. It is able to shuttle to the nucleus and, in cooperation with the TCF/LEF family of transcription factors, regulate cell fate decisions in the embryo and proliferation and tissue renewal in the adult [reviewed in (Cadigan and Peifer, 2009)]. Furthermore, shuttling of β-Catenin from the junction to the nucleus is important for Wnt-dependent regulation of epithelial-to-mesenchymal transitions (reviewed in (Heuberger and Birchmeier, 2010)).

α-Catenin

α-catenin interacts with the cadherin cytoplasmic tail via interaction of its N-term with β-Catenin (Aberle et al., 1994) and with F-actin (Pokutta et al., 2002; Rimm et al., 1995). It is composed of 906 amino acid, and it has strong sequence homology with the actin binding protein vinculin. Three vinculin homology domains (VH) can be identified in α-catenin primary sequence (reviewed in (Pokutta et al., 2008)). α-catenin binds to β-Catenin via its N-terminal domain (aa 57-146) (Pokutta and Weis, 2000), and to actin via its C-term VH domain (Pokutta et al., 2002). In addition, α-catenin is able to homodimerize via aa 82-264 (Pokutta et al., 2002), and formation of the homodimer competes with formation of the α/β-catenin heterodimer (Pokutta and Weis, 2000).

Actin cytoskeleton and adherens junctions have long been thought to be interdependent. Indeed, mutations in the *Drosophila* β-catenin ortholog Armadillo lead to disruption of actin cytoskeleton polarity (Cox et al., 1996). In addition, disruption of the circumferential actin belt in cultured epithelial cells via expression of a constitutively active Rac1 or by direct depolymerisation by Cytochalasin D disrupts organization of adherens junctions (Quinlan and Hyatt, 1999). In summary, given the stoichiometric composition of the cadherin catenin complex, the ability of α-catenin to directly bind F-actin and the functional data suggesting close interrelation between actin cytoskeleton and adherens junction organization, the textbook view of cadherin-actin interactions has long favoured a model in which α-catenin bridges actin to the cadherin tail via β-catenin (reviewed in (Gates and Peifer, 2005). Biochemical studies from the Nelson and from the Weis lab, however, challenged this traditional view, showing that α-

catenin interactions with actin are highly dynamic and mutually exclusive with α/β-catenin dimer formation (Drees et al., 2005; Yamada et al., 2005). Using *in vitro* actin cosedimentation assays with purified α-catenin, β-catenin and E-Cadherin cytoplasmic domain at concentrations compatible with formation of a quaternary complex on the basis of known estimated affinity constants, Drees and colleagues demonstrated that α-catenin either binds to actin or to cadherin, and that the α/β-catenin dimer does not co-sediment with actin. In addition, α-catenin preferentially binds to actin as a homodimer, while the monomer prefers association with β-catenin and E-Cadherin (Drees et al., 2005), thus suggesting a model for allosteric regulation of α-catenin. In line with this results, the quaternary cadherin/β-catenin/α-catenin/actin complex could not be detected either on isolated native cadherin containing membranes. Furthermore, FRAP analysis of cadherin complex and actin mobility shows that while the half recovery time of E-Cadherin, β-catenin and α-catenin are similar, actin protein mobility is much higher at epithelial adherens junction, further supporting the notion that the interaction between actin filaments and the cadherin-catenin complex might be much more dynamic than previously appreciated (Yamada et al., 2005). In addition, monomeric α-catenin can compete with the Arp2/3 complex for actin binding (Drees et al., 2005), therefore supporting a model in which, upon homophilic cadherin binding, cadherin clustering leads to a local increase in concentration of cadherin/β-catenin complexes, to which monomeric α-catenin can dynamically bind. Free monomers of α-catenin in the cytosol can inhibit Arp2/3 activity by sequestering actin, therefore stopping lamellipodial protrusive activity and promoting junction maturation (Pokutta et al., 2008).

Recent work in *Drosophila melanogaster,* however, shows that, *in vivo,* interactions between monomeric α-catenin and the cadherin catenin complex are required to link the complex to actin, and that the dimers are found only in the cytoplasm and are in equilibrium with monomeric α-catenin (Desai et al., 2013). A recent report from the Nelson laboratory provides an explanation for this apparent conundrum. Using an *in vitro* strategy in which actin filaments attached to two optically trapped beads are suspended above the Cadherin/β-catenin-/α-catenin purified complex immobilized on a coverslip mounted on a motorized stage and imaged by electron tomography, they show that bonds between the ternary complex and the actin filaments can only form when tension is applied to the cadherin-catenin bonds. The authors observed that bond lifetime distributions had a two-phase dependence on the tension applied, consistent with weak binding of the complex to actin in low tension conditions, which transitions to strong binding on increase of the force applied (Buckley et al., 2014). This report suggest that direct binding of the cadherin-catenin complex to actin was not detected in previous in vitro based assays (Drees et al., 2005; Yamada et al., 2005) because such bonds were not strengthened by tension.

α-catenin is able to bind additional actin binding proteins, such as vinculin and α-actinin [reviewed in (Kobielak and Fuchs, 2004)] via its VH2 and VH3 domain. These are important for mechanosensing at the cadherin junction, which will be discussed in detail in the next chapter of this thesis.

Cadherins and Rho GTPases

Formation and maintenance of cadherin junctions requires an interplay between cadherins, small GTPases of the Rho family and the actomyosin cytoskeleton. Several studies suggest Rho GTPase activity to be required for adherens junction formation. Early reports have shown that the small GTPase Rac1 localises at the sites of contact in a Ca^{2+} dependent manner (Nakagawa et al., 2001). In addition, inhibition of endogenous RhoA activity by microinjection of the Rho inhibitor C3 exotransferase or inhibition of Rac1 activity by expression of a dominant negative Rac1 mutant (RacN17) inhibits E-Cadherin accumulation at cell-cell junctions both in newly forming adhesions and in stable junctions (Braga et al., 1997). Conversely, expression of a constitutively active Rac1 mutant (RacV12) induces accumulation of E-cadherin, β-catenin and actin filaments at cell-cell contact sites of MDCK cells (Takaishi et al., 1997). Importantly, E-Cadherin ligation has been reported to trigger activation of Rac1 and PI3K but not of RhoA (Nakagawa et al., 2001). Cadherin ligation has been suggested to activate Rac via a c-Src-C3G-Rap1-PI3K-Vav2 dependent pathway (Fukuyama et al., 2006). However, other authors reported PI3K signalling not to be required for E-Cadherin dependent cell-cell adhesion formation (Ehrlich et al., 2002), and it has been suggested that expression of p120 uncoupled E-cadherin mutants abrogates cadherin-dependent Rac1 activation (Goodwin et al., 2003), thus supporting, as discussed before, a role for p120 in cadherin-mediated Rac1 activation. Furthermore, studies in myoblast C2C12 cells using immobilized N-Cadherin-FC as an adhesive substrate support a role for N-Cadherin/p120 dependent Rac1 activation in promoting formation of a junctional complex and F-Actin assembly, while an initial PI3K-dependent Rac1 activation seem to be

involved in the early formation of lamellipodia in response to cadherin ligation (Lambert et al., 2002).

Live imaging studies have elucidated the temporal dynamics of Rac1 and RhoA activation during *de novo* formation of a cell-cell junction. When two MDCK cells are in close proximity, cell-cell junction formation is initiated by initial engagement of E-Cadherin complexes at the overlapping membranes of the two cells (Yamada and Nelson, 2007). Membrane overlap correlates with increased lamellipodial activity, actin remodelling at the site of cell-cell contact and recruitment of Rac1-GFP at the newly forming cell-cell junction (Ehrlich et al., 2002). Live imaging of active Rac1 and RhoA using FRET probes reveals that Rac1 is active at the overlapping lamellipodia during early steps of cadherin junction assembly, while active RhoA is excluded from the junction at this stage (Yamada and Nelson, 2007). Activation of Rac1 at the site of E-Cadherin ligation is thought to promote actin polymerization and increase lamellipodial protrusion to extend the area of cell-cell adhesion (Yamada and Nelson 2007). Active RhoA is detected laterally at the newly formed adhesions, once cadherin complexes are assembled and a linear junction starts to be observed. RhoA activity promotes ROCK activity and localization of phosphorylated Myosin light chain at the lateral sides of the newly formed adhesion, where actomyosin contraction is required to drive contact expansion and maturation (Yamada and Nelson 2007).

RhoA activity has been found to be essential in mature epithelial junctions for maintenance of junctional integrity via Myosin-II dependent regulation of E-cadherin clustering (Akhmanova et al., 2009; Ratheesh et al., 2012; Smutny et al., 2010). In mature MDCK cells, active RhoA is detected at the adherens junction

(Ratheesh et al., 2012), and its localization depends on the RhoGEF Ect2, which is localised at the adherens junction via interaction with α-catenin (Ratheesh et al., 2012). Inactivation of RhoA at the apical junction by C3 exotransferase results in loss of E-Cadherin from the zonula adherens (Ratheesh et al., 2012), due to a decrease in Myosin IIA accumulation at the junction (Ratheesh et al., 2012). Indeed, MyosinIIA is required for lateral clustering of cadherin complexes in mature MDCK epithelial adherens junctions, and inhibition of MyosinIIA mediated contractility via inhibition of the RhoA-ROCK axis leads to impaired junctional integrity because of impaired E-Cadherin lateral clustering (Smutny et al., 2010).

In summary, in epithelial cells Rho GTPases are required for initiation and maintenance of adherens junctions. In particular, Rac1 activation and local inhibition of RhoA is required for early steps of cell-cell adhesion formation, while RhoA-mediated actomyosin contractility appears to be required for expansion of cell-cell contact during junctional maturation and for maintenance of junctional integrity in mature epithelia.

Regulation of Rho GTPases during mesenchymal cell-cell interactions has been poorly studied. Dynamics of Rac1 and RhoA activity during formation of mesenchymal transient cell-cell contacts in living cells have not been reported so far. However, in neural crest cells RhoA is active at the cell-cell contact during Contact Inhibition of Locomotion (Carmona-Fontaine et al., 2008). N-Cadherin (Theveneau et al., 2010) and the polarity protein Par3 (Moore et al., 2013) are required to mediate inhibition of Rac1 at neural crest cell-cell junctions, thus raising the possibility that Rho GTPases at mesenchymal cell-cell junctions might be regulated in a different manner than at epithelial junctions.

Cadherins and Organization of the Actomyosin Cytoskeleton

Cadherin cell-cell adhesions are closely interrelated with the actin cytoskeleton. Indeed, mutations in the *Drosophila* β-catenin ortholog Armadillo disrupt actin cytoskeleton polarity (Cox et al., 1996). In epithelial cells, actin forms a circumferential actin belt, which is associated with adherens junctions (Quinlan and Hyatt, 1999). Perturbation of the actin belt in cultured epithelial cells via Cytochalasin D mediated actin depolymerisation disrupts organization of adherens junctions (Quinlan and Hyatt, 1999). Cadherins interact with the actin cytoskeleton via α-catenin (Pokutta et al., 2002). Most efforts to understand cadherin-actin cooperation have been directed to elucidate the physical interaction between α-catenin and actin (Drees et al., 2005). However, it is important to note that stable junction components interact with a junctional actin cytoskeleton which is, comparatively, highly dynamic (Yamada et al., 2005). During formation of *de novo* cell-cell junctions in keratinocytes, E-Cadherin is recruited at filopodia forming between the two interacting cells, forming punctate zipper-like cell-cell junctions (Vasioukhin et al., 2000), which recruit actin filaments as well as actin-binding proteins such as vinculin, zyxin, Mena and VASP in an α-catenin dependent manner. Actin polymerization occurs at the nascent adhesions as demonstrated by saponin permeabilization and incorporation of Rhodamine-labelled actin into living keratinocytes (Vasioukhin et al., 2000). In addition, VASP mediated actin assembly is required for junction maturation, which is blocked by dominant-negative VASP (Vasioukhin et al., 2000). Other additional components of the actin polymerization machinery have been found to promote actin assembly at cadherin adhesions. Plating E-Cadherin expressing CHO cells on a E-Cadherin-Fc coated substrate results in lamellipodia

formation and recruitment of Arp2/3 components such as Arp3 and p34Arc at cadherin adhesions. In addition, E-Cadherin interacts biochemically with Arp2/3 complex components and E-Cadherin coated beads trigger Arp2/3 dependent F-actin polymerization at the cell-bead surface (Kovacs et al., 2002). Taken together, these reports highlight cadherin-directed actin assembly during cell-cell junction formation. Further evidence for active F-actin nucleation at sites of E-Cadherin clustering comes from in vitro polymerization assays on reconstituted membranes (Tang and Brieher, 2012). Indeed, Arp2/3 and α-actinin-4 associate with apical cadherin complexes in MDCK cells, and are required for rapid reassembly of junctional actin upon Latrunculin-B mediated actin depolymerisation and washout in cells and on reconstituted membranes (Tang and Brieher, 2012). Other actin regulators, including N-WASP and Cortactin (Helwani et al., 2004; Kovacs et al., 2011) are localized at mature apical junctions in MDCK cells and are required to maintain homeostasis of junctional actin. Indeed, N-WASP siRNA knockdown results in loss of actin from zonula adherens via a non-canonical Arp2/3 nucleation independent pathway: via interaction with WIRE, N-WASP mediates clustering and organization of newly nucleated F-Actin (Kovacs et al., 2011). Knockdown of N-WASP or of WIRE does not result in loss of F-actin, but the polymerized actin is not organised into an apical actin belt (Kovacs et al., 2011).

Actin filaments at adherens junctions associate with a contractile myosin network. Actomyosin structures are responsible for junctional maintenance: in MDCK cells, MyosinIIA is required for clustering of E-Cadherin at the apical zonula adherens (Smutny et al., 2010), while MyosinIIB is required for organization and focussing of F-actin into an apical ring (Smutny et al., 2010).

The architecture of the Cadherin-Actin-Myosin interface can be dynamically rearranged, and such reorganization is essential for morphogenetic rearrangements occurring during development. Cadherin junctions can be found in two prominent forms: linear or punctate. Linear adherens junctions are found in mature epithelial sheets, where a bundle of actin filaments runs parallel to the cell border at the apical side of the cell in close proximity with the plasma membrane, and it is called circumferential actin belt. Here, cadherins accumulate along the actin filaments in clusters (Quinlan and Hyatt, 1999).

During epithelial junction formation, at the edge of epithelial colonies or at mesenchymal cell-cell contacts, adherens junctions are defined as punctate (Vasioukhin et al., 2000) and their organization is rather different. Indeed, actin filaments are organized and attached to cadherins in a perpendicular orientation to the plasma membrane, thus pulling cadherin from both sides of the junction and conferring it a "zigzag" appearance (Vasioukhin et al., 2000). In epithelial cells, punctate junctions can mature into linear junctions (Vasioukhin et al., 2000). However, it is currently unclear whether mesenchymal cells can form linear adherens junctions, and the actin cytoskeletal organization at the mesenchymal cell-cell adhesion has been so far poorly characterized.

Cadherins have been proposed to interact with F-Actin via the C-terminal domain of α-catenin (Pokutta et al., 2002). However, the circumferential actin belt is much thicker than the length of the α-catenin C-terminal domain, and additional actin-binding proteins are required for the conversion of punctate junctions into linear junctions. Importantly, EPLIN, an actin-crosslinking protein (Maul et al., 2003), which binds directly to α-catenin (Taguchi, Ishiuchi et al. 2011), is required for maintenance of linear junctions. Indeed, knockdown of

EPLIN leads to disruption of the zonula adherens and to conversion of linear junctions into punctate junctions (Abe and Takeichi, 2008). At the periphery of epithelial cell colonies punctate junctions can be observed. Importantly, EPLIN is excluded from these punctate junctions (Taguchi et al., 2011). Interestingly, release of local tension by laser ablation of perpendicular actin filaments triggers recruitment of EPLIN to the junction and conversion of the punctate junction into a linear one, thus supporting a role for tension-dependent inhibition of EPLIN recruitment to punctate junctions (Taguchi, Ishiuchi et al. 2011). An overview of actin organization at linear and punctate adherens junction is provided in Figure 5.1.

Actin filaments at both punctate and linear junctions are crosslinked by nonmuscle myosin, which creates a contractile actomyosin network. This is essential, in epithelial cells, for maintenance of cadherin lateral clustering as well as for apical organization of the actin circumferential ring (Smutny et al., 2010). In addition, junction-associated actomyosin contraction is essential for collective tissue remodelling events occurring during morphogenesis. During *Drosophila* gastrulation, apical constriction mediates mesoderm invagination: here, pulsed contraction of a medial actomyosin network is required for apical constriction (Martin et al., 2009). During convergence-extension movements, such as the ones occurring during *Drosophila* germband extension, ROCK and myosin are planar polarized in the epithelium (Simoes Sde et al., 2010), leading to waves of anisotropic contraction along the dorsoventral axis of the tissue and to cell intercalation (Rauzi et al., 2010). Finally, mechanical coupling of cell clusters through actomyosin cables has been suggested to control collective migration of cancer cells. Invasive squamous cell carcinoma A431 cells form motile clusters

which are surrounded by an actomyosin ring, while phosphorylated myosin is excluded from cell-cell contact (Hidalgo-Carcedo et al., 2011). Knockdown of the Par6-E-Cadherin associated protein DDR1 restores myosin accumulation at cell-cell contacts via inhibition of the small GTPase RhoE, which antagonises RhoA, and inhibits collective invasion (Hidalgo-Carcedo et al., 2011), suggesting that mechanical coupling of cell collectives through establishment of a supracellular actomyosin ring at the cell periphery might be required for collective migration.

4. Mechanics of Collective Cell Migration

Collective migration is essential during developmental processes such as neural crest migration and gastrulation, for physiological repair processes such as epithelial wound healing as well as pathological processes such as cancer invasion and metastasis (Friedl and Gilmour, 2009). During collective migration, a group of cells migrates as a cohesive sheet, maintaining stable or transient cell-cell junctions that coordinate the group (Theveneau and Mayor, 2012a). Polarized leader cells at the front edge of the group form new protrusions, exerting traction forces on the extracellular matrix onto which the cells migrate (Reffay et al., 2014). These forces are anisotropically distributed across the cell sheet (Reffay et al., 2014) and need to be counterbalanced by equal and opposite intercellular tensions, transmitted via cell-cell adhesions, for the group of cells to remain cohesive(Tambe et al., 2011; Tseng et al., 2012; Vitorino et al., 2011).

Guidance of single cells and of cell collectives can rely on gradients of chemokines, the source of which might be external (Theveneau et al., 2010) or self generated (Dona et al., 2013). This behaviour is defined as chemotaxis. More recently, increasing evidence established that cells can migrate directionally in response to gradients of mechanical cues in their microenvironment (Lo et al., 2000). Indeed, it has been demonstrated that single NIH3T3 fibroblasts placed on a collagen-coated polyacrylamide gel fabricated with a rigidity gradient directionally migrate towards the stiffer area of the gel (Lo et al., 2000). Cell collectives have also been shown to migrate in a highly coordinated manner on stiff matrices, while on soft substrates coordination of migration is strongly decreased (Ng et al., 2012). In addition, stiffening of the ECM occurs in

pathological conditions such as mammary cancer, and favours collective invasion of cancer cells *in vivo* and *in vitro* (Levental et al., 2009). The ability of cells to respond to gradients of stiffness is defined as durotaxis. Collective migration requires coordination of large groups of cells via cell-cell interactions (Friedl and Gilmour, 2009). It has been suggested that groups of cells are able not only to respond to mechanical features of the extracellular matrix, but they are also able to migrate directionally in response to self-generated gradients of intercellular tensions, a behaviour defined as cohesotaxis (Weber et al., 2012). Indeed, during epithelial wound healing, migrating neighbouring cells join forces to transmit intercellular stresses, a behaviour measured by a technique called monolayer stress microscopy (Tambe et al., 2011), and orientate their movement in a way that minimises shear stress at cell-cell junctions (Tambe et al., 2011). In addition, *Xenopus* mesodermal cells are able to migrate directionally in response to a gradient of intercellular stresses that is transmitted across C-Cadherin junctions (Weber et al., 2012). Application of tension to magnetic beads coated with C-Cadherin in contact with single mesodermal cells is sufficient to polarize cell protrusions in a direction opposite to the applied tension (Weber et al., 2012).

To sense and respond to mechanical cues, cells are equipped with mechanosensitive systems. Such structures need to be localised at cell-matrix adhesions, to respond to changes in compliance of the extracellular environment, and at cell-cell interaction sites, where they allow cells to transmit and respond to tensile information from one another. Here, I will discuss molecular components and cellular responses to mechanosensation at cell matrix adhesions and cell-cell contacts.

Mechanosensation at cell-matrix adhesions

Integrin-Mediated Adhesions

Both in culture conditions and in their native environment *in vivo* cells adhere to the extracellular matrix via a class of specialized receptors called integrins. Integrins were first discovered as the receptors for the extracellular matrix component fibronectin in 1987 (Hynes, 1987). Integrins are heterodimers constituted of one α and one β single pass transmembrane subunits. In mammals there are 24 different α subunits and 8 β subunits, which can form up to 24 different heterodimers whose binding affinities differ according to the composition of the extracellular matrix (Hynes, 2002). As an example, $\alpha_5\beta_1$ heterodimer is a receptor for fibronectin, while $\alpha_6\beta_1$ heterodimer is a laminin receptor (reviewed in (Hynes, 2002)). Similar to cadherins, integrin receptors are indirectly connected with the actin cytoskeleton via proteins, such as talin, which binds to both integrin cytoplasmic tail (Horwitz et al., 1986) and F-Actin (McCann and Craig, 1999). Additional components of the integrin adhesion include integrin binding partners such as paxillin, which interacts directly with integrin cytoplasmic tail (Liu et al., 1999), actin binding proteins such as vinculin (Johnson and Craig, 1995), and multidomain enzymes such as FAK (Focal Adhesion Kinase) (Parsons et al., 2000) which exert both scaffolding (Carragher et al., 2003) and signalling functions (Parsons et al., 2000). The composition of the architectural and signalling platform of the integrin adhesome is extremely complex and includes about 90 components (Zaidel-Bar et al., 2007a). Interactions between these and additional proteins lead to the formation of an adhesion plaque that connects the extracellular matrix with the intracellular

environment via actin stress fibres. Assembly of actin stress fibres connected to integrin adhesions requires the actin nucleator formin/mDia1: knockdown of mDia1 in U2OS cells leads to loss of dorsal stress fibres associated with focal adhesions (Hotulainen and Lappalainen, 2006).

Formation, Maturation and Disassembly of Integrin Adhesions

Assembly of the integrin adhesome is initiated by binding of integrins to the extracellular matrix. A FRET-based approach (Kim et al., 2003) has demonstrated that, upon ligand binding, α and β subunits undergo conformational changes that separate them from one another, thus exposing sites for binding partners of the integrin cytoplasmic tail (Kim et al., 2003). Once the lamellipodium forms the first contacts with the matrix, "inside-out" signalling takes place: interactions of integrin cytoplasmic tail with talin (Wegener et al., 2007) and kindlin-2 (Montanez et al., 2008) enhances integrin activation and stabilize their grip on the extracellular matrix. Actin polymerization and integrin clustering rapidly follows integrin-ECM binding, as demonstrated by high resolution imaging of integrin adhesion of intact cells to their ligands on lipid bilayers with nanofabricated barriers (Yu et al., 2011). The growth of integrin clusters (nascent adhesions) into larger focal complexes depends on assembly of actomyosin stress fibres via mDia1 (Riveline et al., 2001), α-actinin (Choi et al., 2008; Oakes et al., 2012) and MyosinII (Choi et al., 2008). Importantly, maturation of focal complexes into focal adhesions requires the actin crosslinking capabilities of α-actinin and MyosinII, rather than RhoA-ROCK dependent contractility mediated by the myosin motor domain (Choi et al., 2008; Oakes et al., 2012). Mature focal adhesions are about 1 μm wide and up to 3-5

μm long, with lifetimes of tens of minutes (Zaidel-Bar et al., 2007b). Fluorescence speckle microscopy imaging reveals that protrusive migration depends on an adhesion-coupled actomyosin network located at the leading edge of migrating cells, the lamella, where focal adhesions are located (Ponti et al., 2004). Mature focal adhesions are then turned over and disassembled at the trailing edge of the cell, a process that requires microtubule-mediated targeting of focal complexes (Kaverina et al., 1999). Microtubules targeting of focal adhesions at the trailing edge temporally precedes adhesion disassembly (Kaverina et al., 1999). Importantly, nocodazole-induced microtubule depolymerisation blocks focal adhesion disassembly at the rear of the cell (Kaverina et al., 1999). Concerning the mechanisms through which microtubules mediate focal adhesion turnover, the RacGEF STEF/Tiam2 is required for the disassembly of adhesions downstream of microtubules and STEF knockdown by RNA interference results in stabilized focal adhesions (Rooney et al., 2010). In addition, it has been recently proposed that microtubule-mediated delivery of MAP4K4 to focal adhesions via the microtubule end-binding protein EB2 triggers activation of the Arf6-GEF IQSEC1 leading to Arf6-dependent focal adhesion internalization (Yue et al., 2014).

Mechanotransduction at Integrin Adhesions

Integrin adhesions mediate interactions between cells and their extracellular environment and allow cells to sense and respond to mechanical stresses exerted through the extracellular matrix or generated by the actin cytoskeleton machinery. The mechanotransduction function of integrin adhesions is allowed by the intimate link between integrins and the actin cytoskeleton. It has been

shown that the ECM can link via integrin and talin to the actin cytoskeleton, and that a minimal ECM adhesion can resist a force of ≈2pN (Jiang et al., 2003), while forces transmitted across large focal adhesions are in the order of tens of nN (Balaban et al., 2001). Seminal experiments have shown that assembly of focal adhesions is a force dependent process (Balaban et al., 2001; Riveline et al., 2001). Application of external mechanical force to immature, dot-like adhesions at the cell leading edge using a fibronectin-coated micropipette induced assembly and elongation of these immature structures into streak-like focal adhesions positive for Vinculin and Paxillin (Riveline et al., 2001). In addition, plating of cells onto an elastomeric, deformable, micropatterned substrate allowed simultaneous measurement of substrate deformation and of focal adhesion assembly using GFP-Vinculin (Balaban et al., 2001). Importantly, this work showed for the first time that traction forces oriented opposite to the direction of migration are exerted at focal adhesion sites (Balaban et al., 2001). In addition, reduction of intracellular tension via inhibition of actomyosin contractility not only reduces the strength of the traction forces exerted by the cells over the substrate, but also decreases focal adhesion size and intensity of Vinculin-GFP fluorescence at the focal adhesion (Balaban et al., 2001). Experiments using laser traps to restrain movement of Fibronectin-coated beads applied to the lamellipodium of migrating cells (Choquet et al., 1997) have shown that, upon application of a given external force of known magnitude to the bead, the cells are able to increase their linkage to the bead via an integrin-actin axis, a process defined as reinforcement (Choquet et al., 1997).

How do reinforcement of integrin-actin linkage and force dependent assembly of focal adhesions occur?

Integrin adhesions are linked to the actin cytoskeleton via Talin (Horwitz et al., 1986). In vitro experiments using magnetic tweezers to apply tensile force to single talin molecules in vitro (del Rio et al., 2009) has shown that stretching of talin using physiologically relevant force ranges exposes cryptic binding sites for the actin-binding protein vinculin, thus suggesting that mechanotransduction at focal adhesions occurs through exposure of buried vinculin binding sites in the talin protein upon force-induced stretch (del Rio et al., 2009). Importantly, several investigators have reported that vinculin is recruited to focal adhesion in a force dependent manner (Galbraith et al., 2002; Grashoff et al., 2010; Humphries et al., 2007). Indeed, application of fibronectin coated beads of medium (6 m) but not small (1 m) diameter to fibroblast lamellipodia induces focal adhesion assembly and vinculin recruitment in a manner dependent on actomyosin contractility (Galbraith et al., 2002). In addition, vinculin can be recruited at small diameter beads upon optical tweezer-induced stretch (Galbraith et al., 2002). Importantly, additional studies using vinculin deletion mutants (Humphries et al., 2007) have shown that vinculin N-terminal head domain is required for integrin clustering, while its C-terminal tail is required to link vinculin with the mechanotransduction machinery (Humphries et al., 2007). Indeed, expression of vinculin deletion mutants with unmasked actin binding sites induced focal adhesion growth via direct interaction with talin, while actin-vinculin interactions depend on vinculin C-terminal domain (Humphries et al., 2007). A direct measurement of the tension vinculin molecules sustain at focal adhesions has been provided by FRET studies (Grashoff et al., 2010). Grashoff and colleagues developed a tension-sensitive FRET probe for vinculin, in which a tension-sensor FRET module constituted by mTFP, an elastic aminoacid linker

(GPGGA$_8$) and Venus is inserted in between vinculin head and tail domain. When force extends the elastic linker, FRET efficiency decreases. This study shows that force transmitted across single vinculin molecules is ≈2.5 pN (Grashoff et al., 2010). Importantly, this report confirms that recruitment of vinculin to focal adhesions is regulated separately from force transmission, as already suggested by previous studies (Humphries et al., 2007) and it confirms the requirement of vinculin to stabilise focal adhesions under force (Grashoff et al., 2010). In addition, it revealed that vinculin is under highest tension at large focal adhesions at the leading edge of migrating cells and under low tension at disassembling focal adhesion at the trailing edge of the cell (Grashoff et al., 2010).

Another potential candidate for mechanosensing at the cell-ECM adhesion is the actin crosslinking protein filamin-A (Ehrlicher et al., 2011). Filamin-A is able to bind directly to the integrin β subunit and competes with talin for integrin binding (Kiema et al., 2006). Using a minimal *in vitro* reconstituted actin network composed of filamin-A crosslinked actin filaments, β integrin cytoplasmic tail and the filamin-A partner Rac-GAP FilGAP, and by performing fluorescence loss after photoconversion experiments (Sprague et al., 2004) Ehrlicher and colleagues show that both externally imposed bulk shear and myosinII-induced forces differentially regulate binding of Filamin-A to its partners (Ehrlicher et al., 2011). In particular, under stress conditions Filamin-A dissociates from FilGAP and binds to β integrin cytoplasmic tail, thus suggesting a direct molecular mechanism for filamin-A dependent mechanotranduction (Ehrlicher et al., 2011). To summarise, these reports show how forces applied at cell-ECM adhesions can induce conformational changes in adhesion-resident proteins, which eventually

lead to maturation and strengthening of the adhesion, mainly through recruitment of additional actin-binding proteins. In this context, the talin-vinculin axis, and filamin, function as tension-sensitive modules. As forces modify the adhesion, this is in turn able to modify forces by inducing assembly of actomyosin structures and therefore increasing cellular contractility (Figure 6.1 b,d,f,) (Butler et al., 2006; Hotulainen and Lappalainen, 2006). *In vitro* actin polymerization studies using integrin complexes isolated from hematopoietic cells have shown that these complexes are able to polymerize F-actin, in a manner dependent on tyrosine phosphorylation of β_3 integrin and on formin-mediated polymerization of actin (Butler et al., 2006). In addition, another study performed on U2OS cells has demonstrated assembly of actin stress fibres connected to integrin adhesions (Hotulainen and Lappalainen, 2006). This requires, again, the actin nucleator formin/mDia1. Indeed, knockdown of mDia1 leads to loss of dorsal stress fibres associated with focal adhesions (Hotulainen and Lappalainen, 2006).

The mechanical stresses sensed by an adhesion may depend on intrinsic forces or on the mechanical properties of the surrounding environment. In this context, it is important to note that traction forces exerted by a focal adhesion on its substrate are proportional to the rigidity of the extracellular matrix, therefore, the stiffer the matrix, the higher the stress experienced by the adhesion (Saez et al., 2005). Importantly, cells are able to sense and migrate towards gradients of stiffness of the extracellular matrix (Lo et al., 2000), a behaviour defined as durotaxis. It has been proposed that, for a cell to perform durotaxis, the sole detection of an externally applied force might not be sufficient. A cell should exert a force on the substrate, detect the consequent deformation of the

substrate and compute the ratio between force and deformation to measure rigidity (Roca-Cusachs et al., 2013). Several, diverse models have been proposed, including clutch models (Chan and Odde, 2008), local rigidity sensing mechanisms based on submicrometric actomyosin structures (Ghassemi et al., 2012) or "global" stiffness sensing units (Trichet et al., 2012). The first are based on a stochastic model of a "motor clutch" force transmission system, in which integrin-based adhesions act as molecular clutches linking F-actin and mechanically myosin-driven actin retrograde flow to the substrate. The model predicts fast retrograde flow and low traction forces on stiff substrates, and oscillatory "load and fail" dynamics on soft substrates, with slower retrograde flow and higher traction forces (Chan and Odde, 2008). Nanoscale dynamics of traction forces exerted by neuronal growth cone filopodia are consistent with the predictions of the clutch model (Chan and Odde, 2008). Alternative mechanisms for rigidity sensing have been suggested by studies utilising PDMS micropillars to measure matrix forces (Ghassemi et al., 2012; Trichet et al., 2012). A study which compared tractions exerted by cell-matrix adhesions on submicrometric micropillars has shown how cells are able to locally contract pillars with a maximum displacement of about 60 nm (Ghassemi et al., 2012). Myosin filaments localise in between the contracting pillars, and cells mutant for rigidity sensing pathways do not show local contractions, suggesting a correlation between contraction and rigidity sensing (Ghassemi et al., 2012). An alternative model proposes larger scale rigidity sensing mechanism and argues against local ones (Trichet et al., 2012). In this study, using PDMS micropillars the authors show that upon adhesion formation a buildup of traction force on the substrate is observed over time, until it reaches a saturation value. Importantly,

stiffer substrates lead to higher saturation values, and focal adhesions of similar size give rise to higher traction forces on a stiffer substrate, consistently with earlier observations (Saez et al., 2005), thus suggesting the presence of a rigidity sensing mechanism (Trichet et al., 2012). A viscoelastic gel model for rigidity sensing predicts a role for cytoskeleton in mediating large scale mechanosensing, and, consistently, on stiffer substrates the actin cytoskeleton is organized in higher order structures such as stress fibres (Trichet et al., 2012), thus leading the authors to propose that large scale cytoskeletal structures such as stress fibres might be more important for rigidity sensing than local mechanisms. At the cell collective scale, it has been shown that epithelial wound healing is more efficient on stiff substrates than on soft ones (Ng et al., 2012). Stiff substrates increase cell coordination and protrusion polarization, and this depends on formation of myosinII contractile stuctures which depend on cadherin based cell-cell interactions (Ng et al., 2012).

Although additional research might be required to conciliate these models, all of these reports suggest the existence of a sensor mechanism through which cells might be able to assess rigidity of the environment by sensing substrate deformation and appropriately adjust the mechanochemical properties of their cell-ECM adhesions.

Cadherin Mechanotransduction

Cadherin cell-cell adhesions are intimately connected with the actin cytoskeleton. They have long been considered as passive structural elements in force transmission between cells. However, recent findings have challenged this view, and increasing evidence suggest that, by dynamically interacting with the

actin cytoskeleton, cadherin adhesions behave as mechanotransduction elements able to sense and elicit a biochemical response to changes in intercellular tension.

During the last five years, direct evidence for mechanosensing has been demonstrated for most of classical cadherins, including E-Cadherin (Borghi et al., 2012; le Duc et al., 2010), N-Cadherin (Ladoux et al., 2010), VE-Cadherin (Liu et al., 2010) and C-Cadherin (Weber et al., 2012), using a variety of approaches and experimental settings. One of the first reports about the mechanosensitive properties of E-Cadherin used magnetic twist cytometry on F9 cells (le Duc et al., 2010). Upon application of shear stress to E-Cadherin coated beads adherent to F9 cells, bead displacement amplitude decreased with the forcing time, in a manner proportional to the increase in stiffness of the bead-cell interaction. Such force-induced stiffening was found to be dependent on the actin cytoskeleton, as it could be reversed by incubation of the cells with the actin depolymerizing drugs Cytochalasin D or Latrunculin B (le Duc et al., 2010). A more recent study exploited a tension-sensor FRET approach, similar to the one already discussed for Vinculin (Grashoff et al., 2010), to prove that, in MDCK cells, E-Cadherin molecules are under constitutive tension at cell-cell junctions but not when they are localised in junction-free areas of the membrane (Borghi et al., 2012). Junctional tension exerted on E-Cadherin molecules is constitutive and actomyosin dependent as it is released upon Cytochalasin B mediated actin depolymerisation or inhibition of myosin light chain phosphorylation with ML-7 and can be enhanced by externally applied stretch when cells are cultured on a compliant PDMS substrate (Borghi et al., 2012). N-Cadherin mechanosensing has been demonstrated using N-Cadherin-coated polyacrylamide hydrogels and N-

Cadherin coated micropillars of different stiffnesses (Ladoux et al., 2010). C2 myoblasts spread and exert higher traction forces on stiff N-Cadherin coated substrates rather than on soft ones. Such N-Cadherin mediated rigidity sensing strongly suggest that N-Cadherin can act as a mechanosensor. As observed for E-Cadherin (Borghi et al., 2012; le Duc et al., 2010), N-Cadherin mediated mechanosensing requires actomyosin assembly and N-Cadherin mediated spreading and traction force generation on stiff substrates is blocked by the myosinII inhibitor Blebbistatin (Ladoux et al., 2010). Exertion of substrate stiffness dependent traction forces has recently been reported also for E-Cadherin coated substrates (Barry et al., 2014). Another report used a combination of micropatterning on PDMS micropillars to measure tugging forces of endothelial cell doublets (Liu et al., 2010). The size of the VE-Cadherin junction was found to be proportional to the cell-cell tugging force (Liu et al., 2010), and tugging forces grew or decayed upon MyosinII activation or inhibition, thus once more confirming the actomyosin dependence of classical cadherin mechanosensing (Liu et al., 2010). Finally, *Xenopus* mesodermal cells were found to migrate directionally in response to a gradient of intercellular stresses transmitted across C-Cadherin junctions (Weber et al., 2012). Interestingly, mesodermal cells direct their migration in response to tension transmitted across cell-cell contacts: application of tension to magnetic beads coated with C-Cadherin in contact with single mesodermal cells is sufficient to polarize cell protrusions in a direction opposite to the applied tension. In this context, mechanoresponsivity of C-Cadherin junctions depends on tension-dependent recruitment of plakoglobin to the cell-cell contact, which in turn is able to polarize the intermediate filament network and therefore allow collective

directional migration (Weber et al., 2012). Importantly, tension dependent plakoglobin recruitment at the junction suggest that other cadherin-like adhesion such as desmosomes may also act as mechanosensor, although this direction has so far been poorly investigated in other systems. A role for actomyosin tension in C-Cadherin dependent mechanosensing has not so far been investigated, but it cannot be excluded. In summary, accumulating evidence strongly suggest that cadherin cell-cell adhesions may act as *bona fide* mechanosensors, and that such behaviour requires interactions with the actomyosin network, or, at least for C-Cadherin , the intermediate filament cytoskeleton.

α-catenin-Vinculin interaction and mechanosensing

Several reports have shown that cadherin mechanosensing requires actin cytoskeleton and myosin-mediated intracellular tension. Cadherin adhesion molecules physically interact with the actin cytoskeleton via β-catenin and α-catenin. In particular, α-catenin binds directly to actin (Pokutta et al., 2002) and, although the precise molecular details remain controversial, links E-Cadherin to the actin cytoskeleton.

A seminal study has recently demonstrated that α-catenin is the key molecular component mediating E-Cadherin mechanosensitivity (Yonemura et al., 2010). In line with previous observations (le Duc et al., 2010), the authors show that vinculin is recruited at the zonula adherens of epithelial cells in a MyosinII dependent manner. α-catenin binds to Vinculin via its central VH2 domain (Watabe-Uchida et al., 1998). Using a series of α-catenin deletion mutants, the authors show that vinculin is recruited to adherens junctions by α-catenin in a

force dependent manner (Yonemura et al., 2010). The notion that α-catenin may undergo a conformational change that may expose cryptic vinculin binding sites was supported by staining with the α18 antibody, which recognises an epitope exposed in a force dependent manner, located on α-catenin VH2 domain (Yonemura et al., 2010). In addition, FRAP experiments suggested that actomyosin contractility stabilised α-catenin at the adherens junction (Yonemura et al., 2010). Further studies, including X-ray crystallography and in vitro binding assays using purified proteins (Choi et al., 2012) have confirmed that α-catenin is autoinhibited via intramolecular interactions: α-catenin molecule encompasses five α-helical bundles named D1-D5, autoinhibition is mediated by interactions between the N-terminal D1 region and the D5 region in the C-terminal actin binding tail. A deletion mutant including only the D3a vinculin binding region has a 1000 fold higher affinity for vinculin than full length α-catenin (Choi et al., 2012).

These studies indicate how the immediate effector downstream of α-catenin in the cadherin mechanosensitive pathway is vinculin. Vinculin is recruited to junctions under endogenous actomyosin dependent tensional stress. In support for a role of vinculin in sustaining the cadherin mechanoresponse, experiments in which cells were cultured on stretchable PDMS substrates show that vinculin is recruited at adherens junctions also in response to externally applied stretch (Thomas et al., 2013). Importantly, knockdown of Vinculin reduces mechanosensitive responses such as stress-induced stiffening induced by magnetic twist cytometry (le Duc et al., 2010) and strongly decreased separation force of E-Cadherin cell doublets using a dual pipette assay (Thomas et al., 2013).

Although it is currently unclear how vinculin stabilises cell-cell junctions under tension, recruitment of Vinculin and F-actin at cell-bead interface upon stress induced by magnetic twist cytometry suggests that Vinculin may recruit additional F-actin to adherens junctions subject to mechanical stress (Barry et al., 2014). A summary of a possible mechanism for α-catenin-vinculin in promoting cadherin mechanosensing is presented in Figure 6.1a,c,e.

Potential roles for additional actin binding proteins in Cadherin mechanotransduction

Additional actin binding proteins are able to interact with α-catenin at binding sites close to the Vinculin binding region, and may therefore participate in the mechanotransduction response. α-actinin binds α-catenin D3a domain and regulates Arp2/3 activity to assemble F-actin at E-Cadherin adherens junctions (Tang and Brieher, 2012). Formin binds to the D3b and D4 domains and localises to adherens junctions, where it is involved in junction formation (Carramusa et al., 2007). In addition, formin has been recently shown to promote mechanosensitive actin nucleation (Higashida et al., 2013): upon cell cortex deformation formins are able to promote processive actin assembly, which can be observed by single molecule fluorescence speckle microscopy (Higashida et al., 2013).

Finally, EPLIN, which binds to the tail domain of α-catenin (Abe and Takeichi, 2008) localises to linear, mature adherens junctions, but is excluded from vinculin-positive punctate adherens junctions in a tension dependent fashion (Taguchi, Ishiuchi et al. 2011). However, whether EPLIN is important to mediate a mechanoresponsive behaviour is currently unclear.

Additional proteins might be important to sense tension at F-actin structures proximal to the cadherin cell-cell adhesions. In particular, zyxin has been found to be recruited at stressed F-actin structures at stress fibers (Colombelli et al., 2009; Smith et al., 2010) or at focal adhesions (Hirata et al., 2008) and it has also been involved in organization of actin dynamics at adherens junctions (Nguyen et al., 2010; Sperry et al., 2010), thus raising the possibility that zyxin might be involved in sensing stressed F-actin structures at cell-cell junctions.

Cadherin-Integrin Crosstalk

In the previous sections of this chapter, we discussed how cadherin-based cell-cell adhesions and Integrin cell-ECM adhesions can sense and transduce mechanical signals they receive from the extracellular environment. Importantly, we have discussed how these adhesion structures share several molecular components, including signalling components such at the tyrosine-kinases Src and FAK (Giehl and Menke, 2008; Koenig et al., 2006), and core components of the mechanosensory machinery such as vinculin, actin or zyxin. Here, we will focus on signalling and mechanical cross-regulation between cell-cell and cell-matrix adhesions.

During morphogenesis *in vivo*, cell-cell and cell matrix adhesions are often spatially segregated, and functionally antagonise each other. In chick somite morphogenesis, local fibronectin assembly on the basal surface of the somite is required to promote apical N-Cadherin polarization (Martins et al., 2009). Conversely, during *Xenopus* convergence-extension, lateral cadherin-dependent tissue tension is required to promote fibronectin fibrillogenesis on the basal surface of the blastocoel roof (Dzamba et al., 2009). In addition, *in vitro* models of

epithelial cyst formation using MDCK cells show that adhesion of integrins to laminin, a component of the ECM, orientates apicobasal polarity in a PI3K and aPKC dependent manner (Liu et al., 2007; O'Brien et al., 2001).

Integrin signalling antagonises Cell-Cell Adhesion

Several reports suggest that integrin signalling spatially restricts or antagonises cadherin cell-cell adhesions. Seminal work in MDCK cells (Ojakian et al., 2001) has shown that incubation of MDCK monolayers with collagen gel overlays results in protrusion formation at the collagen-coated apical side of the cells. Protrusive activity leads to disruption of adherens and tight junctions and, eventually, to formation of a new, internal epithelial lumen and to adherens junction assembly away from the overlayed extracellular matrix (Ojakian et al., 2001). More recently, biophysical studies exploited micropatterning strategies to produce spatially segregated fibronectin and E-cadherin coated surfaces (Al-Kilani et al., 2011; Tsai and Kam, 2009). MCF-7 breast adenocarcinoma cells were unable to form E-Cadherin contacts close to integrin based contacts (Tsai and Kam, 2009). However, this mutually exclusive response was found to be rigidity and Src-family kinase dependent, as cells were able to form cadherin-based contacts in close proximity to focal adhesions on soft substrates (Tsai and Kam, 2009). In a second study, cells were cultured on square shaped fibronectin micropatterns of different areas, and the strength of E-Cadherin interactions was probed by subjecting to magnetic twist cytometry an E-Cadherin coated bead in contact with the cell (Al-Kilani et al., 2011). Importantly, the rigidity modulus of the cadherin contact upon externally applied stress decreased proportionally to the area of cell-ECM adhesion, thus strongly suggesting that cell-ECM

interactions exert a negative modulatory activity on cell-cell junction strength (Al-Kilani et al., 2011). How do cell-ECM adhesions negatively regulate cadherin cell-cell adhesions? In pancreatic cancer cell lines, collagen I induces disruption of E-Cadherin junctional complexes because of tyrosine phosphorylation of β-Catenin (Koenig et al., 2006). Collagen I triggers Src/β_1 integrin interaction, which in turn leads to recruitment of FAK to adherens junctions, which phosphorylates β-Catenin on tyrosine residues (Koenig et al., 2006). In line with this result, FAK has been shown to be responsible for junctional disassembly via tyrosine phosphorylation of β-Catenin during VEGF induced vascular permeability *in vivo* and during VEGF induced junctional rearrangements *in vitro* (Chen et al., 2012).

Cadherin signalling locally antagonises Cell-Matrix Adhesion

We have discussed how integrin signalling may negatively regulate cadherin cell-cell adhesion. Several studies suggest that cadherins may, conversely, negatively signal to cell-matrix adhesions. Indirect evidence has been suggested by seminal work in which disruption of cell-cell junctions led to an increase in cell migration (Balzac et al., 2005; von Schlippe et al., 2000). Expression of a dominant negative E-Cadherin mutant in breast cancer cell lines leads induces a loss of β-Catenin from the junction (von Schlippe et al., 2000). In parallel, cells acquire the ability to migrate on vitronectin substrates, in a manner dependent on $\alpha_v\beta_5$ and $\alpha_v\beta_1$ integrins (von Schlippe et al., 2000). In addition, it has been shown that upon E-Cadherin endocytosis, the small GTPase Rap1, which is involved in integrin inside-out activation (Bos et al., 2003), is activated in a Src dependent manner (Balzac et al., 2005). Importantly E-Cadherin endocytosis-dependent Rap1

activation is required for integrin activation and focal adhesion formation (Balzac et al., 2005). More recently, several reports have provided evidence for local restriction of focal adhesion formation and, in turn, of integrin-dependent traction forces exerted on the substrate, by cadherin dependent cell-cell adhesion (Borghi et al., 2010; McCain et al., 2012; Ouyang et al., 2013). Using a micropatterning approach in which stripes of E-Cadherin-Fc were alternated with stripes of Collagen IV, Borghi and colleagues have shown that single MDCK cells spatially segregate E-Cadherin cell adhesion complexes and integrins. Importantly, E-Cadherin dampens lamellipodial formation and restricts cell migration exclusively on Collagen IV coated surfaces (Borghi et al., 2010). In addition, traction force microscopy experiments show that E-Cadherin mediated segregation of focal adhesions leads to an asymmetric distribution of traction forces between Collagen IV coated and E-Cadherin FC coated substrates (Borghi et al., 2010). Similar conclusions derived from experiments in cardiac myocites (McCain et al., 2012). Culturing cardiac myocite doublets on fibronectin micropatterns leads to cell-cell contact formation. Upon cell-cell contact maturation, focal adhesions are progressively excluded from the site of cell-cell contact and traction forces become anisotropically distributed at the free edge of the cells (McCain et al., 2012). Comparable results were observed in fibroblast cell doublets stimulated with PDGF, where PDGF treatment polarizes protrusions and integrins away from the cell-cell contact (Ouyang et al., 2013). Importantly, N-Cadherin knockdown or expression of a dominant-negative p120 mutant leads to loss of integrin polarization opposite to the cell-cell contact and to integrin localization in proximity of the junction (Ouyang et al., 2013). In addition, cadherins have been shown to polarize focal adhesions away from the cell-cell

contact also during collective migration. Indeed, in primary cultured astrocytes N-Cadherin polarises focal adhesions opposite to the cell-cell contact upon wound-healing induced migration (Camand et al., 2012), however, high-grade gliomas which express lower levels of N-Cadherin display an increased migration response due to an increase in focal adhesion formation, an effect that can be mimicked by siRNA mediated knockdown of N-Cadherin in normal astrocytes (Camand et al., 2012). Another way through which cell-cell adhesion may locally negatively regulate focal adhesion formation in proximity of cell-cell contacts might be through sequestration and relocation of shared components, such as vinculin or zyxin, from the cell-matrix adhesion to cell-cell junctions. However, such mechanism remains purely speculative and it has not yet been directly investigated.

Intracellular and intercellular forces in cadherin-integrin crosstalk

Both cadherin and integrin cell-cell adhesion are able to actively trigger extensive actin cytoskeleton remodelling, including *de novo* actin nucleation, polymerization of branched actin networks and assembly of actomyosin contractile structures. These activities have to be integrated at the cellular level, as forces exerted on the cadherin and integrin network need to be balanced for a multicellular system to be mechanically stable (Tambe et al., 2011; Tseng et al., 2012; Vitorino et al., 2011). Recent reports have shown that as cells produce a new cell-cell contact, traction forces exerted on the ECM are translated into tugging forces across the newly formed cell-cell junction (Maruthamuthu et al., 2011). Using traction force microscopy, Maruthamuthu and colleagues show that in single MDCK cells, tractions are balanced, being directed from the cell

periphery towards the centre and corresponding to sites of focal adhesions. In cell doublets, focal adhesions are excluded from the cell-cell contact, and, again, tractions are balanced and directed from the periphery of the doublet towards the cell-cell junction (Maruthamuthu et al., 2011). Calculation of traction forces for single cells that are part of a doublet shows that in each cell the force is unbalanced and compensated by the force exerted at the cell-cell interface by its neighbour (Maruthamuthu et al., 2011). Such force is defined as tugging force. Because the cell doublets are in equilibrium, both cells exert equal and opposite forces on each other, which are proportional to the total ECM traction forces (Maruthamuthu et al., 2011). A closely related study exploited micropatterning strategies to explain how tugging forces might control spatial segregation of cell-cell junctions from integrin adhesions (Tseng et al., 2012). Different micropattern shapes were used to constrain the location of intercellular junctions and traction force microscopy was exploited to measure tugging forces at cell-cell contacts: when junctions were positioned in close proximity to focal adhesions such as in square-shaped micropatterns, tugging forces were high (Tseng et al., 2012). On other micropattern shapes, which minimised the proximity between cell-cell junctions and integrin adhesions, such as H configured patterns, tugging forces were minimal and junctional stability was maximised (Tseng et al., 2012). Importantly, these findings highlight how spatial segregation between cadherin and integrin adhesions might occur as a consequence of minimization of the magnitude of tensional forces in a tissue.

In addition, these reports also raise the possibility that stochastic or induced asymmetries between intercellular tugging forces and traction forces exerted on the ECM may lead to imbalances of forces, which may negatively affect junctional

stability and may therefore partially explain how focal adhesion assembly inhibits cell-cell adhesion. Interestingly, it has been reported that EMT-inducing growth factors such as HGF do not alter the strength of E-Cadherin cell-cell adhesions in epithelial cells (de Rooij et al., 2005; Hoj et al., 2014), but induce cell scattering by promoting formation of focal adhesions on ECM: alteration of the ability of cells to exert traction forces on the ECM by using compliant substrates impairs scattering (Hoj et al., 2014) while stiffer substrates promote EMT (de Rooij et al., 2005) by increasing the formation of focal adhesion and triggering disassembly of the cell-cell junction.

5. The Neural Crest

The neural crest is a highly migratory embryonic cell population, which arises at the border between neural plate and epidermis in all vertebrates, while it is absent in invertebrates. It constituted an important evolutionary novelty which accounts for the acquisition of the greater complexity of the vertebrate head (reviewed in (Munoz and Trainor, 2015)). Neural crest cells, specified at the neural plate border, are able to delaminate, undergo an epithelial to mesenchymal transition and migrate to distant target sites across the embryo to give rise to a variety of tissues including cartilage and bone, neurons, melanocytes, endocrine cells, smooth muscle and tendons (Kalcheim and Le Douarin, 1999). Neural crest migrates along the anteroposterior axis of the head and trunk and can be subdivided into different subpopulations, the cranial, cardiac, vagal, trunk and sacral neural crest. The first gives rise to craniofacial structures such as cranial nerve and ganglia, cartilage and bone, dermis, smooth muscle and connective tissue (Kalcheim and Le Douarin, 1999). Cardiac neural crest contribute to heart valves and arteries; trunk neural crest form the parasympathetic nervous system and vagal and and sacral populations differentiate into the enteric nervous system (Kalcheim and Le Douarin, 1999). Because of the wide variety of tissues to which they contribute, mutations that affect neural crest development can lead to congenital diseases defined as neurocristopathies (Etchevers et al., 2007), and research into the mechanisms of neural crest development may give an important contribution to the understanding of these pathological conditions and may indicate potential therapeutic strategies. In addition, because of its highly migratory and invasive

capabilities, and because it undergoes a physiologically regulated epithelial-to-mesenchymal transition, neural crest has occupied an increasingly relevant position as a model for understanding of malignant invasion and metastasis (Theveneau and Mayor, 2012b). In the context of this thesis, *Xenopus Laevis* cranial neural crest cells have been utilised as a model system to understand the transition from a cohesive epithelial behaviour to a migratory mesenchymal behaviour characterised by transient, unstable cell-cell interactions. In this chapter, I will therefore discuss neural crest epithelial-to-mesenchymal transition, its collective migration and the role of cell-cell interactions in determining its migratory capabilities.

Neural Crest Epithelial-to-Mesenchymal Transition

Neural crest cells are formed at late blastula stages at the boundary between neural ectoderm and non-neural ectoderm, in a region named neural plate border. Induction and specification of the neural crest is a complex process (Sauka-Spengler and Bronner-Fraser, 2008), which has been described as a two step model. This includes neural crest induction and neural crest maintenance (Steventon et al., 2009). Because early steps of neural crest formation are beyond the aims of the research described in this thesis, the interested reader may refer to these reviews (Sauka-Spengler and Bronner-Fraser, 2008; Steventon et al., 2009).

Once the neural crest precursors are induced, a gene regulatory network comprising numerous transcription factors maintains the population and further directs their development. SNAI family transcription factors Snail1 and Snail2 are expressed in the premigratory neural crest, and are necessary and sufficient

for neural crest development (del Barrio and Nieto, 2002; LaBonne and Bronner-Fraser, 2000; Mayor et al., 2000). Snail1 promotes the expression of Snail2/Slug (Aybar et al., 2003) and of other maintenance genes which are required for neural crest ontogenesis, such as FoxD3 (Aybar et al., 2003), Sox10 (Honore et al., 2003) and Twist (Aybar et al., 2003). These genes act as survival factors by inhibiting apoptosis (Tribulo et al., 2004; Vega et al., 2004). In addition, they reduce proliferation, as Snail1 arrests neural crest precursors at the G1/S transition of the cell cycle (Vega et al., 2004), altogether ensuring that an appropriate number of neural crest precursors is maintained before the beginning of migration. Importantly, key transcription factors involved in neural crest maintenance such as Snail1, Snail2, Sox10 and Twist also play a pivotal role in promoting neural crest delamination, epithelial to mesenchymal transition and progression to the migratory phenotype.

The terms delamination and epithelial-to-mesenchymal transition are often used as synonyms in the developmental biology literature. However, delamination is defined as the splitting of a tissue into separate populations, regardless of the mechanisms through which this outcome is achieved. On the other hand, epithelial-to-mesenchymal transition refers, as already discussed, to a specific process in which cells lose their epithelial polarity and convert into front-rear polarized cells, which form only transient adhesions and are able to migrate in a mesenchymal fashion (Hay, 1995).

Here, we refer to delamination as the process through which the neural crest separate from the neural plate. In all animal models, neural crest delamination differs along the anteroposterior axis. Cranial neural crest delaminates at once, as a cohesive group of cells. In both mouse (Nichols, 1981, 1987) and *Xenopus*

(Sadaghiani and Thiebaud, 1987), the cephalic neural crest delaminate at a time when the neural plate is still wide open, whereas in chick cranial neural crest delaminate from the dorsal ridge of the neural tube at the time of fusion of the neural folds (Duband and Thiery, 1982). In contrast, trunk neural crest do not delaminate as a cluster, but instead they emigrate from the neural tube progressively, leaving the neuroepithelium as single cells (Ahlstrom and Erickson, 2009b; Berndt et al., 2008; Clay and Halloran, 2014; Erickson and Weston, 1983). Furthermore, trunk neural crest delamination occurs after neural tube closure (Sela-Donenfeld and Kalcheim, 1999). These observations suggest that the molecular mechanisms underpinning delamination and EMT in cranial and trunk neural crest may be differentially regulated along the anteroposterior axis of vertebrate embryos.

The molecular principles underlying neural crest delamination have traditionally been investigated in chick trunk neural crest. Here, I will discuss these seminal findings. However, recent reports highlight important differences between cephalic and trunk neural crest across chick, mouse and *Xenopus*.

I have briefly discussed how a network of transcription factors is required for maintenance of neural crest population and for its further development. These include Snail2, FoxD3, Sox9 and Sox10. Importantly, they activate a cascade that promotes delamination and epithelial to mesenchymal transition of trunk neural crest cells by downregulating expression of the classical type I cadherin N-Cadherin and upregulating type II cadherins such as Cadherin6B, Cadherin7 and Cadherin11 (Chalpe et al., 2010; Cheung and Briscoe, 2003; Cheung et al., 2005; Dottori et al., 2001; McKeown et al., 2005). Differential cadherin expression is traditionally thought to promote delamination through definition of territories of

differential adhesion, as neural plate cells express higher levels of N-Cadherin than trunk neural crest, which in addition strongly express Cadherin6B (Akitaya and Bronner-Fraser, 1992; Duband et al., 1988; Nakagawa and Takeichi, 1995). Cadherin6B downregulation under the control of Snail2 (Coles et al., 2007; Taneyhill et al., 2007) and acquisition of Cadherin 7 and Cadherin 11 (Chalpe et al., 2010; Cheung and Briscoe, 2003) has been traditionally thought to push the cells out of the neural tube through a mechanism of differential adhesion. It is worth mentioning, however, that despite differential adhesion having long been though to play a role in cell sorting and in formation of tissue boundaries, very little experimental evidence supports such a view [reviewed in (Dahmann et al., 2011)]. Indeed, recent reports have pointed out how timed expression of specific cadherins such as Cadherin6B is required to appropriately polarise Rho GTPases and actomyosin contractility in a manner that favours emigration of neural crest cells from the neural tube (Clay and Halloran, 2014). In addition, besides regulation of cadherin switching, the transcription factor cocktail promotes migratory capabilities of neural crest cells by inducing expression of β_1 integrin (Cheung et al., 2005) and of the small GTPase RhoB (Cheung et al., 2005; McKeown et al., 2005). Importantly, upregulation of β_1 integrin may favour delamination through integrin-to-cadherin negative crosstalk (Monier-Gavelle and Duband, 1997). Indeed, treatment of cultured chick neural crest with RGD fibronectin-derived peptides or blocking antibodies against β_1 and β_3 integrin induced rapid cell clustering mediated by an increase in N-Cadherin junctional levels and inhibited single cells from migrating (Monier-Gavelle and Duband, 1997).

In line with the differences in timing and manner of delamination of cephalic and trunk neural crest, several recent reports suggest that the repertoire of cadherin expression and the modality of emigration from the neural plate might differ in cranial neural crest. Indeed, several reports suggest that, prior to delamination, at least a subset of cephalic neural crest may retain E-Cadherin expression (Barriga et al., 2013; Breau et al., 2008; Dady et al., 2012; Weston et al., 2004). Studies in mouse embryos (Breau et al., 2008; Weston et al., 2004) have shown that the E-Cadherin expressing cells at the neural plate border also display immunoreactivity for PDGFRα (Weston et al., 2004). At least a subset of these cells is positive for Cre in the neural crest specific transgenic mouse Wnt1-Cre^{+}. Thus, E-Cadherin expressing Wnt1-Cre^{+} cells are detected at premigratory stages in the neural folds in mouse embryos (Breau et al., 2008). E-Cadherin positive premigratory neural crest cells have also been observed in chick cranial sections, where E-Cadherin expression is detected throughout the whole neural crest population before and just after delamination from the neural ridges, and its lost upon migration (Dady et al., 2012). In addition, E-Cadherin expression has been shown to be detectable at the mRNA level by qPCR in premigratory *Xenopus* cranial neural crest cells (Barriga et al., 2013), while it is lost at migratory stages. Importantly, morpholino knockdown of the EMT transcription factor Twist induced E-Cadherin re-expression at the protein and mRNA level at migratory stages and inhibited neural crest dispersion and EMT *in vitro* (Barriga et al., 2013), thus suggesting that E-Cadherin expression might be physiologically downregulated during *Xenopus* neural crest delamination by the transcription factor Twist. Taken together, mouse, chick and *Xenopus* reports suggest that at least a subset of cranial neural crest express E-Cadherin before delamination,

and that E-Cadherin expression is lost at later developmental stages. Upon delamination, cranial neural crest cells have been reported to express the N-Cadherin in chick (Theveneau et al., 2007), *Xenopus* (Theveneau et al., 2010) and zebrafish (Piloto and Schilling, 2010). Importantly, *Xenopus* neural crest cells delaminate as a cohesive group, and maintain relatively stable N-cadherin dependent cell-cell junctions until the beginning of migration, when they loosen their cell-cell interactions and display a more mesenchymal tissue organization (Sadaghiani and Thiebaud, 1987; Theveneau et al., 2010). Similarly to Cadherin6B, N-Cadherin is required for polarized distribution of the small GTPase Rac1 at the leading edge of migrating neural crest cells (Theveneau et al., 2010).

Additional mechanisms through which neural crest may regulate their cadherin surface levels during their delamination from neural tube, and their transition to a mesenchymal state, is shedding of cadherins by ADAM metalloproteases. Indeed, ADAM10 metalloprotease is expressed in neural crest both in mouse (Reiss et al., 2005) and chick (Hall and Erickson, 2003), and it is required for cleavage of N-Cadherin downstream of BMP4 (Shoval et al., 2007). The cytoplasmic fragment of cleaved N-Cadherin (CTF2) translocates to the nucleus of neural crest cells, promoting cell cycle progression and, importantly, delamination from the neural tube (Shoval et al., 2007). Another ADAM family metalloprotease expressed in the neural crest is ADAM13 (Alfandari et al., 2001; Alfandari et al., 1997), which is required for Cadherin-11 cleavage during neural crest migration (McCusker et al., 2009) but not for delamination. Additional matrix metalloproteinases involved in neural crest delamination include MMP2

(Duong and Erickson, 2004), which is expressed in chick neural crest and whose inhibition blocks neural crest delamination.

How do neural crest cells exit the neural tube? Several recent reports exploited advances in live imaging techniques to observe delamination of chick and zebrafish neural crest cells from the neural tube in slice cultures or in intact embryos (Ahlstrom and Erickson, 2009a; Berndt et al., 2008; Clay and Halloran, 2013, 2014). Imaging of zebrafish trunk neural crest delamination has shown that delaminating cells are motile and extend a variety of actin-based protrusions including blebbling and filopodia (Berndt et al., 2008). Importantly, actomyosin based contractility is essential for delamination, as embryos treated with the myosin ATPase inhibitor Blebbistatin or with the ROCK inhibitor Y-27632 were unable to leave the neural tube (Berndt et al., 2008). Further studies have shown that delaminating zebrafish neural crest cells retract their apical process before delaminating by blebbing-like motility (Clay and Halloran, 2013, 2014). Importantly, RhoA is active at the apically retracting process and perturbation of RhoA/ROCK activity by treatment with C3 exotransferase inhibits delamination (Clay and Halloran, 2013). Furthermore, it has recently been shown that Cadherin6B is required for delamination in zebrafish by controlling RhoA polarization at the apical end of neural crest cells (Clay and Halloran, 2014). Indeed, knockdown of Cadherin6B lead to ectopic distribution of active RhoA along the entire apicobasal axis of neural crest cells, impairment of blebbing-mediated protrusive activity at the basal side of the cells and impaired delamination (Clay and Halloran, 2014).

Imaging of chick trunk neural crest during EMT shows that, consistently with observations in zebrafish, the majority of cells downregulate their adherens

junction-containing apical process before translocating their cell body and delaminating (Ahlstrom and Erickson, 2009a). However, in a minor but significant fraction of cases, the cells start protrusion formation and delamination without downregulating their junctions (Ahlstrom and Erickson, 2009a). As a consequence, the apical tail is ruptured during delamination from the neural tube, thus suggesting that adherens junctions might be broken down as a consequence of tractional forces exerted by the delaminating neural crest cells (Ahlstrom and Erickson, 2009a). Alternatively, chick neural crest have been oserved to have an "indecisive" behaviour in which retraction of the apical process is followed by formation of a new one, which is eventually ruptured as the cell translocates its body basally (Ahlstrom and Erickson, 2009a). Finally, neural crest delamination can also occur via non-apical cell divisions that bring one of the daughter cell bodies in close proximity to the basal side of the neural tube, thus facilitating delamination (Ahlstrom and Erickson, 2009a). Taken together, these findings show that, despite the majority of delamination events in vivo seem to be preceded by downregulation of the apical cell-cell junction, this is not an absolute requirement as neural crest cells display a range of dynamic behaviours that eventually have as a common outcome delamination and EMT.

Neural Crest Migration

Shortly after delamination, cranial and trunk neural crest migrate dorsoventrally to reach their target locations. Here, I will discuss cranial neural crest migration. Migration of cephalic neural crest cells is guided by several mechanisms, which need to be coordinated to achieve correct patterning and targeting. These

include restriction of migrating neural crest cells into discrete streams, co-attraction and collective chemotaxis and contact inhibition of locomotion.

Restriction of neural crest streams

In *Xenopus*, neural crest migrate collectively forming distinct streams, named as mandibular, branchial and hyoid streams following an anterior to posterior orientation. Splitting of the neural crest population into streams might be partially due to the presence of permissive spaces, such as the branchial arches, that the migrating cells are free to occupy. However, precise patterning of the streams appears rather to be due to complementary receptor-ligand expression between neural crest cells and adjacent tissues. Indeed, tissues surrounding the neural crest express non-permissive ligands that restrict migration by binding to their complementary receptors expressed on the surface of neural crest cells. At least three receptor-ligand systems are involved in the formation of neural crest streams: neuropilin/semaphorin, Eph/Ephrin and Robo/Slit. An additional mechanism involved in coordinated morphogenesis of neural crest streams and of the adjacent epibranchial placodes, defined as chase'n'run, requires contact inhibition of locomotion as well as collective chemotaxis and will be discussed in the next sections of this chapter.

Semaphorins of the class 3 –Sema3A, 3F and 3G- and their receptors, neuropilin1 and 2, are expressed in tissues surrounding the cranial neural crest and in neural crest cells, respectively (Eickholt et al., 1999; Gammill et al., 2007; Koestner et al., 2008; Yu and Moens, 2005). Loss of function of either the ligands or the receptors leads to abnormal neural crest migration and, most notably, to the appearance of bridges of ectopic neural crest migrating in between different

streams in mouse embryos (Gammill et al., 2007). Consistently, the zebrafish lbr/pbx4 mutant, in whom cranial neural crest streams are fused, displays an expansion of Sema3F/3G expression (Yu and Moens, 2005). Importantly, fusion of neural crest streams can be rescued by morpholino knockdown of neuropilin2 (Yu and Moens, 2005), thus highlighting the importance of the neuropilin/semaphorin axis for stream formation in cranial neural crest across evolutionary distant species. Semaphorins/neuropilins are expressed in a complementary manner also in *Xenopus* neural crest (Koestner et al., 2008). Although the high functional conservation between chick (Eickholt et al., 1999), mouse (Gammill et al., 2007) and zebrafish (Yu and Moens, 2005) suggests that they may play a similar role in restricting the streams, their function in *Xenopus* has not yet been elucidated. Inhibitory cues define corridors permissive for neural crest to migrate through, and are involved in correctly targeting the neural crest to their destinations: mutations in mouse sema3F or nrp2 also lead to incorrect organization and formation of trigeminal ganglia (Gammill et al., 2007). In addition, the semaphorin/neuropilin system is also required for restriction of trunk neural crest migration across the anterior part of the somite (Gammill et al., 2006).

Eph/Ephrin receptor ligand system has also been shown to control the formation of neural crest streams. Eph are tyrosine kinase receptors which interact with membrane bound ligands called Ephrins in a promiscuous manner; Eph/Ephrin interactions generate bidirectional signalling [reviewed in (Lisabeth et al., 2013)]. Numerous Eph receptor and Ephrin ligands exist in vertebrates, and the particular combinatorial subset of Eph/Ephrin expressed by cranial neural crest and surrounding tissues varies across animal models (Mellott and Burke, 2008;

Smith et al., 1997; Winning and Sargent, 1994). However, their functions seem to be conserved. Eph/Ephrins are required for cell sorting in rhombomeres (Xu et al., 1999) and to direct the adjacent neural crest cells into a specific stream along the anteroposterior axis by providing repulsive cues and restricting migration in permissive areas of the embryo (Smith et al., 1997). In *Xenopus*, EphA4 is expressed in neural crest cells and mesoderm of the third branchial arch, while EphB1 is expressed in neural crest and mesoderm of the third and fourth arch (Smith et al., 1997). The ligand EphrinB2, in turn, is located in the neural crest and mesoderm of the second arch (Smith et al., 1997). Expression of truncated dominant negative receptors leads to abnormal migration of neural crest cells from the third arch into the second and fourth arches territory (Smith et al., 1997). In addition, ectopic activation of the receptors by overexpression of EphrinB2 induces scattering of the third arch neural crest into neighbouring regions (Smith et al., 1997). A cell-autonomous role for Ephrins in directing migration of neural crest streams has also been confirmed in mouse embryos (Davy et al., 2004). Indeed, knockout of EphrinB1 either in the whole embryo or tissue-specifically in neural crest leads to defects in neural crest migration and ectopic neural crest scatter in normally nonpermissive areas (Davy et al., 2004). Similarly to semaphorin/neuropilin system, Eph/Ephrins are also required to restrict migration of trunk neural crest to the anterior half of the somites (Krull et al., 1997; Santiago and Erickson, 2002).

Finally, the Robo/Slit receptor-ligand system has also been involved in restricting early migration of trunk neural crest to the ventromedial migratory pathway (Giovannone et al., 2012; Jia et al., 2005), and it has been shown to be active during cardiac neural crest migration in mouse embryos, where Robo1 is

expressed in cardiac neural crest streams and Slit2 in surrounding tissues (Calmont et al., 2009). However, its expression and function has not yet been investigated in cranial neural crest migration.

Chemotaxis and Co-Attraction

Neural crest cell migration is positively regulated by chemotactic cues, which attract the cells towards their target. In addition, cranial neural crest migrate as a collective, and an autocrine chemotactic loop defined as co-attraction attracts single neural crest cells towards each other, thus helping to maintain collectiveness (Carmona-Fontaine et al., 2011; Woods et al., 2014).

Several factors are important for positive regulation of cephalic neural crest migration; however, their role as *bona fide* chemoattractants is still controversial, at least for most of them. Chick cranial neural crest is able to migrate towards a source of VEGF or of VEGF expressing tissue *in vitro* (McLennan and Kulesa, 2010). *In vivo,* the ectoderm of the second branchial arch endogenously produces VEGF, and blocking of neuropilin-VEGF signaling by injection of the soluble form of VEGFR1 reduces the migration of neural crest cells into the second branchial arch (McLennan and Kulesa, 2010). However, the function of VEGF as a chemoattractant is still debated as introduction of an ectopic VEGF source in the tissue *in vivo* only slightly redirects cells towards the source but does not produce ectopic migration (McLennan and Kulesa, 2010). Another molecule, which may potentially play a role as a chemoattractant in promoting neural crest migration, is PDGF. PDGFRα is expressed in neural crest cells in mouse (Schatteman et al., 1992) and *Xenopus* embryos (Ho et al., 1994), while its ligands PDGF-A and PDGF-C are expressed in surrounding tissues such

as branchial arches and oral and nasal cavities (Ding et al., 2000; Ho et al., 1994; Tallquist et al., 2000). Genetic knockout of PDGFRα in mouse embryos leads to cell autonomous defects in cranial and cardiac neural crest development, including craniofacial cartilage defects and defects in aortic arches (Tallquist and Soriano, 2003). However, neural crest cells are still able to colonise the face mesenchyme, thus suggesting a role for PDGFRα in differentiation of neural crest derivatives rather than during migration (Tallquist and Soriano, 2003). However, whether PDGF signaling also regulates migration of at least a subset of neural crest cells, or whether it regulates migration in model organisms other than mouse has not been yet elucidated.

A third factor, which recently emerged as a possible *bona fide* neural crest chemoattractant, is SDF-1. In mouse, SDF-1 is expressed along the pattern of trunk neural crest migration, and neural crest cells express its receptor CXCR4 (Belmadani et al., 2005). In vitro, trunk neural crest are attracted to an SDF-1 source and mice knockout for CXCR4 exhibit defects in trunk neural crest derived sensory neurons, the dorsal root ganglia (Belmadani et al., 2005). SDF-1 is also expressed in tissues surrounding the cranial neural crest, while CXCR4 is expressed in neural crest cells in zebrafish (Olesnicky Killian et al., 2009) and *Xenopus* embryos (Theveneau et al., 2010). Importantly, blocking SDF-1/CXCR4 signalling with morpholino oligonucleotides directed against either SDF-1 or CXCR4 inhibits neural crest migration (Olesnicky Killian et al., 2009; Theveneau et al., 2010) and leads to defects in cranial cartilages (Olesnicky Killian et al., 2009), while overexpression of CXCR4 (Olesnicky Killian et al., 2009) results in ectopic craniofacial structures (Olesnicky Killian et al., 2009). Strikingly, ectopic SDF-1 sources such as SDF-1 soaked beads induce ectopic migration of *Xenopus*

neural crest cells (Theveneau et al., 2010) as well as of neural crest derived melanocytes in Zebrafish embryos (Svetic et al., 2007). Interestingly, SDF-1/CXCR4 have been suggested to promote neural crest chemotaxis in a cell-cell contact dependent manner (Theveneau et al., 2010), as single neural crest cells are poorly efficient in migration towards an SDF-1 source *in vitro* while cell collectives, which display N-Cadherin dependent cell-cell junctions, are highly persistent in migrating towards an SDF-1 source. In this context, SDF-1 increases stability of protrusions of the neural crest cluster by enhancing N-Cadherin-dependent Rac1 activation at the leading edge of migrating cells (Theveneau et al., 2010).

Taken together, these reports suggest that SDF-1 may indeed act as a chemoattractant for neural crest cells and for some of its derivatives. However, the expression patterns of all the molecules proposed as neural crest chemoattractants (VEGF, PDGFs, SDF-1) appear to be uniform rather than forming a gradient along the tissues surrounding the neural crest, thus raising the possibility that they may act as positive chemokinetic cues rather than chemotactic ones. Although it is worth noting that the presence of a gradient of SDF-1 protein cannot be excluded as its pattern of expression has not so far been investigated at the protein level, a recent report suggest an alternative mechanism through which SDF-1 may promote actual chemotaxis in *Xenopus* neural crest cells (Theveneau et al., 2013). Indeed, SDF-1 is expressed in the epibranchial placodes, which lay adjacent to *Xenopus* cranial neural crest at premigratory stages, and is dynamically regulated during development (Theveneau et al., 2013). Neural crest cells are chemoattracted in vitro to placodal explants, which express SDF-1, but not to ventral ectoderm, which does

not produce SDF-1 (Theveneau et al., 2013). Importantly, upon beginning of migration, neural crest form protrusions which touch the adjacent placodal cells. Placodal cells *per se* are poorly motile, but when contacted by neural crest they engage in a repulsive response, collapsing their focal adhesions at the site of contact and moving away from neural crest cells (Theveneau et al., 2013). Such behaviour is defined as chase'n'run, and it is required for guiding collective co-migration of neural crest and placodes across the head of the embryo: neural crest are chemoattracted to placodes as they express SDF-1, but as soon as they reach them, placodes move away, thus forcing the neural crest further ventrally along the migratory path (Theveneau et al., 2013). This report provides an alternative mechanism for neural crest chemotaxis towards SDF-1 which may account for the lack of evidence for a detectable SDF-1 gradient in neural crest surroundings.

An additional mechanism that contributes to collective guidance of cranial neural crest, named co-attraction has recently been discovered (Carmona-Fontaine et al., 2011). Neural crest cells secrete the complement factor C3a and express its receptor C3aR. The C3a/C3aR system acts in an autocrine fashion to attract neural crest to each other at migratory stages, when they migrate as collective which forms transient contacts (Carmona-Fontaine et al., 2011). C3a signalling contributes to maintain cohesiveness of the group of neural crest cells, and is necessary for efficient chemotaxis towards SDF-1. Indeed, knockdown of C3aR in cells exposed to a SDF-1 gradient in vitro reduces the persistence of the cells towards the chemoattractant due to an increase in cell dispersion (Carmona-Fontaine et al., 2011). Finally, C3a can be considered as a chemotactic factor for neural crest, as an ectopic C3a-soaked bead induces ectopic neural crest

migration *in vivo* (Carmona-Fontaine et al., 2011). Importantly, the complement cascade had previously been described as part of the innate immune system and this work highlights a novel, previously uncharacterized, role for these molecules in embryo development and chemotaxis.

Contact Inhibition of Locomotion and Collective Migration

Restriction of migration in streams and chemotaxis provide mechanisms that promote migration of cranial neural crest streams along the appropriate pathways and enhance protrusion stability and persistent migration. However, they are not sufficient to drive directional collective migration. An additional phenomenon, defined as Contact Inhibition of Locomotion (CIL), is required to confer appropriate polarity to the migrating neural crest collectives.

As discussed in the second chapter of this introduction, CIL was first observed by Abercrombie and colleagues as early as 1953 (Abercrombie and Heaysman, 1953) in chick heart fibroblasts, and it is defined at the ability of a migrating cell to halt its movement and to change the direction of its motion after contact with another cell (Abercrombie and Heaysman, 1953). CIL is essential not only for neural crest migration, but also for other migratory phenomena occurring during embryo development, such as dispersion of *Drosophila* hemocytes (Davis et al., 2012; Stramer et al., 2010b) and of Cajal-Retzius neurons in the mammalian brain (Villar-Cervino et al., 2013) and it has been suggested to promote prostate cancer cell invasion into stroma (Astin et al., 2010b).

Concerning neural crest migration, contact inhibition of locomotion has been observed to occur both in zebrafish and *Xenopus* migrating neural crest cells (Carmona-Fontaine et al., 2008) *in vivo* and *in vitro*. When two isolated neural

crest cells interact *in vitro*, they form a transient cell-cell contact, but after some time they repolarize in opposite directions and move away from one another; this has been correlated with the observation that interacting neural crest cells collapse their protrusion at the cell-cell contact and produce a new one in the opposite direction (Figure 7.1a)(Carmona-Fontaine et al., 2008). At the tissue level, neural crest clusters cultured in close proximity do not invade each other, while they retain the ability to invade other surrounding tissues such as the mesoderm (Carmona-Fontaine et al., 2008). To date, it is not clear whether CIL is an intrinsic property of neural crest cells or whether it is a behaviour that these cells acquire during migratory stages. In neural crest cells, CIL has been shown to be dependent on establishment of Wnt/Planar Cell Polarity (PCP) signalling: upon cell-cell interactions, Wnt11, its receptor Frizzled7 and the downstream effector Dishevelled are recruited at the cell cell contact, where they induce the activation of the small GTPase RhoA (Carmona-Fontaine et al., 2008). Perturbation of Wnt/PCP signalling leads to impaired CIL response in vitro, and to loss of directionality of migration *in vivo* (Carmona-Fontaine et al., 2008). Importantly, Wnt/PCP dependent CIL is essential to confer appropriate contact dependent cell polarity to neural crest collectives. Indeed, *Xenopus* neural crest cell clusters display a strong contact-dependent polarity, in which small, cryptic protrusions are formed at the cell-cell contact, while large lamellipodial protrusions are oriented outwards, towards the free edge of the group (Carmona-Fontaine et al., 2008; Theveneau et al., 2010). Perturbation of Wnt/PCP signalling disrupts such polarity, leading to misoriented protrusions in the centre of the group (Carmona-Fontaine et al., 2008). As a consequence of this behaviour, cells exhibiting CIL do not crawl over their neighbours leading to

monolayer formation in groups and eventually, as cell density decreases as a consequence of monolayering, to scattering to single cells (Figure 7.1b)(Mayor and Carmona-Fontaine, 2010). Importantly, while RhoA is activated at the cell-cell contact through Wnt/PCP, Rac1 activity is polarized towards the leading edge of the cell, where it promotes lamellipodia formation (Theveneau et al., 2010). Polarization of Rac1 has been reported to depend on N-Cadherin. Importantly, N-Cadherin is also required in neural crest for CIL, and N-Cadherin dependent cell-cell interactions are essential for efficient chemotaxis towards SDF-1, thus highlighting how different molecular mechanisms are integrated at the cell collective level to achieve correct migration (Theveneau et al., 2010). Another protein involved in epithelial and mesenchymal front-rear polarity, Par3, has been recently shown to be required for neural crest CIL response in *xenopus* as well as in zebrafish embryos (Moore et al., 2013). Par 3 localises at cell-cell contacts upon neural crest collisions, and it is required to trigger microtubule catastrophe at the site of cell-cell contact (Moore et al., 2013). Morpholino knockdown of Par3 results in impaired migration in vivo due to impaired contact inhibition response as microtubules are not properly depolymerized at the cell-cell junction due to hyperactivation of Rac via the Rac GEF Trio (Moore et al., 2013). Thus, appropriate polarization of small GTPase is required for CIL to occur. This, in turn ensures that a variety of cytoskeletal events such as microtubule depolymerisation and lamellipodial protrusion collapse are correctly orchestrated in space and time.

In addition to regulating neural crest migration *per se,* CIL has recently been shown to be involved in coordinating the collective co-migration of neural crest and epibranchial placodes during the chase'n'run process. As already discussed,

neural crest cells are chemoattracted to placodes, which produce SDF-1. However, upon neural crest-placode cell-cell interaction, a CIL response is induced in the placodal cells via Wnt/PCP and N-Cadherin mediated signalling, which leads to placodal protrusion collapse, focal adhesion disassembly and displacement of the placodes away from the neural crest. Thus, CIL is important to coordinate complex collective migratory responses not only by polarizing cells inside a group (homotypic CIL), but also by triggering heterotypic repulsive responses, that, in coordination with additional mechanisms such as chemotaxis, orchestrate morphogenesis across different tissues.

In summary, we have discussed how a variety of mechanisms cooperate to achieve correct migration of cranial neural crest cells. Repulsive cues restrict neural crest streams to the appropriate territories; contact inhibition of locomotion polarises the group and promotes scattering and monolayering; co-attraction partially contrasts CIL by promoting cohesion within the group and by maintaining collectiveness enables neural crest cells to respond efficiently to chemotactic cues such SDF-1. The mechanisms orchestrating collective neural crest migration are summarised in Figure 8.1.

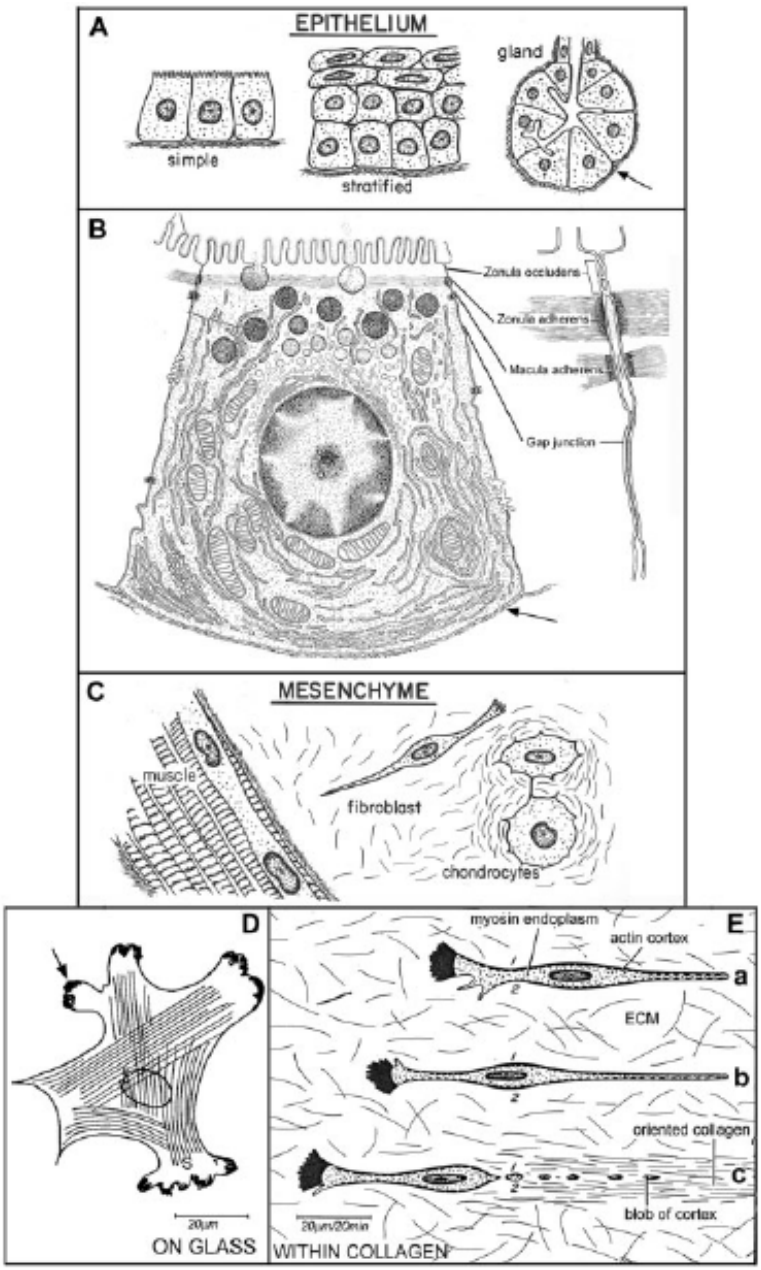

Figure1.1Epithelial and Mesenchymal Cells.

(A) Epithelia are cohesive tissues characterized by apicobasal polarity and confined by a basal lamina. They can be found as simple, stratified or glandular epithelia. **(B)** Polarized epithelial cell: apical adhesion complexes include Zonula Occludens (tight junctions), Zonula Adherens (Adherens junctions) and Macula Adherens (desmosomes). Basement membrane is indicated by an arrow. **(C)** Example of mesenchymal tissues include muscle, fibroblasts and chondrocytes. **(D,E)** Morphology of mesenchymal cells in 2-dimensional or 3-dimensional

culture. Mesenchymal cells display an elongated morphology and front-rear polarity, with an actin-rich leading edge (arrow) and a retracting pseudopod at the back.

Adapted from Hay, E.D., 2005.

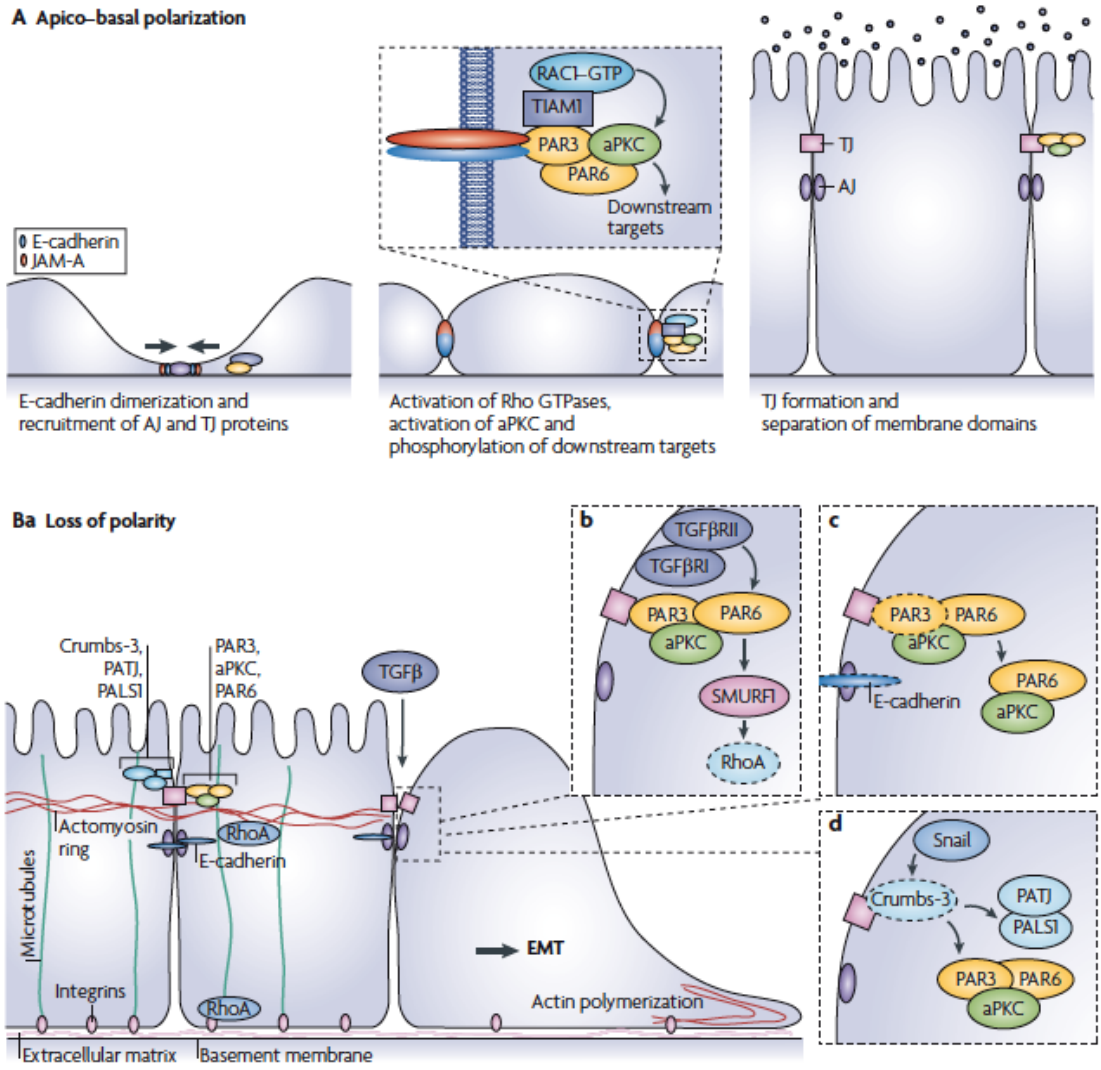

Figure 2.1 Establishment and Loss of Apicobasal Polarity

(A) Establishment of apicobasal polarity in epithelial cells requires initial E-Cadherin dimerization, recruitment of tight junction and adherens junction proteins, which leads to PAR3-dependent recruitment of Tiam-1 and aPKC to the nascent junction, which in turn can activate Rac1 and Cdc42. Maturation of junctions leads to discrete adherens junction and tight junctions domains in the lateral membrane. **(B)** Loss of apicobasal polarity during EMT occurs through several mechanisms (b) TGFβ mediates recruitment of the E3-ubiquitin ligase SMURF1 to PAR6, RhoA proteasomal degradation and loss of the apical actomyosin belt .(c) Direct repression of E-Cadherin and tight junction

components by EMT inducing TF leads to loss of PAR complex from the cell-cell contact. (d) Snail mediated repression of Crumbs3 leads to disassembly of apical polarity complexes.

Adapted from Iden, S. and Collard, J.G., 2008.

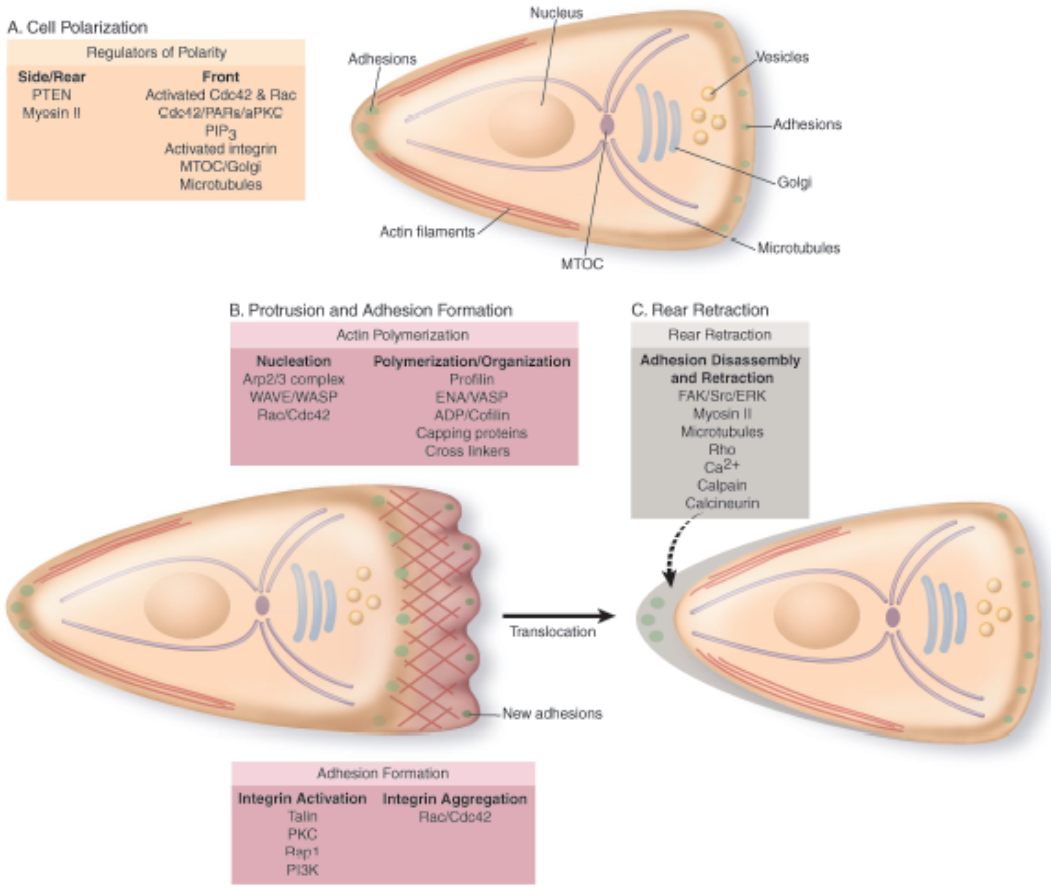

Figure 2.2 Front-Rear Polarity in Migratory Cells

(A) Front-rear polarization is mediated by polarity factors such as Cdc42/Par3/aPKC and PIP_3, while PIP_2 and MyosinII are polarized at the back of the cell. **(B)** Lamellipodial protrusion is mediated by Rho GTPases such as Rac and Cdc42, which in turn promote assembly of branched actin networks by activation of Arp2/3 complex via WAVE/WASP and by promoting polymerization of F-actin via Profilins, Ena/VASP and others. **(C)** Tail retraction is mediated by RhoA/Rock mediated contractility and microtubule dependent disassembly of focal adhesions.

Adapted from Ridley A.J *et al.*, 2003.

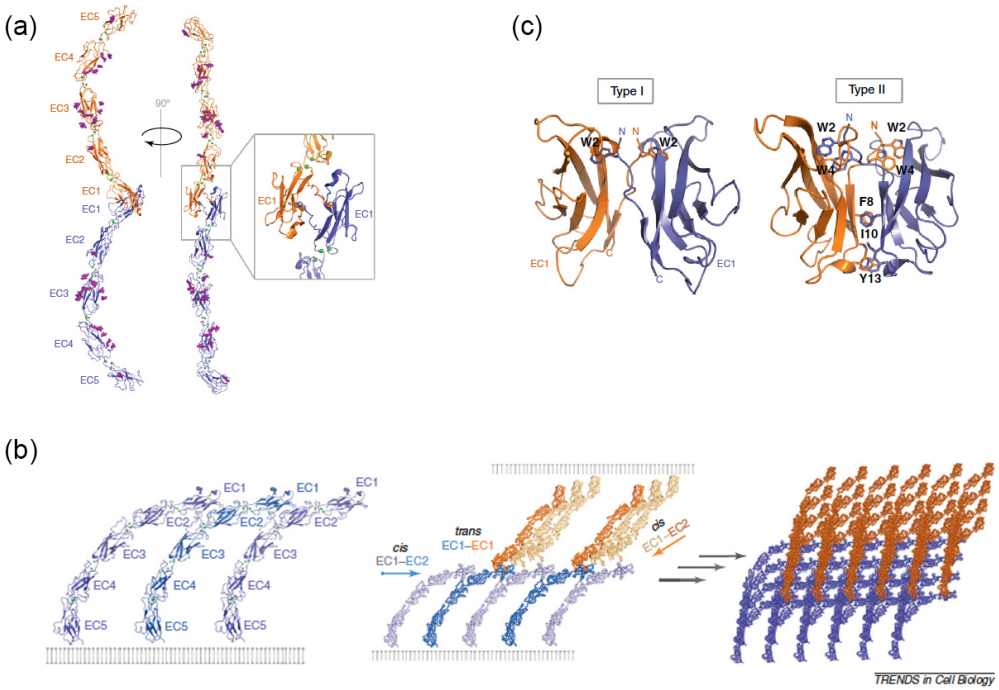

Figure 3.1 Mechanisms of trans and cis cadherin interactions

(A) Classical cadherins form trans homophilic bounds by exchanging the N-terminal β-strand of their EC1 domain. **(B)** Strand-swapped trans dimers form together with cis interactions in the same crystal lattice. trans interactions orient opposing cis arrays approximately perpendicularly such that each cis array (blue) forms trans interactions with multiple opposing cis arrays (orange). The combination of cis and trans interactions enables cadherin ectodomains to form an ordered network that is thought to be the basis for the extracellular architecture of adherens junction. **(C)** In type I cadherins, residue Trp2 in domain EC1 is swapped between binding partners. In type II cadherins, two Trp residues, Trp2 and Trp4, are exchanged, and, in addition, hydrophobic interactions occur between conserved residues Phe8, Ile10 and Tyr13.

Adapted from Brasch, J. *et al.*, 2012.

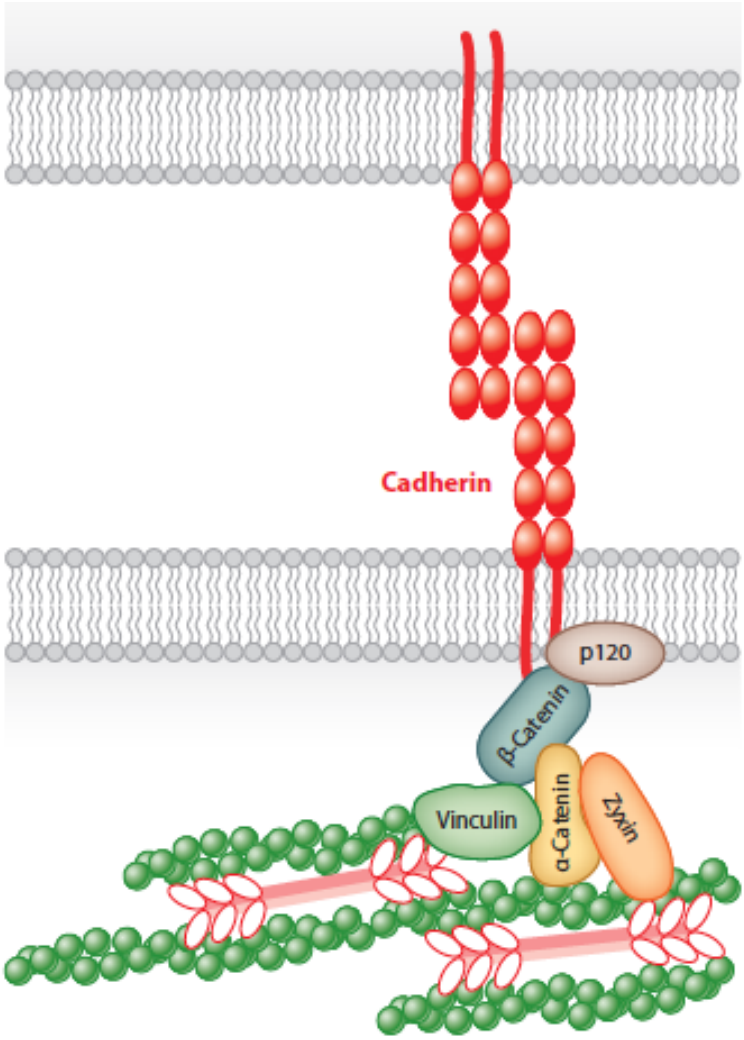

Figure 4.1 Overview of the classical cadherin-catenin complex.

Classical cadherins such as N- and E- Cadherin form homophilic trans and cis bounds through their EC1 domain. The cadherin cytoplasmic tail interacts with p120 catenin via the juxtamembrane region, and with β-catenin via the most C-terminal domain. β-catenin in turn links the cadherin cytoplasmic domain to F-actin via recruitment of α-catenin. Additional actin binding proteins such as Vinculin can interact with α-catenin or can directly bind to actin, as Zyxin,

Adapted from Leckband D. and De Rooij J., 2014.

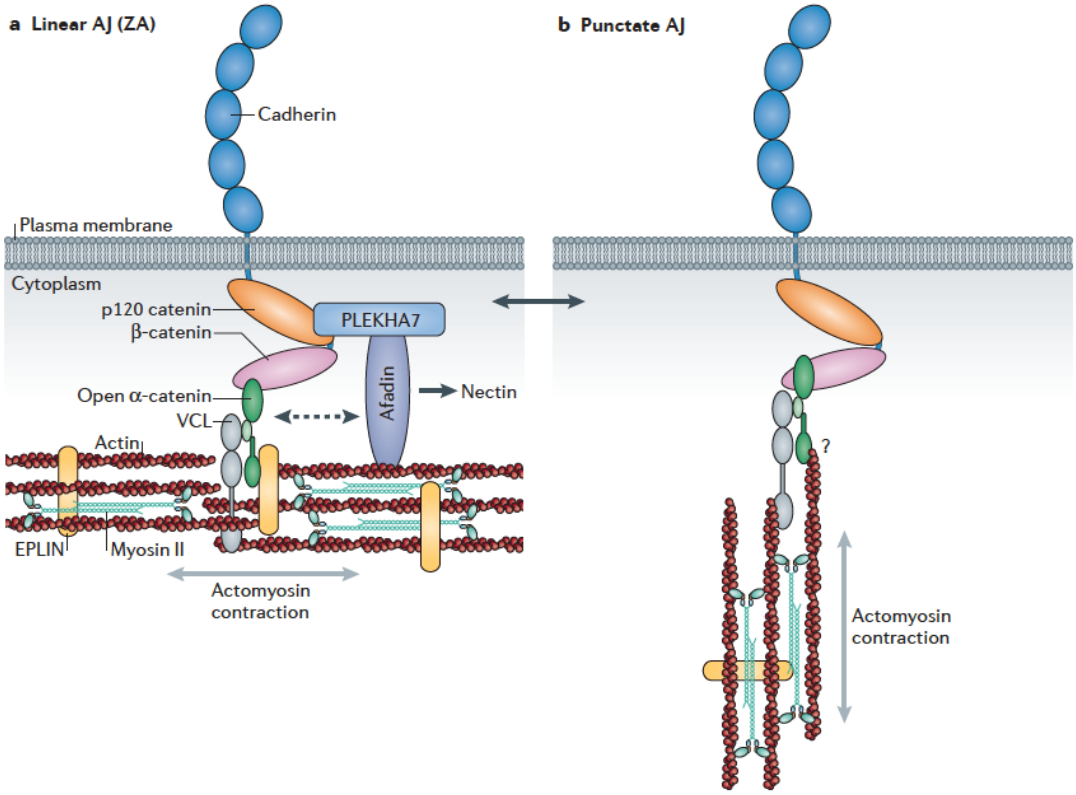

Figure 5.1 Actomyosin organization at linear and punctate adherens junctions.

(A) At linear adherens junctions, actin filaments run parallel to the plasma membrane. α-catenin, vinculin and additional actin binding proteins such as EPLIN help bundling the actin filaments. Myosin colocalises with the actin bundles at the zonula adherens and is required for clustering of cadherin complexes and junction maintenance. **(B)** At punctate adherens junctions, actomyosin filaments are attached to the cadherin complex via α-catenin, but not EPLIN, they are perpendicular to the plasma membrane and exert tugging stresses onto the cell-cell junction.

Adapted from Takeichi, M., 2014.

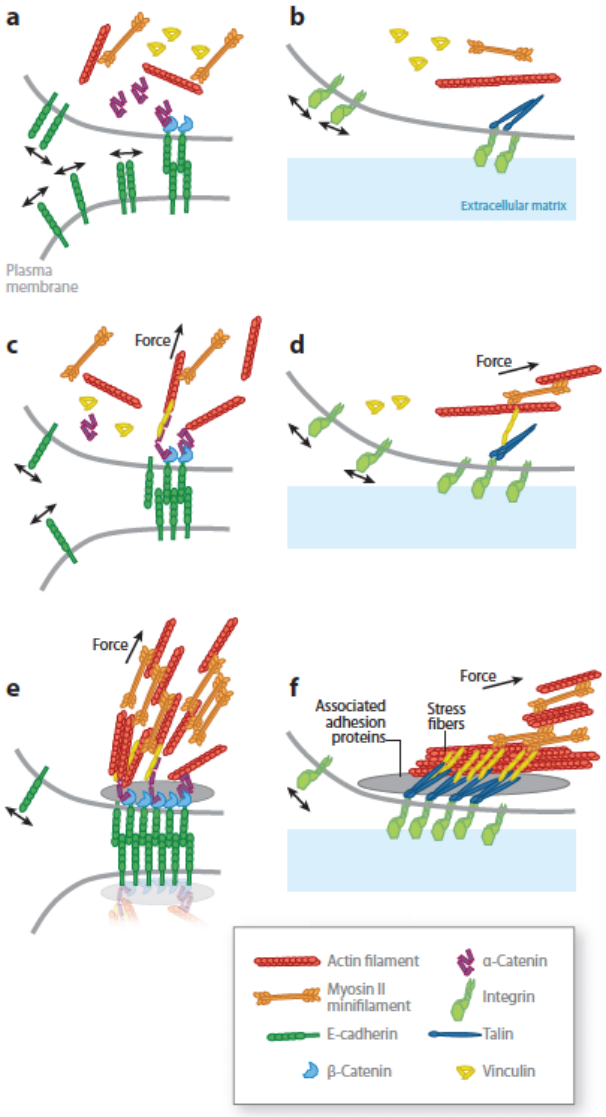

Figure 6.1 Force dependent reinforcement of cell-cell and cell-ECM adhesions.

(A,C,E) At cadherin cell-cell junction, tension dependent stretching of α-catenin molecules exposes binding sites for Vinculin (C), which promotes stabilization of junction associated actomyosin cytoskeleton and further cadherin clustering (E). **(B,D,F)** Similarly, binding of Vinculin to talin is enhanced upon tension-induced unmasking of Vinculin binding sites in talin (D), thus enhancing F-actin assembly and actomyosin contractility associated with focal adhesion, and increasing focal adhesion size by integrin clustering (F).

Adapted from Lecuit, T. *et al.*, 2011.

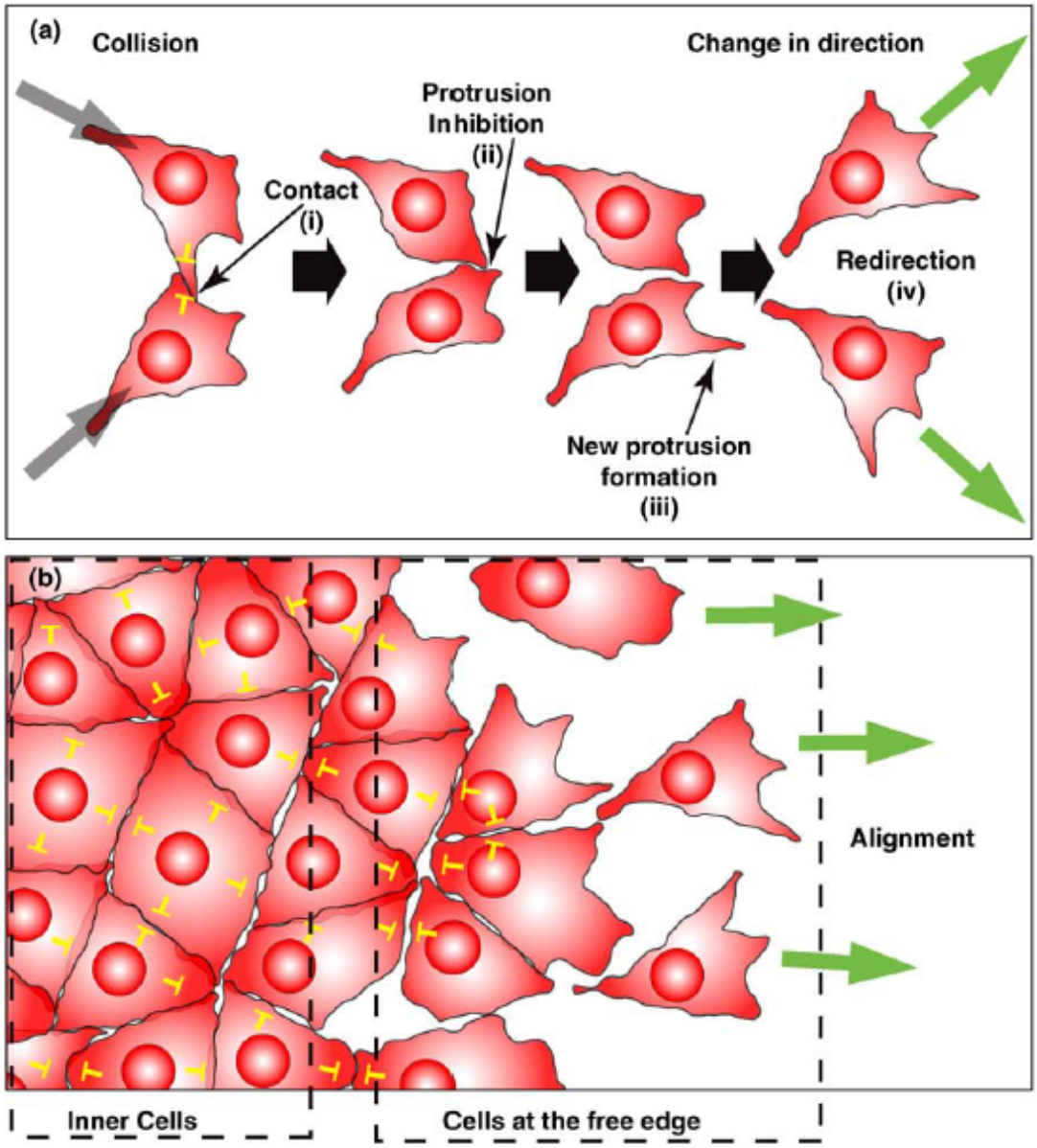

Figure 7.1 Contact Inhibition of Locomotion and Contact Dependent Polarity.

(A) At the single cell level, CIL causes two colliding cells (i) to collapse their protrusion at the site of cell-cell contact (ii), form new protrusions opposite to the contact (iii) and move away in opposite directions (iv).**(B)** In groups of cells, CIL causes the leader cells to orient their protrusion towards the free space, because protrusion formation is inhibited at the cell-cell contact. This results in orientation of the direction of movement of the group, monolayering and, eventually, cell dispersion.

Adapted from Mayor, R. and Carmona-Fontaine, C., 2010.

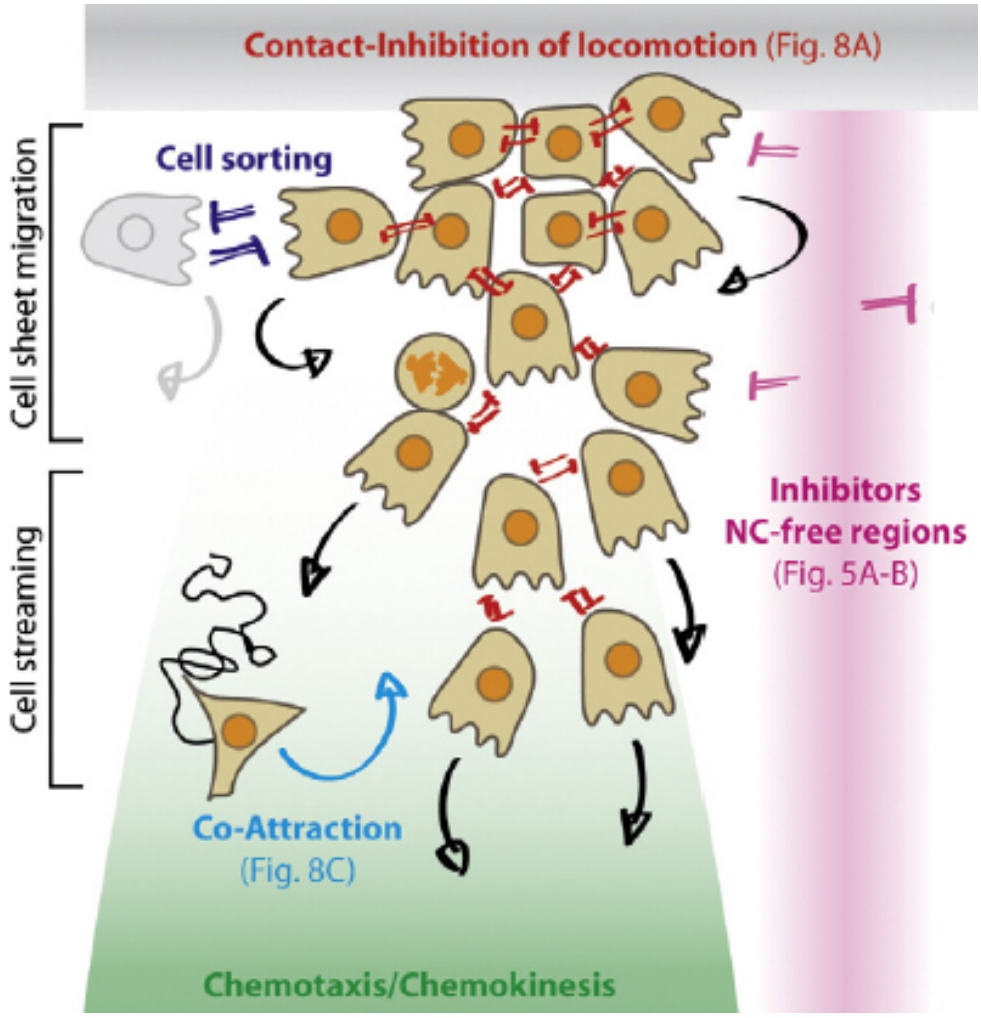

Figure8.1 Interplay of CIL, co-A, Chemotaxis and restrictive cues orchestrates neural crest migration.

CIL orientates protrusions towards the cell-free space and promotes monolayering and directionality. Co-Attraction prevents dispersion of single cells and promotes clustering, thus enhancing collectivity and cooperating with chemotactic cues in directing the migration of the stream towards the target. Inhibitory cues expressed by surrounding tissues ensure neural crest streams follow the correct migratory path.

Adapted from Theveneau, E. and Mayor, R., 2012.

6. Hypothesis

Contact inhibition of Locomotion occurs between migratory mesenchymal cells, it is essential for directional migration and patterning in development and it favours invasion of malignant cells into stromal tissues. Numerous reports have highlighted the importance of cell-cell interactions for CIL, and in particular, a classical cell adhesion complex, based on N-Cadherin, is assembled during CIL in migratory neural crest cells. However, these adherens junctions are relatively transient, and are disassembled after a short time. The molecular mechanisms underlying the breakdown of the cell-cell junction during CIL are currently unknown.

CIL is not a universal property shared by all cell types. Why certain cell types undergo CIL while other cells do not? Why some cell-cell interactions lead to the formation of a stable adherens junction while during CIL these junctions are transient?

Here, we used neural crest (NC) cells, a migratory embryonic stem cell population, to address these questions. Neural crest undergoes an epithelial to mesenchymal transition during their normal development, and CIL is required for collective directional migration of neural crest at migratory stages. I propose the following hypotheses:

a) *Neural crest cells acquire CIL as part of their developmental EMT program*
b) *Acquisition of CIL correlates which changes in cell-cell adhesion and motility during EMT, and such changes are required to promote acquisition of contact-dependent front-rear polarity in migratory neural crest cells*

c) *Contact dependent polarity and its effects on cell protrusive activity, rather than intrinsic properties of the cadherin junction, determine its breakdown during CIL*

II. Experimental Procedures

1. Embryology

Xenopus Laevis In Vitro Fertilization and Embryo Collection

Adult *Xenopus Laevis* were provided from Portsmouth Animal Facility, UK or Nasco, USA and maintained in standard conditions. To promote ovulation, females were injected with 100 units of Pregnant Serum Mare Gonadotropin (PMSG, Intervert) 3 to 6 days in advance. A second injection of 500 units of Chorion Gonadotropin (Chorulon, Intervert) was performed 16 hours before the planned fertilization. Induced females were kept in MMR solution (1M NaCl 20mM KCl 10mM MgSO4 20mM CaCl2 50mM HEPES) when laying eggs. MMR maintains the eggs susceptible of fertilization. For testes collection, adult males were anaesthetised in 0.5% Tricaine solution (Sigma, E10521) for 45 minutes. Testes were then dissected and transferred in Leibovitz L-15 medium (Invitrogen, 11415) supplemented with streptomycin (5 ug/ml, Sigma 85886), in which they could be maintained at 4°C for up to one week.

To obtain embryos, eggs were collected in a dish and most of the MMR solution removed. A piece of the testis tissue was cut, crushed in an eppendorf tube containing 500 ul of MMR and mixed with the eggs.

After 30 minutes, the dish was filled with NAM 1/10 solution (1% NAM A, 1% NAMB, 0.1% NAM C, 50 ug/ml Streptomycin). When the first cleavage division occurred, embryos were incubated for 5 minutes in 2% Cysteine (Sigma) to remove the jelly surrounding the eggs. Embryos were maintained in NAM 1/10.

Normal Amphibian Media for X.Laevis Embryo Maintenance

NAM A 1.1 M NaCl, 20mM KCl ,10mM Ca (No3)2, 10 mM MgSO4, 1mM EDTA

NAM B 20mM NaH2PO4, ph 7.5

NAM C 100 mM NaHCO3

Microinjection of X.Laevis embryos

Xenopus embryos were collected at the 2, 4 or 8-cell stage of cleavage division.

Embryos were microinjected using a Narishige IM300 microinjector under a Leica MZ6 or Nikon SMZ645 dissecting microscope.

To inject, borosilicate glass capillaries (Intracel, 01-001-06) with an internal diameter of 0.5 mm were pulled using a Narishige PC-10 needle puller on two step mode, both the first and second step were adjusted to 69.5% capacity. The needles obtained were calibrated using an eyepiece graticule to a volume of 5 or 10 nl per injection.

The needles were filled with the appropriate mRNA, DNA, morpholino oligonucleotide, or cell tracer.

To target the neural crest, embryos were injected at 8-cell stage on the dorsal and ventral animal blastomeres when mRNA, morpholinos or cell tracers were used. For DNA injections, embryos were injected 4 times at 2-4 cell stages and then 2 injections per cell on the dorsal and ventral animal blastomeres were performed at the 8-cell stage.

For microinjection, embryos were transferred in a dish containing 3% Ficoll (Polysucrose 400, Sigma) in NAM 3/8 and maintained in it until the onset of gastrulation, when they were transferred back to NAM 1/10. Embryos were maintained in a 14.5 °C incubator. Temperature was occasionally altered to 18 °C to increase the speed of development.

Neural Crest Tissue Dissection and Cell Culture

For pre-migratory and migratory neural crest dissection, embryos were collected at Stage 14-15 or 19 (according to Nieuwkoop and Faber) respectively. Embryos were transferred in a dish containing NAM 3/8 and the vitelline membranes were removed using forceps. Embryos were allowed to heal for 20 minutes, then transferred to a plasticine dish filled with NAM 3/8 and embedded in the plasticin using a fire-polished Pasteur pipette. The pigmented superficial layer of the ectoderm was removed using an eyebrow knife. The neural crest appears as a light grey clump of cohesive tissue at the neural plate border and can be removed using the eybrow knife. Using a micropipette, neural crest explants were transferred to a 30 mm plastic dish (Falcon) containing Danilchick's Solution (DFA: 53 mM NaCl 5mM Na2CO3 4.5mM Potassium Gluconate 32 mM Sodium Gluconate 1mM MgSO4 1mM CaCl2 0.1% BSA .Adjusted to pH 8.3 with 1M Bicine (Sigma). Supplemented with 50 μg/ml Streptomycin).

There, they were cut in smaller clusters with the eyebrow knife and eventually plated on fibronectin coated dishes.

When analysing migration of single neural crest cells, the explants were incubated for 5 minutes in Ca2+/Mg2+ free DFA (53 mM NaCl 5mM Na2CO3 4.5mM Potassium Gluconate 32 mM Sodium Gluconate 0.1% BSA, adjusted to pH 8.3 with 1M Bicine) to promote cell dissociation before plating.

Cells were allowed to spread on fibronectin for 30-45 minutes.

To prepare the fibronectin coating, dishes were incubated for 1 hour at 37 °C or overnight at 4 °C with a solution of 10 ug/ml Fibronectin(Sigma F1141)/PBS for

plastic dishes (50mm, sealable, Falcon) or on 100 ug/ml Fibronectin/PBS for glass bottom dishes (WillCo-Dish) . Dishes were then washed once with PBS and blocked for 30 minutes in PBS 0.1% BSA (Sigma) before the cells were plated.

For cell confinement experiments, micropatterned fibronectin coated coverslips were obtained from CYTOO and immobilised on a 50 mm plastic dish using silicone grease (Dow Corning). Explants were carefully dissociated to maximise the yield of single isolated neural crest cells and finally cells were plated on the micropatterns and allowed to spread for 1 hour before imaging.

2. Molecular Biology

Amplification of Plasmid DNA clones

DNA clones spotted onto filter paper were resuspended using 50 ul of nuclease free water (Ambion). Plasmid DNA was then amplified.

First, it was transformed using the DH5a strain of E.Coli competent cells. Briefly, DNA was added to the cells on ice and incubated for 30 minutes. Cells were heat-shocked for 5 minutes at 37 °C, incubated on ice again for 2 minutes and then cultured for an hour at 37 °C after addition 800 μl of LB (20 g/l LB Broth, Sigma). 100 μl of the culture were spread on a LB agar plate (37 g/l LB Agar, Sigma) supplemented with either 100 μg/ml Ampicillin or 50 μg/ml Kanamycin (Gibco) and incubated overnight at 37 °C.

Colonies were picked and amplified in 50 ml of LB supplemented with 50 μg/ml Ampicillin overnight at 37 °C.

Plasmid DNA was purified using a Plasmid Midiprep Kit (Qiagen). DNA was resuspended in 50-150 μl of nuclease-free water and quantified using a

Nanodrop Spectrophotometer ND-2000.

Molecular Cloning

Plasmids were obtained as described above.

For subcloning into pCS2+, plasmids were digested, when possible, with the appropriate restriction enzyme (Promega). Alternatively, DNA primers were custom synthesized from Life Technologies.

cDNA fragments were amplified by PCR using a GoTaq DNA polymerase kit (Promega). A table of the primers and of their amplification conditions is provided.

Fragments were isolated from the PCR reaction mix using a PCR Purification Kit (Qiagen), band size and integrity was verified by agarose gel electrophoresis and DNA concentration was determined using a Nanodrop Spectrophotometer ND-2000. They were then digested with the appropriate set of restriction enzymes.

Fragments were then isolated by agarose gel electrophoresis, the band was cut of from the gel using a sharp blade and DNA was purified from agarose using a QiaQuick Gel Extraction Kit (Qiagen). DNA concentration was determined using a Nanodrop Spectrophotometer ND-2000 before ligation reaction.

A ligation reaction was set up using a proportion of 1:3 plasmid to insert molecules, using 100 ng of insert. T4 DNA ligase was from NEB and reaction was performed overnight at 16 °C using a PCR machine (Eppendorf).

5 µl of the ligation reaction were then transformed into DH5a competent cells and plated on LB-Agar supplemented with Ampicillin or Kanamycin, as appropriate.

12-24 single clones were picked in sterile conditions with a fire polished Pasteur

pipette and cultured in a shaker overnight at 37 °C.

Plasmid DNA was purified using a Plasmid Mini Kit (Qiagen), and 5 µl of miniprep were digested with the appropriate restriction enzyme (Promega) to screen for positive clones.

Once a positive clone was found, it was sent to sequencing to the Source Biosciences sequencing facility in Cambridge, UK. Once verified, the clone was cultured overnight in 50 ml of LB and the plasmid DNA extracted with a Plasmid Midiprep Kit.

A list of the clonings performed, together with cloning strategy and primers used is included.

Construct	**Step**	**Template**	**Destination Plasmid**	**Forward Primer**	**Reverse Primer**	**Restriction Digest**
ECadherin-GFP	1	pCS2- XE-Cadherin-Myc	pCS2-XX-GFP	SP6	EcadRev	ClaI-XhoI
E/N	1	pCS2- XE-Cadherin-Myc		SP6	3ECadEC-NCadCyto	-
	2	pCS2-XNcad NIBB Clone 403		NcadCyto-ECadEc5	Ncad3-XhoI	-
	3	Product of Step 1 + Product of Step 2	pCS2+	SP6	Ncad3-XhoI	ClaI-XhoI
N/E	1	pCSf107-		Ncad5 EC	NCadEC -	

		XNCad FL		XhoI	ECadCyto3	
	2	pCS2- XE-Cadherin-Myc		ECadCyto-NCadEC 5	ECad3XbaI	
	3	Product of Step 1 + Product of Step 2	pCS2+	Ncad5 EC XhoI	ECad3XbaI	XhoI-XbaI
pCS2+-Rac FRET	1	pRaichuRac	pCS2+			BamHI-EcoRI
PCS2+ Cdc42 FRET	1	pRaichuCdc42	pCS2+			BamHI-EcoRI

Table 1. Clonings and their strategies.

Forward Primer	**Sequence**
NcadCyto-ECadEc5	5'-CTGTTGTTGCTCTTACTATTTATGAAGCGTCGTGACAAGGAG-3'
Ncad5 EC XhoI	5'-CAATAACTCGAGATGTGCGGGAAAGAGCCCTTC-3'
ECadCyto-NCadEC 5	5'-GTTTTGATGTTTGTTGTATGGGTACGAAGAAAGAAAGTGGTA-3'
Reverse Primer	**Sequence**
EcadRev	5'-TGCTTCCTCGAGATCCTCATCACCTCCATACAT-3'
3ECadEC-NCadCyto	5'-CTCCTTGTCACGACGCTTCATAAATAGTAAGAGCAAC

	AACAG-3'
Ncad3-XhoI	5-CAATAACTCGAGTCAGTCGTCGCTCCCTCCATA-3'
NCadEC -ECadCyto3	5'- TACCACTTTCTTTCTTCGTACCCATACAACAAACATCA AAAC-3'
ECad3XbaI	5'- CTACCGTCTAGATTAATCCTCATCACCTCCATACAT-3'

Table 2.Primers used and their sequences.

In vitro Transcription

To transcribe mRNA from plasmid DNA *in* vitro, DNA was linearized by using an appropriate restriction enzyme for digestion (Promega Restriction Enzymes). Linearization efficiency was verified by agarose gel electrophoresis. Digested DNA was separated from proteins in the enzyme mix using a Phenol:Chloroform:Isoamyil Alcohol (24:24:1, Sigma) solution. Briefly, equal volumes of restriction digestion mix and Phenol:Chloroform were mixed together, vortexed and centrifuged for 5 minutes at 4 °C at 13000 rpm.

The aqueous fraction containing the DNA was collected in a new tube. DNA was then precipitated with a double volume of 100% ethanol and 10 % v/v of a 3 M Sodium Acetate solution and incubated for 1 hour at -20 °C.

The DNA-Ethanol mix was then centrifuged for 30 minutes at 13000 rpm at 4 °C to retrieve DNA. DNA was washed once in 70% Ethanol, the mix was centrifuged for 10 minutes at 13000 rpm at 4 °C, ethanol solution discarded and DNA air-dried on the tube for 10 minutes at room temperature. DNA was finally resuspended in 10 µl of Nuclease-free water.

For the *in vitro* transcription reaction, either a SP6 or a T7 mMessage Machine Kit (Ambion) were utilised, according to the promoter sequence encoded in the plasmid of interest. Shortly, 1 µg of linearized DNA template was mixed with 2 µl of 10x Reaction Buffer, 10 µl of NTP/CAP solution, 1 µl of GTP , 2 µl of Enzyme Mix and nuclease-free water up to a final volume of 20 µl. The reaction was incubated for 2 hours at 37 °C, then 1 µl of Turbo DNAse was added to the mix to digest the DNA template and incubated for another hour at 37 °C.

An Rneasy Mini Kit (Qiagen) was used to purify the mRNA from the reaction mix. Finally, RNA concentration was measured using A Nanodrop Spectrophotometer ND-2000 and the quality of the *in vitro* transcribed mRNA assessed by agarose gel electrophoresis.

In situ Hybridization

In situ hybridization was performed as described by Harland (Harland, 1991). Briefly, embryos were fixed at the appropriate stage using MEMFA (10% Formaldehyde, MOPS) 0.1M ph 7.4, 1mM MgSO4, 2mM EGTA) either overnight at 4°C or one hour at room temperature. Embryos were then dehydrated in 100% methanol, let overnight at -20 °C and rehydrated by performing several washes with decreasing concentrations of methanol in PBS (Phosphate Buffer Saline: 137mM NaCl 2.7 mM KCl 4.3mM NaHPO4 1.4 mM H2PO4 pH7.3). Embryos were then washed twice in PBT (PBS 0.1% Tween-20, Sigma) and then bleached for 20 minutes in the dark in Bleaching Solution (20% H_2O_2, 5% Formamide, 2.5% SSC 20X). Bleached embryos were postfixed for 20 minutes in 3.7% Formaldehyde/PBS. After postfixation, embryos were quickly washed in

PBT and then washed twice in Hybridization Buffer (50% Formamide, 5X SSC, 1x Denhardt's Solution, 1mg/ml Ribonucleic Acid, 100 μg/ml Heparin, 0.1% CHAPS, 10 mM EDTA, 0.1% Tween-20). Embryos were then incubated for 30 minutes at 65 °C in Hybridization Buffer before adding the probe at 1μg/μl concentration. Hybridization of the digoxigenin-labelled probe was performed overnight at 65 °C. The next day, embryos were washed with Washing Solutions 1, 2, 3, 4 for 10 minutes at 65 °C each and Washing Solution 5 for 30 minutes at 65 °C (Solution1 :50% Formamide, 2X SSC, 0.1%Tween; Solution2 : 25% Formamide, 2X SSC, 0.1%Tween; Solution3 : 12.5 % Formamide, 2X SSC, 0.1%Tween; Solution4 : 2X SSC, 0.1% Tween; Solution5 : 0.2X SSC, 0.1% Tween). Embryos were then washed twice in PBT at room temperature and twice in TBS (NaCl 137mM, KCl 2.7 mM, Tris-HCl 19mM) before being blocked for two hours at room temperature in TBS 10% Fetal Calf Serum (FCS). Embryos were then incubated overnight at 4°C with an AP-conjugated anti-Digoxigenin antibody (Roche). Four 2 hours washes in TBS 10% FCS at room temperature were then performed before washing the embryos in AP buffer (0.1 M NaCl, 0.1 M Tris-HCl pH 9.5, 50 μM $MgCl_2$, 1% Tween-20) three times for 15 minutes at room temperature. AP staining was revealed using 4-nitro blue-tetrazolium-chloride (NBT, Roche) and 5-bromo-4choloro-3 indolyl- phosphate (BCIP, Roche) diluted 1:4000 in AP buffer at room temperature. The reaction was stopped washing quickly the embryos in PBT. Background staining was removed by washing the embryos in methanol for 30 minutes. Finally, embryos were postfixed in 3.7% formaldehyde in PBS.

3. Morpholinos

Xenopus E-Cadherin Morpholino (Nandadasa et al., 2009) (ECad MO 5'-AACCAGGGCCTCTTAACCCCATTG-3') was purchased from Gene Tools. For knockdown in the neural crest, the E-Cadherin MO was injected in a final amount of 10 ng/ blastomere at the 8-cell stage, dorsal and ventral animal blastomere. An equimolar concentration of a standard control morpholino (Control MO 5'-CCTCTTACCTCAGTTACAATTTA -3') was used.

Xenopus p120-Catenin Morpholino(Ciesiolka et al., 2004) (p120 MO 5'-ACTCTGGCTCATCCATATAGAAAGG 3′) was purchased from Gene Tools. For knockdown in the neural crest, the p120 MO was injected in a final amount of 10 ng/ blastomere at the 8-cell stage, dorsal and ventral animal blastomere. An equimolar concentration of a standard control morpholino (Control MO 5'-CCTCTTACCTCAGTTACAATTTA -3') was used.

4. Immunofluorescence

For immunofluoresce, Neural Crest Cells were dissected and cultured on 13 mm glass coverslips .Cells were allowed to migrate for 3 to 4 hours and then fixed in 3.7% formaldehyde (Sigma)/PBS for 30 minutes at room temperature or overnight at 4°C. Cells were washed three times with PBS.

According to the requirements of each different antibody, the cells were then permeabilised for 10 minutes at room temperature in PBS 0.1%-0.5% Triton –X-100 (Sigma) or incubated for 30 minutes in a blocking-permeabilising solution of PBS/0.3 M Glycine (Sigma)-10% FCS- 1% BSA- 0.1 %Tween (Sigma).

When treated with Triton-X-100, cells were then washed again three times in PBS and blocked with PBS 5%BSA. The primary antibody was then diluted at its

working concentration in blocking buffer and cells were incubated overnight at 4°C. The next morning, cells were washed three times in PBS for 5 minutes and then incubated with the appropriate fluorescently conjugate secondary antibody in blocking buffer for 30 minutes at room temperature. Cells were finally washed three times in PBS for 5 minutes each and coverslips were mounted on slides with Mowiol (Polyvinyl Alcohol 40-88/Fluka) mounting medium supplemented with DABCO (Sigma).

A table of the antibodies and their immunostaining conditions is provided.

Antibody	**α-Catenin**	**β-Catenin**	**E-Cadherin**	
Species	Rabbit	Rabbit	Mouse	
Mono/Polyclonal	Polyclonal	Polyclonal	Monoclonal	
Producer	Abcam	Sigma	Developmental Studies Hybridoma Bank	
Fixation	3.7% Formaldehyde/ PBS	3.7% Formaldehyde/ PBS	3.7% Formaldehyde/ PBS	
Permeabilisation	-	0.5% Triton-X-100/PBS	0.1% Triton-X-100/PBS	
Blocking	1% BSA- 10% FCS-0.3M Glycine-0.1% Tween-20/ PBS	3% FCS-5 % BSA/ PBS	3% FCS-5 % BSA/ PBS	
Working Dilution	1 in 50	1 in 200	1 in 200	
Incubation	Overnight 4 °C	Overnight 4 °C	1 hour RT/Overnight 4 °C	

Antibody	N-Cadherin	Myosin Phospho-Serin 19	Paxillin Phospho-Tyrosin 118	Vinculin
Species	Rat	Rabbit	Rabbit	Mouse
Mono/ Polyclonal	Monoclonal	Polyclonal	Polyclonal	Monoclonal
Producer	Developmental Studies Hybridoma Bank	Cell Signaling	Upstate	Sigma
Fixation	3.7% Formaldehyde/PBS	3.7% Formaldehyde/PBS	3.7% Formaldehyde/PBS	3.7% Formaldehyde/PBS
Permeabilisation	0.1% Triton-X-100/PBS	0.1% Triton-X-100/PBS	0.2% Triton-X-100/PBS	0.1% Triton-X-100/PBS
Blocking	3% FCS-5 % BSA/ PBS	3% FCS-5 % BSA/ PBS	2% FCS/PBS	3% FCS-5 % BSA/ PBS
Working Dilution	1 in 50	1 in 50	1 in 50	1 in 500
Incubation	30 minutes 37°C +Overnight 4 °C	Overnight 4 °C	30 minutes 37°C +Overnight 4 °C	Overnight 4 °C

Table 3. List of primary antibodies and of their immunostaining conditions.

Antibody	Species	Mono/Polyclonal	Producer	Working Dilution	Incubation
Anti Mouse Alexa 488	Goat	Polyclonal	Molecular Probes	1 in 500	30 minutes at RT
Anti Mouse Alexa 555	Goat	Polyclonal	Molecular Probes	1 in 500	30 minutes at RT
Anti Rat Alexa 488	Goat	Polyclonal	Life Technologies	1 in 500	30 minutes at RT
Anti Rabbit Alexa 488	Donkey	Polyclonal	Life Technologies	1 in 500	30 minutes at RT

Table 4.List of secondary antibodies and of their immunostaining conditions.

5. Biochemistry

Preparation of X.L. embryo lysates and immunoprecipitation

Vitelline membrane was removed from Stage 19 *Xenopus* embryos and they were collected in an eppendorf tube. They were then lysed in Lysis Buffer (100 mM NaCl, 50 mM Tris-HCl, 1% Triton-X-100) supplemented with the protease inhibitors antipain, leupeptin, pepstatin and PMSF (Sigma) at 10 μg/mL each using 5 μl per embryo. Briefly, embryos were incubated in Lysis Buffer for 10 minutes on ice, then vortexed for 30 seconds. The samples were then centrifuged for 10 minutes at 4 at 13000 rpm. The clear cytoplasmic fraction was recovered and transferred in a new tube. Protein concentration was then determined by using a BCA Protein Assay Kit (Novagen). Absorbance at 560 nm was determined using a spectrophotometre (Bio-Tek). For total lysate samples, 50 ug of total protein were diluted in NuPAGE LDS sample buffer (Invitrogen, NP0007) and denatured for 5 minutes at 95°C.

For immunoprecipitation, supernatants were diluted to a concentration of 6 mg/ml in a 250 μl volume. They were then incubated at 4°C for 3 hours 30 minutes with 10 μl of a 50% slurry of GFP-TRAP beads (Chromotek). Afterwards, beads were centrifuged for 2 minutes at 2000 rpm at 4°C and washed three times in Lysis Buffer. Bound material was eluted by adding NuPAGE LDS sample buffer and denaturing the samples for 5 minutes at 95°C.

Western Blot

Polyacrilamide gels at 8% concentration were prepared by mixing appropriate volumes of 1M Tris-HCl pH 8.8, 30% Acrilamyde-Bisacrylamide Mix (Sigma), 10% SDS, 10% Ammonium Persulfate (Sigma), 0.02% Temed (Sigma), filling a

mould and letting the mix to polymerise for 30 minutes. A stacking gel made by mixing appropriate volumes of 0.625M Tris-HCl pH 6.8, 30% Acrilamyde (Biorad), 10% SDS, 10% Ammonium Persulfate (Sigma) , 0.02% Temed (Sigma) was added on top of the running gel together with a comb to form wells to load the samples and allowed to polymerise for 15 minutes. To run the samples, the comb was removed, the mould with the gel placed in an electrophoretic chamber and the chamber filled with running buffer (250 mM Tris-HCl, 1,92 M Glycine, 0.1% SDS). Samples were loaded together with a standard protein ladder (Bio-Rad) to estimate protein molecular weight. Gel electrophoresis was then performed at 150 V for 45 minutes.

Afterwards, the gel was incubated in transfer buffer (250 mM Tris-HCl, 1,92 M Glycine, 20% Methanol (WWR Chemicals), 0.03% SDS) and proteins were transferred to a PVDF membrane (Amersham Hybond, RPNFL/02/10), which had previously activated by bathing for 2 minutes in methanol, by using a semi-dry blotting apparatus (Bio-Rad) at 15 V for 50 minutes. To assess for efficient protein transfer, the PVDF protein membrane was washed with Red Ponceau/Acetic Acid (Bio-rad) and then the Red Ponceau staining was washed away with filtered water.

The membrane was then blocked with 5% milk (Marvel) in TBST (NaCl 137mM, KCl 2.7 mM, Tris-HCl 19mM, 1% Tween-20) for two hours at room temperature and the appropriate antibody at its working dilution was incubated overnight at 4°C in blocking solution.

The next day, the membrane was washed three times for 10 minutes in TBST, and then the appropriate HRP-conjugated secondary antibody was incubated for 1 hour at room temperature at its working dilution.

Finally, membrane was washed again three times for 10 minutes in TBST, then signal was detected using a chemiluminescent-based reaction (Amersham ECL Prime Western Blotting Detection Reagent, GE) and pictures were captured using a Chemi-Doc gel detection device (Bio-Rad) and the Image Lab software (Bio-Rad). Band Intensity was quantified using the Volume Tools of the Image Lab software (Bio-Rad).

A table of the antibodies and their western blotting conditions is provided.

Antibody	**Species**	**Mono/Polyclonal**	**Producer**	**Working Dilution**	**Incubation**
α-Catenin	Rabbit	Polyclonal	Abcam	1 in 1000	Overnight 4 °C
β-Catenin	Rabbit	Polyclonal	Sigma	1 in 1500	2 hours RT/Overnight 4 °C
E-Cadherin	Mouse	Monoclonal	Developmental Studies Hybridoma Bank	1 in 2000	2 hours RT/Overnight 4 °C
N-Cadherin	Rat	Monoclonal	Developmental Studies Hybridoma Bank	1 in 800	30 minutes 37°C +Overnight 4 °C
GFP	Rabbit	Polyclonal	Molecular Probes	1 in 1000	Overnight 4 °C

Table 5. List of primary antibodies and of their Western Blotting conditions.

Antibody	**Species**	**Mono/Polyclo**	**Producer**	**Working**	**Incubation**

		nal		Dilution	
anti-Mouse HRP	Goat	Polyclonal	Santa Cruz	1 in 2000	2 hours RT
anti-Rabbit HRP	Donkey	Polyclonal	GE Healthcare Life Sciences	1 in 2000	2 hours RT

Table 6. List of secondary antibodies and of their Western Blotting conditions.

Polyacrylamide Hydrogels

Glass slides were pre-treated overnight with a 1:1:14 solution of Bind-Silane (GE Healthcare Life Sciences): Acetic Acid: Ethanol then washed once with 70% Ethanol and allowed to dry.

Shortly before hydrogel preparation, 13 mm diameter glass coverslips were incubated for 10 minutes in Repel-Silane (GE Healthcare Life Sciences) and allowed to dry on a paper towel.

For preparation of polyacrilamide hydrogels, 428 µl of a 7.6 mM HCl solution were mixed with 0.25 µl TEMED. On ice, 37.5 µl of 40% Acrylamide (Bio-Rad) and 20 µl 2% Bis-Acrylamide (Bio-Rad) were added to the mix. This combination of acrylamide-bisacrylamide allows to obtain a final gel stiffness of about 600 Pa (Theveneau et al., 2013).

To obtain crosslinking of the polyacrylamide with the fibronectin coating, 20 µl of a solution of 5 mg/ml NHS (Acrylic acid *N*-hydroxysuccinimide ester/Sigma-Aldrich) in DMSO was added to the mix. Finally, 2 µl of fluorescent microspheres (Invitrogen) and 2.5 µl of 10% Ammonium Persulfate were added to the mix.

A drop of 12 µl of gel mix was deposited on a dry slide previously treated with Bind-Silane and a Repel-Silane treated coverslip was placed on top of it.

The hydrogel was allowed to polymerize for 35 minutes. The coverslip was then carefully removed with a blade, the gel was covered in filtered water and UV-

treated for 10 minutes in a tissue culture hood. UV treatment is required for activation of the NHS crosslinker.

Water was removed from the hydrogel, which was then coated with 100 μg/ml Fibronectin (Sigma) for 2 hours at room temperature. The hydrogel was finally washed once with PBS, a plastic chamber was mounted on top of it using silicone grease and filled with Danilchick's Solution.

6. Imaging

Time-Lapse Imaging of *Xenopus* Neural Crest Cells

NC cells cultured on 50 mm sealable plastic dishes (Falcon) were imaged using a compound upright microscope. For cell dispersion and explant overlap experiments, around 30 minutes after plating the dish was inverted upside-down so that the NC cells would be placed directly under the microscope lens. Cells were imaged using a 10X lens.

Microphotographs were acquired every 5 minutes for 10 hours using either the Las AF or the SimplePCI6 software.

For single cell collision experiments, a 20X water immersion lens was utilised. Microphotographs were acquired either every 3 minutes or every 5 minutes for a period of 4 hours using either the Las AF or the SimplePCI6 software.

Images were exported as .avi files and analysed as appropriate using the Image J free software.

Confocal Imaging

For confocal imaging of living neural crest cells, either a Leica-TCS SP8 upright confocal microscope or a PerkinElmer UltraVIEW Vox Spinning Disk system

mounted on a Nikon *Ti* Eclipse microscope were used.

For imaging of fluorescent junctional proteins using the SP8 system, images were acquired every 3 minutes performing Z-stacks of a thickness of 1 μm using a Leica 40X Water Immersion Lens.

For high-time resolution imaging of neural crest cell-cell junctions and cytoskeleton, microphotographs were acquired using the Vox Spinning Disk system with a frequency of 10 to 20 seconds performing Z-stacks of a thickness of 1 μm using Nikon 60X or 100X oil immersion lenses. Images were exported as TIFF files and further analysed utilising the Image J free software.

For imaging of immunofluorescent stained neural crest samples, either an Olympus Fluoview 1000 or a Leica SPE1 confocal microscope were used.

Images were acquired using a 60x or a 63x oil immersion lens, respectively. Imaging conditions were adjusted according to the characteristics of the specimen.

Fluorescence Resonance Energy Transfer (FRET)

For expression of FRET probes in *Xenopus* embryos, Raichu-Rac (Itoh et al, 2002) was subcloned into pCS2+ as previously described in the Molecular Cloning section of this thesis and mRNA was synthesised. The mRNA encoding RhoA biosensor (Pertz et al., 2006) was synthesised exploiting the presence of a T7 promoter upstream of its coding sequence.

mRNAs were microinjected at a concentration of 50 pg/nl at a volume of 10 nl in two of the dorsal and ventral animal blastomeres in embryos at the 8-cell stage.

For Vinculin Tension Sensor FRET probe, plasmid DNA was microinjected at a concentration of 25 pg/nl performing 4 injections of a volume of 10 nl in 2-4 cell

stage embryos. The same amount was injected again in two of the dorsal and ventral animal blastomeres once the embryo reached the 8 cell stage.

Neural crest cells were dissected at stage 15 or at stage 19 as appropriate and plated on glass coverslips or on glass bottom dishes.

Ratiometric FRET Imaging and Analysis

Confocal imaging was carried out using a Nikon A1R confocal laser scanning microscope equipped with environmental chamber and Perfect Focus System (PFS). Images were using a 40× oil-immersion objective. CFP and YFP were excited with 440 diode and 514 nm Argon ion laser lines respectively and detected through 470–500 nm bandpass and 530 nm longpass filters, respectively. FRET was detected by excitation of CFP and collection of emission signal with a 530nm longpass filter. Images were acquired every 20 seconds using 512x512 pixel resolution and averaging. Movies were corrected for bleedthrough between channels prior to background subtraction. The data obtained were analysed using the ImageJ RiFRET plugin(Roszik et al., 2009). Heatmap ratios represent YFP/CFP signal and were normalized to run in a scale of 1.7-2.9. Further image analysis was performed on Image J.

Acceptor Photobleaching FRET Imaging and Analysis

For Acceptor Photobleaching Imaging, neural crest cells were cultured for 4 hours on glass coverslips, fixed overnight at 4 °C in 3.7% Formaldehyde/PBS and mounted in Mowiol on glass slides for observation.

Images were acquired using a Zeiss ISM 510 META confocal microscope and a 63x Plan Apochromat NA 1.4 Ph3 oil lens. CFP/TFP and YFP channels were excited with the 405 nm blue diode laser and 514 nm argon laser, respectively.

Emission was split using a 545 nm dichroic mirror, followed by a 475-525 bandpass filter for CFP/TFP and a 530 nm longpass filter for YFP. Pinholes were opened to reach a depth of focus of 3 mm for each channel. For each channel, gain was set to an approximate 75% of dynamic range and offset such as background was zero. For image collection, time –lapse mode was used: one pre-bleach image for each channel was acquired, followed by a 50 scans bleaching performed with the 514 nm laser line at 100% power to bleach YFP, finally a postbleach image was acquired for each channel. Afterwards, pre and post bleach images were imported into the Mathematica (Wolfram) software for processing: images were smoothed utilizing a 3x3 box mean filter, background was subtracted and the postbleach images were fade-compensated.

A FRET efficiency ratio map over the cell area was then calculated using the following equation:

$$FRET_{efficiency} = CFP_{postbleach} - CFP_{prebleach}/CFP_{postbleach}$$

Ratio values were extracted from pixels inside the bleach region and from another equally sized area outside of the bleach region. The mean ratio was determined for each area and plotted on a histogram. The non-bleach ratio was then subtracted from the bleach region ratio to give a final value for the FRET effciency. Data from images were used only when the efficiency of YFP bleaching was above 70%.

Fluorescence Recovery After Photobleaching (FRAP) Imaging

For Fluorescence Recovery After Photobleaching imaging, embryos were injected at the 8-cell stage, dorsal and ventral animal blastomeres, with mRNAs encoding for N-Cadherin-GFP or E-Cadherin-GFP . Alternatively, embryos were injected with p120-GFP or α-catenin-GFP with or without addition of E-Cadherin-Myc

mRNA. Neural crest cells were dissected at stage 19 and plated on glass bottom dishes.

For imaging, an UltraVIEW Vox Spinning Disk microscope system was used.

FRAP movies were acquired using the FRAP module of the Volocity imaging software. Briefly, GFP signal was excited with 5 % power of the 488 laser line and images were acquired in time lapse mode using a 200-350 ms exposure according to the mRNA probe injected. Five prebleach images were acquired.

For photobleaching, a region of interest lying onto a junction in the central region of a neural crest cell cluster was selected and bleached using 90% power of the 488 laser line for 10 cycles of 20 ms each. Postbleach images were then acquired with the appropriate time interval until GFP signal recovery plateau (0.5 second interval, 90 second plateau for N- and E-Cadherin-GFP; 1 second interval, 120 second plateau for p120 and α-catenin-GFP).

An average of 25 to 30 regions of interest per experiment per condition were acquired. Images were then exported as TIFF and further analysed.

Traction Force Microscopy

To perform traction force microscopy, NC cell clusters were plated on fibronectin-coated polyacrylamide hydrogels with a stiffness of 600 Pa. Cells were imaged on a Zeiss inverted epifluorescence microscope or on a Vox Spinning Disk system for 3 to 6 hours. The focus was set on the first layer of fluorescent beads in the polyacrylamide gel and three Z-Stacks with a 1μm thickness were acquired. This allowed to image the cells and the gel at the same time and allowed for selection of the gel best focus. After imaging, gels were treated with Proteinase K for 5 minutes to promote cell detaching from the

extracellular matrix and a picture of the gel in its relaxed state was acquired.

Photoactivation

For photoactivation experiments, embryos were co-injected at the 8-cell stage with either 800 pg of E-Cadherin-GFP and 1 ng of PA-Rac-Cherry mRNA (Wu et al., 2009) or 300 pg of membraneGFP and 1 ng of DN PA-Rac-Cherry mRNA (Wu et al., 2009). Neural Crest were then dissected, dissociated with Ca^{2+} free DFA and cultured on glass bottom dishes as single cells.

Photoactivation of PA-Rac and DN-PA-Rac has been previously described both in cell lines and in embryonic tissues *in vivo* (Wang et al., 2010; Wu et al., 2009; Yoo et al., 2010). Briefly, cells were imaged under a Zeiss 710 LSM confocal microscope. FRAP mode was used to image GFP/Cherry and transmitted light. Photoactivation was performed using either the 514 nm or the 458 nm laser line at 10%. A region of interest covering about one third of the cell cytoplasm was selected and illuminated for 45 seconds. Images were acquired every minute for 25 minutes.

7. Methods of Analysis

Explant Overlap Assay

For Explant Overlap Assays, neural crest clusters differentially labelled with fluorescein-dextran (FDX -Invitrogen D1821) or rhodamine dextran (RDX-Invitrogen D1824) were plated close to each other and imaged on a 10X magnification on a compound epifluorescence microscope for 10 hours. To analyse the extent of overlap between two differentially labelled neural crest explants, .avi movies were imported into ImageJ. Red and green channels were

split and each of them tresholded to obtain a binary image. Thresholded images were then merged. The frame showing the maximum overlap (represented by the area of overlay between the two channels) was identified and the overlap area was normalised as the ratio between the area of overlap between the two explants and the area of the smallest of the two.

Collision Assay

For analysis of single cell collisions, neural crest cells derived from embryos injected with membrane-targeted GFP and nuclear-localised mCherry were dissociated by a brief treatment in low Ca2+ medium, plated and imaged on a 20X magnification on a compound epifluorescence microscope for 4 hours.

.avi movies were then imported into ImageJ. The beginning of a cell-cell interaction event was identified as the first frame in which a cell-cell contact could be observed (t0).

For analysis of the angle of collision, the angle tool of the ImageJ software was used. The first vertex of the angle was defined by the position of the nucleus of the chosen cell at t_0 , the second as the position of the same nucleus two frames (10 minutes) later and the third as the position of the nucleus at the moment of junction disassembly (t_{end}). The angle of collision was only measured when the overall duration of the collision from t_0 to t_{end} did not exceed 30 minutes.

Collisions which exceeded 30 minutes were considered as adhesion events. To compare quantitatively adhesion and contact inhibition of locomotion events, the duration of cell-cell interaction from t_0 to t_{end} was measured regardless of duration of cell-cell interaction.

In addition, the distance between the nuclei of the two interacting cells after 30

minutes of cell-cell contact was measured. If two cells assemble a stable junction, the distance between their nuclei results relatively steady over time, and lends itself as a useful parameter to distinguish between and adhesive and a contact-inhibition-like behaviour (Scarpa et al., 2013).

Quantitation of Cell Dispersion

To investigate the ability of NC cells to undergo EMT, cell dispersion assays were performed. Neural crest cells clusters derived from embryos injected with membrane-targeted GFP and nuclear-localised mCherry were plated and imaged on a 10X magnification on a compound epifluorescence microscope for 10 hours.

To analyse cell dispersion, the Delaunay triangulation algorithm was utilised (Carmona-Fontaine et al., 2011).

This algorithm allows to connect every cell to its closest neighbour and to build a network of triangles which covers the entire explant. Furthermore, it retrieves the area of each triangle, making therefore possible to compare different explants independent of their initial size. Delaunay triangulation is available as an ImageJ plugin. Briefly, .avi movies were imported into ImageJ, channels were split and the nCherry channel was used for triangulation.

The initial timepoint and a late timepoint of the movie were used for triangulation to compare the extent of cell dispersion over time. In most of the experiments the latest timepoint corresponded to 8 hours from the beginning of the movie.

Images were background subtracted using a rolling ball of 5 or 10 pixels depending on signal intensity. Afterwards, images were tresholded and single frames saved as JPEG. The Delaunay Batch plugin on ImageJ was used.

To colour-code triangles, the best representative example was chosen for each condition. Triangulation was run using the Delaunay Triangulation Plugin; afterwards, the Colour-Code 16bit Individual Plugin of the Delaunay Triangulation package in ImageJ was deployed.

Cell Tracking

To analyse migratory features of NC cells such as velocity, distance of migration and directionality, neural crest cells clusters or dissociated NC cells derived from embryos injected with membrane-targeted GFP and nuclear-localised mCherry were plated and imaged on a 10X magnification on a compound epifluorescence microscope for 4-10 hours.

.avi movies were imported into ImageJ for further quantitation. To measure velocity, directionality and distance of migration, the Manual Tracking plugin and the Chemotaxis Tool of ImageJ were used in combination. First, single cells in a cluster (10 cells per cluster, 5-10 clusters per experimental condition) or single dissociated cells (30-40 cells per experimental condition) were manually tracked following the nuclear Cherry signal using the Manual Tracking plugin for the whole duration of the movie or up until the cell left the field of view. The cell coordinates obtained were saved and imported into the ImageJ Chemotaxis tool, which, knowing the XY calibration of the images acquired, allows to calculate parameters such as cell velocity, euclidean and linear distance of migraton and directionality of migration.

Analysis of Lifeact distribution in Living NC Cells

To investigate actin cytoskeleton organization in living NC cells, NC cell clusters derived from embryos microinjected with Lifeact-GFP or Lifeact-Cherry

biosensors were plated on fibronectin coated glass bottom dishes and imaged at high time resolution (10 seconds) on a Vox Spinning Disk machine.

Movies were imported into ImageJ. To analyse actin distribution at cell-cell contacts and leading edges of cells, first, a maximum projection of the Z-stacks was performed. The average grey levels of the lifeact signal in a square of 40x40 pixels at cell-cell junctions, at leading edge and in the nucleus (for normalisation) were measured for at least 5 cells per movie, 5 movies per condition (n=25 cells). Normalised grey levels were obtained by dividing the junctional or leading edge grey level values by the average grey level value in the nucleus for each cell.

Analysis of Protrusion Polarity in Living NC Cells

For analysis of protrusion polarity in NC cell clusters, cells explants derived from embryos injected with membrane-targeted GFP and nuclear-localised mCherry were plated on fibronectin coated glass bottom dishes and imaged at high time resolution (10 seconds) on a Vox Spinning Disk machine.

Movies were imported into ImageJ. To analyse cell protrusions at the free edge of the explants a maximum projection of the Z-stacks was performed. The channels were split and the mGFP channel used for further analysis. Images were thresholded and converted to binary images. A copy of the thresholded movie was generated, in which the first frame was deleted and an additional empty frame was added at the end of the movie. The Image Calculator function of ImageJ was used to subtract the second movie from the first, in order to retrieve a third movie which contains the information about the displacement of the cell membranes from one frame to the other. The total protrusion area was measured for each timepoint using the Analyse Particle function of ImageJ and was then

normalised to the number of cells in each movie, which could be counted by means of the nuclear-localised mCherry.

To analyse cell protrusions at the cell-cell contacts, only the basal-most stack, closest to the extracellular matrix, of the movies was used, because most protrusions events at contact sites happen basally. Images were tresholded at higher values so that only the overlapping membranes at cell-cell contact sites would result in the binary image. To calculate protrusion rate, the same procedure applied for leading edge protrusions was used, and total area of protrusion per timepoint was again normalised to the number of nuclei in each movie.

Analysis of Junctional Protein Recruitment in Living NC Cells

To quantify junctional assembly during NC collisions, NC cells derived from embryos microinjected with p120-GFP, α-catenin-GFP or N-Cadherin-Cherry were dissociated in Ca2+ free medium, plated on fibronectin coated glass bottom dishes or on fibronectin-650 coated micropatterns (CYTOO) and imaged at high or medium time resolution (20 seconds or 3 minutes) on a Vox Spinning Disk machine or on a Leica SP8 confocal machine, respectively.

Movies were imported into ImageJ and a maximum projection of the Z-Stacks was carried out. Junctional recruitment was measured by measuring the average grey levels in 3 squares of 20x20 pixels each across the cell-cell contact for each timepoint. Signal intensity was normalised to the intensity measured in the cell nucleus, which for junctional proteins is close to background, for each timepoint.

Analysis of Actomyosin spatiotemporal distribution in Living NC Cells

To observe actomyosin dynamics during NC collisions, NC cells derived from

embryos microinjected with MRLC2-GFP and lifeact-Cherry were dissociated in Ca2+ free medium, plated on fibronectin coated glass bottom dishes or on fibronectin-650 coated micropatterns (CYTOO) and imaged at high or medium time resolution (20 seconds or 3 minutes) on a Vox Spinning Disk machine or on a Leica SP8 confocal machine, respectively.

The polarity of myosin distribution over NC-NC collisions was quantified. Movies were first imported into ImageJ and Z-Stacks were maximally projected. A straight segment spanning from the cell trailing edge to the cell leading edge was traced for each timepoint, and the profile of myosin intensity along the traced segment was retrieved using the Plot Profile function of Image J. Signal intensity was normalised to the intensity profile of a randomly oriented segment for each time point and the normalised intensity distribution was then normalised to each segment length.

Analysis of Endogenous Protein Recruitment at the Cell-Cell Junction

To determine the distribution of the endogenous cadherin complex proteins, NC cells clusters were plated on fibronectin-coated glass coverslips and allowed to spread for 3 to 5 hours before fixation and immunostaining with the appropriate antibodies.

For quantitation, confocal stacks were acquired and then analysed on Image J.

First, a maximum or an average projection of the Z-Stacks was carried out. A straight segment of 5 μm in length was traced across each cell-cell junction and its intensity profile retrieved using the e Plot Profile function of Image J. Signal intensity was then normalised to the intensity profile of a segment spanning the cell cytoplasmic region.

Analysis of ratiometric FRET imaging

The polarity of active Rac1 signal at the cell free edge during NC-NC collisions was calculated using ImageJ. Briefly, 16-bit movies of the YFP/CFP signal were imported into ImageJ. Signal intensity at the cell free edge during collisions was quantified by measuring the average grey levels of 3 20x20 pixel squares in the cell lamellipodia per each timepoint. Data were normalised to signal intensity in the cell cytoplasm, in which the signal of the membrane-targeted Raichu-Rac probe is close to background.

FRAP Analysis

For FRAP normalization, the FRAP Analysis ImageJ plugin was used. Briefly, each region of interest was normalised to background, to whole-cell fluorescence and corrected for bleaching.

FRAP data were then normalised as :

F(t)= Fr (t)-Fr(0)/Fr(-)-Fr(0)

where Fr (t) is the measured intensity at time *t* , Fr(0)is the intensity measured at photobleaching *(t=0)*, Fr(-) is the average intensity of the 5 timepoints preceeding photobleaching.

FRAP data were fitted using a single exponential equation

Fs (t)= A (1-e-ln(2)xt/τ)

The mobile fraction and half recovery time were determined directly from the fitted parameters of the single exponentials. Confidence intervals of 95% were calculated from the asymptotic standard errors of the fits.

Analysis of the Spatial Distribution of Traction Forces in Living NC Cells

To derive traction forces from fluorescent bead displacement, a Particle Intensity

Velocimetry (PIV) analysis was performed.

First, the single frames were imported as Tiff images into ImageJ. Pictures were median-filtered with a radius equal to 1 to remove the pixel errors of the camera. Then, the best focus was selected from the z-Stacks. The best focus was defined as the one that has the biggest standard deviation in the grayscale values. The same was done to the reference frame obtained after the cells were removed with Proteinase K, which represents the relaxed state of the gel. Images were then converted to 8-bit and background was subtracted with a rolling ball of a radius of 3 pixels.

The xy shift between the relaxed state frame and each time frame was registered using a StackReg with Rigid Body transformation procedure.

Finally, a 3-step PIV was calculated using the following parameters:

*piv*1=128 *sw*1=256 *vs*1=64

*piv*2=64 *sw*2=128 *vs*2=32

*piv*3=48 *sw*3=128 *vs*3=24

in which *piv* stands for PIV grid, *sw* stands for search window size and the *vs* represents vector spacing.

The PIV was then post-filtered with a median-filter, using a threshold of 2 and noise of 0.1: if the vector was an outlier from the neighbourhood, it was replaced by the median of the neighbourhood. To decide whether a vector is an outlier, the median deviation of the vectors from the neighbourhood median was analysed. If the deviation of the vector resulted to be bigger than [threshold * (median deviation in neighbourhood + noise)], then it was regarded as an outlier.

The PIV calculated from bead displacement was then used to calculate traction

forces by using an algorithm for finite thickness gels (Lin et al., 2010) with the following parameters: thickness of the gel 100 μm; Young's Modulus 600 Pa; Poisson's ratio 0.5.

Free edge and cell-contact measurement were then performed using a custom-built ImageJ plugin. Briefly, a series of selections were made around each explant perimeter or in its centre, in which tractions were averaged and normalized to the overall traction in the total explant area. NC cells were injected with membrane Cherry and the fluorescence signal was used as a reference to locate the cells.

Analysis of Photoactivatable Rac-induced Protrusion Formation

To assess for the efficiency of the PA-Rac probe, the protrusion area of the illuminated cells was measured before and after illumination using Image J.

Statistical analysis

Comparison of percentages was performed using contingency tables(Carmona-Fontaine et al., 2008; Taillard et al., 2008). Two data sets were considered significantly different (null hypothesis rejected) if $T>3.841$ ($\alpha = 0.05$,*), $T>6.635$ ($\alpha = 0.01$,**) or $T>10.83$ ($\alpha = 0.001$,***). Normality of data sets was tested using Kolmogorov–Smirnov's test, d'Agostino and Pearson's test using Prism6 (GraphPad). A data set was considered normal if found as normal by the two tests. Data sets following a normal distribution were compared with Student's *t*-test (two-tailed, unequal variances) in Excel or a one-way analysis of variance (ANOVA) with a Dunnett's multiple comparisons post-test in Prism6 (GraphPad). Data sets that did not follow a normal distribution were compared using Mann–Whitney's test or a non-parametric ANOVA (Kruskal–Wallis with Dunn's multiple

comparisons post-test) using Prism6 (GraphPad). Cross-comparisons were performed only if the overall *P* value of the ANOVA was <0.05.

III. Results

1. Neural crest cells acquire Contact Inhibition of Locomotion during Epithelial to Mesenchymal transition

CIL is a developmentally regulated property of Neural Crest Cells acquired during EMT

Neural Crest acquire CIL during EMT

Xenopus Neural Crest Cells (NC) are an archetypal model for CIL, whose CIL response is well characterised and it is essential for their directional migration *in vivo* and *in vitro* (Carmona-Fontaine et al., 2008; Moore et al., 2013; Theveneau et al., 2010). However, CIL behaviour of neural crest cells has exclusively been studied during neural crest migration, and it is currently unknown whether CIL is an intrinsic property of neural crest cells or whether it is acquired, together with other features associated with enhanced migratory capabilities -such as integrin upregulation, ability to remodel the extracellular matrix and changes in cell-cell adhesion- upon neural crest delamination from the neural plate border and EMT.

To investigate whether CIL is an intrinsic property of NC or whether it is acquired during NC development, I cultured *Xenopus laevis* pre-migratory NC (Premig-NC) before they undergo Epithelial to Mesenchymal Transition (EMT), at developmental stage 15 (Nieuwkoop and Faber) and compared them with Migratory NC (Mig-NC) dissected at stage 19 (Nieuwkoop and Faber), after EMT has taken place. To analyse CIL during individual cell-cell collisions, neural crest were dissociated in Ca^{2+} free medium and cultured as single cells. Nearly 80% of observed cell-cell collisions of Mig-NC showed typical CIL. These cells formed a

transient contact, arrested their migration and eventually moved away, while only 40% of Premig-NC collisions exhibited CIL (Fig. 9.1 A-B, Supplemental Movie S1) with most Premig-NC forming a stable contact and their nuclei remaining within a short cell-cell distance (Fig. 9.1C). At the cell population level, CIL is known to prevent cell mixing. Indeed, Mig-NC explants exhibiting CIL do not overlap when cultured in close proximity to each other (Carmona-Fontaine et al., 2008). While our observations in Mig-NC explants confirm this result (Fig.9.1D), the Premig-NC explants overlapped extensively, and individual cells from one group intermingled with the other (Fig 9.1E, arrows, Supplemental Movie S2). Taken together, cell-cell collision experiments and explant overlap assays strongly suggest that CIL is a property acquired by neural crest cells as they progress in development. At migratory stages, NC explants are known to undergo spontaneous EMT *in vitro* (Kuriyama et al., 2014) and disperse due to CIL (Carmona-Fontaine et al., 2011; Woods et al., 2014). We investigated whether the ability of NC cells to undergo CIL correlated with their capability to disperse *in vitro.* Interestingly, dispersion was observed in Mig-NC explants but not in Premig-NC (Fig. 9.2A, Supplemental Movie S3) as shown by Delaunay triangulation analysis, which quantifies cell dispersion by retrieving a parameter, the triangle area between triplets of cell neighbours, proportional to the distance between adjacent cells (Carmona-Fontaine et al., 2011) (Fig. 9.2B, C). Importantly, this result suggests that acquisition of CIL correlates with epithelial to mesenchymal transition in neural crest cells. In summary, here I show that neural crest gain CIL behaviour during their development, and that acquisition of CIL strikingly correlates in time with neural crest EMT.

Contact dependent polarity is differentially regulated before and after EMT

During CIL, cell protrusions are oriented by polarized activation of the small GTPases RhoA and Rac1, which leads to the formation of lamellipodia away from the cell contact in migrating NC clusters and confers an outward directed polarity to the group (Carmona-Fontaine et al., 2008; Theveneau et al., 2010). I sought to determine whether orientation of protrusion and Rac1 activity correlated with loss of epithelial features and acquisition of CIL in developing neural crest cells. I analysed the dynamics of newly formed membrane protrusions (Fig. 9.3A, B; Supplemental Movie S4) and F-actin distribution (Fig 9.3 C, D, Supplemental Movie S5). In Mig-NC explants most newly formed protrusions pointed away from the cell contact and towards the free space while in Premig-NC most lamellipodia were formed beneath the cell-cell contacts (Fig. 9.3A, B; Supplemental Movie S4). Consistently, in Mig-NC most F-actin was found at lamellipodia, while in Premig-NC F-actin was mainly detected at protrusions forming underneath cell-cell contacts in the centre of cell clusters (Fig 9.3 C, D, Supplemental Movie S5). Because contact-dependent cell polarity has been shown to rely on polarized distribution of the small GTPase Rac1 (Theveneau et al., 2010), we investigated whether Rac1 activity was differentially regulated in Premig-NC and Mig-NC by expressing a Rac FRET probe (Itoh et al., 2002) in neural crest cells and performing FRET acceptor photobleaching. In line with previous observations (Theveneau et al., 2010), Rac1 activity in Mig-NC was high at the free edge (Fig. 9.4A, top, arrows, Fig. 9.4B) and low at cell-cell contacts (Fig. 9.4A, top, arrowheads, Fig. 9.4B) as detected by FRET (Itoh et al., 2002; Theveneau et al., 2010). Importantly, the distribution of Rac1 activity in Premig-NC was reversed, being low at the free edge (Fig. 9.4A, bottom, arrows, Fig. 9.4B)

and high at cell-cell contacts (Fig. 9.4A bottom, arrowheads, Fig. 9.4B). In addition, because RhoA activity has been suggested to be required for CIL (Carmona-Fontaine et al., 2008), we investigated whether RhoA activity changed during neural crest development by using a RhoA specific FRET biosensor (Pertz et al., 2006). In contrast with the observations of Rac1 activity, active RhoA was mainly detected at cell-cell contacts, and its distribution was not significantly affected during neural crest EMT (Fig. 9.4C, D). Taken together, the observations shown in Figure 9.3 and Figure 9.4 strongly suggest that Rac1 activity, but not that of RhoA, and contact-dependent protrusion polarity change during neural crest epithelial to mesenchymal transition, and that such change may correlate with acquisition of contact inhibition of locomotion behaviour by migratory neural crest cells. Previous work from our laboratory has suggested an antagonistic relationship between RhoA and Rac (Matthews et al., 2008), while my results suggest both RhoA and Rac1 to be active in proximity of the cell-cell junction in premigratory neural crest . However, high resolution cross-correlation analysis of RhoA and Rac activity measured by FRET in migrating fibroblasts has suggested that the two GTPases are active in different micrometric-scale domains of the migrating cell lamella (Machacek et al., 2009). Due to technical limitation, I have not been able to measure RhoA and Rac1 activity in the same cell, however, it remains possible that RhoA and Rac1 might be active in different subdomains in proximity of the premigratory neural crest cell-cell adhesion.

Analysis of cell junctions during CIL

I have shown how neural crest acquire contact inhibition of locomotion at the same time they undergo a developmentally regulated epithelial to mesenchymal transition. Acquisition of CIL and of mesenchymal migratory features might be related to changes in cell-cell adhesion properties of neural crest cells, as discussed in the Introduction of this thesis. In particular, I reasoned that changes in cell-cell adhesion dynamics, in the composition of the cell adhesion complex or in the cadherin isoform expressed by the cell may affect contact inhibition of locomotion behaviour. I therefore investigated these aspects. First, I sought to determine whether the distinct behaviour of Mig-NC and Premig-NC in response to cell-cell interactions might arise from differential dynamics of junction formation. To test this, I expressed p120-GFP or α-Catenin-GFP in Mig-NC or Premig-NC and imaged cell collisions with high time resolution. During collisions, both Mig-NC and Premig-NC formed junctions containing p120 (Fig. 9.5A-C, Supplemental Movie S6) and α-catenin (Fig. 9.5D-F, Supplemental Movie S7) with similar dynamics. I observed that the timing of junction assembly was undistinguishable between Premig-NC and Mig-NC: as soon as the colliding cells lamellipodia overlapped, p120-GFP (Fig. 9.5B) and α-catenin (Fig. 9.5E) were recruited to the cell-cell contact site within seconds. In addition, the normalised levels of fluorescence intensity at the cell-cell junction were similar between Premig-NC and Mig-NC (Fig.9.5B, E), thus further supporting the idea that these cells are able to assemble a cadherin junction with similar efficiency. However, in Mig-NC cell-cell contacts were disassembled, normally within 15 minutes or less (Fig. 9.5 C, F), while they persisted in Premig-NC, suggesting that Mig-NC are unable to stabilise their junctions. Based on these observations, I postulated that

the composition of endogenous adherens junctions might be different in Mig-NC and Premig-NC, thus resulting in differential stability of these contacts. Indeed, I observed that α-catenin and β-catenin levels of immunostaining were higher in Premig-NC adhesions than in Mig-NC junctions (Fig. 9.6A-C), which may partially explain the higher stability of premigratory neural crest adherens junctions. Secondly, I analysed the expression of classical cadherins in Mig-NC and Premig-NC, since cadherin switching has been observed during EMT in cancer cells and during cranial NC development in other organisms (Dady et al., 2012; Wheelock et al., 2008), and since my data demonstrate that the acquisition of CIL correlates with EMT. I found that Mig-NC predominantly expressed N-cadherin, consistent with previous observations (Theveneau et al., 2010), whilst Premig-NC expressed E-cadherin (Fig. 9.7A-C). The differential cadherin expression suggests that cadherin switching might be linked to the acquisition of CIL.

In summary, I observed that dynamics of junction formation do not differ between premigratory and migratory neural crest cells, but that migratory neural crest cell-cell junctions are unstable despite their ability to accumulate comparable levels of p120-GFP or α-Catenin-GFP. Endogenous levels of α-Catenin and β-Catenin are lower at the Mig-NC cell-cell junction, further supporting the hypothesis that these junctions might be more dynamic and less stable. Investigation of endogenous cadherin expression pattern reveals that an E- to N- cadherin switch occurs during *Xenopus* neural crest EMT, with loss of E-Cadherin and acquisition of N-Cadherin occurring concomitantly with acquisition of CIL. Given the well-established role for N-Cadherin in controlling CIL response in migratory neural crest (Theveneau et al., 2010; Theveneau et al., 2013) and given that Twist-induced repression of E-Cadherin is required for

neural crest EMT (Barriga et al., 2013), here we hypothesise that E-Cadherin might act as a repressor of CIL behaviour before the onset of EMT.

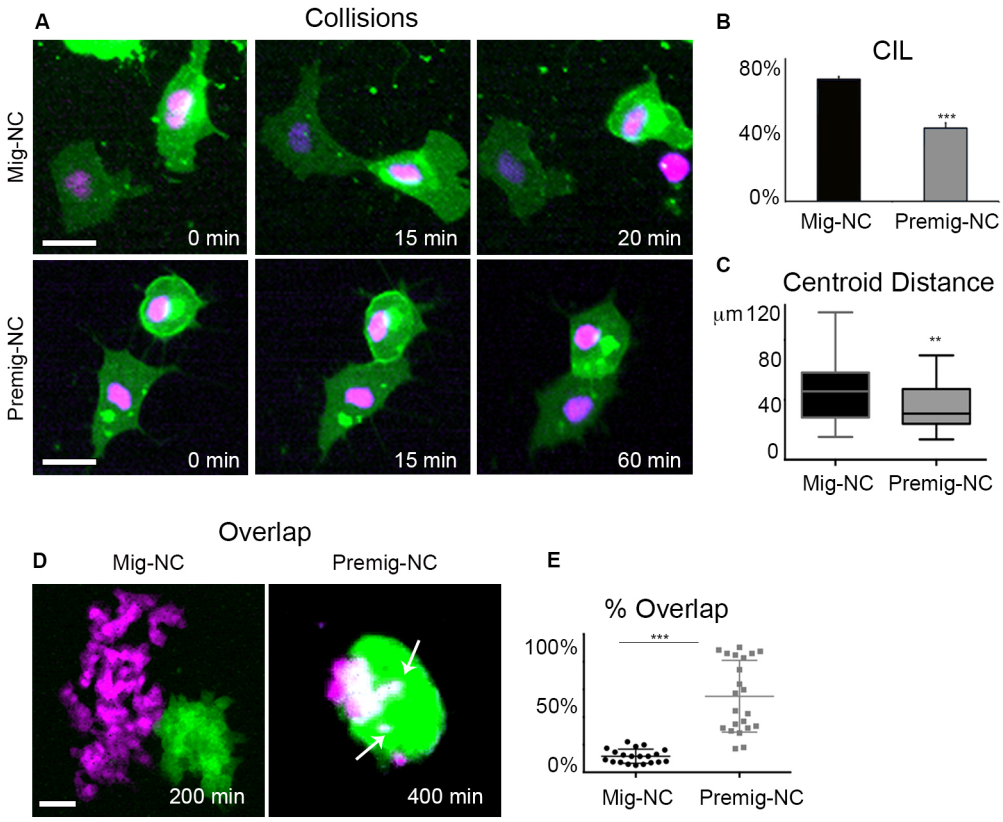

Figure 9.1 . Migratory, but not premigratory NC exhibit CIL.

(A) Collisions of Mig-NC and Premig-NC, scale bar 20 µm. **(B)** Percentage of collisions displaying CIL (Mig-NC n=132, Premig-NC n=98 collisions, 3 independent experiments, error bars: s.e.m., Taillard Contingency Tables for Proportion Comparison***α=0.1%). **(C)** Distance between cells centroids 30 min after collision (Mig-NC n=80, Premig-NC n=64, 2 independent experiments, error bars: s.d., ** P<0.01 Mann-Whitney test). **(D)** Overlap assay for Mig-NC or Premig-NC, scale bar 60 µm. **(E)** Percentage of overlap between explants at time point of maximum superimposition. (Mig-NC n= 19, Premig-NC n=19, 2 independent experiments, error bars: s.d., *** P<0.001 Student's t –test).

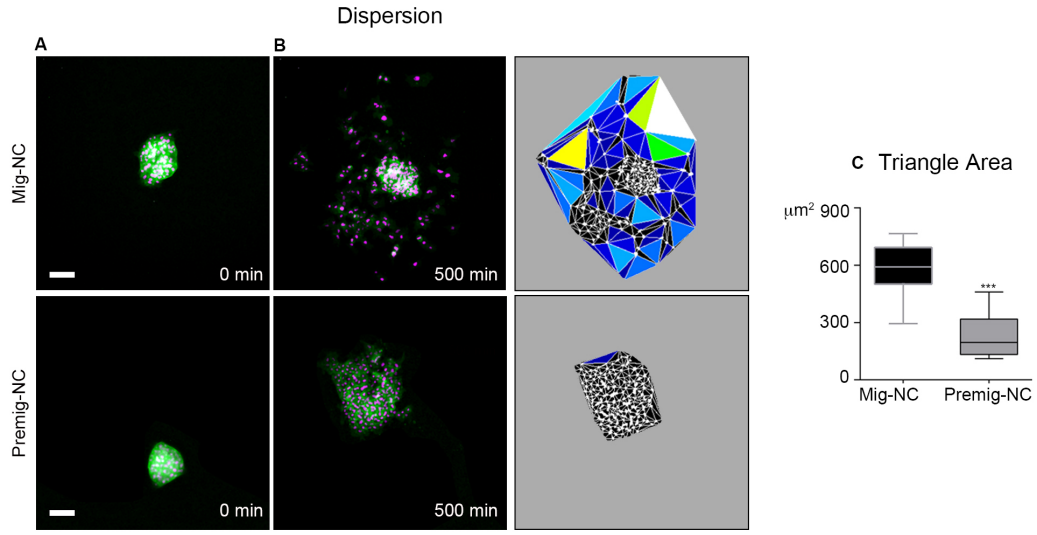

Figure 9.2. Migratory, but not premigratory NC undergo EMT.

(A) Dispersion assay for Mig-NC and Premig-NC explants, scale bar 50 µm. **(B)** Triangulation at 500 min, colour coded according to size of triangles. **(C)** Triangle Area at 500 minutes (Mig-NC n= 10, Premig-NC n=23, 3 independent experiments, error bars : s.d., *** P<0.001 Mann-Whitney test).

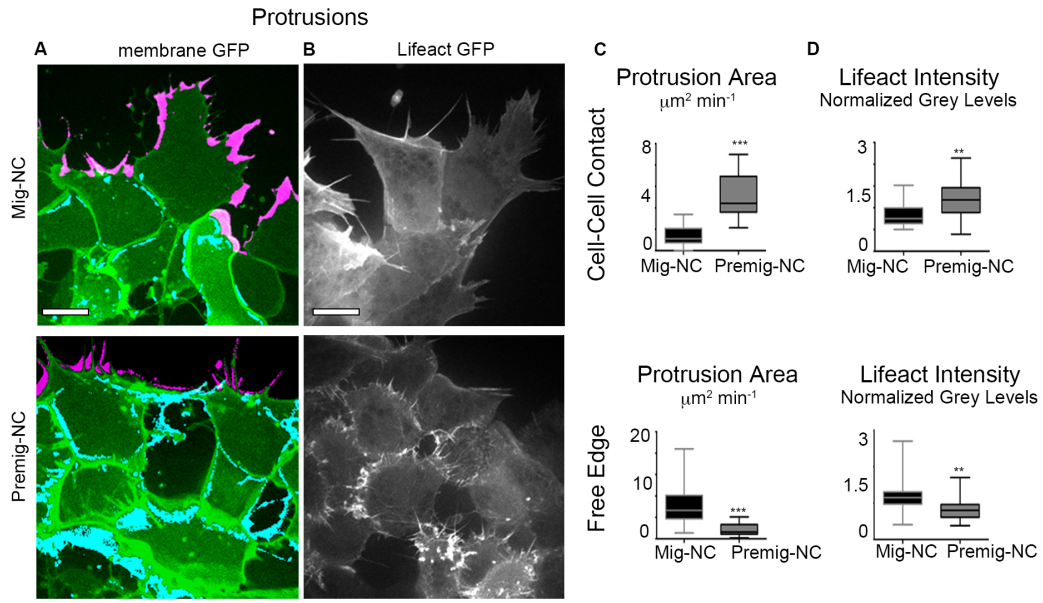

Figure 9.3. Contact-dependent protrusion polarity is acquired upon NC EMT.

(I) Protrusive activity of Mig-NC and Premig-NC. Maximal projection, free edge protrusions labelled in magenta, cell-cell contact protrusions in cyan, scale bar 10 μm. **(J)** Protrusion Area per minute per cell obtained by subtraction analysis (Mig-NC n= 45, Premig-NC n=80, 2 independent experiments, error bars: s.d., Top:*** P<0.001 Student's t –test Bottom: *** P<0.001 Mann-Whitney test). **(K)** Lifeact-GFP, scale bar 10 μm. **(L)** Lifeact-GFP fluorescence intensity (Mig-NC n= 12, Premig-NC n=15, 3 independent experiments, error bars: s.d., *** P<0.001 Student's t –test).

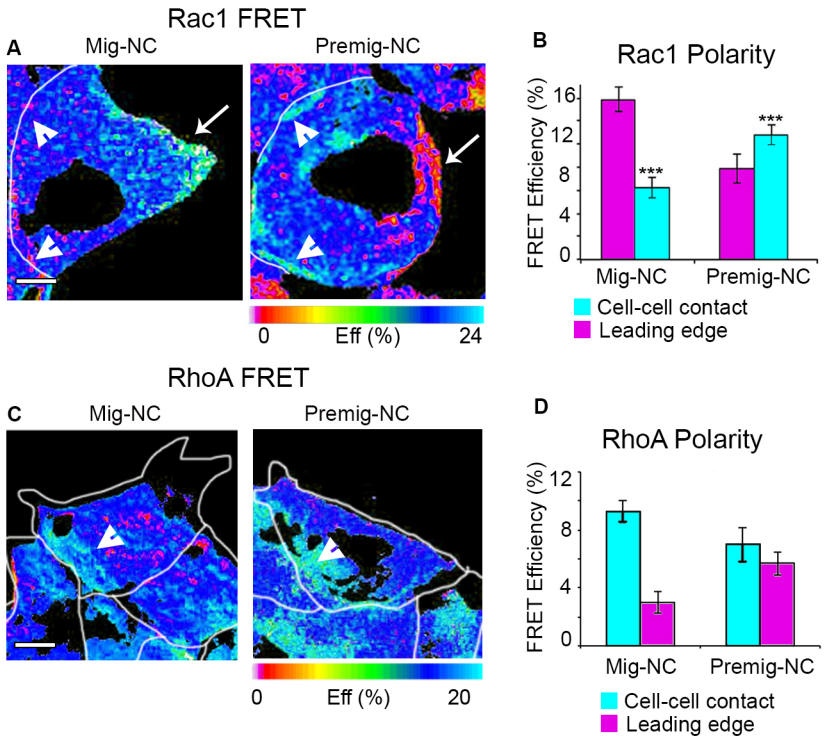

Figure 9.4. Rac1, but not RhoA, is differentially polarised in migratory and premigratory NC.

(A) Spatial distribution of Rac1 FRET efficiency. Cell-cell junctions outlined in white, scale bar 5 µm. **(B)** Rac1 polarity (Mig-NC n= 24, Premig-NC n=24, 3 independent experiments, error bars: s.e.m, *** P<0.001 Student's t –test). **(C)** Spatial distribution of RhoA FRET efficiency. Cell perimeter outlined in white, scale bar 5 µm. **(D)** RhoA polarity (Mig-NC n= 24, Premig-NC n=20, 2 independent experiments, error bars: s.e.m).

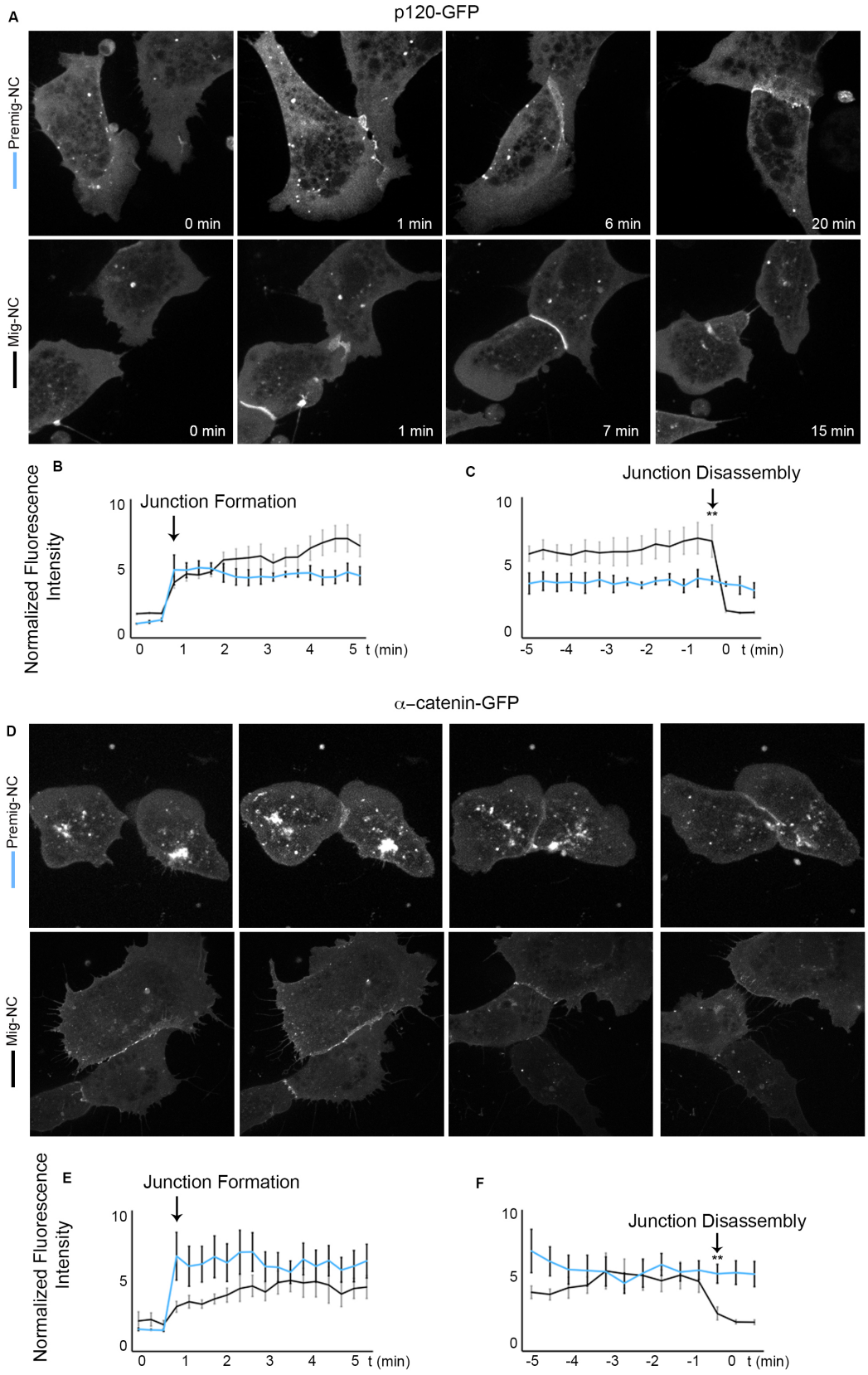

Figure 9.5. Junction dynamics of migratory and premigratory NC collisions.

Assembly and disassembly of cell-cell junctions during collisions of Mig-NC or Premig-NC expressing p120-GFP (**A**) and α-catenin-GFP (**D**); scale bars 10 μm. Fluorescence intensity of p120-GFP (**B**) and α-catenin-GFP (**E**) at cell-cell contact normalised to adjacent cytoplasm during first 5 minutes of collisions. (p120-GFP: Mig-NC n=6 , Premig-NC n=4, α-catenin-GFP Mig-NC n=9, Premig-NC n=7 collisions, 4 independent experiments, error bars: s.e.m.). Normalised fluorescence intensity of p120-GFP(**C**) and α-catenin-GFP (**F**) at cell-cell contact during the last 5 minutes of cell-cell collisions (p120-GFP: Mig-NC n=6, Premig-NC n=4 , α-catenin-GFP: Mig-NC n=9, Premig-NC n=7, 4 independent experiments, error bars: s.e.m.).

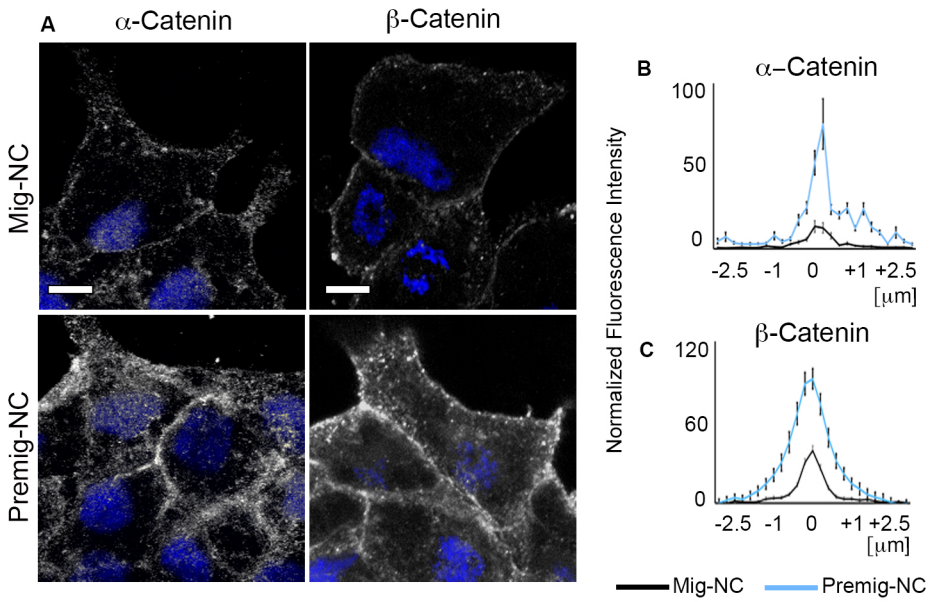

Figure 9.6. Endogenous expression of junctional complex components in migratory and premigratory neural crest.

(A) Immunostaining for α-catenin and β-catenin in Mig-NC and Premig-NC, scale bars 10 μm, nuclear staining: DAPI. **(B, C)** Fluorescence intensity across cell-cell junctions normalised to fluorescence in adjacent cell cytoplasm (α-catenin: Mig-NC n=50; Premig-NC n=50, 3 independent experiments, β-catenin: Mig-NC n=50; Premig-NC n=50, 3 independent experiments, error bars: s.em.).

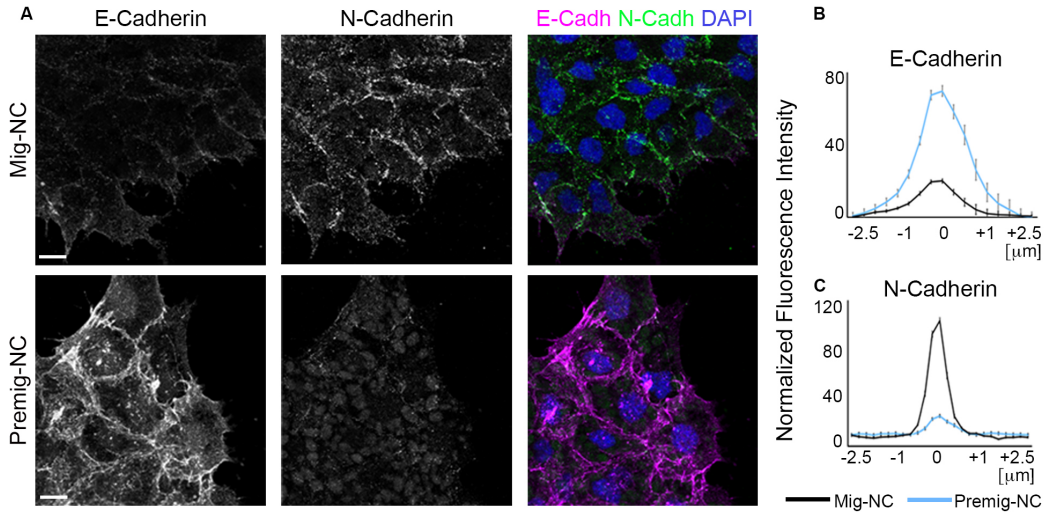

Figure 9.7. A cadherin switch occurs during NC EMT.

(A) Double immunostaining for E- and N-Cadherin in Mig-NC and Premig-NC, scale bars 20 µm. **(B, C)** Normalised fluorescence intensity diagrams (Mig-NC n=74, Premig-NC n=74, 3 independent experiments, error bars: s.em.).

2. E-Cadherin suppresses collective migration *in vivo* and Contact Inhibition of Locomotion by controlling contact-dependent polarity of Rac1

Neural crest cells acquire CIL during their EMT. This correlates with a change in contact dependent Rac1 and protrusion polarity and with a switch from E- to N-Cadherin expression. E-Cadherin is typically associated with epithelial behaviour, stable cell-cell adhesions and poor motility, while it is known that N-Cadherin is required to polarize Rac1 away from the cell-cell contacts in migratory neural crest cells as well as for CIL. I therefore reasoned that loss of E-Cadherin expression during neural crest development might be a permissive event that allows neural crest cells to transition to a front-rear polarized, migratory status in which cells may loosen their cell-cell contacts due to acquisition of N-Cadherin expression and CIL-induced polarization of protrusive activity.

E-Cadherin inhibits collective migration of Neural Crest in vivo

To explore whether the E- to N-Cadherin switching is required for acquisition of CIL by migratory neural crest, we expressed E-cadherin ectopically in Mig-NC. As CIL is required for migration *in vivo* (Carmona-Fontaine et al., 2008), I analysed the consequences of ectopic E-cadherin expression on NC migration. Overexpressing E-cadherin by microinjection at the 8-cell stage of the blastomeres that give rise to neural crest tissues was sufficient to reduce the migration of NC cells *in vivo* (Fig. 10.1 A-B). However, as such injections may also target adjacent ectodermal tissues such as placodes, which are important for

correct neural crest migration (Theveneau et al., 2013), I decided to assess whether the observed inhibition of neural crest migration was cell-autonomous. For this reason, graft experiments were performed, in which control fluorescein-injected neural crest cells or E-Cadherin injected neural crest cells were dissected and grafted into a wild type embryo. Importantly, this experiment revealed that the effect of E-cadherin on NC migration is cell autonomous, as grafting E-cadherin expressing NC in wild type embryos severely impaired migration compared to control grafts (Fig. 10.1 C, D).

E-Cadherin suppresses Contact Inhibition of Locomotion and EMT by controlling contact-dependent Rac1 polarity

The finding that E-Cadherin ectopic expression is able to cell-autonomously inhibit collective migration of neural crest *in vivo* supported the hypothesis that loss of E-Cadherin expression in development is required to allow correct neural crest migration. I therefore proceeded to investigate whether E-Cadherin ectopic expression may affect neural crest behaviour *in vitro*. Interestingly, observation of cell-cell collisions *in vitro* shows that E-cadherin expression reduces CIL compared to control Mig-NC (Fig. 10.2 A-C; Supplemental Movie S8). Such inhibitory effect of E-Cadherin on CIL was further confirmed by overlap assays demonstrating that intermixing between Mig-NC cell clusters was increased by E-cadherin overexpression (Fig. 10.2 D, E). I also investigated whether repression of CIL by E-Cadherin may affect EMT of neural crest and I found that, accordingly, ectopic E-cadherin strongly affected cell dispersion (Fig. 10.3 A, B; Supplemental Movie S9). Next, I investigated the effect of E-cadherin expression on the polarity of cell protrusions. Control Mig-NC produced large lamellipodial

protrusions towards the free edge (Fig. 10.4 A-B), and few protrusions at cell-cell contacts. This polarity was reversed in E-cadherin overexpressing Mig-NC (Fig. 10.4 A-B, Supplemental Movie S10). Analysis of the distribution of the activity of the small GTPases Rac1 and RhoA shows that, strikingly, E-Cadherin expression is able to reverse the polarity of Rac1 distribution, leading to a depletion of active Rac1 from the cell's leading edge and to a strong increase in active Rac1 at the cell-cell contacts (Fig. 10.4 C,D), while the distribution of active RhoA was not affected by E-Cadherin expression (Fig. 10.4 E, F). Importantly, E-Cadherin dependent redistribution of protrusive activity and active Rac1 was reminiscent of the protrusive activity and Rac1 distribution observed in premigratory neural crest, which express E-Cadherin endogenously.

E-Cadherin-mediated suppression of CIL is not due to downregulation of N-Cadherin expression

My results suggested that E-Cadherin might inhibit neural crest migration in vivo by suppressing EMT and CIL. However, it has been reported that increasing cell-cell adhesion might similarly repress neural crest migration *in vivo* (Kuriyama et al., 2014; Theveneau et al., 2010) and EMT *in vitro* (Kuriyama et al., 2014). To test whether these effects were specific to E-Cadherin or simply due to an overall increase of cell-cell adhesion strength, I overexpressed N-cadherin in Mig-NC and assessed its effect on cell collisions (Fig. 10.5 A), explant overlap assays (Fig. 10.5 B, C) and cell dispersion (Fig. 10.5 D, E). Contrary to the E-cadherin expression experiments, none of these assays were affected by N-cadherin overexpression, indicating an E-cadherin-specific effect on CIL and polarity. Because CIL has been reported to be dependent on N-cadherin (Theveneau et al., 2010; Theveneau et

al., 2013) and ectopic expression of one cadherin isoform may result in downregulation of another at the protein level via competition for binding to p120 (Xiao et al., 2003), I tested whether expression of E-cadherin in Mig-NC might result in downregulation of N-cadherin levels. I found that E-cadherin did not decrease endogenous N-cadherin expression or other components of the cell adhesion complex, such as α– or β-catenin (Fig. 10.6 A-F). Taken together, these results strongly suggest that E-cadherin acts as a repressor of CIL in Mig-NC.

E-Cadherin knockdown in premigratory neural crest promotes a CIL-like behaviour and mesenchymal-like polarity

To further substantiate the notion that E-Cadherin might be important in neural crest development to ensure timely acquisition of the CIL behaviour, I performed E-cadherin loss-of-function experiments in Premig-NC, which do not exhibit CIL and express E-Cadherin endogenously. To inhibit E-cadherin function, I used a morpholino oligonucleotide (MO) targeted against E-cadherin (Nandadasa et al., 2009) or an E-cadherin blocking antibody, which targets E-Cadherin extracellular domain (5D3)(Theveneau et al., 2013). I used explant overlap assays to assess for CIL of Premig-NC. These experiments show that intermixing between explants was reduced in Premig-NC following E-cadherin inhibition (Fig. 10.7 A, B). Single cell collisions were not analysed in this context due to technical difficulties. Indeed, at developmental stage 15 (Nieuwkoop and Faber), when Premig-NC were dissected, the premig-NC rely on E-Cadherin for cell-cell adhesion. Indeed, morpholino mediated knockdown of E-Cadherin results in loosening of tissue integrity, and incubation of MO cells in Ca^{2+} free medium to obtain single dissociated cells resulted in cell death, thus making impossible to

analyse single cell collisions in E-Cadherin MO cells. I therefore decided to probe Premig-NC in which E-Cadherin was knocked down for contact-dependent polarity, which is considered as a readout for CIL in neural crest cells (Carmona-Fontaine et al., 2008). I assessed the dynamics of protrusion formation in Premig-NC injected with a control MO or E-cadherin MO. In control Premig-NC, protrusions were formed predominantly at cell-cell contacts and were small at free edges, while E-cadherin MO injected cells showed a reverted, mesenchymal-like, outward directed polarity (Fig. 10.7 C, D). Taken together, these two assays suggest that E-Cadherin is required to suppress CIL-like features in Premig-NC cells. Together with my ectopic expression experiments, these results indicate that E-cadherin acts as a repressor of CIL and its downregulation during EMT is a required step for acquisition of CIL in normal development.

Analysis of junction composition, dynamics and biochemical interactions in E-Cadherin expressing neural crest

I have shown that E-Cadherin represses CIL in migratory neural crest, and that, conversely, knockdown of E-Cadherin in premigratory cells leads to a CIL-like behaviour. To gain further insight into the mechanism through which E-cadherin inhibits CIL, I analysed whether E-cadherin affects the composition of Mig-NC cell-cell junctions. No qualitative difference was observed in the molecular composition of the cell adhesion complex between Mig-NC and E-cadherin expressing Mig-NC, as both express α- and β-catenins, although both proteins were accumulated at higher levels in Mig-NC +E-cadherin cell-cell junctions (Fig. 10.8 A-C). In addition, I measured the intensity of junctional recruitment of p120-GFP in Mig-NC and Mig-NC expressing E-Cadherin and I found that, similar

to endogenous α- and β-catenins, higher levels of p120-GFP were recruited at the E-Cadherin cell-cell adhesion (Figure 10.8 A, D). I reasoned that the higher recruitment of junctional complex molecules at E-Cadherin based cell-cell adhesions might be consequence of a higher affinity of E-Cadherin for α- and β-catenin or p120. Therefore, I decided to compare the biochemical interaction of E- and N- Cadherin with catenins by performing immunoprecipitation experiments from *Xenopus* embryos injected with either E-Cadherin or N-Cadherin. Surprisingly, comparison of the N- and E-cadherin immunoprecipitations demonstrates that both cadherins interact with endogenous α- and β-catenins with comparable affinity (Fig. 10.9 A-D). This result suggests that E-Cadherin does not stabilise the junctional complex because of a higher binding affinity for α- and β-catenin. In Mig-NC, the endogenous N-Cadherin-Catenin complex undergoes fast endocytic recycling (Kuriyama et al., 2014), and impaired recycling of N-Cadherin results in inhibition of EMT and of migration in vivo (Kuriyama et al., 2014). For this reason, I assessed whether E-Cadherin expression affected the mobility of the cadherin-catenin complex by performing FRAP for p120-GFP and α-Catenin-GFP. The mobile fractions of p120-GFP and α-Catenin-GFP resulted slightly, but significantly, decreased upon E-Cadherin expression (Fig. 10.10 C-E) and the halftime of recovery was significantly increased for both p120-GFP and α-Catenin-GFP (Fig. 10.10 D-F). Therefore, the effects observed in Mig-NC upon E-Cadherin expression might be, partially ascribed to a mild stabilization of the catenin complex protein dynamics. However, given that the effect of E-Cadherin on junctional complex mobility appears to be very mild (Fig. 10.10), it is likely that E-Cadherin

mediated suppression of CIL may require an additional mechanism. Importantly, we observed a striking relocation of active Rac1 at the cell-cell junction site upon E-Cadherin ectopic expression, which may account for the ability of E-Cadherin to repress cell dispersion and cell separation during CIL, as protrusions do not correctly polarize outwards in E-Cadherin overexpressing neural crest clusters. Overall, these results suggest that E-cadherin does not affect CIL via the composition of the adhesion complex components, but may regulate CIL through an alternative mechanism.

The interaction between E-Cadherin and p120ctn is required to suppress CIL

The cytoplasmic juxtamembrane domain of E-Cadherin inhibits NC migration in vivo

My results indicate that E-Cadherin suppresses collective migration, CIL and EMT. In E-Cadherin expressing neural crest cells, cell-cell adhesion appears to be mildly stabilised although the biochemical interaction with α- and β-catenin does not significantly differ between N- and E-Cadherin and, importantly, Rac1 is redistributed at the cell-cell adhesion sites and depleted from the cell's free edge. I reasoned that E-Cadherin might mediate its effects either via an increase in homophilic adhesion and *cis* lateral clustering mediated by its EC domains, or by mediating intracellular signalling via its cytoplasmic tail. To address this problem, I sought to identify which functional domain of E-cadherin inhibits CIL. As discussed in detail in the Introduction of this thesis, N- and E-cadherin are single pass transmembrane proteins, with an extracellular (EC) domain mediating cis- and trans- homophilic interactions, a transmembrane domain (TM), and a highly conserved cytoplasmic domain with a direct binding site for p120 and β-catenin at the juxtamembrane and C-term regions respectively (Fig.

10.11 A). To address whether the extracellular or the cytoplasmic domain of E-Cadherin represses migration *in vivo*, EMT and CIL, I generated two chimeric mutants by exchanging the EC domains of E and N-cadherin (Fig. 10.11 A). In addition, since I observed a clear change in Rac1 activity upon E-cadherin expression and because p120 is the only direct classical cadherin binding partner involved in activating Rac1 (Goodwin et al., 2003; Wildenberg et al., 2006), I abolished E-cadherin-p120 interaction by using two E-cadherin mutants uncoupled from p120 that carry point mutations in the core p120 binding region of the juxtamembrane domain (Ciesiolka et al., 2004): E-cadherin750AAA and E-cadherin753AAA (Fig. 10.11 A). Double immunostaining with N-cadherin and E-cadherin antibodies reactive against their respective EC domain confirmed that all mutants were expressed and correctly localised at cell-cell junctions in neural crest cells (Fig.10.11 B). I first addressed whether the mutants may affect neural crest collective migration *in vivo*. I therefore expressed the wild type, chimeric or point mutant E-cadherin in embryos and compared their effects on NC migration in vivo (Fig. 10.12 A, B). Observation and quantitation of dorsoventral migration of the neural crest streams revealed that the N/E chimeric mutant, which carries N-Cadherin EC domain and wild type E-Cadherin cytoplasmic domain, was the only mutant that mimicked E-cadherin overexpression by reducing NC migration *in vivo*. Expression of full length E-Cadherin carrying point mutations that abolish p120 binding resulted in normal neural crest migration (Fig. 10.12 A, B). Altogether, these results indicate that the inhibitory effect of E-cadherin on neural crest migration requires the cytoplasmic domain and, in particular, E-Cadherin interaction with p120 appears to be required.

The cytoplasmic juxtamembrane domain of E-Cadherin inhibits CIL, dispersion and Rac1 activation

I then sought to confirm whether a similar requirement would be needed for E-Cadherin to repress EMT and CIL *in vitro*. In line with the *in vivo* findings, dispersion (Fig. 10.13A, B) and collision assays (Fig. 10.13 C, D) showed that the E-Cadherin cytoplasmic domain and its interaction with p120 are also required to inhibit cell dispersion and CIL.

How does the E-cadherin-p120 signalling impact on polarity and CIL? FRET analysis of total Rac1 activity in neural crest cell clusters shows that Mig-NC+E Cadherin exhibit higher Rac1 activity than control cells or cells expressing the p120 uncoupled E-Cadherin mutants (Fig. 10.13 E), indicating that E-cadherin promotes Rac1 activity in NC cells via p120.

p120 is required for E-Cadherin mediated suppression of CIL and EMT

In vivo and *in vitro* experiments of expression of chimaeric cadherins and p120-uncoupled E-Cadherin strongly suggest that the E-Cadherin cytoplasmic domain inhibits neural crest migration, EMT and CIL, and that such inhibitory activity requires interaction between E-Cadherin and p120. I therefore proceeded to confirm the importance of E-cadherin-p120 interaction by knocking down endogenous p120 in Mig-NC or Mig-NC + E-cadherin using a p120 MO (Ciesiolka et al., 2004) and by assessing the ability of neural crest cells to disperse as well as the polarity and dynamics of protrusion formation (Supplemental Movie S11). Dispersion assays show that p120 knockdown *per se* mildly, but not significantly, affects neural crest dispersion (Figure 10.14 A, B), however, knockdown of p120 in E-Cadherin overexpressing explants is able to partially rescue the inhibition of

dispersion mediated by E-Cadherin (Figure 10.14 A, B), thus suggesting that p120 is required downstream of E-Cadherin for repression of EMT. Importantly, p120 knockdown did not *per se* affect the polarity and size of lamellipodial protrusions (Fig. 10.14A, B) but was sufficient to fully rescue the reduction in protrusive activity due to E-cadherin ectopic expression (Fig. 10.14 A, B). The partiality of the rescue obtained upon p120 knockdown in cell dispersion assays might be due to additional E-Cadherin partners involved in mainteinance of cell-cell junction stability. Indeed, immunofluorescence (Fig. 10.8) and FRAP experiments (Fig. 10.10) suggest that not only p120, but also α-Catenin might be more stably recruited at E-Cadherin cell-cell junctions. Interestingly, α-N-Catenin controls chick cranial neural crest EMT: knockdown of α-Catenin increases EMT of neural crest cells in vitro and migration in vivo, while overexpression of α-Catenin is sufficient to inhibit neural crest migration (Jhingory et al., 2010), thus raising the possibility of a similar role for α-Catenin in E-Cadherin mediated EMT inhibition in our system, which will need further investigation. Nevertheless, outward directed contact-dependent protrusion polarity is fully restored by p120 knockdown, and FRET measurements suggest a requirement for E-Cadherin/p120 interaction for Rac1 activation (Figure 10.13 E). Taken together, these observations strongly suggest that p120 might be a key element in controlling Rac1 activity at the cell-cell contact downstream of E-Cadherin. In conclusion, these results show that E-cadherin cytoplasmic domain signals via p120 to activate Rac1 at NC cell-cell junctions, and leads to suppression of CIL and altered NC migratory behaviour *in vivo* via inhibition of contact-dependent Rac1 and protrusion repolarization.

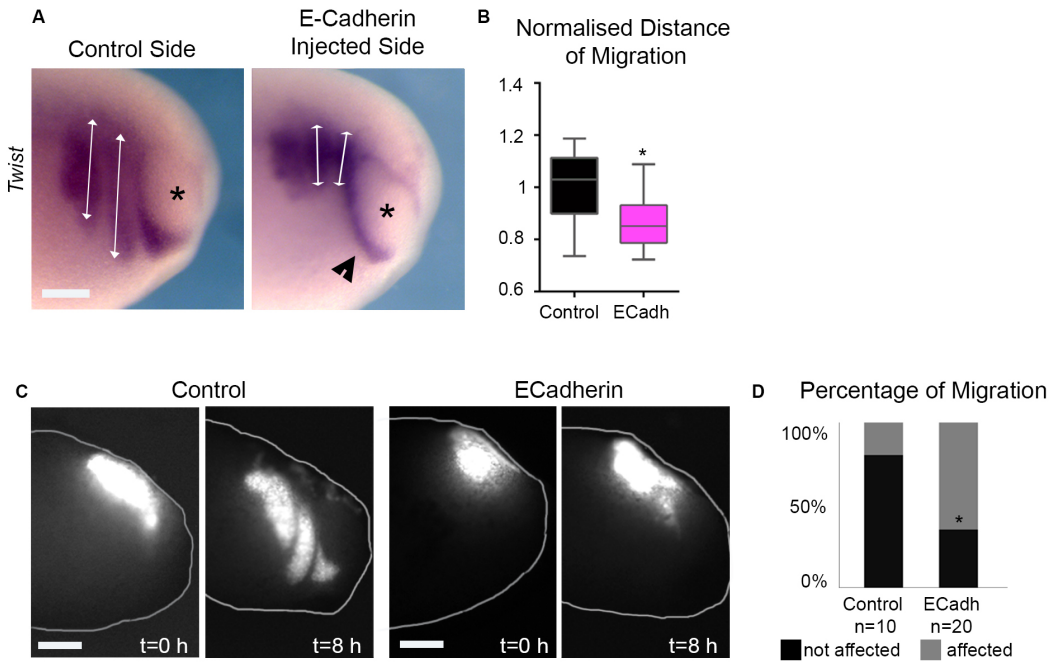

Figure 10.1. E-Cadherin inhibits collective migration of neural crest *in vivo*. **(A)** *Twist* in situ hybridization (ISH) of Stage 25 *Xenopus laevis* embryo. Asterisks: eye, scale bar 200 µm. **(B)** Distance of migration. Injected side normalised to the uninjected side (n=19 embryos, error bars: s.d, * P<0.05). **(C)** Fluorescently labelled WT or E-Cadh expressing NC grafted into WT embryos before (t=0) and after (t=8 hours) migration. Scale bars 250 µm. **(D)** Percentage of migrating NC grafts (Control n=10, E-Cadh n=20, 2 independent experiments, Taillard Contingency Tables for Proportion Comparison *α=5%).

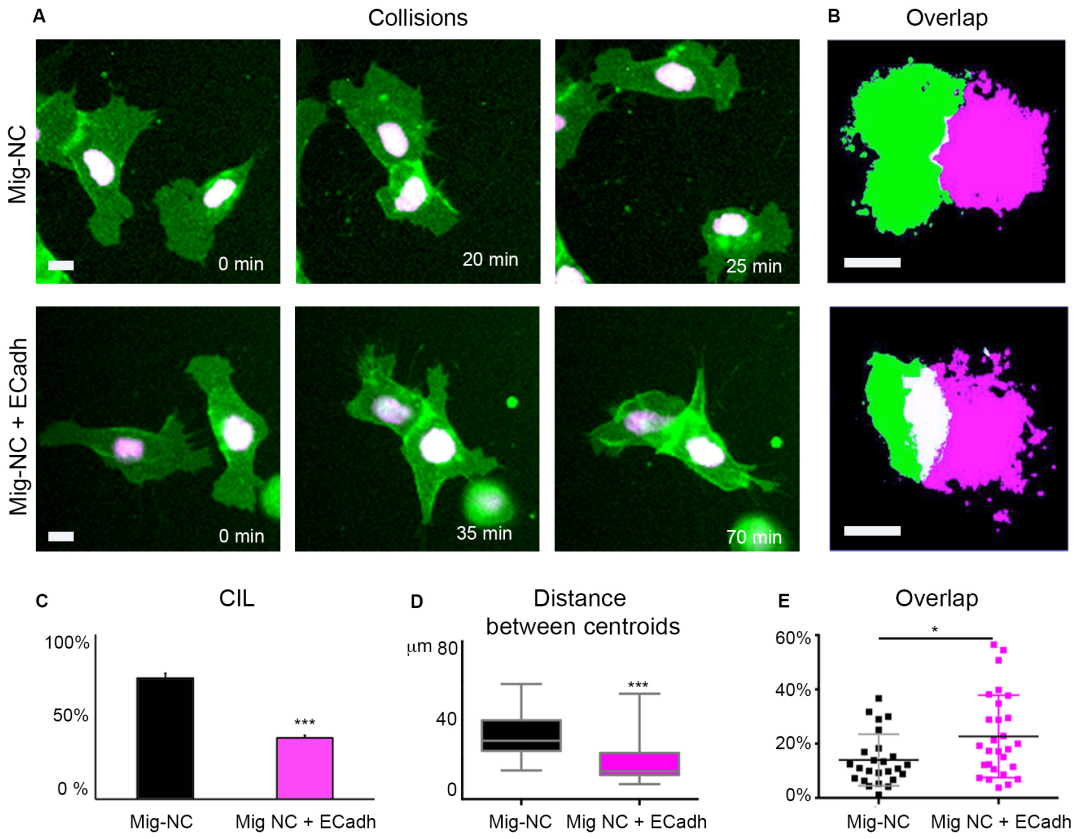

Figure 10.2 E-Cadherin suppresses CIL in migratory NC.

(A) Collisions of Mig-NC or Mig-NC+ECadh cells, scale bar 10 µm. **(B)** Percentage of CIL (Mig-NC n=40, Mig-NC+E-Cadh n=29, 3 independent experiments, error bars: s.e.m. Taillard Contingency Tables for Proportion Comparison ***α=0.1%). **(C)** Distance between cells centroids (Mig-NC n=40, Mig-NC+E-Cadh n=29, 3 independent experiments, error bars: s.d., *** P<0.001 Mann-Whitney test). **(D)** Explant overlap assay, thresholded images; scale bar 60 µm. **(E)** Percentage of overlap between explants (Mig-NC n= 25, Mig-NC+E-Cadh n=28, 3 independent experiments, error bars: s.d., * P<0.05 Student's t –test).

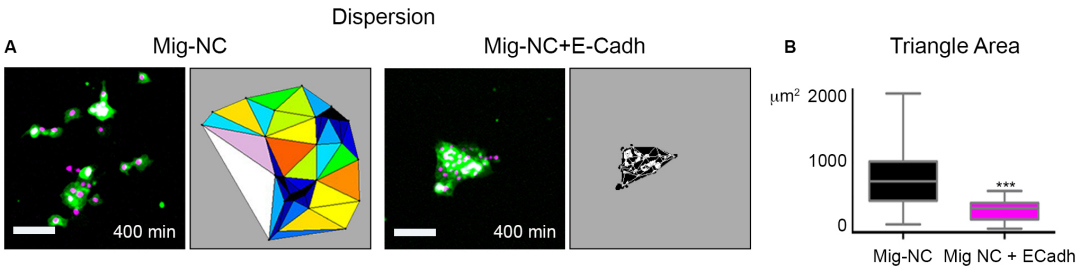

Figure 10.3 E-Cadherin suppresses EMT in migratory neural crest.

(A) Dispersion assay. Mig-NC and Mig-NC+ E-Cadh at 400 min (Left panel) and colour coded triangulation diagram (Right panel), scale bar 50 µm. **(B)** Triangle Area (Mig-NC n= 28, Mig-NC+E-Cadh n=22, 3 independent experiments, error bars: s.d., *** P<0.001 Student's t –test).

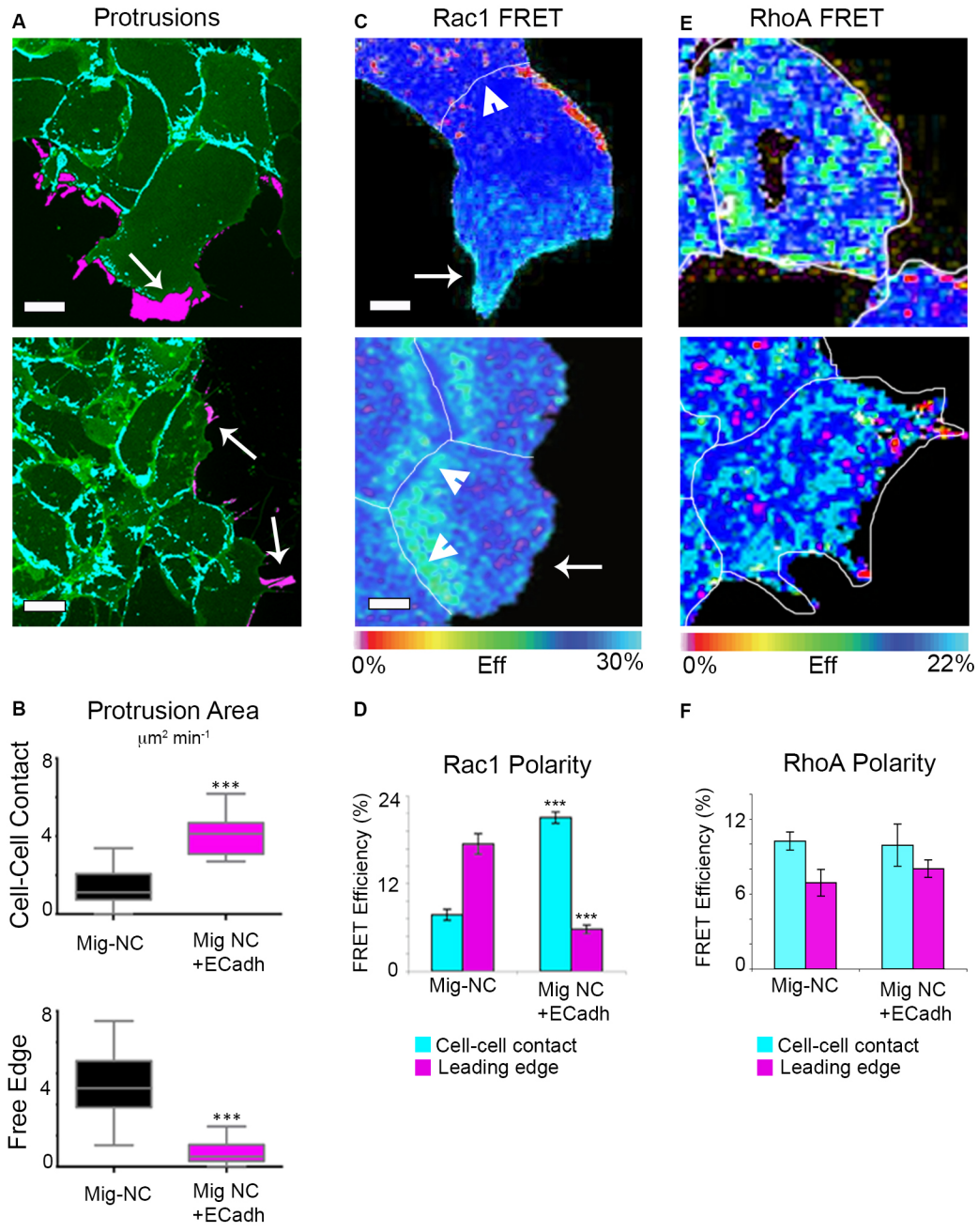

Figure 10.4 E-Cadherin controls Rac1-dependent repolarization of cell protrusions.

(A) Protrusive activity of Mig-NC and Mig-NC+E-Cadh. Maximum projection, Free Edge protrusions in magenta, Cell-Cell contact protrusions in cyan, scale bar 10 µm. **(B)** Quantitation of Protrusion Area per minute per cell (Mig-NC n= 43, Mig-NC+E-Cadh n=66, 3 independent experiments, error bars: s.d., top*** P<0.001

Student's t –test bottom: *** P<0.001 Mann-Whitney test). **(C)** Rac1 FRET efficiency distribution. Cell-cell junctions outlined in black, scale bar 5 μm. **(D)** Rac1 FRET efficiency at cell-cell contact and at leading edge (Mig-NC n= 24, Mig-NC+E-cadh n=24, 3 independent experiments, error bars: s.e.m, *** P<0.001 Student's t–test). **(E)** RhoA FRET efficiency distribution. Cell-cell junctions outlined in black, scale bar 5 μm. **(F)** RhoA FRET efficiency at cell-cell contact and at leading edge (Mig-NC n= 32, Mig-NC+E-cadh n=32, 3 independent experiments, error bars: s.e.m).

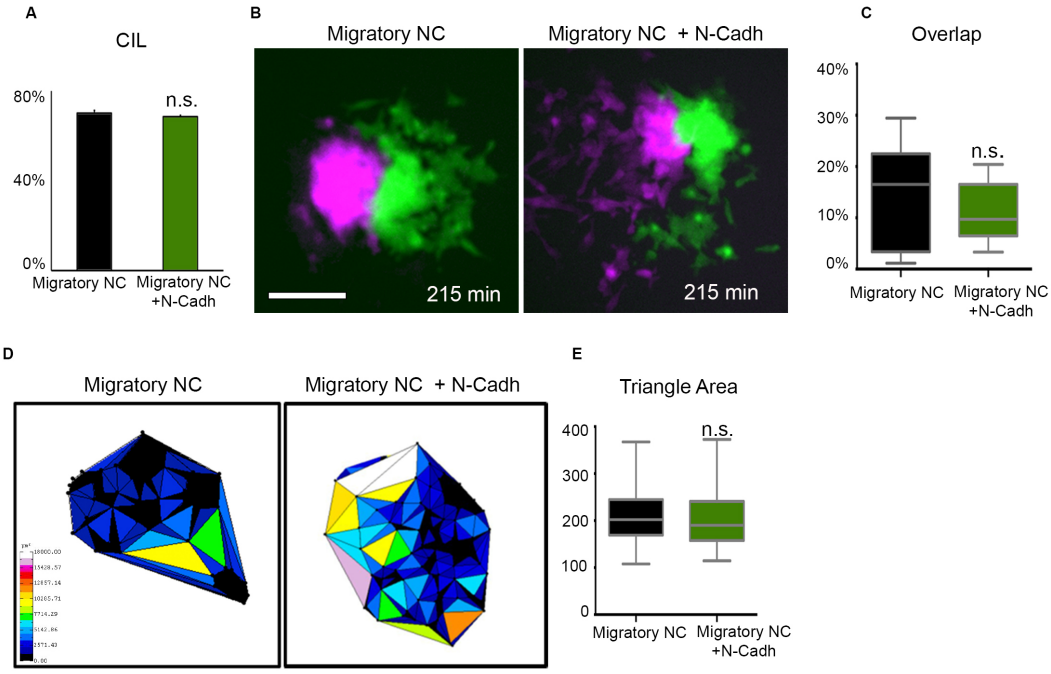

Figure 10.5. N-Cadherin overexpression does not affect neural crest CIL or EMT.

(A) Percentage of CIL (n=47 collisions Mig-NC, n=86 collisions Mig-NC+N-Cadh, 2 independent experiments, error bars : s.e.m., n.s. not significant). **(B)** Explant overlap assay for Mig-NC or Mig-NC+N-Cadh, scale bar 100 µm. **(C)** Percentage of overlap between the explants (n= 19 explants Mig-NC, n=18 explants Mig-NC+N-Cadh, 2 independent experiments, error bars : s.d., n.s. not significant, Student's t –test). **(D)** Dispersion Assay. Colour coded Delaunay triangulation diagrams. **(E)** Triangle Area at 400 minutes after plating (Mig-NC n=28, Mig-NC+N-Cadh n=27 explants, 3 independent experiments, error bars : s.d., n.s. not significant, Student's t–test).

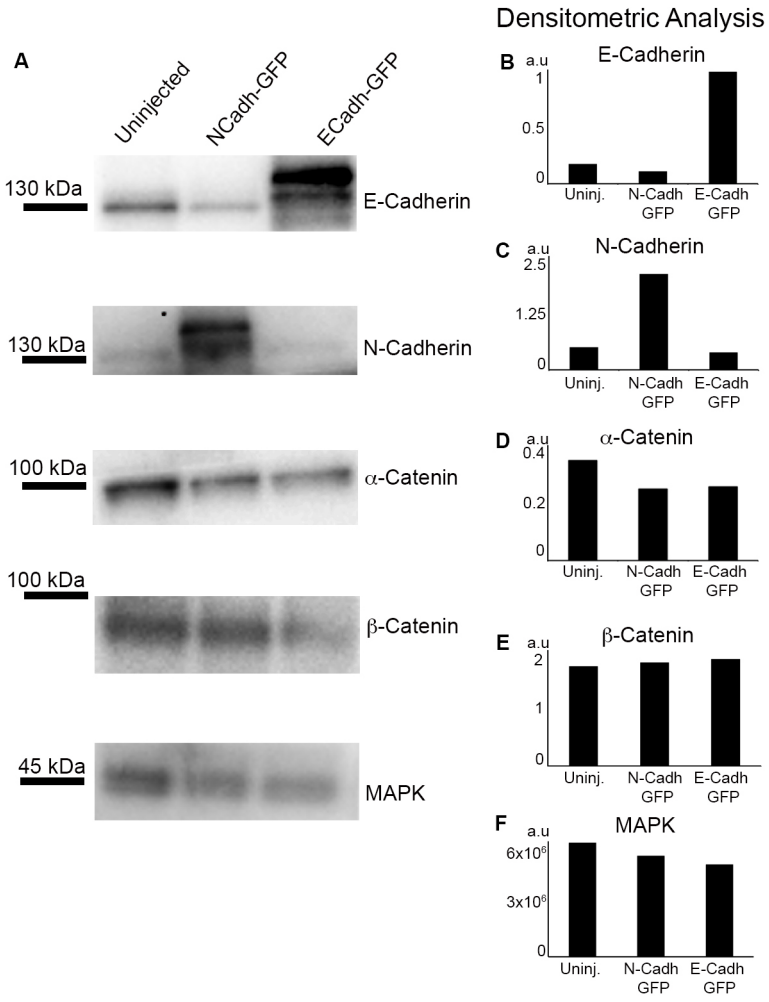

Figure 10.6. E-Cadherin ectopic expression does not affect N-Cadherin, α– or β-catenin expression levels.

(A) Western blot (WB) of stage 19 embryo lysates. Antibody blotting as illustrated. **(B-F)** Densitometric analysis of the WB shown in **(A),** with **(B-E)** representing ratio between the antibody band intensity and the pixel intensity for MAPK **(F)**.

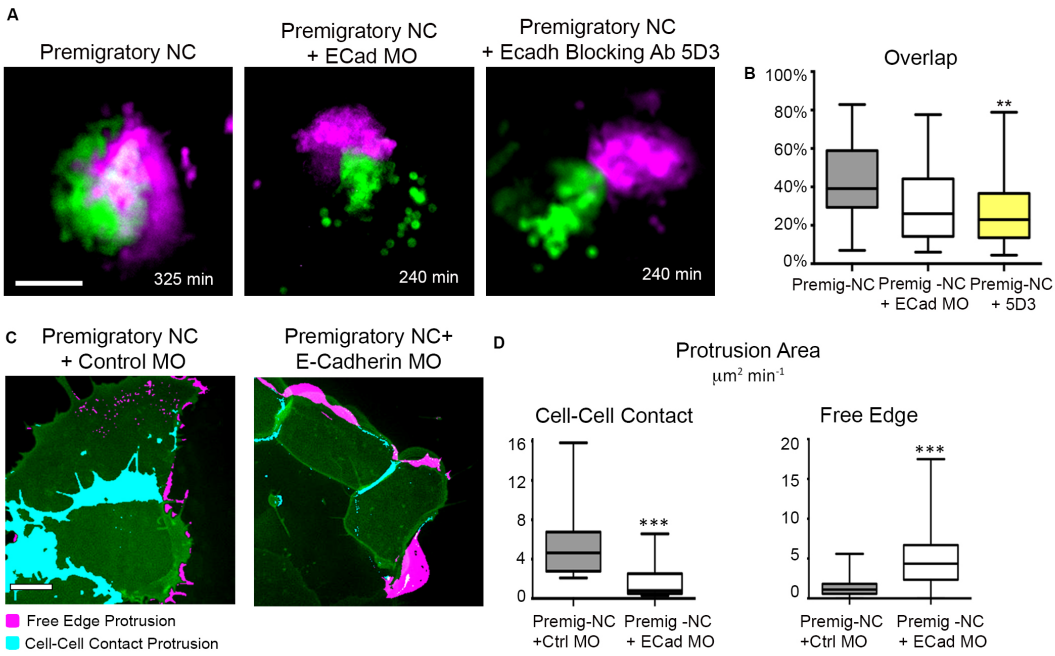

Figure 10.7. E-Cadherin loss of function in premigratory NC triggers a CIL-like behaviour and a reversal of protrusion polarity.

(A) Time lapse stills of explant overlap assay for Premig-NC or Premig-NC+E-Cadh MO or E-Cadh blocking antibody (5D3), scale bar 100 µm. **(B)** Percentage of overlap between the explants at the time point of maximum superimposition.(Premig-NC n= 33, Premig-NC+E-Cadh n=7 MO, Premig-NC+5D3 n=31 explants, 2 independent experiments, error bars : s.d., **P<0.01Dunn's multiple comparisons, n.s. not significant). **(C)** Protrusive activity of Premig-NC+ Control MO and Premig-NC+E-Cadh MO. Still time-lapse photographs of a maximal projection, Free Edge protrusions labelled in magenta, Cell-Cell contact protrusions labelled in cyan (Right), scale bar 10 µm. **(D)** Quantitation of Protrusion Area per minute per cell obtained by subtraction analysis (n= 22 cells Premig-NC+Standard Control MO, n=30 cells Premig-NC+E-Cadh MO, 4 independent experiments, error bars : s.d., *** P<0.001, Mann-Whitney test).

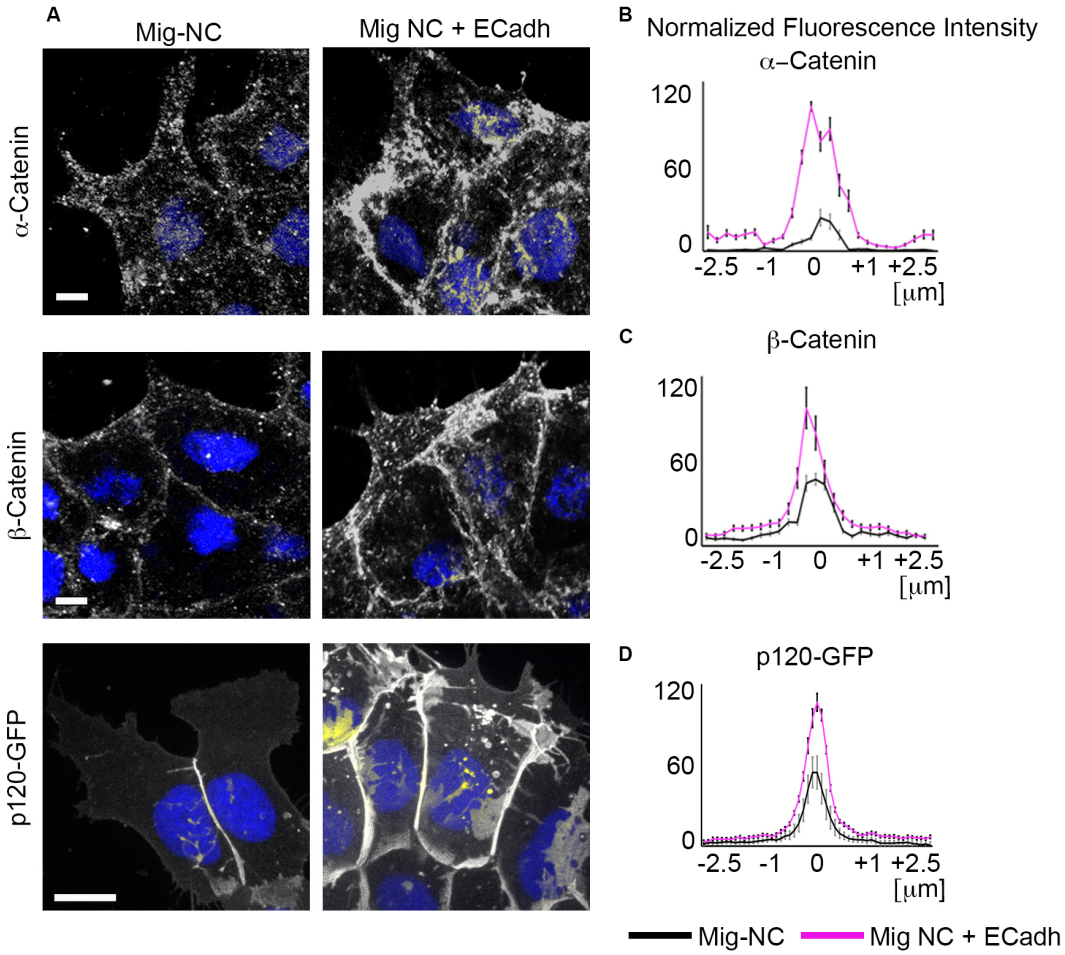

Figure 10.8. E-Cadherin ectopic expression increases recruitment of endogenous α– and β-catenin at cell-cell junctions.

(A) Immunostaining for α-catenin and β-catenin in Mig-NC and Premig-NC, scale bars 10 μm, nuclear staining: DAPI. **(B, C, D)** Fluorescence intensity across cell-cell junctions normalised to fluorescence in adjacent cell cytoplasm (α-catenin: Mig-NC n=50; Mig-NC+E-Cadh n=50 junctions, 2 independent experiments, β-catenin: Mig-NC n=50; Mig-NC+E-Cadh n=50, 3 independent experiments, error bars: s.em., p120-GFP Mig-NC n=30 Mig-NC+E-Cadh n=30, 3 independent experiments).

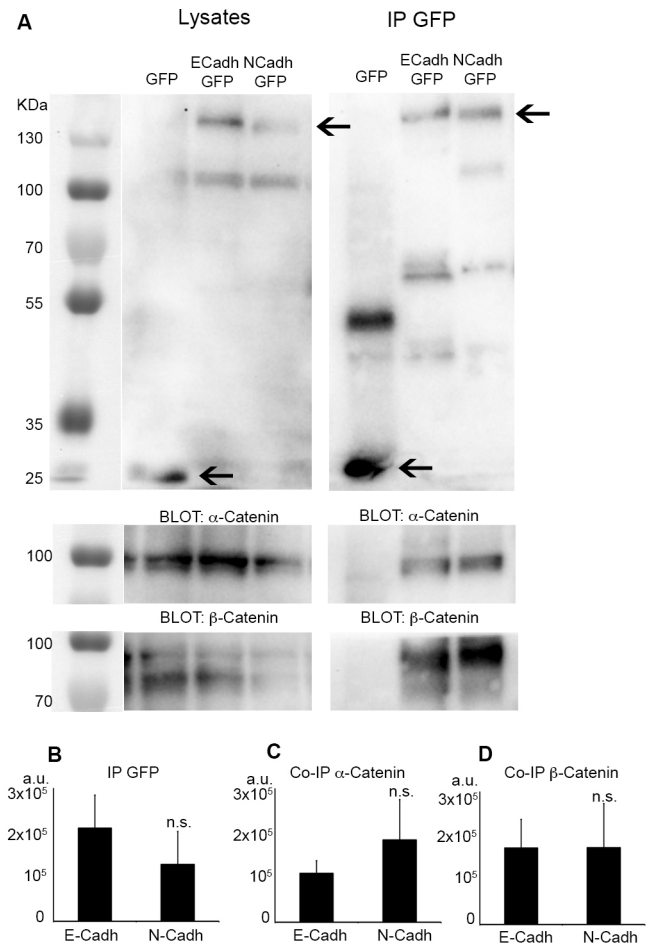

Figure 10.9. Biochemical interaction of N- and E-Cadherin with endogenous α– and β-catenin is comparable.

(A) Immunoprecipitation (IP) of GFP, E-cadh-GFP, N-Cadh-GFP from Stage 19 embryo lysates. A WB of lysates is shown in left panel. Pull down of GFP is shown in right panel. Coimmunoprecipitation of a- and b-Catenin and their corresponding lysates is shown in the bottom panels. **(B-D)** Pixel volumetric intensity of GFP IP **(B)** and corresponding co-immunoprecipitates for a-catenin **(C)** and b-Catenin **(D)** (n=5 independent experiments, error bars : s.e.m, n.s. not significant, Student's t-test).

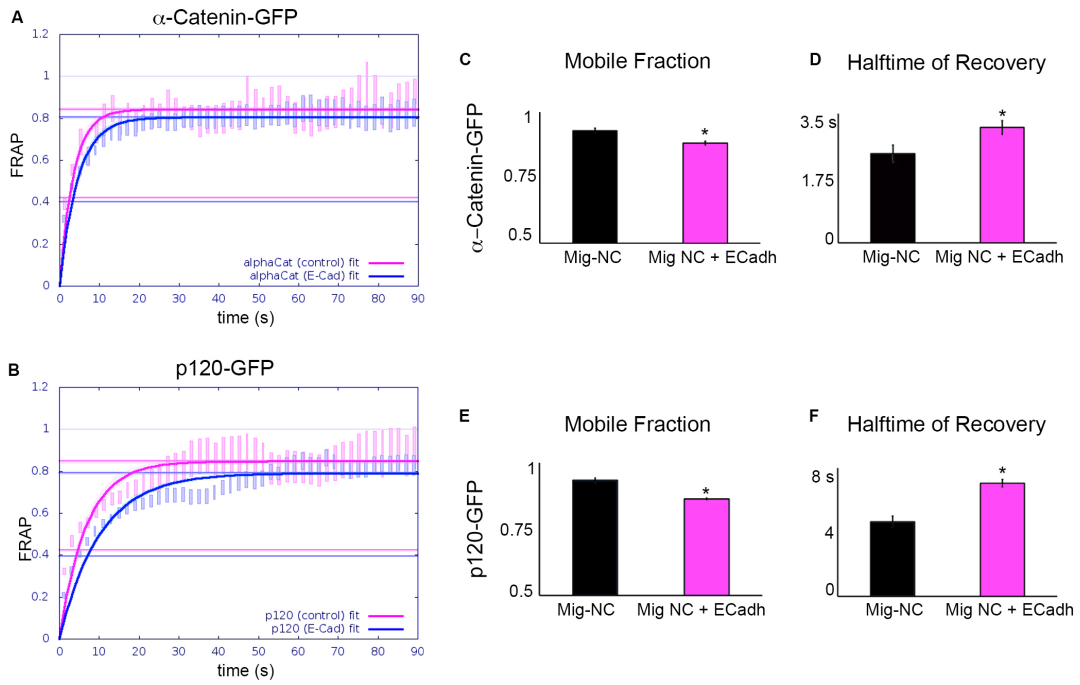

Figure 10.10. E-Cadherin ectopic expression mildly affects α–catenin and p120-GFP dynamics at the cell-cell junction.

(A,B). FRAP single exponential fits for recovery curves for α-Catenin-GFP (A) and p120-GFP (B) and vertical bars :s.d of FRAP data. Shades around fitting curves : 95% c.i. **(C-F)** Fitting FRAP parameters for and α-catenin-GFP (C,D) and p120-GFP (E,F) in Mig-NC and Mig-NC+E-Cadh. Mobile fraction in (C,E), Halftime of recovery in (D,F) (n=18 FRAP regions for Mig-NC, n=24 FRAP regions for Mig-NC+ECadh for p120-GFP; n=29 FRAP regions for Mig-NC, n=36 FRAP regions for Mig-NC+ECadh for α-catenin-GFP FRAP, 3 independent experiments, error bars : 95% c.i., *P<0.05).

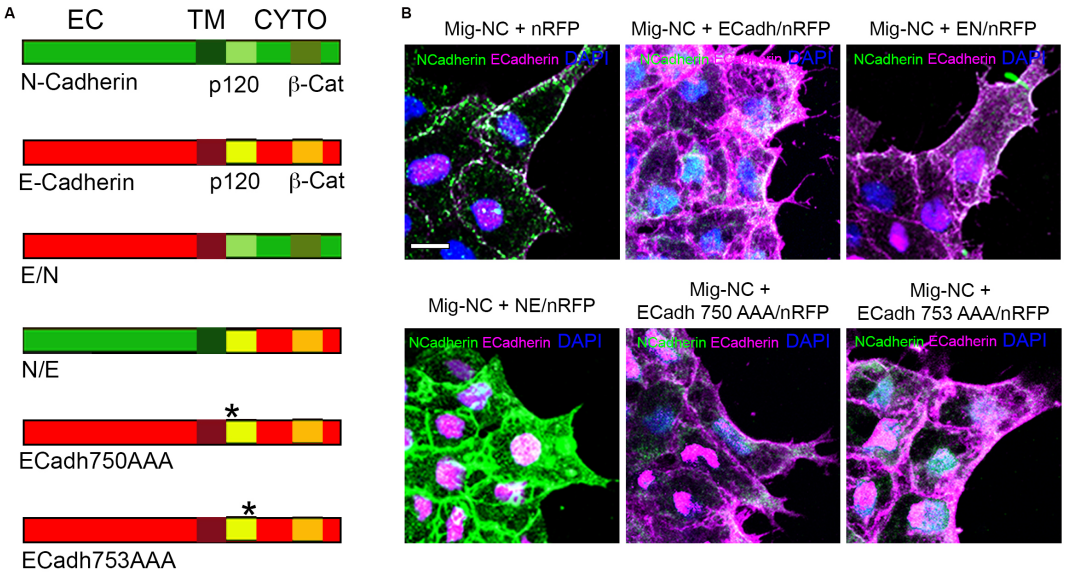

Figure 10.11. Diagram of E-Cadherin mutants and expression in neural crest cells.

(A) Diagram of N- and E-Cadherin domain organization: extracellular domain (EC), transmembrane domain (TM) and cytoplasmic domain (CYTO). E/N mutant: E-Cadh EC/N-Cadh CYTO. N/E mutant : N-Cadh EC/E-Cadh CYTO. Point mutations (750 GGG-> AAA), (753 EED-> AAA) in the juxtamembrane domain of E-Cadh are represented by the asterisk. **(B)** Double immunostaining for E- and N-Cadherin in Mig-NC, Mig-NC+E-Cadh, Mig-NC+E/N, Mig-NC+N/E, Mig-NC+E-Cadh750AAA, Mig-NC+E-Cadh753AAA, all constructs co-injected with nuclear RFP (nRFP) scale bar 10 µm. Both antibodies are specific for the EC domain of each cadherin, therefore allowing distinguishing the expression of the swapped CYTO domains mutants.

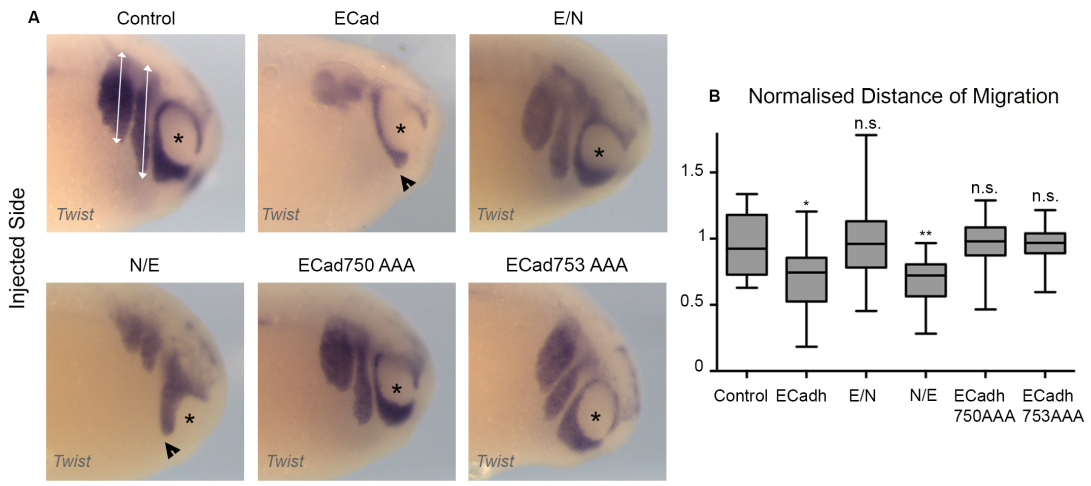

Figure 10.12. E-Cadherin cytoplasmic tail inhibits neural crest migration *in vivo.*

(A) *Twist* ISH of Stage 25 X.L. embryos. Asterisks indicate the eye, scale bar 200 µm. **(B)** Distance of migration. Injected side normalised to uninjected side (Control n=14, E-Cadh n=23, E/N n=20, N/E n=23, 750AAA n=10, 753AAA n=17 embryos, 3 independent experiments, error bars: s.d, One-way Anova P<0.001, multiple comparisons *P<0.05, **P<0.01).

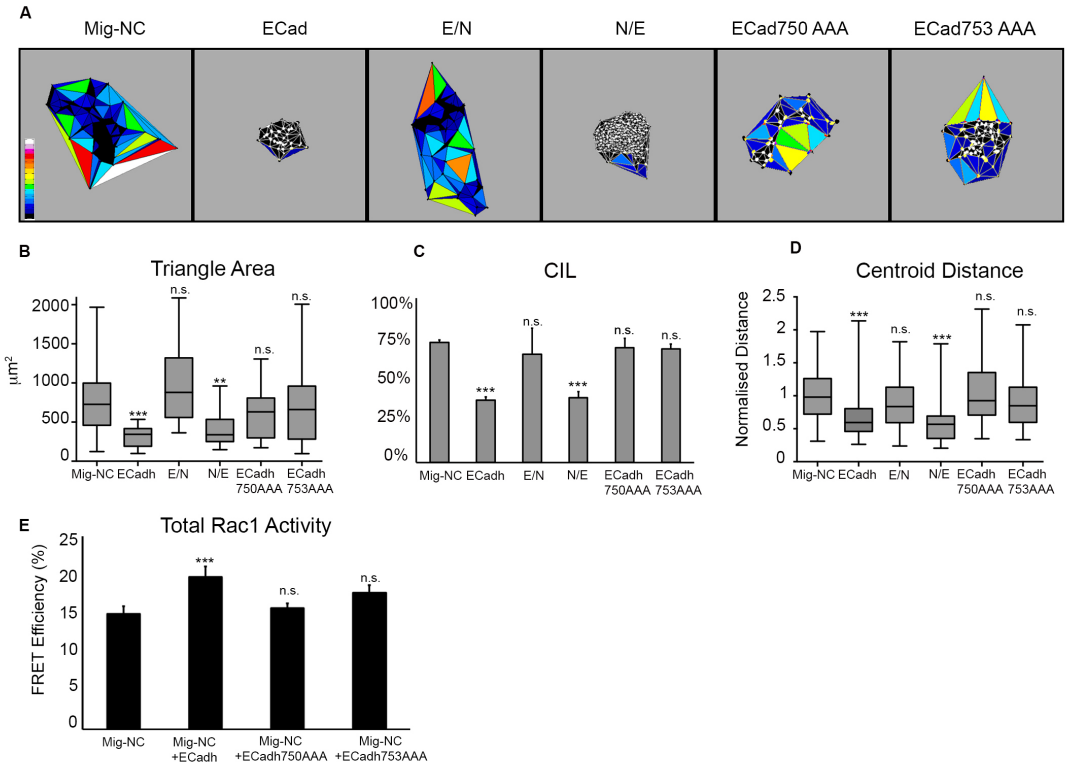

Figure 10.13. E-Cadherin cytoplasmic domain suppresses EMT, CIL and promotes Rac1 activity via its p120 binding site.

(A) Dispersion Assay triangulation diagrams and **(B)** Triangle areas at 400 minutes (Mig-NC n=28, E-Cadh n=22, E/N n=24, N/E n=19, 750AAA n=31, 753AAA n=27, 3 independent experiments, error bars: s.d., * P<0.05 *** P<0.01 *** P<0.001, Dunn's multiple comparison test). **(C)** Percentage of CIL (Mig-NC n=105, E-Cadh n=71, E/N n=80, N/E n=55, 750AAA n=50, 753AAA n=60, 2 independent experiments, error bars: s.e.m., Taillard Contingency Tables for Proportion Comparison ***α=0.1%). **(D)** Distance between cells centroids 30 minutes after collision (Mig-NC n=105, E-Cadh n=71, E/N n=80, N/E n=55, 750AAA n=50, 753AAA n=60 collisions, 2 independent experiments, error bars: s.d., *** P<0.001, Dunn's multiple comparison test). **(E)** Total Rac1 FRET efficiency measured by acceptor photobleaching for Mig-NC, Mig-NC+E-Cadh and the p120-uncoupled mutants E-Cadh750AAA and E-Cadh753AAA (n=16 Mig-NC,

n=22 Mig-NC+E-Cadh, n=15 Mig-NC+E-Cadh750AAA, n=12 Mig-NC+E-Cadh753AAA, 5 independent experiments * P<0.05, *** P<0.001).

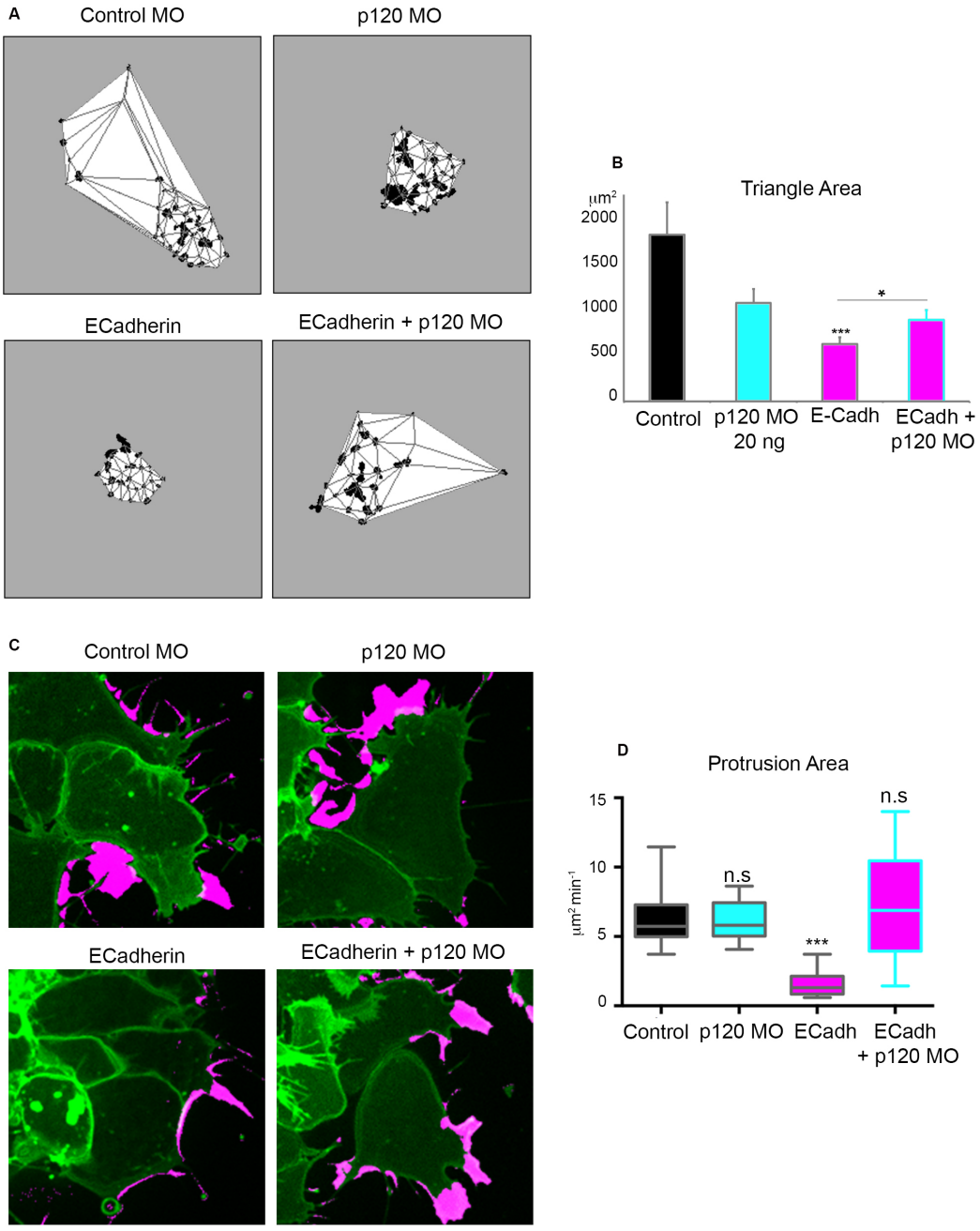

Figure 10.14. p120 is required downstream of E-Cadherin to suppress EMT and contact-dependent protrusion polarity.

(A) Dispersion Assay triangulation diagrams. **(B)** Triangle areas at 400 minutes (Mig-NC n=18, E-Cadh n=16, p120 MO n=36, p120 MO+ E-Cadh n=38, 3 independent experiments, error bars: s.e.m., * P<0.05 *** P<0.001, Dunn's multiple comparison test).**(C)** Protrusive activity of Mig-NC and Mig-NC+ECadh upon p120 knockdown. Time-lapse stills of a maximal projection, Free Edge

protrusions labelled in magenta, scale bar 10 μm. **(D)** Quantitation of Protrusion Area per minute at cluster free edge per cell by subtraction analysis (Control n= 43, p120-MO n=50, E-Cadh n=58, E-cadh+p120 MO n=69, 2 independent experiments, error bars: s.d., *** P<0.001, Dunn's multiple comparison test).

3. Repolarization of protrusions and of forces triggers cell-cell junction disassembly during CIL

I have shown that neural crest cells acquire CIL at the time of their EMT and that acquisition of CIL behaviour and of the ability to disassemble cell-cell junctions correlates with the loss of E-Cadherin expression and with the acquisition of N-Cadherin expression and of Rac1 dependent polarity of protrusions. I have then proceeded to investigate whether E-Cadherin might repress CIL before the onset of EMT, and I found that E-Cadherin inhibits migration in vivo and CIL and EMT in vitro by controlling the polarity of cell protrusions and of Rac1 distribution in a p120 dependent manner. Based on these results, I reasoned that the repolarization of Rac1 and in turn, of lamellipodial protrusions away from the cell contact might be a causal factor in promoting the disassembly of the cell-cell junction that occurs during CIL and during EMT-mediated neural crest dispersal.

Repolarization of protrusions induces cell-cell junction breakdown during CIL

To support causality between protrusion repolarization and junctional breakdown, I analysed the temporal sequence of cell-cell junction disassembly and lamellipodial protrusion formation in collisions of Mig-NC, using p120-GFP and lifeact-Cherry to identify cell-cell junctions and lamellipodial protrusions respectively (Fig. 11.1 A, Supplemental Movie S12). I found that new protrusions formed away from the cell contact whilst cell-cell adhesion complexes were still present (Fig. 11.1 A, arrows, 11.1 D). Moreover, protrusion area and junction width inversely correlated during CIL of Mig-NC (Spearman r=-0.9426, *P=0.017) (Fig.11.1 C). In addition, ratiometric Rac1 FRET imaging of live Mig-NC collisions (Fig. 11.1 B, Supplemental Movie S12) demonstrates that active

Rac1 increases opposite to the cell contact upon collision when the cells are still in contact. These observations show that repolarization of protrusions opposite of the cell-cell contact site precede, and therefore could promote, junction disassembly during CIL. On the other hand, in line with previous observations in fixed samples (Carmona-Fontaine et al., 2008), live FRET imaging showed RhoA activity to be high at the cell-cell contact for the duration of the whole cell collision (Figure 11.1 C, arrows), while little active RhoA was observed at the newly repolarizing protrusion (Fig. 11.1 C, arrowhead). Importantly, unlike Rac1, RhoA activity did not seem to be dynamically reoriented during the repolarization phase of CIL. In neural crest cells, CIL relies on Wnt/PCP signalling, which in turn activates a RhoA/ROCK signalling pathway (Carmona-Fontaine et al., 2008). Because ROCK activation downstream of RhoA mainly impinges on phosphorylation of the myosin regulatory light chain (MRLC), which is important for tail retraction in migrating mesenchymal cells (Ridley et al., 2003) and because actomyosin distribution has not yet been investigated during CIL in neural crest cells, I imaged collisions of migratory neural crest cells expressing MRLC2-GFP (Fig. 11.2). I observed that actomyosin structures are localised at the cell leading edge before and at early timepoints of collision (Fig. 11.2 A, B and Supplemental Movie S15, left panel), are then disassembled upon cell-cell contact formation (2-7 minutes, Fig.11.2 B) and finally accumulate at the rear of the cell, in proximity of the contact shortly before junction disassembly, after the cells have repolarised their protrusions (Fig. 11.2 A, B). In contrast with RhoA activity, actomyosin distribution seems to be dynamically regulated during CIL. It is worth noting, however, that accumulation of myosin seem to occur at very late timepoints of cell-cell collisions, after protrusion repolarization has

taken place (Fig. 11.2, arrows), which suggest it may have a secondary role in junction disassembly. In addition, functional studies of CIL in chick heart fibroblasts have suggested that ROCK might promote CIL in a myosin-independent manner, as blockade of myosin contractility using the ATPase inhibitor Blebbistatin only mildly affects the polarity switch occurring during CIL (Kadir et al., 2011). Although inhibition of myosin function remains to be tested in our system, these findings suggest that myosin contractility might not be essential for repolarization during CIL. In summary, these observations show that repolarization of protrusions and of Rac1 activity, but not of RhoA activity and actomyosin assembly, opposite of the cell-cell contact site precede, and therefore could promote, junctional disassembly during CIL.

To address the hypothesis of a causal relationship between protrusion repolarization and cell-cell adhesion disassembly, we inhibited the formation of new protrusions in Mig-NC cell doublets by restricting them on H-shaped or circular-shaped micropatterns of two different sizes (Tseng et al., 2012). I then compared their ability to separate and undergo CIL with the same ability of cells without confinement. CIL occurred efficiently between freely migrating Mig-NC (Fig11.3, A top panels), while its frequency was significantly decreased in cells plated on micropatterns (Fig. 11.3 A, middle and bottom panels; Fig. 11.3 B) where cells maintained cell-cell contacts (Fig. 11.3 A, middle and bottom panels; Fig. 11.3 C). These effects were even more evident on smaller micropatterns (Fig. 11.3 B, C; Supplemental Movie S13), thus suggesting that the higher the confinement, the lesser the probability of cell separation. These findings suggest that repolarization of protrusions opposite to the cell-cell contact might a requirement for cell-cell adhesion breakdown. The analysis displayed in Fig.

11.3 was performed using neural crest cells expressing membrane GFP and nuclear RFP to identify the cell-shape and the number of nuclei on the micropattern to identify cell doublets, and it could not therefore be excluded that confined cells doublets whose plasma membrane was in close proximity to each other did not maintain a functional cadherin junction. For this reason, I investigated whether classical cell-cell adhesions were retained upon confinement of neural crest cells doublets on micropatterns by imaging the tagged cell-adhesion complex components N-Cadherin-Cherry, p120-GFP and α-Catenin-GFP. Cell-cell junctions in cells under confinement were maintained throughout, as evidenced by the continued presence of junctional markers N-cadherin-Cherry, p120-GFP, and α-Catenin-GFP (Fig. 11.4 A, C, E), while junctions were disassembled between unconstrained cells (Figs 11.4 A-F; Supplemental Movie S14). These results suggest that inhibition of protrusion repolarization is sufficient to maintain the cell-cell junction. Because actomyosin cytoskeleton also reorganises dynamically during CIL, we investigated the organization of actomyosin in confined conditions (Fig. 11.5). Interestingly, we observed that MRCL2-GFP accumulated in close proximity of cell-cell contacts when neural crest cells were confined in micropatterns (Fig. 11.5 A), thus suggesting that the RhoA/ROCK pathway is intact under confinement conditions and that the cells are able to specify a "back" identity at the cell-cell contact site. Prolonged, polarized myosin accumulation (Fig. 11.5 B, Supplemental Movie S16), however, is not sufficient to trigger cell-cell junction disassembly as neural cells in confined conditions were able to maintain their adherens junctions for long times (Fig. 11.3-11.4). In summary, I conclude that repolarization of protrusions is required for junction disassembly during CIL.

Protrusion repolarization via Rac1 is sufficient to trigger cell separation during CIL

The cell confinement experiments indicate that polarized formation of new protrusions opposite to the cell-cell contact is necessary for CIL. To confirm this conclusion and further test whether repolarization of protrusions upon collision is sufficient to drive CIL, I reasoned that manipulation of Rac1 activity in a spatiotemporally regulated manner might prove a good strategy to promote protrusion repolarization in neural crest cells. As a tool, I employed photoactivatable analogs of Rac1 (PA-Rac, and dominant-negative DN-PA-Rac) (Wu et al., 2009), which have been successfully used to stimulate localized lamellipodia formation in vitro (Wu et al., 2009) as well as directional cell migration in *Drosophila* and Zebrafish embryos in vivo (Wang et al., 2010; Yoo et al., 2010). Localized illumination of the cell membrane in PA-Rac expressing cells triggers induction of lamellipodia formation in a spatiotemporally tight manner, which allowed to further test the hypothesis that repolarization of protrusions is required to induce a CIL-like behaviour (Fig. 11. 6 A, B). We first verified the efficiency of Rac1 photoactivation in NC by illuminating single cells with control (control-514nm) or photoactivating wavelengths (PA-458nm) and measuring the protrusion area in the illuminated box over time (Fig. 11.6 A, B; Supplemental Movie S16). Only the PA-458nm was able to induce protrusions (Fig. 11.6B) in PA-Rac expressing cells or to trigger protrusion collapse in DN-PA Rac expressing cells (Fig.11.6 C, D, Supplemental Movie S17). Consistently with what previously observed in cell confinement experiments (Fig. 11.3-11.4), inhibition of protrusion formation in Mig-NC doublets by using a dominant-negative-PA-Rac1 (Wu et al., 2009) (DN-PA-Rac; Supplemental Movie S17) prevented the separation of cells (Fig. 11.7 A-D; and Movie S18).

We then employed the PA-Rac1 to induce protrusion repolarization in E-Cadherin expressing NC cell doublets, which do display CIL due to active Rac1 accumulation at the cell-cell contact and to depletion of active Rac1 from the free edge (Figure 11.8 A). Illumination of the free edges of Mig-NC+ECadh-GFP doublets with control-514nm (Fig. 11.8 B, top) did not result in new protrusions and cells maintained their cell-cell junction. Illumination with PA-458nm however, resulted in cell repolarization (Fig. 11.8 B, bottom) and in a significantly increased rate of cell separation (Fig. 11.8 C-D; Supplemental Movies S19 and S20). In addition, measurement of the intensity of E-Cadherin-GFP at the cell-cell junction in 514 nm and 458 nm illuminated cell doublets showed that cell separation was not due to non-specific downregulation of junctional E-cadherin caused by laser illumination (Fig. 11.9 A, B, Supplemental Movie S20). These results show that photoactivation of Rac1 at the free edges of E-Cadherin expressing cells is sufficient to trigger cell separation and rescues the inhibitory effect of E-Cadherin on CIL, thus indicating, first, that repolarization of protrusions is sufficient to trigger cell-cell junctional breakdown and, secondly, further supporting the notion that E-Cadherin mediated inhibition of CIL depends on the depletion of active Rac1 and therefore of lamellipodial protrusive activity at the cell free edges.

Taken together, cell confinement and Rac1 photoactivation experiments strongly suggest that formation of new protrusions opposite to the cell contact is necessary and sufficient to promote junction disassembly.

E-cadherin impairs CIL by perturbing the distribution of forces in Mig-NC

Why does repolarization trigger junction disassembly? During collective migration, a polarized group of cells forms new protrusions at its leading edge, exerting on the ECM traction forces, which are anisotropically distributed at the sites of cell protrusions (Reffay et al., 2014) and need to be counterbalanced by equal and opposite intercellular tensions for the group of cells to remain cohesive (Tambe et al., 2011; Tseng et al., 2012; Vitorino et al., 2011). I have shown that repolarization of protrusions occurs during CIL in Mig-NC and is necessary and sufficient for adherens junction disassembly. Based on this evidence, I postulate that cells move away from each other during CIL because traction forces generated by the polarised protrusions give rise to a stress sufficient to overcome the tensile strength of cell-cell adhesion sites and this subsequently acts to pull the cells apart. To test my hypothesis, I performed traction force microscopy to image and measure traction forces in Mig-NC explants, which exhibit polarised protrusions. Measurements of traction forces revealed that major forces are localized to the edge of the neural crest cluster and are oriented inwards (Fig. 11.10A). In contrast, Mig-NC+E-cadherin explants, that do not display polarised protrusions, exhibit randomly oriented traction forces in the middle of the clusters and significantly lower traction at the free edges compared with Mig-NC explants (Fig. 11.10 A, B). Overall, these results show that, while in polarized migratory neural crest traction forces are anisotropically distributed and oriented inwards, in neural crest explants which fail to polarise their protrusions, such as E-Cadherin expressing explants, traction forces are uniformly distributed across the centre of the explant and, in addition, they are depleted from the leading edges.

The polarised distribution of focal adhesion is perturbed in E-Cadherin expressing neural crest

As discussed in the Introduction of this thesis, cells adhere, migrate, sense tension and exert traction forces on their extracellular matrix by means of specialised adhesive structures that engage integrin receptors, signalling proteins, actin binding proteins and the actomyosin cytoskeleton, called focal adhesions. The area of focal adhesions (FA) through which cells migrate onto the extracellular matrix correlates with the traction force generated (Trichet et al., 2012). Because I observed a clear decrease in traction forces at the free edge of E-Cadherin expressing neural crest clusters when compared to Mig-NC, I reasoned that such decrease in traction forces might arise from a decrease in the number or size of focal adhesions in E-Cadherin expressing clusters. Therefore, I analysed the distribution, size and dynamics of FAs by expressing Focal Adhesion Kinase (FAK)-GFP and imaging it in living neural crest cell clusters (Fig. 11.11 A-B; E-F) or by immunostaining against Phospho-paxillin (Fig. 11.11 C-D) to detect endogenous focal adhesions. In line with the asymmetric distribution of traction forces at the border of neural crest clusters, Mig-NC explants show large and dynamic FAs distributed in a highly polarized fashion towards the free protruding edge (Fig 11.11 A, left). By overexpressing E-cadherin, however, the total area of FAs as well as their dynamics was reduced (Fig. 11.11 B-F). Importantly, FA numbers were strongly reduced at the free edge in cells overexpressing E-cadherin (Fig. 11.11 A, arrows, 11.11 D), and a mild increase in the number of focal adhesions detected in proximity of cell-cell contacts was observed (Fig. 11.11 A, arrows, 11.11 D). These observations are

consistent with the finding that traction forces are decreased at the free edge and increased in the centre of the explant in E-Cadherin expressing cells.

Intercellular tension and tension across focal adhesions is differentially polarized in E-Cadherin expressing neural crest cells

Our observation of traction forces show that in repolarizing Mig-NC explants such forces are anisotropically distributed towards the border of the cluster, and that this asymmetry is lost upon E-Cadherin expression, where cells fail to repolarize. Traction force microscopy solely allows direct measurement of tractions applied to the ECM, while intercellular tensions may only be derived indirectly (Maruthamuthu et al., 2011; Tseng et al., 2012). Such calculations are possible upon observation of traction forces in cell doublets (Maruthamuthu et al., 2011; Tseng et al., 2012) or in epithelial monolayers (Tambe et al., 2013), but not in multi-layered mesenchymal cell clusters such as neural crest explants. Therefore, to measure intercellular tensions in N-Cadherin expressing migratory neural crest and in E-Cadherin overexpressing cells, I had to use an alternative experimental strategy. Vinculin localises to both FA and cell-cell contacts in neural crest cells (Kuriyama et al., 2014), and, as discussed in the Introduction of this thesis, a vinculin tension sensor (Vinculin-TS) FRET probe has been developed, which allows the measurement of tension across vinculin molecules both at FAs (Grashoff et al., 2010) and at cell-cell contacts (Grashoff et al., 2010; Kuriyama et al., 2014). Using the Vinculin-TS probe, I found that in Mig-NC, tension across Vinculin was high at the cell leading edges, where most FAs are localised, and lower at cell-cell contacts, a finding suggestive of a disproportion between traction forces at the cell-extracellular matrix interface and N-Cadherin

mediated intercellular tensions. On the other hand, Mig-NC+E-cadherin cells showed increased tension at cell-cell contacts and a strong reduction in tension across FAs at the free edge (Fig. 11.12 A, B). Given that in E-Cadherin expressing cells FA can also occasionally be found in proximity of the cell-cell junction, I cannot exclude that the observed increase in tension across Vinculin at the cell-cell adhesion may partially derive from Vinculin-positive focal adhesions located in proximity of the cell-cell contact. Nevertheless, these results show that in E-Cadherin expressing cells the disproportion between traction forces and intercellular tensions is reversed, compared to polarized migratory neural crest, in favour of intercellular tensions.

Overall, these data indicate that during EMT there is a dramatic repolarization of forces, consistent with Mig-NC cells undergoing CIL and breaking down the junction, as the traction forces pull them apart. Such repolarization of forces is not observed in E-Cadherin expressing neural crest, which are unable to undergo EMT and CIL as they do not break down their cell-cell junction.

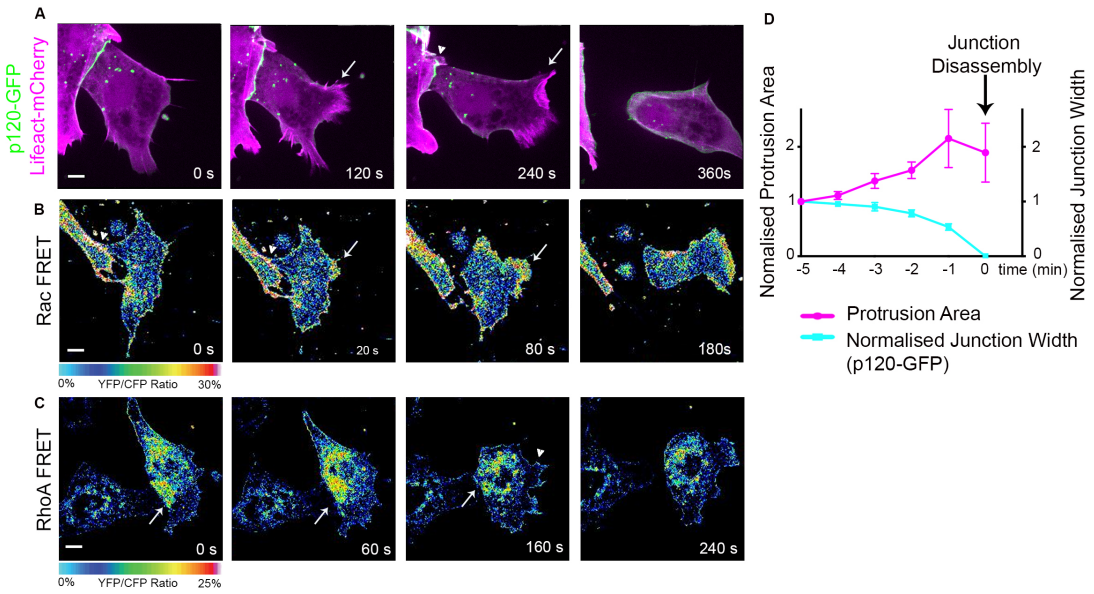

Figure 11.1. Repolarization of protrusions and of Rac1 activity precedes junctional disassembly.

(A) Time lapse stills of junction disassembly in a Mig-NC cell-cell collision. Cells expressing p120-GFP and lifeact-Cherry, scale bar 5 μm. **(B)** heatmap stills of Raichu-Rac1 FRET, scale bar 7.5 μm, representative image for n=9 collisions from 3 independent experiments. **(C)** heatmap stills of Raichu-RhoA FRET, scale bar 7.5 μm, representative image for n=11 collisions from 3 independent experiments. **(D)** Protrusion area and junction width over time. Junction disassembly occurs at t=0. Cell-cell junctions were identified by recruitment of p120-GFP (n=11 cell-cell collisions, 4 independent experiments, error bars: s.e.m, Spearman correlation coefficient r=-0.943 *P=0.017).

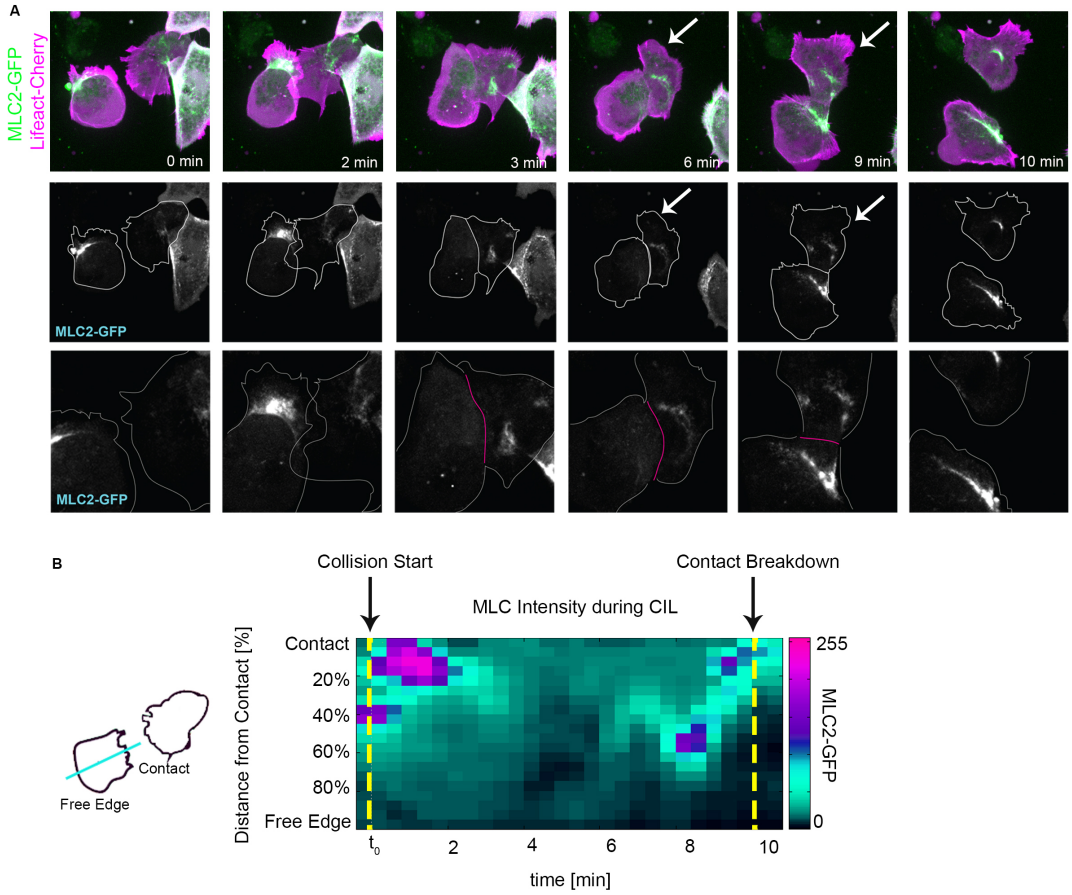

Figure 11.2. Accumulation of MLC2 in proximity of the cell-cell contact precedes junctional disassembly.

(A) Time lapse stills of a representative collision between two migratory neural crest cells expressing MRLC2-GFP and Lifeact-Cherry (top), MRLC2 channel only (centre) and zoom-ins of the cell-cell contact site (bottom). Myosin accumulates in proximity of the cell-cell contact after repolarization of protrusions has taken place (arrow). **(B)** Linescan analysis of myosin intensity over time for the collision depicted in (A). Actomyosin structures localise at the cell leading edge before and at early timepoints of collision, are then disassembled upon cell-cell contact formation (2-7 minutes) and finally accumulate at the rear of the cell, in proximity of the contact shortly before junction disassembly. Representative image and analysis for n=11 collisions from 4 independent experiments.

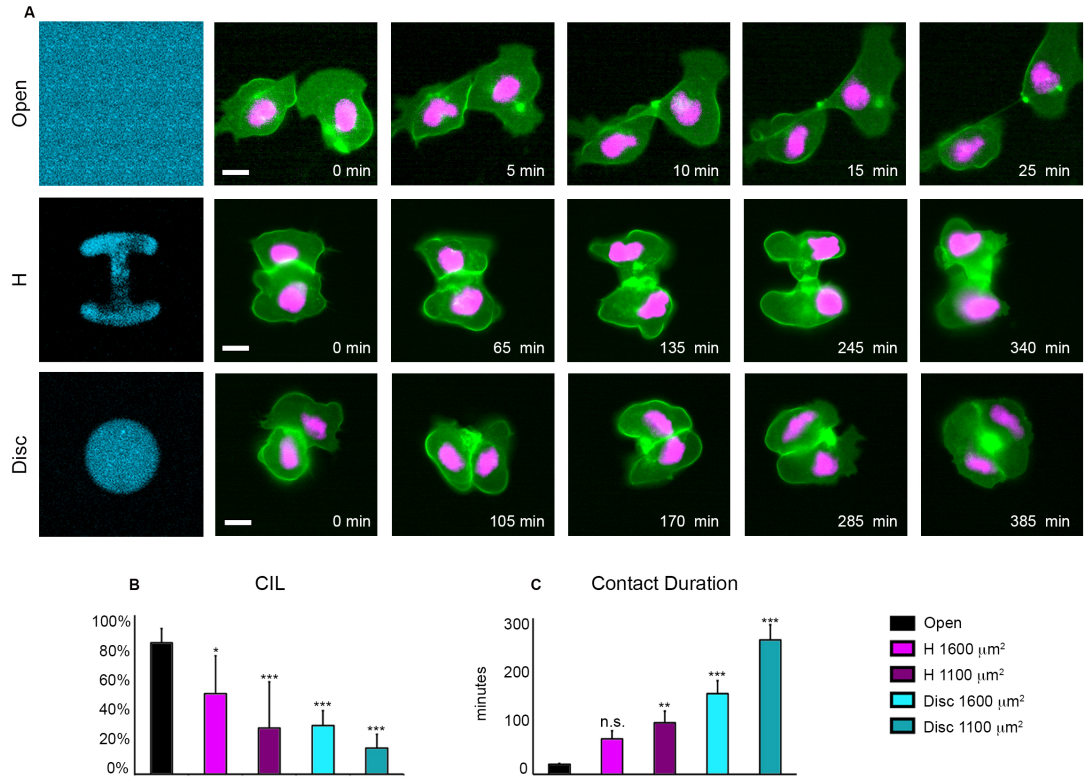

Figure 11.3. Repolarization of protrusions is required to promote junction disassembly.

(A) Time lapse photographs of confined cells. Mig-NC labelled with membrane GFP and nuclearRFP (nRFP) cultured on uniform or H-shaped or Disc-shaped micropatterns of fibronectin (Fn-650). Scale bar 10 μm. **(B)** Percentage of CIL (Freely Migrating (FM) n=139, H 1600 μm^2 n=61, H 1100 μm^2 n=35, Disc 1600 μm^2 n=34, Disc 1100 μm^2 n=22 collisions, 2 independent experiments, error bars: s.e.m., Taillard Contingency Tables for Proportion Comparison *α=5%, ***α=0.1%). **(C)** Duration of cell-cell contact (FM n=139, H 1600 μm^2 n=61, H 1100 μm^2 n=35, Disc 1600 μm^2 n=34, Disc 1100 μm^2 n=22 collisions, 2 independent experiments, error bars: s.e.m., ** P<0.01 *** P<0.001 Dunn's multiple comparisons.).

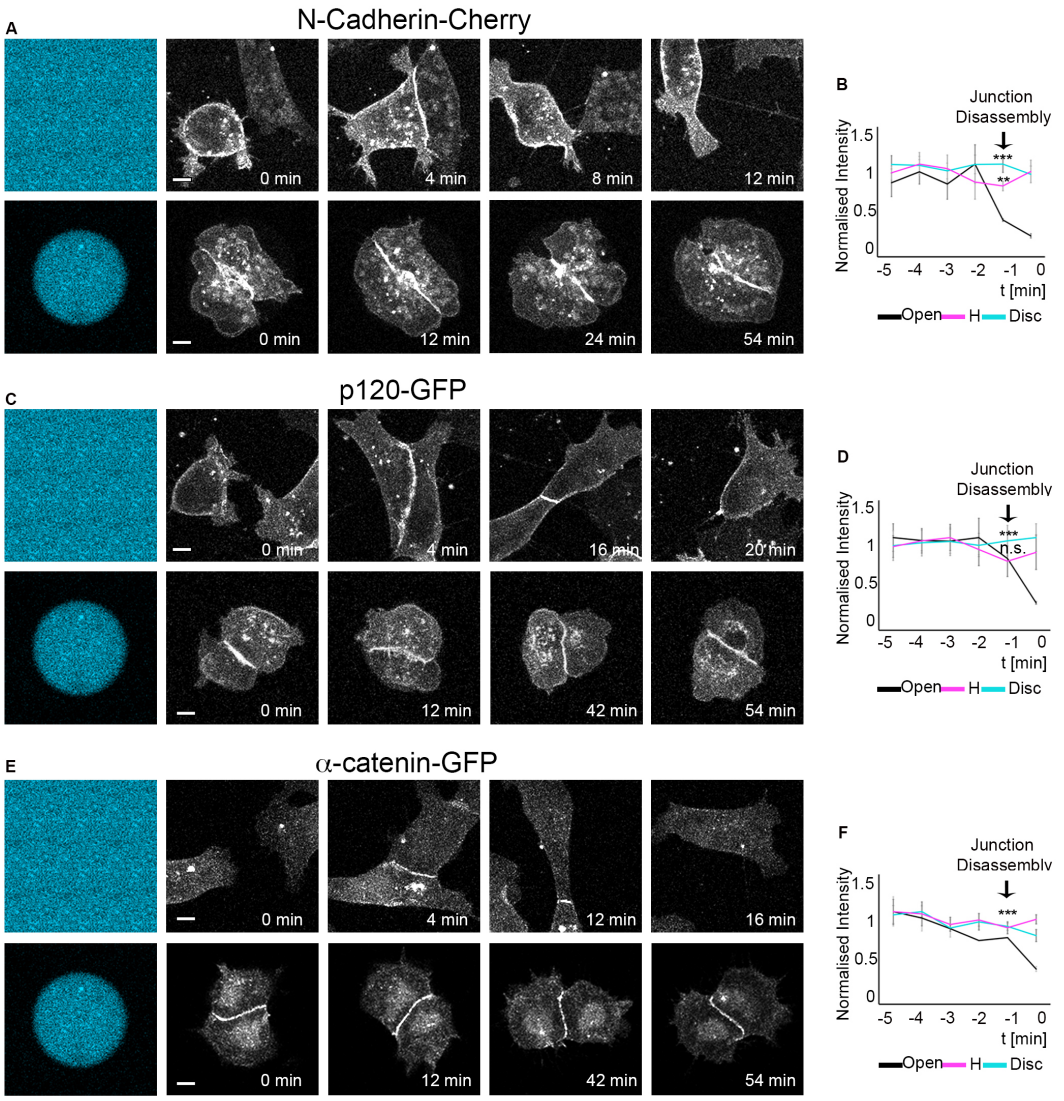

Figure 11.4. Cell confinement is sufficient to maintain adherens junctions.

(A, C, E) Time-lapse stills of of Mig-NC confined on a disc micropattern expressing N-Cadherin-Cherry (A), p120-GFP (C), α-catenin-GFP (E), scale bar 5 µm. **(B, D, F)** Normalised fluorescence intensity over time for N-Cadherin-Cherry (B), p120-GFP (D), α-catenin-GFP (F). N-Cadherin-Cherry FM n=7, H n=4, Disc n=6; p120-GFP FM n=7, H n=4 Disc n=8; α-catenin-GFP FM n=9, H n=4 Disc n=4; 4 independent experiments, error bars: s.e.m. Representative image and analysis for n=11 collisions from 4 independent experiments.

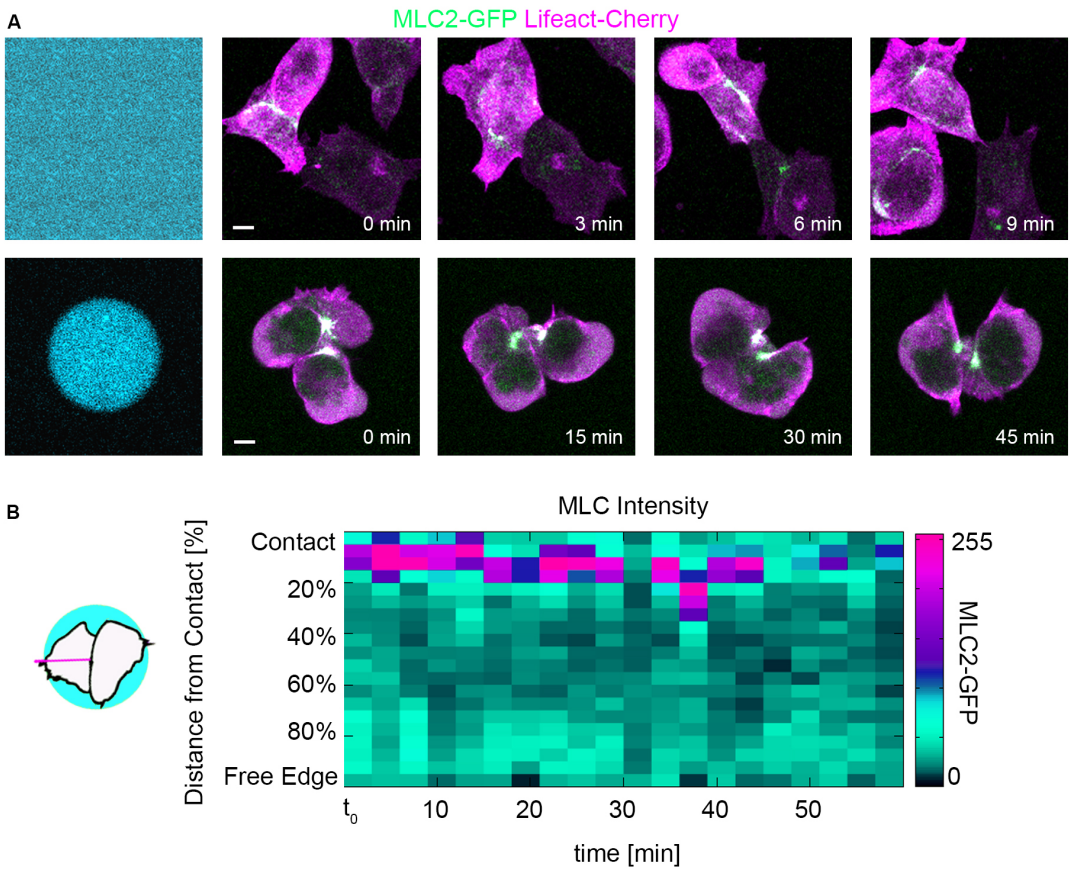

Figure 11.5. Distribution of actomyosin in confined neural crest cells.

(A) Time lapse stills of a representative collision between two migratory neural crest cells expressing MRLC2-GFP and Lifeact-Cherry in open fibronectin(top) or confined on disc-shaped micropatterns (bottom), scale bar 5 µm. **(B)** Linescan analysis of myosin intensity over time for the collision depicted in (A). Representative image and analysis for n=7 cell doublets.

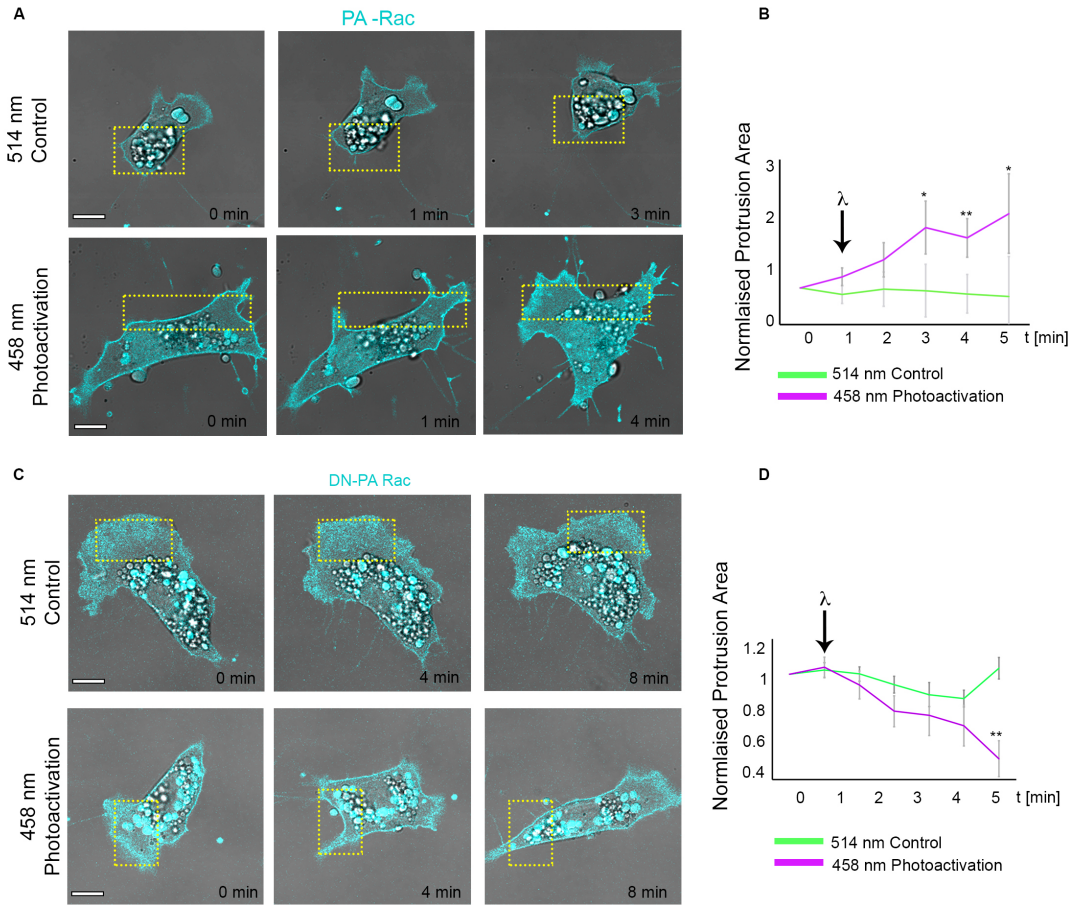

Figure 11.6. Validation of Photoactivatable Rac1 analogs in *Xenopus* neural crest cells.

(A) Photograms from a photoactivation experiment. Mig-NC expressing PA-Rac-Cherry. Illumination of the area in the box (white dashed lines) with 514 nm control wavelength (top) does not trigger cell protrusion; illumination of the area in the box (white dashed lines) with 458 nm wavelength results in formation of a new protrusion(bottom), scale bar 10 µm. **(B)** Protrusion area over time. Illumination occurs at t=1 min (arrow) (514 nm n=5 cells, 458 nm n=6 cells, * P<0.05 **P<0.01). **(C)** Photograms from a DN-Rac photoactivation experiment. Mig-NC expressing DN-PA-Rac-Cherry. Illumination of the area in the box (white dashed lines) with 514 nm control wavelength (top) does not trigger protrusion collapse; illumination of the area in the box (white dashed

lines) with 458 nm wavelength results in collapse of the protrusion in the illumination area(bottom), scale bar 10 μm. **(D)** Protrusion area over time. Illumination occurs at t=1 min (arrow) (514 nm n=5 cells, 458 nm n=5 cells, **P<0.01).

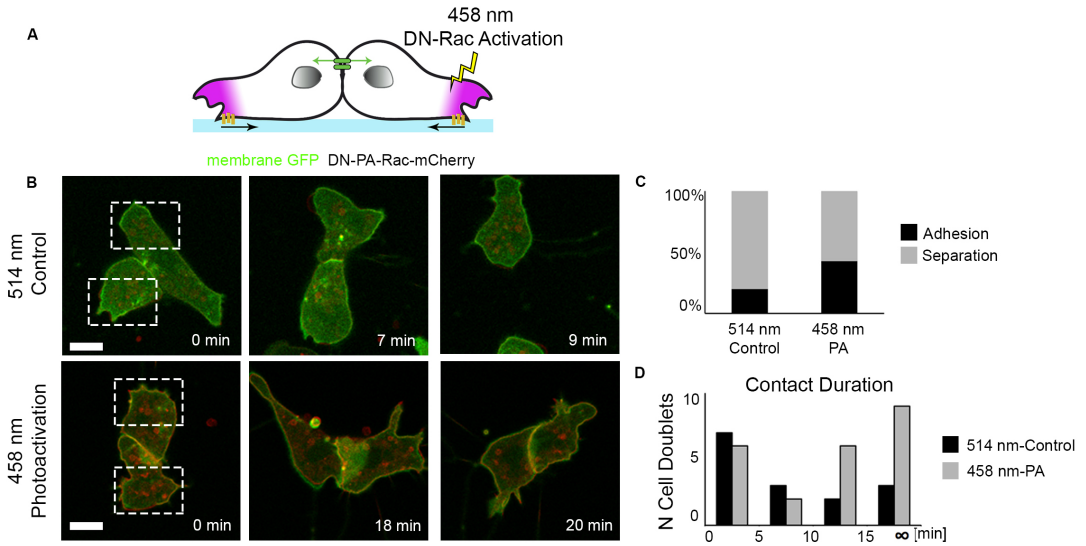

Figure 11.7. Blockade of protrusion repolarization by DN-Rac1 photoactivation inhibits cell separation.

(A) Strategy of DN-PA-Rac1 photoactivation experiments. **(B)** Stills of Mig-NC doublets expressing DN-PA-Rac-Cherry. Illumination in boxed areas with 514 nm control wavelength (top) or with 458 nm wavelength (bottom), scale bar 10 µm. Numbers indicate each cell. **(C)** Percentages of adhesion and separation upon Photoactivation in DN-PA-Rac-Cherry Mig-NC (n= 15 cells 514 nm, n=21 cells 458 nm, 3 independent experiments). **(D)** Histogram of contact duration upon Photoactivation in DN-PA-Rac-Cherry expressing Mig-NC; ∞: cell adhesion (n= 15 cells 514 nm, n=21 cells 458 nm, 3 independent experiments).

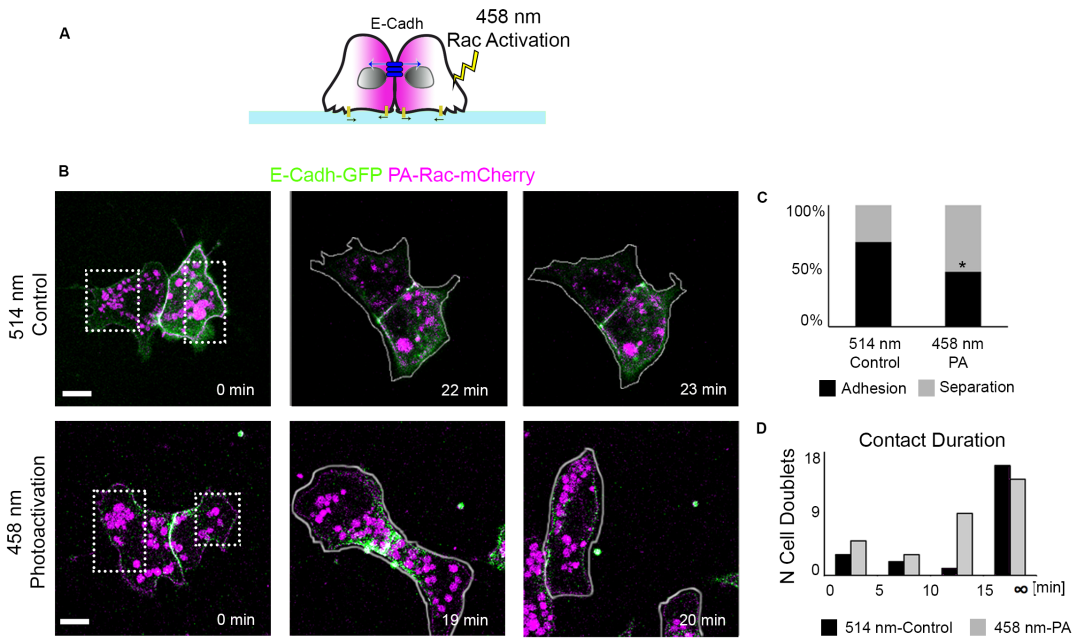

Figure 11.8. Inducing protrusion repolarization by Rac1 photoactivation is sufficient to trigger CIL and junction disassembly.

(A) Strategy of PA-Rac1 photoactivation experiments. **(B)** Stills of E-Cadh-GFP/PA-Rac-Cherry expressing Mig-NC doublets. Illumination of boxed areas with 514 nm control wavelength (top) or with 458 nm wavelength (bottom), scale bar 10 µm. **(C)** Percentages of adhesion and separation upon Photoactivation in E-Cadh-GFP/PA-Rac-Cherry Mig-NC (n= 24 cells 514 nm, n=31 cells 458 nm, 6 independent experiments**,** Taillard Contingency Tables for Proportion Comparison *α=5%) **(D)** Histogram of contact duration in E-Cadh-GFP/PA-Rac-Cherry Mig-NC upon Photoactivation; ∞: cell adhesion (n= 24 cells 514 nm, n=31 cells 458 nm, 6 independent experiments).

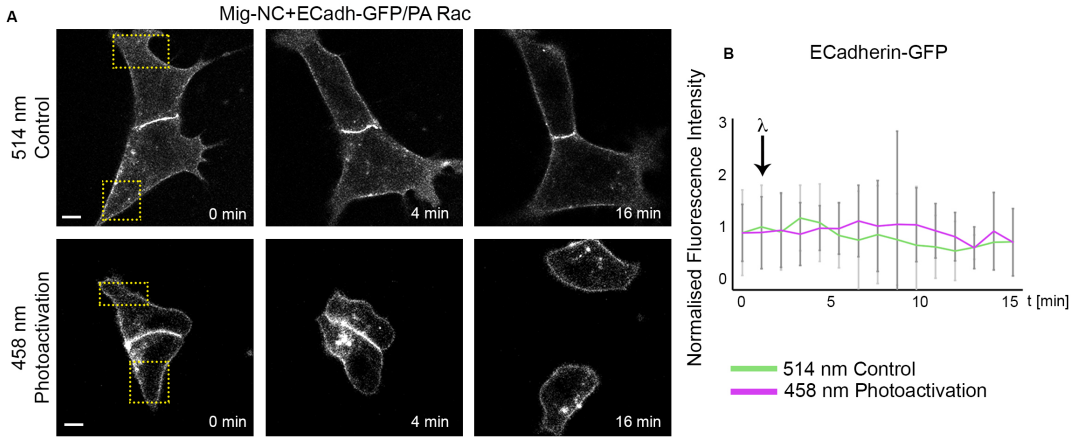

Figure 11.9. Photoactivation of PA-Rac1 does not affect E-Cadherin intensity at the cell-cell junction.

(A) Time lapse stills from a photoactivation experiment. Mig-NC expressing E-Cadh-GFP and PA-Rac Cherry. Illumination of the area in the box (yellow dashed lines) with 514 (top)or 458 nm (bottom) wavelength does not alter E-Cadh-GFP localization, scale bar 10 µm. **(B)** Normalised E-Cadh-GFP junctional intensity over time. Illumination occurs at t=1 min (arrow) (514 nm n=6 cells, 458 nm n=6 cells).

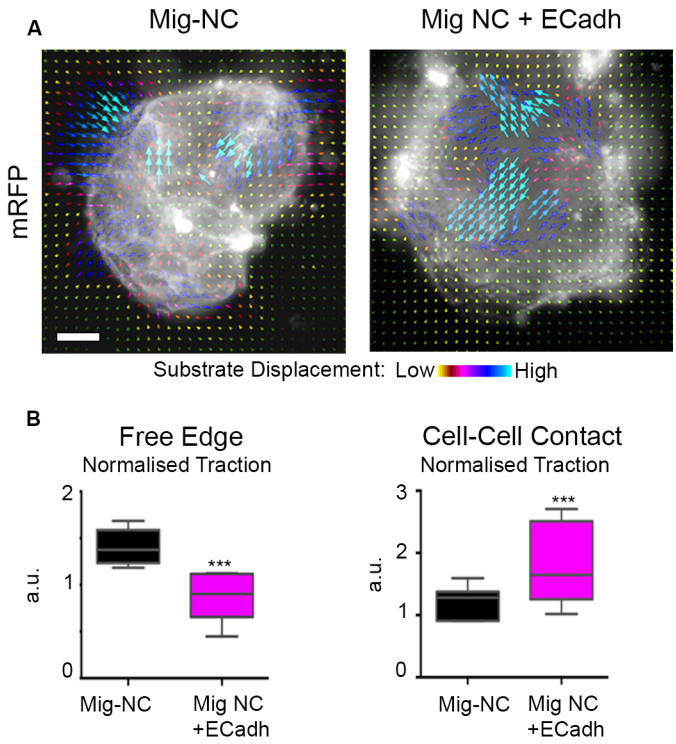

Figure 11.10. E-cadherin impairs CIL by perturbing the distribution of forces in Mig-NC.

(A) Traction Force Microscopy superimposed to membrane RFP, arrows: magnitude and direction of bead displacement, scale bar 20 µm. **(B)** Normalised traction forces (TF) at free edge (left) and cell-contacts (right). (Mig-NC n=9, Mig-NC+E-Cadh n=7 explants, 3 independent experiments, error bars: s.d. *** P<0.001 Student's t-test).

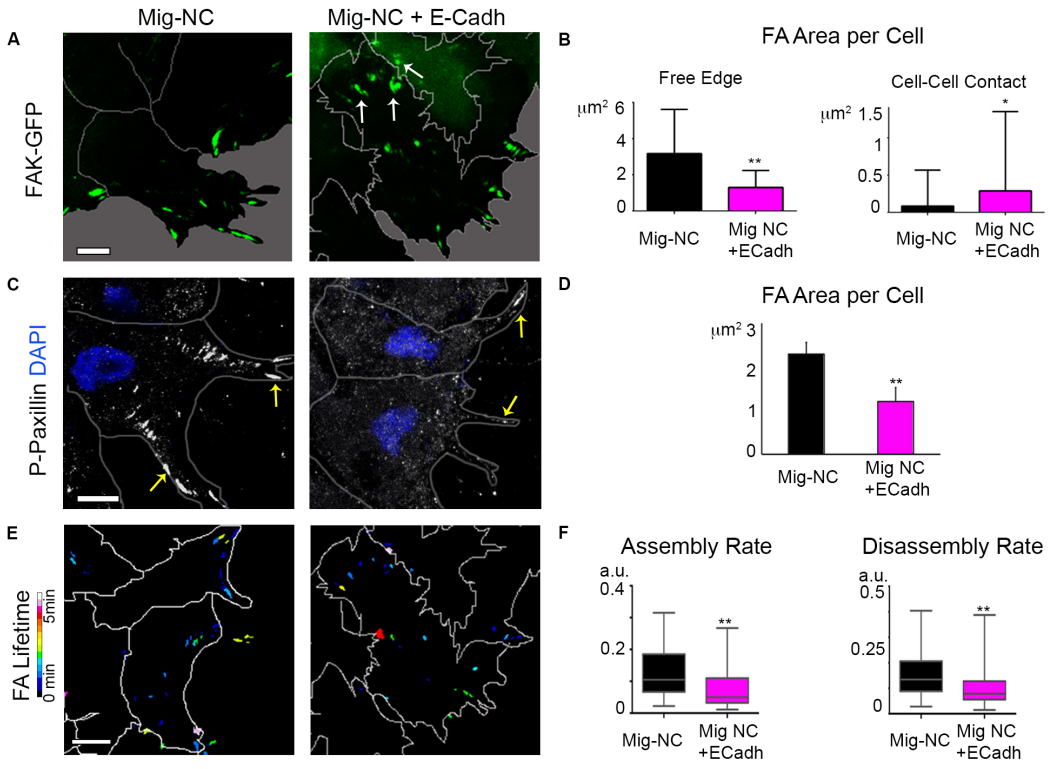

Figure 11.11. Focal Adhesion area, polarity and dynamics are reduced in E-Cadherin expressing migratory neural crest cells.

(A) Stills of Mig-NC and Mig-NC+E-Cadh explants expressing FAK-GFP, cell borders outlined, scale bar 5 µm. **(B)** Focal adhesion (FA) area per cell at free edge (left) and cell-contacts (right) (Mig-NC n=32, Mig-NC+E-Cadh n=56 cells, 2 independent experiments, error bars: s.d. * P<0.05 ** P<0.01 Mann-Whitney test). **(C)** P-Paxillin immunostaining in Mig-NC and Mig-NC+ECadh, FA: arrows, cell borders outlined, scale bar 10 µm, nuclear staining: DAPI. **(D)** FA area per cell (Mig-NC n=10, Mig-NC+E-Cadh n=10 explants, 2 independent experiments, error bars: s.e.m. ** P<0.01 Student's t-test). **(E)** Heatmap of focal adhesion (FA) lifetime in Mig-NC and Mig-NC+E-Cadh, scale bar 10 µm. **(F)** Left: Assembly Rate of FA in Mig-NC and Mig-NC+E-Cadh (Mig-NC n= , Mig-NC+E-Cadh n= **P<0.01 Mann-Whitney test). Right: Disassembly Rate of FA in Mig-NC and Mig-NC+E-Cadh (Mig-NC n= , Mig-NC+E-Cadh n= **P<0.01 Mann-Whitney test).

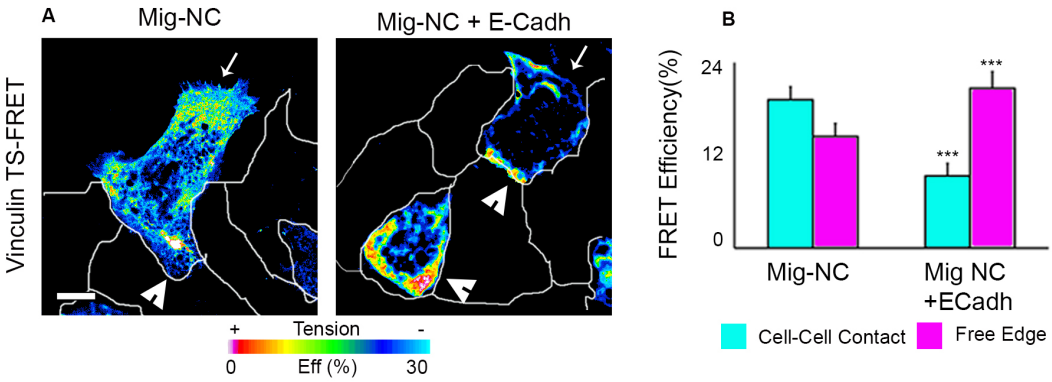

Figure 11.12. Tension across Vinculin is anisotropically distributed in migratory neural crest cells and its pattern is reversed by E-Cadherin ectopic expression.

(A) Spatial distribution of tension in Mig-NC and Mig-NC+E-Cadh clusters measured by Vinculin-TS FRET. In Mig-NC, tension is high at leading edge (arrow) and inhibited at cell-cell contact (arrowheads); in Mig-NC+E-Cadh tension distribution is opposite. Cell borders outlined, scale bar 5 μm. **(B)** Vinculin-TS FRET efficiency at cell-cell contact and leading edge (n= 24 cells Mig-NC, n=24 cells Mig-NC+E-cadh, 2 independent experiments, error bars: s.e.m, *** P<0.001 Student's t–test).

IV. Discussion

1. Model Overview

During CIL, neural crest cells form transient cell-cell contacts, which disassemble as the cells repolarize in opposite directions. Here, I propose a model for Contact Inhibition of Locomotion in which polarization of Rac1 activity, protrusions, and focal adhesions in mesenchymal Mig-NC leads to strongly polarized traction forces, which may override intercellular tension across N-cadherin junctions that eventually disassemble (Fig. 12.1 i). In epithelial Premig-NC or in Mig-NC ectopically expressing E-cadherin, Rac1 activity and FAs are polarized towards the cell-cell junction and protrusions away from the contact are small, leading to smaller traction forces at the free edge counterbalanced by E-cadherin cell-cell junctions (Fig. 12.1 ii). Importantly, these findings suggest a correlation between acquisition of CIL behaviour and EMT in neural crest cells. I propose that, during EMT, loss of E-Cadherin and switching to N-cadherin results in a switch in contact-dependent polarity of Rac1 in neural crest cells. They acquire the ability of forming highly polarized protrusions and exert high traction forces over the substrate, which N-Cadherin intercellular tensions (Fig. 12.1 iii). I propose that this disproportion of tension leads to cell dispersion during neural crest EMT (Fig. 12.1 iii). In summary, I conclude that CIL behaviour is acquired concomitantly with EMT through downregulation of E-cadherin (Fig. 12.1iii).

2. Is adhesion between E-Cadherin and N-Cadherin different?

I have shown that neural crest acquire CIL during their development. Before the onset of EMT, neural crest cells express E-Cadherin and do not display a contact

inhibition of locomotion behaviour, whereas at migratory stages neural crest downregulate E-Cadherin expression to switch to another classical cadherin, N-Cadherin, and acquire CIL behaviour. I have shown that knockdown of E-Cadherin or its functional blockade using an antibody results in a CIL-like behaviour in premigratory neural crest, while ectopic expression of E-Cadherin in migratory neural crest inhibits collective migration *in vivo* and EMT and CIL *in vitro*. Inhibition of collective neural crest migration has been reported to occur in increased cell-cell adhesion conditions: indeed, impaired N-Cadherin recycling by knockdown of the LPA receptor Edg4 leads inhibits migration of neural crest *in vivo* and EMT *in vitro* (Kuriyama et al., 2014). My results suggest that increased cell-cell adhesion *per se* is not responsible for the observed phenotypes, as overexpression of equivalent levels of N-Cadherin does not inhibit EMT or CIL. Nevertheless, to understand whether the inhibition of cell separation driven by E-Cadherin might be imputable to stronger cell-cell adhesion, I characterized the composition of E- and N-Cadherin junctions in neural crest cells. Our results show that both E- and N-cadherin are able to organize an adhesion containing the junction components p120, β-catenin and α-catenin, although in both premigratory and E-Cadherin overexpressing neural crest cells the recruitment of catenins at the cell-cell junction is increased. However, my analysis of the biochemical interaction of E- or N- cadherin with β-catenin and α-catenin shows no significant difference in affinity of the two cadherins to the complex. Considering that, in neural crest, EMT is inhibited by impaired cadherin recycling (Kuriyama et al., 2014), I analysed p120 and β-catenin molecular dynamics by FRAP to address whether E-Cadherin expression would affect the half-life of these proteins at the cell-cell junction. However, my

results suggest that E-Cadherin exerts a mild effect on junctional stability of the cadherin-catenin complex in neural crest, which may not account for the strong inhibition of EMT, CIL and migration I observe. Altogether, my results do not clearly show a difference in adhesion between E-Cadherin and N-Cadherin junctions in neural crest cells. Interestingly, it is currently still unclear whether the strength of E- and N-Cadherin based junctions is different. Indeed, in vitro studies of analytical ultra centrifugation show that the homophilic binding affinity of N-Cadherin extracellular domain is about fourfold higher than in E-Cadherin (Katsamba et al., 2009). In contrast, dual pipette separation studies performed in cells in suspension suggest the E-Cadherin junction to be stronger than the N-Cadherin one (Chu et al., 2004), thus making unclear whether there might be any difference in N- and E- Cadherin adhesive strength. It is worth noting that AUC experiments as well as dual pipette separation assays use highly purified proteins or cells grown in suspension, respectively, to assess for cadherin binding affinity. Such experimental conditions are highly artificial and very far from the conditions in which cadherins are found in cells *in vivo* or even in culture, and do not take into account any influences on the strength of cell-cell interactions exerted by interactions of the cell with the extracellular matrix (Borghi et al., 2010), or by actomyosin cytoskeletal structures, which control maintenance and clustering of cadherins junctions in their native configuration (Ratheesh et al., 2012; Smutny et al., 2010). In addition, to rule out whether the inhibition of CIL and migration exerted by E-Cadherin might be mediated by an increase in adhesion strength via its extracellular domain, I generated chimaeric cadherins in which the extracellular and cytoplasmic domain of N- and E-Cadherin had been exchanged. Importantly, my findings suggest that the

intracellular domain of E-Cadherin rather the extracellular adhesive domain is responsible for the suppression of CIL, EMT and migration, thus supporting the notion that E-Cadherin might suppress CIL through a mechanism alternative to a simple increase in junctional strength via homophilic *trans* and *cis* clustering of its extracellular domain. Indeed, I have found that in premigratory neural crest cells endogenously expressing E-Cadherin, as well as in E-Cadherin overexpressing migratory neural crest cells, E-cadherin inhibits the formation of outward protrusions by controlling the distribution of active Rac1. In addition, experiments using chimaeric cadherin mutants as well as p120 uncoupled E-Cadherin mutants suggest that E-cadherin-dependent regulation of Rac1 and lamellipodial protrusion polarity might be regulated by E-Cadherin cytoplasmic domain by signalling via p120.

3. How is the polarized distribution of Rac1 activity regulated?

In my working model, a key factor that triggers a switch between epithelial behaviour and migratory mesenchymal behaviour and CIL is the polarised distribution of Rac1 activity. E-Cadherin endogenous or ectopic expression in premigratory and migratory neural crest, respectively, leads to redistribution of active Rac1 at the sites of cell-cell contact, while in migratory neural crest Rac1 is strongly polarized opposite to the junction at the leading edge of the cell. Importantly, the polarized distribution of Rac1 at the free edge of migratory neural crest clusters has been previously shown to rely on N-Cadherin. Indeed, functional blockade of N-Cadherin function using a monoclonal antibody leads to a decrease in global Rac1 activity and to an increase in Rac1 activity at the cell-

cell contact (Theveneau et al., 2010), thus suggesting that E- and N- Cadherin have opposing effects on the distribution of active Rac1. How may such a differential effect be achieved?

As discussed in the Introduction, N- and E- Cadherin are classical type I cadherins. Their overall domain organisation is highly conserved between the two, and, in particular, their cytoplasmic domain is very similar, with a 73% homology in *Xenopus Laevis*.

One possibility for differential signalling between E- and N-Cadherin might arise from differential interaction with additional cofactors. Indeed, N-Cadherin, but not E-Cadherin, has been reported to functionally and physically interact with FGF receptors (Skaper et al., 2000; Williams et al., 2001). Interestingly, FGF8 has been recently shown to act as a chemoattractant for chick cardiac neural crest, which express FGFR1 and FGFR3 (Sato et al., 2011), and N-Cadherin is also required for neural crest chemotaxis (Theveneau et al., 2010). In neuronal growth cones, N-Cadherin facilitates the dimerization of the FGF receptor to initiate a growth factor independent signal, and N-Cadherin mediated FGF-signalling appears to be distinct from its adhesive activity (Utton et al., 2001; Williams et al., 2002). Importantly, treatment with downstream inhibitors of FGF signalling reduces N-Cadherin mediated invasion in cancer cells (Nieman et al., 1999). It is worth considering, however, that the interaction between FGF and N-Cadherin has been mapped to the EC 4 domain of N-Cadherin (Kim et al., 2000a). Using chimaeric cadherin mutants, I have shown that E-Cadherin mediates its inhibitory effect on neural crest migration and CIL via its cytoplasmic domain, and that expression of a chimaeric cadherin consisting of E-Cadherin EC domain fused with N-Cadherin cytoplasmic domain has a phenotype indistinguishable

from wild type neural crest, thus suggesting that interaction of N-Cadherin with additional cofactors via its extracellular domain might not be important for CIL and migration in neural crest.

How does E-Cadherin cytoplasmic domain mediate such a distinct effect on Rac1 distribution? My results using E-Cadherin mutants unable to interact with p120 suggest a requirement for E-Cadherin/p120 interaction in suppression of EMT, CIL and in E-Cadherin dependent upregulation of Rac1 activity. Consistently, knockdown of p120 partially rescues dispersion of E-Cadherin expressing explants, and fully rescues contact-dependent protrusion polarity.

Importantly, p120 interacts with both N- and E-Cadherin, and, although the overall aminoacid sequence of the p120 binding domain are not 100% homologous between the two cadherins, the core binding sites on the juxtamembrane domain required for interaction with p120 are conserved between the two isoforms (Ishiyama et al., 2010; Nanes et al., 2012). However, one possible explanation for a differential requirement of p120 in mediating Rac1 activity at the N-Cadherin and E-Cadherin cell-cell junction might be found in my analysis of junctional protein dynamics. Indeed, FRAP analysis of p120-GFP at N- and E-Cadherin junctions shows that p120 is mildly, but significantly, less dynamic at the E-Cadherin junction. It is therefore likely that p120 molecules are more stable at E-Cadherin adhesion sites, thus increasing the probability of Rac1 activation at the site of cell-cell contact.

Our results suggest that E-Cadherin promotes Rac1 activation via interaction with p120. This observation is consistent with previous reports that suggest p120 is required to promote Rac1 activation downstream of E-Cadherin ligation (Goodwin et al., 2003; Oas et al., 2013). In addition, p120 inhibits RhoA activity

at cell-cell junction via interaction with p190A RhoGAP (Wildenberg et al., 2006), which positively contributes to increase Rac1 activity by antagonising RhoA activation (Wildenberg et al., 2006).

However, it is currently unclear how p120 may promote Rac1 activation at the cadherin junction. Indeed, p120 has been suggested to promote Rac1 activity directly via the Rac GEF Vav2 in the cytoplasm, but not at the cell-cell junction (Noren et al., 2000; Valls et al., 2012). Additional Rac GEFs such as Tiam1 have been reported to be active upon cadherin ligation (Sander et al., 1998). However, whether a biochemical or functional interaction may occur between p120 and Tiam1 has not been yet investigated. In neural crest the Rho/Rac GEF Trio has been reported to interact with the type II mesenchymal Cadherin11 (Kashef et al., 2009) and to control CIL and Rac1 polarized distribution at the cell-cell contact downstream of Par3 (Moore et al., 2013). Although Trio has been shown to interact with Cadherin 11 via its β-catenin binding domain (Kashef et al., 2009), its interaction with classical type I cadherins has not yet been investigated, and it remains a potential candidate to mediate Rac1 polarized distribution downstream of classical cadherins. Whether other Rac GEFs or may interact with the junctional pool of p120 in neural crest cells remains to be investigated.

An alternative possibility may arise from a differential regulation of Rho GTPases via p120 by N-Cadherin. Indeed, a study in myoblasts, which endogenously express N-Cadherin, suggested RhoA rather than Rac1 to be activated downstream of p120 upon N-Cadherin-p120 interaction (Taulet et al., 2009). However, how p120 may activate RhoA at the junction, given that –as discussed in the Introduction- p120 is *per se* a Rho GDI and has been shown to inhibit RhoA

activity in the cytoplasm (Anastasiadis et al., 2000), remains elusive. My observations of RhoA FRET imaging in living migratory neural crest cell collisions, which express endogenous N-Cadherin, show that upon cell-cell interaction RhoA is activated at the cell-cell contact. Although the relationship between N-Cadherin and active RhoA distribution has not been yet determined in neural crest cells, considering that Wnt/PCP is required for polarized RhoA activation at the cell-cell contact (Carmona-Fontaine et al., 2008) and that I observed that RhoA distribution does not change upon the E- to N- Cadherin switch occurring in neural crest EMT or upon E-Cadherin ectopic expression, it is tempting to speculate that RhoA activity at cell-cell contacts might be regulated in an N-cadherin-independent fashion.

Finally, a study in PDGF-stimulated fibroblasts proposed that p120 may indirectly inhibit Rac1 downstream of N-Cadherin by controlling integrin activation in the vicinity of the cell-cell contact (Ouyang et al., 2013). This result is in line with my observations that very few focal adhesions are found in proximity of the cell-cell contact in clusters of migratory neural crest cells. Given that integrin activity promotes Rac1 activation (del Pozo et al., 2000; Etienne-Manneville and Hall, 2001), inhibition of focal adhesion formation might indirectly lead to inhibition of Rac1 activity in proximity of migratory neural crest cell-cell contacts. Interestingly, p120 is phosphorylated by Src (Reynolds et al., 2014), thus raising the possibility that p120 phosphorylation might be also involved in Src mediated inhibition of focal adhesion formation in migratory neural crest cells.

4. EMT and CIL are promoted by changes in cell-substrate adhesion rather than in cell-cell adhesion

Does protrusion repolarization specify a front-rear identity?

I have shown that, in the absence of E-Cadherin mediated inhibition of protrusion repolarization, cell separation during CIL is driven by such protrusions. I observed that during repolarization of protrusions traction forces are generated on the substrate by the newly forming lamellipodium, and that, in migratory neural crest, intercellular tension across vinculin molecules is lower than tension at interface with the extracellular matrix. Here, I propose that such a disproportion between intercellular and traction forces eventually leads to disassembly of the cell-cell adhesion.

How the forces generated by the newly formed protrusions are transmitted to the cell-cell junction is currently unclear. One possibility might be that protrusive forces are necessary to polarize the cell and generate a "trailing back" environment in proximity to the junction (Houk et al., 2012; Martin et al., 2014). Because my observations suggest that in repolarising migratory neural crest cells Rac1 is active at the leading edge and promotes a "front" identity (Houk et al., 2012; Ridley et al., 2003), and because it is well established that RhoA and Rac antagonise each other and that RhoA/ROCK pathway is required for trailing edge retraction at the back of migrating cells (Ridley et al., 2003), I investigated the dynamic localization of active RhoA and of its effector protein Myosin during collisions of migratory neural crest cells. Interestingly, RhoA distribution is not as dynamic as that of Rac1 and active RhoA localises at the site of cell-cell contact, which can be identified as the prospective "back" of the repolarising cell,

along the whole duration of neural crest cell collisions. Because Rac1 is dynamically redistributed to the leading edge of the colliding cells during protrusion repolarization while active RhoA is invariably found at the contact, it might be possible that "back" identity via RhoA might be, as found in migrating neutrophils (Wang et al., 2013), more robust. Interestingly, RhoA has been found to inhibit Rac1 activation in neural crest cells via ROCK (Matthews et al., 2008). Whether back identity via RhoA is specified first remains to be investigated, because currently available FRET probes for RhoA and Rac have overlapping spectra and cannot be expressed and analysed in the same cell at the same time. In order to have a deeper understanding of the dynamics of downstream RhoA signalling during CIL, I performed live imaging of neural crest expressing MLC2-GFP. I found that also Myosin localises at the back of the cell, but its accumulation is delayed compared to RhoA as myosin bundles can be detected in proximity of the cell-cell contact only after the cells have started repolarizing their protrusions, about a minute before the cells break down their adherens junction. Because actomyosin contractility at cell-cell contact sites can drive junctional constriction thus leading to EMT (Hidalgo-Carcedo et al., 2011; Martin et al., 2009), it is possible that the accumulation of myosin filaments I observed before cell separation might mediate a pulse of contraction that contributes to junctional breakdown. Such aspect still needs investigation. However, myosin II activity appears to affect contact inhibition of locomotion only mildly in chick heart fibroblasts (Kadir et al., 2011), and my cell confinement experiments in which protrusion repolarization was inhibited by culturing neural crest cell doublets on fibronectin micropatterns suggest that repolarization of protrusions rather than myosin contractility in proximity of the contact might be the driving

force triggering cell separation. Indeed, cells on micropatterns are unable to separate despite showing a strongly polarized myosin localization pattern. In addition, experiments using a photoactivatable Rac1 probe suggest that promoting protrusion formation opposite to the cell-cell adhesion site is sufficient to trigger junctional breakdown and to rescue E-Cadherin mediated suppression of CIL, thus further supporting the idea that repolarization of lamellipodial protrusions, rather than contraction that may occur at the back of the cell in proximity of the cell-cell adhesion, triggers junctional disassembly. It is true that the localisation of MLC2-GFP has not been investigated during the photoactivation experiments, and it may still be possible that activation of Rac1 at the free edge of the cell induces polarization of myosin activity at the back. Such a possibility seems unlikely, however, as in neural crest the RhoA/ROCK pathway has been shown to antagonise Rac1 activation, but Rac1 activity does not seem to antagonise RhoA (Matthews et al., 2008).

Interestingly, a recent report has proposed an intriguing mechanism that links polarization of Rac1 activity with force transmission at cell-cell contact sites in collectively migrating epithelial cells. The tumour suppressor protein merlin localises at cell-cell contacts in epithelial cells, however, upon wound healing induced migration, a fraction of merlin relocalises to the cytoplasm in a manner dependent on intercellular pulling forces of the leader cells and actomyosin contractility (Das et al., 2015). Redistribution of merlin in the cytoplasm induces polarised Rac1 activation in the follower cell thus providing a mechanism for tension induced planar polarization of Rac1 activity (Das et al., 2015). In addition, studies in polarised migrating neutrophils have suggested that an increase in membrane tension induced by Arp2/3 mediated branched actin

polymerization at the lamellipodium is sufficient to sustain Rac1 activation at the leading edge (Houk et al., 2012). My observations show that Rac1 is active at the free edge of N-Cadherin expressing migratory neural crest cells, where lamellipodial activity is prominent, and that E-Cadherin relocalises Rac1 to the cell-cell adhesion site. Vinculin-TS FRET measurements show that tension is significantly higher at E-Cadherin cell-cell contact sites compared to N-Cadherin junctions. Considering these reports, it is tempting to speculate that a tension-sensitive mechanism might play a role downstream or in parallel to cadherins in contact-dependent Rac1 activation in neural crest cells, although such possibility has not been investigated yet and further work might be required to address this aspect. Interestingly, in this context, BAR domain proteins, which are sensitive to membrane curvature and control cell architecture and endocytosis, have recently been found to be recruited to the plasma membrane in response to external push forces or to internal, actomyosin contractility mediated, pulling forces (Galic et al., 2012). Among BAR domain proteins are several Rac GAPs, and it has been demonstrated that ArhGAP44 mediates highly localised Rac1 inactivation at neuronal filopodia (Galic et al., 2014). A possible scenario might see BAR domain proteins recruited at the cell-cell contacts to locally regulate small GTPase activity in response to tension. However, such a possibility remains purely speculative and awaits further investigations.

Changes in substrate adhesions are responsible for EMT and CIL in neural crest

I have shown how repolarization of lamellipodial protrusion precedes, and it is necessary and sufficient for, junctional disassembly occurring during CIL. By measuring traction forces exerted by repolarizing and non-repolarizing neural

crest clusters on their substrate, and by measuring tension across vinculin molecules, I propose that the disassembly of cell-cell junctions taking place during CIL relies on a disproportion between intercellular tensions and traction forces exerted on the ECM by the repolarizing cells.

Such disproportion may arise from the strong polarization of focal adhesion distribution observed in migratory neural crest cells, which may origin from negative cross-talk between cadherin cell-cell adhesion and integrin adhesions. Importantly, a seminal study in cranial chick neural crest cells has suggested an antagonism between β_1 and β_3 integrins and N-Cadherin cell-cell adhesion(Monier-Gavelle and Duband, 1997). More recently, studies using micropatterned substrates have demonstrated that cadherin adhesions cannot form in close proximity of cell-ECM adhesions, and that mutual exclusion between cell-cell and cell-matrix adhesions results in asymmetric distribution of traction forces between CollagenIV- and E-Cadherin- coated substrata (Borghi et al., 2010). Another report has demonstrated that upon cell-cell contact maturation between cardiomyocites, which express N-Cadherin, focal adhesions are excluded from the site of cell-cell contact and traction forces become increasingly anysotropically distributed at the free edge of the cells (McCain et al., 2012).

As previously discussed, my experiments show little evidence for a major difference in junctional stability or in strength between E-Cadherin, expressed in premigratory cells, and N-Cadherin, expressed in migratory cells which undergo CIL and EMT. For this reason, and given the results of the traction forces and vinculin-TS measurements, I propose that protrusion and, in turn, focal adhesion and traction forces polarization induces EMT and CIL.

Interestingly, it has been reported that EMT-inducing growth factors such as HGF do not alter the strength of E-Cadherin cell-cell adhesions in epithelial cells (de Rooij et al., 2005; Hoj et al., 2014), but induce cell scattering by increasing their ability to form focal adhesions on ECM. Importantly, the efficiency of scattering is integrin-dependent and proportional to the concentration of ECM (de Rooij et al., 2005). Direct alteration of the ability of cells to exert traction forces on the ECM by using compliant substrates impairs scattering (Hoj et al., 2014) while stiffer substrates promote EMT (de Rooij et al., 2005). In addition, direct measurement of traction forces during Snail-induced EMT in epithelial cells shows that single Snail-expressing mesenchymal cells exert higher traction forces on the ECM (McGrail et al., 2014) than epithelial cells. Finally, a recent report suggests β_1 integrin and adhesion to collagen to be activated in response to immobilized but not to soluble EphrinA1 ligands in prostate PC3 cells (Yu et al., 2015), which display an Eph-Ephrin dependent CIL response(Astin et al., 2010b). Taken together, these reports support our model in which repolarization of traction forces rather than changes in the strength of adhesion promote junction breakdown during CIL. I hypothesise that during repolarization of protrusions, as neural crest increase the size of their lamella, polarised focal adhesion formation leads to a progressive buildup of tension at the cell-ECM interface. Due to technical restrictions, I have so far been unable to observe traction forces during junctional breakdown events in living cell doublets and I have not so far been able to image the Vinculin-TS FRET probe in living neural crest cells. Although my measurements from neural crest clusters and fixed samples are consistent with the model I am proposing, measurements of traction forces and

of tension across vinculin during migratory neural crest collisions in living cells may provide additional experimental evidence to support my hypothesis.

Traditionally, the cadherin switches occurring during neural crest delamination and EMT have been thought to drive separation of the neural crest tissue from the adjacent neural tube via a mechanism involving differential adhesion between tissues expressing different cadherin isoforms and, consequently, cell sorting (Akitaya and Bronner-Fraser, 1992; Chalpe et al., 2010; Cheung and Briscoe, 2003; Coles et al., 2007; Duband et al., 1988; Nakagawa and Takeichi, 1995; Taneyhill et al., 2007). However, there is so far little experimental evidence for differential adhesion regulation of tissue boundary formation [reviewed in (Dahmann et al., 2011)]. Instead, recent reports have highlighted a role for tensional forces in mediating separation between tissues (Calzolari et al., 2014; Landsberg et al., 2009; Monier et al., 2010).

The concept that neural crest cells undergo EMT due to changes in tractional forces and protrusive activity rather than because of downregulation of cell-adhesion complexes, as it has been demonstrated for other cell types *in vitro* (de Rooij et al., 2005; Hoj et al., 2014), has been proposed as early as 1989. In a seminal study from Elizabeth Hay laboratory (Bilozur and Hay, 1989) upon inhibition of normal neural crest emigration from the neural tube by low serum condition, neural crest have been shown instead to migrate into the neural tube lumen by sliding their cell body past their apical junctions and by breaking down the adherens junction complex as the final step of their delamination (Bilozur and Hay, 1989).

In line with these early results, more recently, live imaging experiments of chick and zebrafish trunk neural crest delamination *in vivo* have shown that during

their EMT the cells start producing a variety of protrusions, including lamellipodia, filopodia and blebs, at their basal side, opposite to the adherens junction, which is located at the apical side of the neural tube (Ahlstrom and Erickson, 2009a; Berndt et al., 2008). Importantly, the apical tail of the cells, which contains adherens junctions, is often ruptured during delamination from the neural tube without downregulation of the junctional complex components p120 and α-catenin, thus suggesting that cell-cell junctions might be broken down as a consequence of tractional forces exerted by the delaminating neural crest cells *in vivo* (Ahlstrom and Erickson, 2009a). These findings are consistent with my hypothesis, that during neural crest EMT junctional disassembly occurs because of repolarization of protrusions and of tractional forces. Although most of my experiments have been performed *in vitro*, ectopic expression of E-Cadherin leads to a cell-autonomous inhibition of neural crest migration in *Xenopus*, and given my results on the role of E-Cadherin in suppression of repolarization of Rac activity, protrusion formation and traction forces, it is reasonable to speculate that migration is inhibited by E-Cadherin *in vivo* due to the same mechanisms. Interestingly, the PA-Rac1 tool has been reported to efficiently promote directed cell migration in zebrafish embryos in vivo (Yoo et al., 2010). It might be very interesting to test whether spatiotemporally controlled polarization of protrusions, which can be obtained by laser illumination of PA-Rac1, might be sufficient to promote premature delamination of neural crest cells *in vivo*.

In conclusion, here I propose a molecular mechanism linking two processes, EMT and CIL, leading to cell dissociation and cell dispersion. Importantly, similar to what has been observed upon growth factor induced EMT in epithelial cells,

junctional breakdown and cell dispersion appear to be rather a consequence of a change in cell polarity and in the protrusive and migratory abilities due to the E- to N-Cadherin switch of the emigrating neural crest cells rather than a consequence of differential adhesion. The generality of the EMT and CIL processes raises the possibility that a wider range of cell types (i.e metastatic cancer cells, other embryonic cells) undergoing similar qualitative changes of their cadherin repertoire might acquire CIL through a similar mechanism as part of their progression through EMT, contributing to disease progression or developmental morphogenesis.

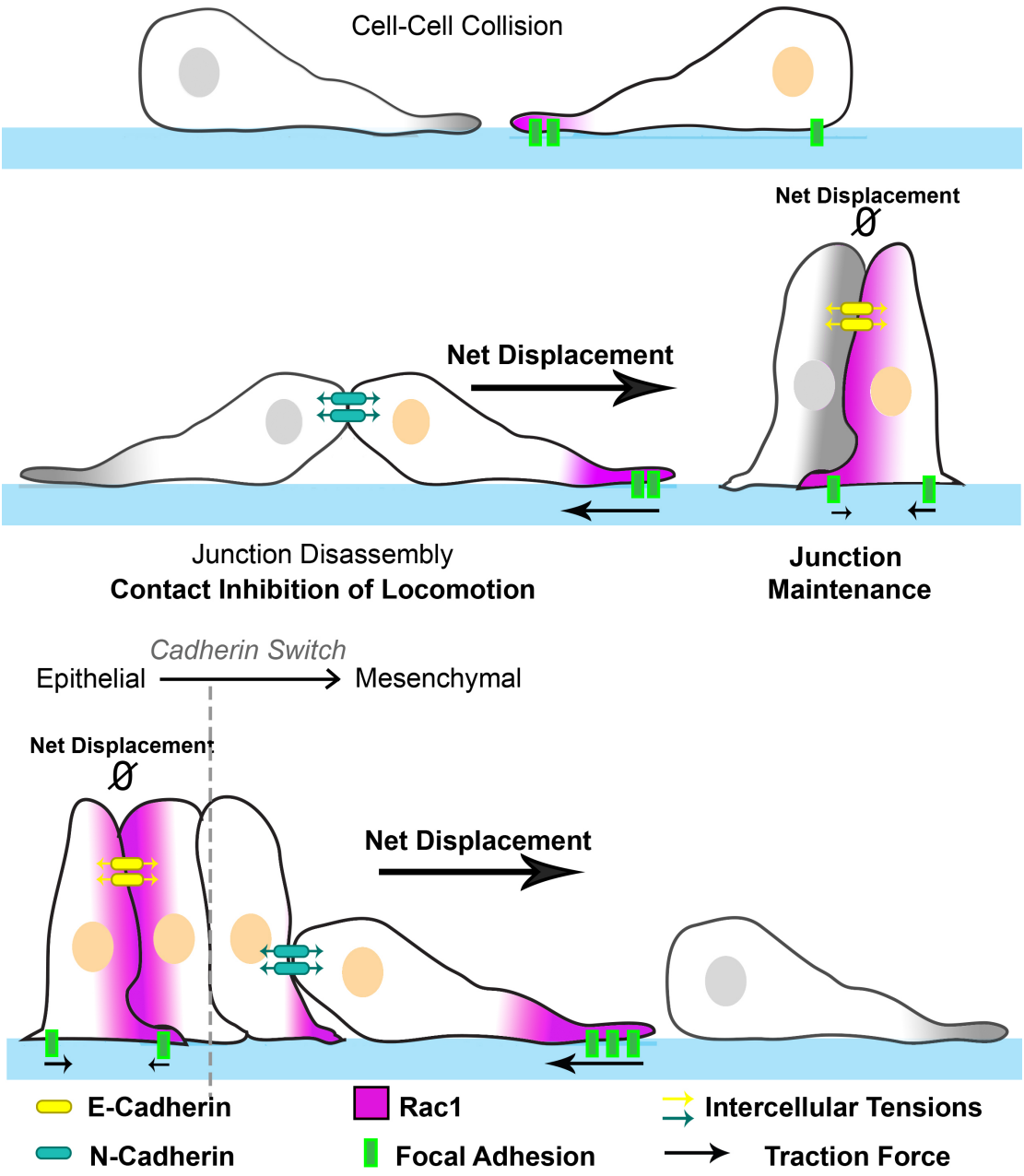

Figure 12.1. Working Model.

(Top). During single cell-cell collisions, a cell-cell junction is formed. Migratory neural crest (left), which display a CIL behaviour, form an N-Cadherin cell-cell contact, which leads to repolarizations of protrusions and, in turn of focal adhesions, which exert high traction forces on the substrate, while N-Cadherin mediated intercellular tensions are weaker. This disproportion between forces

results in a net displacement of the cell, which eventually leads to junction disassembly and cell separation. On the other hand, premigratory E-Cadherin expressing neural crest cells do not repolarise Rac1 activity and protrusions, therefore tractions forces are small and are counterbalanced by intercellular tensions across E-Cadherin junctions, therefore leading to maintenance of the cell-cell contact. A similar mechanism could explain the occurrence of EMT and the acquisition of CIL upon the E- to N- cadherin switch (Bottom).

References

Abe, K., and Takeichi, M. (2008). EPLIN mediates linkage of the cadherin catenin complex to F-actin and stabilizes the circumferential actin belt. Proceedings of the National Academy of Sciences of the United States of America *105*, 13-19.
Abercrombie, M. (1979). Contact inhibition and malignancy. Nature *281*, 259-262.
Abercrombie, M., and Ambrose, E.J. (1962). The surface properties of cancer cells: a review. Cancer research *22*, 525-548.
Abercrombie, M., and Heaysman, J.E. (1953). Observations on the social behaviour of cells in tissue culture. I. Speed of movement of chick heart fibroblasts in relation to their mutual contacts. Experimental cell research *5*, 111-131.
Abercrombie, M., and Heaysman, J.E. (1954). Invasiveness of sarcoma cells. Nature *174*, 697-698.
Aberle, H., Butz, S., Stappert, J., Weissig, H., Kemler, R., and Hoschuetzky, H. (1994). Assembly of the cadherin-catenin complex in vitro with recombinant proteins. Journal of cell science *107 (Pt 12)*, 3655-3663.
Ahlstrom, J.D., and Erickson, C.A. (2009a). The neural crest epithelial-mesenchymal transition in 4D: a 'tail' of multiple non-obligatory cellular mechanisms. Development *136*, 1801-1812.
Ahlstrom, J.D., and Erickson, C.A. (2009b). New views on the neural crest epithelial-mesenchymal transition and neuroepithelial interkinetic nuclear migration. Communicative & integrative biology *2*, 489-493.
Aigner, K., Dampier, B., Descovich, L., Mikula, M., Sultan, A., Schreiber, M., Mikulits, W., Brabletz, T., Strand, D., Obrist, P.*, et al.* (2007). The transcription factor ZEB1 (deltaEF1) promotes tumour cell dedifferentiation by repressing master regulators of epithelial polarity. Oncogene *26*, 6979-6988.
Akhmanova, A., Stehbens, S.J., and Yap, A.S. (2009). Touch, grasp, deliver and control: functional cross-talk between microtubules and cell adhesions. Traffic *10*, 268-274.
Akitaya, T., and Bronner-Fraser, M. (1992). Expression of cell adhesion molecules during initiation and cessation of neural crest cell migration. Developmental dynamics : an official publication of the American Association of Anatomists *194*, 12-20.
Al-Kilani, A., de Freitas, O., Dufour, S., and Gallet, F. (2011). Negative feedback from integrins to cadherins: a micromechanical study. Biophysical journal *101*, 336-344.
Alfandari, D., Cousin, H., Gaultier, A., Smith, K., White, J.M., Darribere, T., and DeSimone, D.W. (2001). Xenopus ADAM 13 is a metalloprotease required for cranial neural crest-cell migration. Current biology : CB *11*, 918-930.
Alfandari, D., Wolfsberg, T.G., White, J.M., and DeSimone, D.W. (1997). ADAM 13: a novel ADAM expressed in somitic mesoderm and neural crest cells during Xenopus laevis development. Developmental biology *182*, 314-330.
Anastasiadis, P.Z., Moon, S.Y., Thoreson, M.A., Mariner, D.J., Crawford, H.C., Zheng, Y., and Reynolds, A.B. (2000). Inhibition of RhoA by p120 catenin. Nature cell biology *2*, 637-644.

Assemat, E., Bazellieres, E., Pallesi-Pocachard, E., Le Bivic, A., and Massey-Harroche, D. (2008). Polarity complex proteins. Biochimica et biophysica acta *1778*, 614-630.
Astin, J.W., Batson, J., Kadir, S., Charlet, J., Persad, R.A., Gillatt, D., Oxley, J.D., and Nobes, C.D. (2010a). Competition amongst Eph receptors regulates contact inhibition of locomotion and invasiveness in prostate cancer cells. Nat Cell Biol *12*, 1194-1204.
Astin, J.W., Batson, J., Kadir, S., Charlet, J., Persad, R.A., Gillatt, D., Oxley, J.D., and Nobes, C.D. (2010b). Competition amongst Eph receptors regulates contact inhibition of locomotion and invasiveness in prostate cancer cells. Nature cell biology *12*, 1194-1204.
Audebert, S., Navarro, C., Nourry, C., Chasserot-Golaz, S., Lecine, P., Bellaiche, Y., Dupont, J.L., Premont, R.T., Sempere, C., Strub, J.M.*, et al.* (2004). Mammalian Scribble forms a tight complex with the betaPIX exchange factor. Current biology : CB *14*, 987-995.
Aybar, M.J., Nieto, M.A., and Mayor, R. (2003). Snail precedes slug in the genetic cascade required for the specification and migration of the Xenopus neural crest. Development *130*, 483-494.
Balaban, N.Q., Schwarz, U.S., Riveline, D., Goichberg, P., Tzur, G., Sabanay, I., Mahalu, D., Safran, S., Bershadsky, A., Addadi, L.*, et al.* (2001). Force and focal adhesion assembly: a close relationship studied using elastic micropatterned substrates. Nature cell biology *3*, 466-472.
Balzac, F., Avolio, M., Degani, S., Kaverina, I., Torti, M., Silengo, L., Small, J.V., and Retta, S.F. (2005). E-cadherin endocytosis regulates the activity of Rap1: a traffic light GTPase at the crossroads between cadherin and integrin function. Journal of cell science *118*, 4765-4783.
Barrallo-Gimeno, A., and Nieto, M.A. (2005). The Snail genes as inducers of cell movement and survival: implications in development and cancer. Development *132*, 3151-3161.
Barriga, E.H., Maxwell, P.H., Reyes, A.E., and Mayor, R. (2013). The hypoxia factor Hif-1alpha controls neural crest chemotaxis and epithelial to mesenchymal transition. The Journal of cell biology *201*, 759-776.
Barry, A.K., Tabdili, H., Muhamed, I., Wu, J., Shashikanth, N., Gomez, G.A., Yap, A.S., Gottardi, C.J., de Rooij, J., Wang, N.*, et al.* (2014). alpha-catenin cytomechanics--role in cadherin-dependent adhesion and mechanotransduction. Journal of cell science *127*, 1779-1791.
Batlle, E., Sancho, E., Franci, C., Dominguez, D., Monfar, M., Baulida, J., and Garcia De Herreros, A. (2000). The transcription factor snail is a repressor of E-cadherin gene expression in epithelial tumour cells. Nature cell biology *2*, 84-89.
Becker, S.F., Mayor, R., and Kashef, J. (2013). Cadherin-11 Mediates Contact Inhibition of Locomotion during Xenopus Neural Crest Cell Migration. PloS one *8*, e85717.
Belmadani, A., Tran, P.B., Ren, D., Assimacopoulos, S., Grove, E.A., and Miller, R.J. (2005). The chemokine stromal cell-derived factor-1 regulates the migration of sensory neuron progenitors. The Journal of neuroscience : the official journal of the Society for Neuroscience *25*, 3995-4003.
Benton, R., and St Johnston, D. (2003). Drosophila PAR-1 and 14-3-3 inhibit Bazooka/PAR-3 to establish complementary cortical domains in polarized cells. Cell *115*, 691-704.

Berndt, J.D., Clay, M.R., Langenberg, T., and Halloran, M.C. (2008). Rho-kinase and myosin II affect dynamic neural crest cell behaviors during epithelial to mesenchymal transition in vivo. Developmental biology *324*, 236-244.
Betancur, P., Bronner-Fraser, M., and Sauka-Spengler, T. (2010). Assembling neural crest regulatory circuits into a gene regulatory network. Annual review of cell and developmental biology *26*, 581-603.
Bilder, D., Li, M., and Perrimon, N. (2000). Cooperative regulation of cell polarity and growth by Drosophila tumor suppressors. Science *289*, 113-116.
Bilder, D., Schober, M., and Perrimon, N. (2003). Integrated activity of PDZ protein complexes regulates epithelial polarity. Nature cell biology *5*, 53-58.
Bilozur, M.E., and Hay, E.D. (1989). Cell migration into neural tube lumen provides evidence for the "fixed cortex" theory of cell motility. Cell motility and the cytoskeleton *14*, 469-484.
Boggon, T.J., Murray, J., Chappuis-Flament, S., Wong, E., Gumbiner, B.M., and Shapiro, L. (2002). C-cadherin ectodomain structure and implications for cell adhesion mechanisms. Science *296*, 1308-1313.
Bolos, V., Peinado, H., Perez-Moreno, M.A., Fraga, M.F., Esteller, M., and Cano, A. (2003). The transcription factor Slug represses E-cadherin expression and induces epithelial to mesenchymal transitions: a comparison with Snail and E47 repressors. Journal of cell science *116*, 499-511.
Borghi, N., Lowndes, M., Maruthamuthu, V., Gardel, M.L., and Nelson, W.J. (2010). Regulation of cell motile behavior by crosstalk between cadherin- and integrin-mediated adhesions. Proceedings of the National Academy of Sciences of the United States of America *107*, 13324-13329.
Borghi, N., Sorokina, M., Shcherbakova, O.G., Weis, W.I., Pruitt, B.L., Nelson, W.J., and Dunn, A.R. (2012). E-cadherin is under constitutive actomyosin-generated tension that is increased at cell-cell contacts upon externally applied stretch. Proceedings of the National Academy of Sciences of the United States of America *109*, 12568-12573.
Bos, J.L., de Bruyn, K., Enserink, J., Kuiperij, B., Rangarajan, S., Rehmann, H., Riedl, J., de Rooij, J., van Mansfeld, F., and Zwartkruis, F. (2003). The role of Rap1 in integrin-mediated cell adhesion. Biochemical Society transactions *31*, 83-86.
Braga, V.M., Machesky, L.M., Hall, A., and Hotchin, N.A. (1997). The small GTPases Rho and Rac are required for the establishment of cadherin-dependent cell-cell contacts. The Journal of cell biology *137*, 1421-1431.
Brasch, J., Harrison, O.J., Ahlsen, G., Carnally, S.M., Henderson, R.M., Honig, B., and Shapiro, L. (2011). Structure and binding mechanism of vascular endothelial cadherin: a divergent classical cadherin. Journal of molecular biology *408*, 57-73.
Breau, M.A., Pietri, T., Stemmler, M.P., Thiery, J.P., and Weston, J.A. (2008). A nonneural epithelial domain of embryonic cranial neural folds gives rise to ectomesenchyme. Proceedings of the National Academy of Sciences of the United States of America *105*, 7750-7755.
Brieher, W.M., and Yap, A.S. (2013). Cadherin junctions and their cytoskeleton(s). Current opinion in cell biology *25*, 39-46.
Buckley, C.D., Tan, J., Anderson, K.L., Hanein, D., Volkmann, N., Weis, W.I., Nelson, W.J., and Dunn, A.R. (2014). Cell adhesion. The minimal cadherin-catenin complex binds to actin filaments under force. Science *346*, 1254211.

Butler, B., Gao, C., Mersich, A.T., and Blystone, S.D. (2006). Purified integrin adhesion complexes exhibit actin-polymerization activity. Current biology : CB *16*, 242-251.
Cadigan, K.M., and Peifer, M. (2009). Wnt signaling from development to disease: insights from model systems. Cold Spring Harbor perspectives in biology *1*, a002881.
Calmont, A., Ivins, S., Van Bueren, K.L., Papangeli, I., Kyriakopoulou, V., Andrews, W.D., Martin, J.F., Moon, A.M., Illingworth, E.A., Basson, M.A*., et al.* (2009). Tbx1 controls cardiac neural crest cell migration during arch artery development by regulating Gbx2 expression in the pharyngeal ectoderm. Development *136*, 3173-3183.
Calzolari, S., Terriente, J., and Pujades, C. (2014). Cell segregation in the vertebrate hindbrain relies on actomyosin cables located at the interhombomeric boundaries. The EMBO journal *33*, 686-701.
Camand, E., Peglion, F., Osmani, N., Sanson, M., and Etienne-Manneville, S. (2012). N-cadherin expression level modulates integrin-mediated polarity and strongly impacts on the speed and directionality of glial cell migration. Journal of cell science *125*, 844-857.
Cano, A., Perez-Moreno, M.A., Rodrigo, I., Locascio, A., Blanco, M.J., del Barrio, M.G., Portillo, F., and Nieto, M.A. (2000). The transcription factor snail controls epithelial-mesenchymal transitions by repressing E-cadherin expression. Nature cell biology *2*, 76-83.
Carmona-Fontaine, C., Matthews, H.K., Kuriyama, S., Moreno, M., Dunn, G.A., Parsons, M., Stern, C.D., and Mayor, R. (2008). Contact inhibition of locomotion in vivo controls neural crest directional migration. Nature *456*, 957-961.
Carmona-Fontaine, C., Theveneau, E., Tzekou, A., Tada, M., Woods, M., Page, K.M., Parsons, M., Lambris, J.D., and Mayor, R. (2011). Complement fragment C3a controls mutual cell attraction during collective cell migration. Developmental cell *21*, 1026-1037.
Carragher, N.O., Westhoff, M.A., Fincham, V.J., Schaller, M.D., and Frame, M.C. (2003). A novel role for FAK as a protease-targeting adaptor protein: regulation by p42 ERK and Src. Current biology : CB *13*, 1442-1450.
Carramusa, L., Ballestrem, C., Zilberman, Y., and Bershadsky, A.D. (2007). Mammalian diaphanous-related formin Dia1 controls the organization of E-cadherin-mediated cell-cell junctions. Journal of cell science *120*, 3870-3882.
Carver, E.A., Jiang, R., Lan, Y., Oram, K.F., and Gridley, T. (2001). The mouse snail gene encodes a key regulator of the epithelial-mesenchymal transition. Molecular and cellular biology *21*, 8184-8188.
Chalpe, A.J., Prasad, M., Henke, A.J., and Paulson, A.F. (2010). Regulation of cadherin expression in the chicken neural crest by the Wnt/beta-catenin signaling pathway. Cell adhesion & migration *4*, 431-438.
Chan, C.E., and Odde, D.J. (2008). Traction dynamics of filopodia on compliant substrates. Science *322*, 1687-1691.
Chen, X., and Gumbiner, B.M. (2006). Paraxial protocadherin mediates cell sorting and tissue morphogenesis by regulating C-cadherin adhesion activity. The Journal of cell biology *174*, 301-313.
Chen, X., Kojima, S., Borisy, G.G., and Green, K.J. (2003). p120 catenin associates with kinesin and facilitates the transport of cadherin-catenin complexes to intercellular junctions. The Journal of cell biology *163*, 547-557.

Chen, X., and Macara, I.G. (2005). Par-3 controls tight junction assembly through the Rac exchange factor Tiam1. Nature cell biology *7*, 262-269.
Chen, X.L., Nam, J.O., Jean, C., Lawson, C., Walsh, C.T., Goka, E., Lim, S.T., Tomar, A., Tancioni, I., Uryu, S.*, et al.* (2012). VEGF-induced vascular permeability is mediated by FAK. Developmental cell *22*, 146-157.
Cheung, M., and Briscoe, J. (2003). Neural crest development is regulated by the transcription factor Sox9. Development *130*, 5681-5693.
Cheung, M., Chaboissier, M.C., Mynett, A., Hirst, E., Schedl, A., and Briscoe, J. (2005). The transcriptional control of trunk neural crest induction, survival, and delamination. Developmental cell *8*, 179-192.
Choi, C.K., Vicente-Manzanares, M., Zareno, J., Whitmore, L.A., Mogilner, A., and Horwitz, A.R. (2008). Actin and alpha-actinin orchestrate the assembly and maturation of nascent adhesions in a myosin II motor-independent manner. Nature cell biology *10*, 1039-1050.
Choi, H.J., Pokutta, S., Cadwell, G.W., Bobkov, A.A., Bankston, L.A., Liddington, R.C., and Weis, W.I. (2012). alphaE-catenin is an autoinhibited molecule that coactivates vinculin. Proceedings of the National Academy of Sciences of the United States of America *109*, 8576-8581.
Choquet, D., Felsenfeld, D.P., and Sheetz, M.P. (1997). Extracellular matrix rigidity causes strengthening of integrin-cytoskeleton linkages. Cell *88*, 39-48.
Chu, Y.S., Thomas, W.A., Eder, O., Pincet, F., Perez, E., Thiery, J.P., and Dufour, S. (2004). Force measurements in E-cadherin-mediated cell doublets reveal rapid adhesion strengthened by actin cytoskeleton remodeling through Rac and Cdc42. The Journal of cell biology *167*, 1183-1194.
Ciesiolka, M., Delvaeye, M., Van Imschoot, G., Verschuere, V., McCrea, P., van Roy, F., and Vleminckx, K. (2004). p120 catenin is required for morphogenetic movements involved in the formation of the eyes and the craniofacial skeleton in Xenopus. Journal of cell science *117*, 4325-4339.
Clark, H.F., Brentrup, D., Schneitz, K., Bieber, A., Goodman, C., and Noll, M. (1995). Dachsous encodes a member of the cadherin superfamily that controls imaginal disc morphogenesis in Drosophila. Genes & development *9*, 1530-1542.
Clay, M.R., and Halloran, M.C. (2013). Rho activation is apically restricted by Arhgap1 in neural crest cells and drives epithelial-to-mesenchymal transition. Development *140*, 3198-3209.
Clay, M.R., and Halloran, M.C. (2014). Cadherin 6 promotes neural crest cell detachment via F-actin regulation and influences active Rho distribution during epithelial-to-mesenchymal transition. Development *141*, 2506-2515.
Coles, E.G., Taneyhill, L.A., and Bronner-Fraser, M. (2007). A critical role for Cadherin6B in regulating avian neural crest emigration. Developmental biology *312*, 533-544.
Colombelli, J., Besser, A., Kress, H., Reynaud, E.G., Girard, P., Caussinus, E., Haselmann, U., Small, J.V., Schwarz, U.S., and Stelzer, E.H. (2009). Mechanosensing in actin stress fibers revealed by a close correlation between force and protein localization. Journal of cell science *122*, 1665-1679.
Comijn, J., Berx, G., Vermassen, P., Verschueren, K., van Grunsven, L., Bruyneel, E., Mareel, M., Huylebroeck, D., and van Roy, F. (2001). The two-handed E box binding zinc finger protein SIP1 downregulates E-cadherin and induces invasion. Molecular cell *7*, 1267-1278.

Cox, R.T., Kirkpatrick, C., and Peifer, M. (1996). Armadillo is required for adherens junction assembly, cell polarity, and morphogenesis during Drosophila embryogenesis. The Journal of cell biology *134*, 133-148.
Dady, A., Blavet, C., and Duband, J.L. (2012). Timing and kinetics of E- to N-cadherin switch during neurulation in the avian embryo. Developmental dynamics : an official publication of the American Association of Anatomists *241*, 1333-1349.
Dahmann, C., Oates, A.C., and Brand, M. (2011). Boundary formation and maintenance in tissue development. Nature reviews Genetics *12*, 43-55.
Daniel, J.M., and Reynolds, A.B. (1995). The tyrosine kinase substrate p120cas binds directly to E-cadherin but not to the adenomatous polyposis coli protein or alpha-catenin. Molecular and cellular biology *15*, 4819-4824.
Das, T., Safferling, K., Rausch, S., Grabe, N., Boehm, H., and Spatz, J.P. (2015). A molecular mechanotransduction pathway regulates collective migration of epithelial cells. Nature cell biology *17*, 276-287.
Davis, J.R., Huang, C.Y., Zanet, J., Harrison, S., Rosten, E., Cox, S., Soong, D.Y., Dunn, G.A., and Stramer, B.M. (2012). Emergence of embryonic pattern through contact inhibition of locomotion. Development *139*, 4555-4560.
Davis, M.A., Ireton, R.C., and Reynolds, A.B. (2003). A core function for p120-catenin in cadherin turnover. The Journal of cell biology *163*, 525-534.
Davy, A., Aubin, J., and Soriano, P. (2004). Ephrin-B1 forward and reverse signaling are required during mouse development. Genes & development *18*, 572-583.
de Rooij, J., Kerstens, A., Danuser, G., Schwartz, M.A., and Waterman-Storer, C.M. (2005). Integrin-dependent actomyosin contraction regulates epithelial cell scattering. The Journal of cell biology *171*, 153-164.
del Barrio, M.G., and Nieto, M.A. (2002). Overexpression of Snail family members highlights their ability to promote chick neural crest formation. Development *129*, 1583-1593.
del Pozo, M.A., Price, L.S., Alderson, N.B., Ren, X.D., and Schwartz, M.A. (2000). Adhesion to the extracellular matrix regulates the coupling of the small GTPase Rac to its effector PAK. The EMBO journal *19*, 2008-2014.
del Rio, A., Perez-Jimenez, R., Liu, R., Roca-Cusachs, P., Fernandez, J.M., and Sheetz, M.P. (2009). Stretching single talin rod molecules activates vinculin binding. Science *323*, 638-641.
Desai, R., Sarpal, R., Ishiyama, N., Pellikka, M., Ikura, M., and Tepass, U. (2013). Monomeric alpha-catenin links cadherin to the actin cytoskeleton. Nature cell biology *15*, 261-273.
Di Paolo, G., and De Camilli, P. (2006). Phosphoinositides in cell regulation and membrane dynamics. Nature *443*, 651-657.
Dickinson, D.J., Nelson, W.J., and Weis, W.I. (2011). A polarized epithelium organized by beta- and alpha-catenin predates cadherin and metazoan origins. Science *331*, 1336-1339.
Ding, H., Wu, X., Kim, I., Tam, P.P., Koh, G.Y., and Nagy, A. (2000). The mouse Pdgfc gene: dynamic expression in embryonic tissues during organogenesis. Mechanisms of development *96*, 209-213.
Dona, E., Barry, J.D., Valentin, G., Quirin, C., Khmelinskii, A., Kunze, A., Durdu, S., Newton, L.R., Fernandez-Minan, A., Huber, W.*, et al.* (2013). Directional tissue migration through a self-generated chemokine gradient. Nature *503*, 285-289.

Dottori, M., Gross, M.K., Labosky, P., and Goulding, M. (2001). The winged-helix transcription factor Foxd3 suppresses interneuron differentiation and promotes neural crest cell fate. Development *128*, 4127-4138.
Drees, F., Pokutta, S., Yamada, S., Nelson, W.J., and Weis, W.I. (2005). Alpha-catenin is a molecular switch that binds E-cadherin-beta-catenin and regulates actin-filament assembly. Cell *123*, 903-915.
Duband, J.L., and Thiery, J.P. (1982). Distribution of fibronectin in the early phase of avian cephalic neural crest cell migration. Developmental biology *93*, 308-323.
Duband, J.L., Volberg, T., Sabanay, I., Thiery, J.P., and Geiger, B. (1988). Spatial and temporal distribution of the adherens-junction-associated adhesion molecule A-CAM during avian embryogenesis. Development *103*, 325-344.
Duong, T.D., and Erickson, C.A. (2004). MMP-2 plays an essential role in producing epithelial-mesenchymal transformations in the avian embryo. Developmental dynamics : an official publication of the American Association of Anatomists *229*, 42-53.
Dzamba, B.J., Jakab, K.R., Marsden, M., Schwartz, M.A., and DeSimone, D.W. (2009). Cadherin adhesion, tissue tension, and noncanonical Wnt signaling regulate fibronectin matrix organization. Developmental cell *16*, 421-432.
Ebnet, K. (2008). Organization of multiprotein complexes at cell-cell junctions. Histochemistry and cell biology *130*, 1-20.
Egeblad, M., and Werb, Z. (2002). New functions for the matrix metalloproteinases in cancer progression. Nature reviews Cancer *2*, 161-174.
Eger, A., Aigner, K., Sonderegger, S., Dampier, B., Oehler, S., Schreiber, M., Berx, G., Cano, A., Beug, H., and Foisner, R. (2005). DeltaEF1 is a transcriptional repressor of E-cadherin and regulates epithelial plasticity in breast cancer cells. Oncogene *24*, 2375-2385.
Ehrlich, J.S., Hansen, M.D., and Nelson, W.J. (2002). Spatio-temporal regulation of Rac1 localization and lamellipodia dynamics during epithelial cell-cell adhesion. Developmental cell *3*, 259-270.
Ehrlicher, A.J., Nakamura, F., Hartwig, J.H., Weitz, D.A., and Stossel, T.P. (2011). Mechanical strain in actin networks regulates FilGAP and integrin binding to filamin A. Nature *478*, 260-263.
Eickholt, B.J., Mackenzie, S.L., Graham, A., Walsh, F.S., and Doherty, P. (1999). Evidence for collapsin-1 functioning in the control of neural crest migration in both trunk and hindbrain regions. Development *126*, 2181-2189.
Erickson, C.A., and Weston, J.A. (1983). An SEM analysis of neural crest migration in the mouse. Journal of embryology and experimental morphology *74*, 97-118.
Escriva, M., Peiro, S., Herranz, N., Villagrasa, P., Dave, N., Montserrat-Sentis, B., Murray, S.A., Franci, C., Gridley, T., Virtanen, I.*, et al.* (2008). Repression of PTEN phosphatase by Snail1 transcriptional factor during gamma radiation-induced apoptosis. Molecular and cellular biology *28*, 1528-1540.
Etchevers, H.C., Amiel, J., and Lyonnet, S. (2007). [Genetic and molecular bases of neurocristopathies]. Archives de pediatrie : organe officiel de la Societe francaise de pediatrie *14*, 668-672.
Etienne-Manneville, S., and Hall, A. (2001). Integrin-mediated activation of Cdc42 controls cell polarity in migrating astrocytes through PKCzeta. Cell *106*, 489-498.
Etienne-Manneville, S., and Hall, A. (2003). Cdc42 regulates GSK-3beta and adenomatous polyposis coli to control cell polarity. Nature *421*, 753-756.

Etienne-Manneville, S., Manneville, J.B., Nicholls, S., Ferenczi, M.A., and Hall, A. (2005). Cdc42 and Par6-PKCzeta regulate the spatially localized association of Dlg1 and APC to control cell polarization. The Journal of cell biology *170*, 895-901.
Franci, C., Takkunen, M., Dave, N., Alameda, F., Gomez, S., Rodriguez, R., Escriva, M., Montserrat-Sentis, B., Baro, T., Garrido, M.*, et al.* (2006). Expression of Snail protein in tumor-stroma interface. Oncogene *25*, 5134-5144.
Franke, W.W. (2009). Discovering the molecular components of intercellular junctions--a historical view. Cold Spring Harbor perspectives in biology *1*, a003061.
Franz, C.M., and Ridley, A.J. (2004). p120 catenin associates with microtubules: inverse relationship between microtubule binding and Rho GTPase regulation. The Journal of biological chemistry *279*, 6588-6594.
Friedl, P., and Gilmour, D. (2009). Collective cell migration in morphogenesis, regeneration and cancer. Nature reviews Molecular cell biology *10*, 445-457.
Fujita, Y., Krause, G., Scheffner, M., Zechner, D., Leddy, H.E., Behrens, J., Sommer, T., and Birchmeier, W. (2002). Hakai, a c-Cbl-like protein, ubiquitinates and induces endocytosis of the E-cadherin complex. Nature cell biology *4*, 222-231.
Fukuhara, T., Shimizu, K., Kawakatsu, T., Fukuyama, T., Minami, Y., Honda, T., Hoshino, T., Yamada, T., Ogita, H., Okada, M.*, et al.* (2004). Activation of Cdc42 by trans interactions of the cell adhesion molecules nectins through c-Src and Cdc42-GEF FRG. The Journal of cell biology *166*, 393-405.
Fukuyama, T., Ogita, H., Kawakatsu, T., Inagaki, M., and Takai, Y. (2006). Activation of Rac by cadherin through the c-Src-Rap1-phosphatidylinositol 3-kinase-Vav2 pathway. Oncogene *25*, 8-19.
Funamoto, S., Meili, R., Lee, S., Parry, L., and Firtel, R.A. (2002). Spatial and temporal regulation of 3-phosphoinositides by PI 3-kinase and PTEN mediates chemotaxis. Cell *109*, 611-623.
Furuse, M., and Tsukita, S. (2006). Claudins in occluding junctions of humans and flies. Trends in cell biology *16*, 181-188.
Galbraith, C.G., Yamada, K.M., and Sheetz, M.P. (2002). The relationship between force and focal complex development. The Journal of cell biology *159*, 695-705.
Galic, M., Jeong, S., Tsai, F.C., Joubert, L.M., Wu, Y.I., Hahn, K.M., Cui, Y., and Meyer, T. (2012). External push and internal pull forces recruit curvature-sensing N-BAR domain proteins to the plasma membrane. Nature cell biology *14*, 874-881.
Galic, M., Tsai, F.C., Collins, S.R., Matis, M., Bandara, S., and Meyer, T. (2014). Dynamic recruitment of the curvature-sensitive protein ArhGAP44 to nanoscale membrane deformations limits exploratory filopodia initiation in neurons. eLife *3*, e03116.
Gallin, W.J., Edelman, G.M., and Cunningham, B.A. (1983). Characterization of L-CAM, a major cell adhesion molecule from embryonic liver cells. Proceedings of the National Academy of Sciences of the United States of America *80*, 1038-1042.
Gammill, L.S., Gonzalez, C., and Bronner-Fraser, M. (2007). Neuropilin 2/semaphorin 3F signaling is essential for cranial neural crest migration and trigeminal ganglion condensation. Developmental neurobiology *67*, 47-56.
Gammill, L.S., Gonzalez, C., Gu, C., and Bronner-Fraser, M. (2006). Guidance of trunk neural crest migration requires neuropilin 2/semaphorin 3F signaling. Development *133*, 99-106.

Gassama-Diagne, A., Yu, W., ter Beest, M., Martin-Belmonte, F., Kierbel, A., Engel, J., and Mostov, K. (2006). Phosphatidylinositol-3,4,5-trisphosphate regulates the formation of the basolateral plasma membrane in epithelial cells. Nature cell biology *8*, 963-970.
Gates, J., and Peifer, M. (2005). Can 1000 reviews be wrong? Actin, alpha-Catenin, and adherens junctions. Cell *123*, 769-772.
Ghassemi, S., Meacci, G., Liu, S., Gondarenko, A.A., Mathur, A., Roca-Cusachs, P., Sheetz, M.P., and Hone, J. (2012). Cells test substrate rigidity by local contractions on submicrometer pillars. Proceedings of the National Academy of Sciences of the United States of America *109*, 5328-5333.
Giehl, K., and Menke, A. (2008). Microenvironmental regulation of E-cadherin-mediated adherens junctions. Frontiers in bioscience : a journal and virtual library *13*, 3975-3985.
Giovannone, D., Reyes, M., Reyes, R., Correa, L., Martinez, D., Ra, H., Gomez, G., Kaiser, J., Ma, L., Stein, M.P.*, et al.* (2012). Slits affect the timely migration of neural crest cells via Robo receptor. Developmental dynamics : an official publication of the American Association of Anatomists *241*, 1274-1288.
Goodwin, M., Kovacs, E.M., Thoreson, M.A., Reynolds, A.B., and Yap, A.S. (2003). Minimal mutation of the cytoplasmic tail inhibits the ability of E-cadherin to activate Rac but not phosphatidylinositol 3-kinase: direct evidence of a role for cadherin-activated Rac signaling in adhesion and contact formation. The Journal of biological chemistry *278*, 20533-20539.
Gort, E.H., Groot, A.J., van der Wall, E., van Diest, P.J., and Vooijs, M.A. (2008). Hypoxic regulation of metastasis via hypoxia-inducible factors. Current molecular medicine *8*, 60-67.
Grashoff, C., Hoffman, B.D., Brenner, M.D., Zhou, R., Parsons, M., Yang, M.T., McLean, M.A., Sligar, S.G., Chen, C.S., Ha, T.*, et al.* (2010). Measuring mechanical tension across vinculin reveals regulation of focal adhesion dynamics. Nature *466*, 263-266.
Grosheva, I., Shtutman, M., Elbaum, M., and Bershadsky, A.D. (2001). p120 catenin affects cell motility via modulation of activity of Rho-family GTPases: a link between cell-cell contact formation and regulation of cell locomotion. Journal of cell science *114*, 695-707.
Grosshans, J., and Wieschaus, E. (2000). A genetic link between morphogenesis and cell division during formation of the ventral furrow in Drosophila. Cell *101*, 523-531.
Grotegut, S., von Schweinitz, D., Christofori, G., and Lehembre, F. (2006). Hepatocyte growth factor induces cell scattering through MAPK/Egr-1-mediated upregulation of Snail. The EMBO journal *25*, 3534-3545.
Gumbiner, B., and Simons, K. (1987). The role of uvomorulin in the formation of epithelial occluding junctions. Ciba Foundation symposium *125*, 168-186.
Halbleib, J.M., and Nelson, W.J. (2006). Cadherins in development: cell adhesion, sorting, and tissue morphogenesis. Genes & development *20*, 3199-3214.
Hall, R.J., and Erickson, C.A. (2003). ADAM 10: an active metalloprotease expressed during avian epithelial morphogenesis. Developmental biology *256*, 146-159.
Harland, R.M. (1991). In situ hybridization: an improved whole-mount method for Xenopus embryos. Methods in cell biology *36*, 685-695.

Harrison, O.J., Jin, X., Hong, S., Bahna, F., Ahlsen, G., Brasch, J., Wu, Y., Vendome, J., Felsovalyi, K., Hampton, C.M., *et al.* (2011). The extracellular architecture of adherens junctions revealed by crystal structures of type I cadherins. Structure *19*, 244-256.
Hay, E.D. (1995). An overview of epithelio-mesenchymal transformation. Acta anatomica *154*, 8-20.
Hay, E.D. (2005). The mesenchymal cell, its role in the embryo, and the remarkable signaling mechanisms that create it. Developmental dynamics : an official publication of the American Association of Anatomists *233*, 706-720.
Helwani, F.M., Kovacs, E.M., Paterson, A.D., Verma, S., Ali, R.G., Fanning, A.S., Weed, S.A., and Yap, A.S. (2004). Cortactin is necessary for E-cadherin-mediated contact formation and actin reorganization. The Journal of cell biology *164*, 899-910.
Heuberger, J., and Birchmeier, W. (2010). Interplay of cadherin-mediated cell adhesion and canonical Wnt signaling. Cold Spring Harbor perspectives in biology *2*, a002915.
Hidalgo-Carcedo, C., Hooper, S., Chaudhry, S.I., Williamson, P., Harrington, K., Leitinger, B., and Sahai, E. (2011). Collective cell migration requires suppression of actomyosin at cell-cell contacts mediated by DDR1 and the cell polarity regulators Par3 and Par6. Nature cell biology *13*, 49-58.
Higashida, C., Kiuchi, T., Akiba, Y., Mizuno, H., Maruoka, M., Narumiya, S., Mizuno, K., and Watanabe, N. (2013). F- and G-actin homeostasis regulates mechanosensitive actin nucleation by formins. Nature cell biology *15*, 395-405.
Hirano, M., Hashimoto, S., Yonemura, S., Sabe, H., and Aizawa, S. (2008). EPB41L5 functions to post-transcriptionally regulate cadherin and integrin during epithelial-mesenchymal transition. The Journal of cell biology *182*, 1217-1230.
Hirata, H., Tatsumi, H., and Sokabe, M. (2008). Mechanical forces facilitate actin polymerization at focal adhesions in a zyxin-dependent manner. Journal of cell science *121*, 2795-2804.
Ho, L., Symes, K., Yordan, C., Gudas, L.J., and Mercola, M. (1994). Localization of PDGF A and PDGFR alpha mRNA in Xenopus embryos suggests signalling from neural ectoderm and pharyngeal endoderm to neural crest cells. Mechanisms of development *48*, 165-174.
Hoj, J.P., Davis, J.A., Fullmer, K.E., Morrell, D.J., Saguibo, N.E., Schuler, J.T., Tuttle, K.J., and Hansen, M.D. (2014). Cellular contractility changes are sufficient to drive epithelial scattering. Experimental cell research *326*, 187-200.
Hong, S., Troyanovsky, R.B., and Troyanovsky, S.M. (2010). Spontaneous assembly and active disassembly balance adherens junction homeostasis. Proceedings of the National Academy of Sciences of the United States of America *107*, 3528-3533.
Honore, S.M., Aybar, M.J., and Mayor, R. (2003). Sox10 is required for the early development of the prospective neural crest in Xenopus embryos. Developmental biology *260*, 79-96.
Horwitz, A., Duggan, K., Buck, C., Beckerle, M.C., and Burridge, K. (1986). Interaction of plasma membrane fibronectin receptor with talin--a transmembrane linkage. Nature *320*, 531-533.
Hotulainen, P., and Lappalainen, P. (2006). Stress fibers are generated by two distinct actin assembly mechanisms in motile cells. The Journal of cell biology *173*, 383-394.

Houk, A.R., Jilkine, A., Mejean, C.O., Boltyanskiy, R., Dufresne, E.R., Angenent, S.B., Altschuler, S.J., Wu, L.F., and Weiner, O.D. (2012). Membrane tension maintains cell polarity by confining signals to the leading edge during neutrophil migration. Cell *148*, 175-188.
Huen, A.C., Park, J.K., Godsel, L.M., Chen, X., Bannon, L.J., Amargo, E.V., Hudson, T.Y., Mongiu, A.K., Leigh, I.M., Kelsell, D.P.*, et al.* (2002). Intermediate filament-membrane attachments function synergistically with actin-dependent contacts to regulate intercellular adhesive strength. The Journal of cell biology *159*, 1005-1017.
Hulsken, J., Behrens, J., and Birchmeier, W. (1994a). Tumor-suppressor gene products in cell contacts: the cadherin-APC-armadillo connection. Current opinion in cell biology *6*, 711-716.
Hulsken, J., Birchmeier, W., and Behrens, J. (1994b). E-cadherin and APC compete for the interaction with beta-catenin and the cytoskeleton. The Journal of cell biology *127*, 2061-2069.
Humphries, J.D., Wang, P., Streuli, C., Geiger, B., Humphries, M.J., and Ballestrem, C. (2007). Vinculin controls focal adhesion formation by direct interactions with talin and actin. The Journal of cell biology *179*, 1043-1057.
Hynes, R.O. (1987). Integrins: a family of cell surface receptors. Cell *48*, 549-554.
Hynes, R.O. (2002). Integrins: bidirectional, allosteric signaling machines. Cell *110*, 673-687.
Ikenouchi, J., Matsuda, M., Furuse, M., and Tsukita, S. (2003). Regulation of tight junctions during the epithelium-mesenchyme transition: direct repression of the gene expression of claudins/occludin by Snail. Journal of cell science *116*, 1959-1967.
Ireton, R.C., Davis, M.A., van Hengel, J., Mariner, D.J., Barnes, K., Thoreson, M.A., Anastasiadis, P.Z., Matrisian, L., Bundy, L.M., Sealy, L.*, et al.* (2002). A novel role for p120 catenin in E-cadherin function. The Journal of cell biology *159*, 465-476.
Ishiyama, N., Lee, S.H., Liu, S., Li, G.Y., Smith, M.J., Reichardt, L.F., and Ikura, M. (2010). Dynamic and static interactions between p120 catenin and E-cadherin regulate the stability of cell-cell adhesion. Cell *141*, 117-128.
Itoh, R.E., Kurokawa, K., Ohba, Y., Yoshizaki, H., Mochizuki, N., and Matsuda, M. (2002). Activation of rac and cdc42 video imaged by fluorescent resonance energy transfer-based single-molecule probes in the membrane of living cells. Molecular and cellular biology *22*, 6582-6591.
Ivanov, A.I., Hunt, D., Utech, M., Nusrat, A., and Parkos, C.A. (2005). Differential roles for actin polymerization and a myosin II motor in assembly of the epithelial apical junctional complex. Molecular biology of the cell *16*, 2636-2650.
Ivanov, A.I., Nusrat, A., and Parkos, C.A. (2004). Endocytosis of epithelial apical junctional proteins by a clathrin-mediated pathway into a unique storage compartment. Molecular biology of the cell *15*, 176-188.
Jaffe, A.B., and Hall, A. (2005). Rho GTPases: biochemistry and biology. Annual review of cell and developmental biology *21*, 247-269.
Jhingory, S., Wu, C.Y., and Taneyhill, L.A. (2010). Novel insight into the function and regulation of alphaN-catenin by Snail2 during chick neural crest cell migration. Developmental biology *344*, 896-910.
Jia, L., Cheng, L., and Raper, J. (2005). Slit/Robo signaling is necessary to confine early neural crest cells to the ventral migratory pathway in the trunk. Developmental biology *282*, 411-421.

Jiang, G., Giannone, G., Critchley, D.R., Fukumoto, E., and Sheetz, M.P. (2003). Two-piconewton slip bond between fibronectin and the cytoskeleton depends on talin. Nature *424*, 334-337.
Johnson, R.P., and Craig, S.W. (1995). F-actin binding site masked by the intramolecular association of vinculin head and tail domains. Nature *373*, 261-264.
Jorda, M., Olmeda, D., Vinyals, A., Valero, E., Cubillo, E., Llorens, A., Cano, A., and Fabra, A. (2005). Upregulation of MMP-9 in MDCK epithelial cell line in response to expression of the Snail transcription factor. Journal of cell science *118*, 3371-3385.
Jou, T.S., Stewart, D.B., Stappert, J., Nelson, W.J., and Marrs, J.A. (1995). Genetic and biochemical dissection of protein linkages in the cadherin-catenin complex. Proceedings of the National Academy of Sciences of the United States of America *92*, 5067-5071.
Junghans, D., Haas, I.G., and Kemler, R. (2005). Mammalian cadherins and protocadherins: about cell death, synapses and processing. Current opinion in cell biology *17*, 446-452.
Kadir, S., Astin, J.W., Tahtamouni, L., Martin, P., and Nobes, C.D. (2011). Microtubule remodelling is required for the front-rear polarity switch during contact inhibition of locomotion. Journal of cell science *124*, 2642-2653.
Kashef, J., Kohler, A., Kuriyama, S., Alfandari, D., Mayor, R., and Wedlich, D. (2009). Cadherin-11 regulates protrusive activity in Xenopus cranial neural crest cells upstream of Trio and the small GTPases. Genes & development *23*, 1393-1398.
Katsamba, P., Carroll, K., Ahlsen, G., Bahna, F., Vendome, J., Posy, S., Rajebhosale, M., Price, S., Jessell, T.M., Ben-Shaul, A.*, et al.* (2009). Linking molecular affinity and cellular specificity in cadherin-mediated adhesion. Proceedings of the National Academy of Sciences of the United States of America *106*, 11594-11599.
Kaverina, I., Krylyshkina, O., and Small, J.V. (1999). Microtubule targeting of substrate contacts promotes their relaxation and dissociation. The Journal of cell biology *146*, 1033-1044.
Kawakatsu, T., Shimizu, K., Honda, T., Fukuhara, T., Hoshino, T., and Takai, Y. (2002). Trans-interactions of nectins induce formation of filopodia and Lamellipodia through the respective activation of Cdc42 and Rac small G proteins. The Journal of biological chemistry *277*, 50749-50755.
Kemphues, K.J., Priess, J.R., Morton, D.G., and Cheng, N.S. (1988). Identification of genes required for cytoplasmic localization in early C. elegans embryos. Cell *52*, 311-320.
Kiema, T., Lad, Y., Jiang, P., Oxley, C.L., Baldassarre, M., Wegener, K.L., Campbell, I.D., Ylanne, J., and Calderwood, D.A. (2006). The molecular basis of filamin binding to integrins and competition with talin. Molecular cell *21*, 337-347.
Kim, J.B., Islam, S., Kim, Y.J., Prudoff, R.S., Sass, K.M., Wheelock, M.J., and Johnson, K.R. (2000a). N-Cadherin extracellular repeat 4 mediates epithelial to mesenchymal transition and increased motility. The Journal of cell biology *151*, 1193-1206.
Kim, M., Carman, C.V., and Springer, T.A. (2003). Bidirectional transmembrane signaling by cytoplasmic domain separation in integrins. Science *301*, 1720-1725.

Kim, S.H., Li, Z., and Sacks, D.B. (2000b). E-cadherin-mediated cell-cell attachment activates Cdc42. The Journal of biological chemistry *275*, 36999-37005.
Kiosses, W.B., Shattil, S.J., Pampori, N., and Schwartz, M.A. (2001). Rac recruits high-affinity integrin alphavbeta3 to lamellipodia in endothelial cell migration. Nature cell biology *3*, 316-320.
Kobielak, A., and Fuchs, E. (2004). Alpha-catenin: at the junction of intercellular adhesion and actin dynamics. Nature reviews Molecular cell biology *5*, 614-625.
Koenig, A., Mueller, C., Hasel, C., Adler, G., and Menke, A. (2006). Collagen type I induces disruption of E-cadherin-mediated cell-cell contacts and promotes proliferation of pancreatic carcinoma cells. Cancer research *66*, 4662-4671.
Koestner, U., Shnitsar, I., Linnemannstons, K., Hufton, A.L., and Borchers, A. (2008). Semaphorin and neuropilin expression during early morphogenesis of Xenopus laevis. Developmental dynamics : an official publication of the American Association of Anatomists *237*, 3853-3863.
Kohmura, N., Senzaki, K., Hamada, S., Kai, N., Yasuda, R., Watanabe, M., Ishii, H., Yasuda, M., Mishina, M., and Yagi, T. (1998). Diversity revealed by a novel family of cadherins expressed in neurons at a synaptic complex. Neuron *20*, 1137-1151.
Kolsch, V., Seher, T., Fernandez-Ballester, G.J., Serrano, L., and Leptin, M. (2007). Control of Drosophila gastrulation by apical localization of adherens junctions and RhoGEF2. Science *315*, 384-386.
Kovacs, E.M., Goodwin, M., Ali, R.G., Paterson, A.D., and Yap, A.S. (2002). Cadherin-directed actin assembly: E-cadherin physically associates with the Arp2/3 complex to direct actin assembly in nascent adhesive contacts. Current biology : CB *12*, 379-382.
Kovacs, E.M., Verma, S., Ali, R.G., Ratheesh, A., Hamilton, N.A., Akhmanova, A., and Yap, A.S. (2011). N-WASP regulates the epithelial junctional actin cytoskeleton through a non-canonical post-nucleation pathway. Nature cell biology *13*, 934-943.
Kraemer, A., Goodwin, M., Verma, S., Yap, A.S., and Ali, R.G. (2007). Rac is a dominant regulator of cadherin-directed actin assembly that is activated by adhesive ligation independently of Tiam1. American journal of physiology Cell physiology *292*, C1061-1069.
Krull, C.E., Lansford, R., Gale, N.W., Collazo, A., Marcelle, C., Yancopoulos, G.D., Fraser, S.E., and Bronner-Fraser, M. (1997). Interactions of Eph-related receptors and ligands confer rostrocaudal pattern to trunk neural crest migration. Current biology : CB *7*, 571-580.
Kuriyama, S., Theveneau, E., Benedetto, A., Parsons, M., Tanaka, M., Charras, G., Kabla, A., and Mayor, R. (2014). In vivo collective cell migration requires an LPAR2-dependent increase in tissue fluidity. The Journal of cell biology *206*, 113-127.
LaBonne, C., and Bronner-Fraser, M. (2000). Snail-related transcriptional repressors are required in Xenopus for both the induction of the neural crest and its subsequent migration. Developmental biology *221*, 195-205.
Ladoux, B., Anon, E., Lambert, M., Rabodzey, A., Hersen, P., Buguin, A., Silberzan, P., and Mege, R.M. (2010). Strength dependence of cadherin-mediated adhesions. Biophysical journal *98*, 534-542.

Lambert, M., Choquet, D., and Mege, R.M. (2002). Dynamics of ligand-induced, Rac1-dependent anchoring of cadherins to the actin cytoskeleton. The Journal of cell biology *157*, 469-479.
Landsberg, K.P., Farhadifar, R., Ranft, J., Umetsu, D., Widmann, T.J., Bittig, T., Said, A., Julicher, F., and Dahmann, C. (2009). Increased cell bond tension governs cell sorting at the Drosophila anteroposterior compartment boundary. Current biology : CB *19*, 1950-1955.
le Duc, Q., Shi, Q., Blonk, I., Sonnenberg, A., Wang, N., Leckband, D., and de Rooij, J. (2010). Vinculin potentiates E-cadherin mechanosensing and is recruited to actin-anchored sites within adherens junctions in a myosin II-dependent manner. The Journal of cell biology *189*, 1107-1115.
Lee, M., and Vasioukhin, V. (2008). Cell polarity and cancer--cell and tissue polarity as a non-canonical tumor suppressor. Journal of cell science *121*, 1141-1150.
Levental, K.R., Yu, H., Kass, L., Lakins, J.N., Egeblad, M., Erler, J.T., Fong, S.F., Csiszar, K., Giaccia, A., Weninger, W.*, et al.* (2009). Matrix crosslinking forces tumor progression by enhancing integrin signaling. Cell *139*, 891-906.
Lickert, H., Bauer, A., Kemler, R., and Stappert, J. (2000). Casein kinase II phosphorylation of E-cadherin increases E-cadherin/beta-catenin interaction and strengthens cell-cell adhesion. The Journal of biological chemistry *275*, 5090-5095.
Lin, Y.C., Tambe, D.T., Park, C.Y., Wasserman, M.R., Trepat, X., Krishnan, R., Lenormand, G., Fredberg, J.J., and Butler, J.P. (2010). Mechanosensing of substrate thickness. Physical review E, Statistical, nonlinear, and soft matter physics *82*, 041918.
Lisabeth, E.M., Falivelli, G., and Pasquale, E.B. (2013). Eph receptor signaling and ephrins. Cold Spring Harbor perspectives in biology *5*.
Liu, K.D., Datta, A., Yu, W., Brakeman, P.R., Jou, T.S., Matthay, M.A., and Mostov, K.E. (2007). Rac1 is required for reorientation of polarity and lumen formation through a PI 3-kinase-dependent pathway. American journal of physiology Renal physiology *293*, F1633-1640.
Liu, S., Thomas, S.M., Woodside, D.G., Rose, D.M., Kiosses, W.B., Pfaff, M., and Ginsberg, M.H. (1999). Binding of paxillin to alpha4 integrins modifies integrin-dependent biological responses. Nature *402*, 676-681.
Liu, Z., Tan, J.L., Cohen, D.M., Yang, M.T., Sniadecki, N.J., Ruiz, S.A., Nelson, C.M., and Chen, C.S. (2010). Mechanical tugging force regulates the size of cell-cell junctions. Proceedings of the National Academy of Sciences of the United States of America *107*, 9944-9949.
Lo, C.M., Wang, H.B., Dembo, M., and Wang, Y.L. (2000). Cell movement is guided by the rigidity of the substrate. Biophysical journal *79*, 144-152.
Lochter, A., Galosy, S., Muschler, J., Freedman, N., Werb, Z., and Bissell, M.J. (1997). Matrix metalloproteinase stromelysin-1 triggers a cascade of molecular alterations that leads to stable epithelial-to-mesenchymal conversion and a premalignant phenotype in mammary epithelial cells. The Journal of cell biology *139*, 1861-1872.
Lu, Z., Ghosh, S., Wang, Z., and Hunter, T. (2003). Downregulation of caveolin-1 function by EGF leads to the loss of E-cadherin, increased transcriptional activity of beta-catenin, and enhanced tumor cell invasion. Cancer Cell *4*, 499-515.

Macara, I.G. (2004). Par proteins: partners in polarization. Current biology : CB *14*, R160-162.
Machacek, M., Hodgson, L., Welch, C., Elliott, H., Pertz, O., Nalbant, P., Abell, A., Johnson, G.L., Hahn, K.M., and Danuser, G. (2009). Coordination of Rho GTPase activities during cell protrusion. Nature *461*, 99-103.
Mahoney, P.A., Weber, U., Onofrechuk, P., Biessmann, H., Bryant, P.J., and Goodman, C.S. (1991). The fat tumor suppressor gene in Drosophila encodes a novel member of the cadherin gene superfamily. Cell *67*, 853-868.
Martin, A.C., Kaschube, M., and Wieschaus, E.F. (2009). Pulsed contractions of an actin-myosin network drive apical constriction. Nature *457*, 495-499.
Martin, K., Vilela, M., Jeon, N.L., Danuser, G., and Pertz, O. (2014). A growth factor-induced, spatially organizing cytoskeletal module enables rapid and persistent fibroblast migration. Developmental cell *30*, 701-716.
Martin-Belmonte, F., Gassama, A., Datta, A., Yu, W., Rescher, U., Gerke, V., and Mostov, K. (2007). PTEN-mediated apical segregation of phosphoinositides controls epithelial morphogenesis through Cdc42. Cell *128*, 383-397.
Martinez-Estrada, O.M., Culleres, A., Soriano, F.X., Peinado, H., Bolos, V., Martinez, F.O., Reina, M., Cano, A., Fabre, M., and Vilaro, S. (2006). The transcription factors Slug and Snail act as repressors of Claudin-1 expression in epithelial cells. The Biochemical journal *394*, 449-457.
Martins, G.G., Rifes, P., Amandio, R., Rodrigues, G., Palmeirim, I., and Thorsteinsdottir, S. (2009). Dynamic 3D cell rearrangements guided by a fibronectin matrix underlie somitogenesis. PloS one *4*, e7429.
Maruthamuthu, V., Sabass, B., Schwarz, U.S., and Gardel, M.L. (2011). Cell-ECM traction force modulates endogenous tension at cell-cell contacts. Proceedings of the National Academy of Sciences of the United States of America *108*, 4708-4713.
Massague, J. (2008). TGFbeta in Cancer. Cell *134*, 215-230.
Matthews, H.K., Marchant, L., Carmona-Fontaine, C., Kuriyama, S., Larrain, J., Holt, M.R., Parsons, M., and Mayor, R. (2008). Directional migration of neural crest cells in vivo is regulated by Syndecan-4/Rac1 and non-canonical Wnt signaling/RhoA. Development *135*, 1771-1780.
Maul, R.S., Song, Y., Amann, K.J., Gerbin, S.C., Pollard, T.D., and Chang, D.D. (2003). EPLIN regulates actin dynamics by cross-linking and stabilizing filaments. The Journal of cell biology *160*, 399-407.
Mayor, R., and Carmona-Fontaine, C. (2010). Keeping in touch with contact inhibition of locomotion. Trends in cell biology *20*, 319-328.
Mayor, R., Guerrero, N., Young, R.M., Gomez-Skarmeta, J.L., and Cuellar, C. (2000). A novel function for the Xslug gene: control of dorsal mesendoderm development by repressing BMP-4. Mechanisms of development *97*, 47-56.
McCain, M.L., Lee, H., Aratyn-Schaus, Y., Kleber, A.G., and Parker, K.K. (2012). Cooperative coupling of cell-matrix and cell-cell adhesions in cardiac muscle. Proceedings of the National Academy of Sciences of the United States of America *109*, 9881-9886.
McCann, R.O., and Craig, S.W. (1999). Functional genomic analysis reveals the utility of the I/LWEQ module as a predictor of protein:actin interaction. Biochem Biophys Res Commun *266*, 135-140.

McCusker, C., Cousin, H., Neuner, R., and Alfandari, D. (2009). Extracellular cleavage of cadherin-11 by ADAM metalloproteases is essential for Xenopus cranial neural crest cell migration. Molecular biology of the cell *20*, 78-89.
McGrail, D.J., Mezencev, R., Kieu, Q.M., McDonald, J.F., and Dawson, M.R. (2014). SNAIL-induced epithelial-to-mesenchymal transition produces concerted biophysical changes from altered cytoskeletal gene expression. FASEB journal : official publication of the Federation of American Societies for Experimental Biology.
McKeown, S.J., Lee, V.M., Bronner-Fraser, M., Newgreen, D.F., and Farlie, P.G. (2005). Sox10 overexpression induces neural crest-like cells from all dorsoventral levels of the neural tube but inhibits differentiation. Developmental dynamics : an official publication of the American Association of Anatomists *233*, 430-444.
McLennan, R., and Kulesa, P.M. (2010). Neuropilin-1 interacts with the second branchial arch microenvironment to mediate chick neural crest cell dynamics. Developmental dynamics : an official publication of the American Association of Anatomists *239*, 1664-1673.
Mellott, D.O., and Burke, R.D. (2008). Divergent roles for Eph and ephrin in avian cranial neural crest. BMC developmental biology *8*, 56.
Mertens, A.E., Rygiel, T.P., Olivo, C., van der Kammen, R., and Collard, J.G. (2005). The Rac activator Tiam1 controls tight junction biogenesis in keratinocytes through binding to and activation of the Par polarity complex. The Journal of cell biology *170*, 1029-1037.
Monier, B., Pelissier-Monier, A., Brand, A.H., and Sanson, B. (2010). An actomyosin-based barrier inhibits cell mixing at compartmental boundaries in Drosophila embryos. Nature cell biology *12*, 60-65; sup pp 61-69.
Monier-Gavelle, F., and Duband, J.L. (1997). Cross talk between adhesion molecules: control of N-cadherin activity by intracellular signals elicited by beta1 and beta3 integrins in migrating neural crest cells. The Journal of cell biology *137*, 1663-1681.
Montanez, E., Ussar, S., Schifferer, M., Bosl, M., Zent, R., Moser, M., and Fassler, R. (2008). Kindlin-2 controls bidirectional signaling of integrins. Genes & development *22*, 1325-1330.
Moore, R., Theveneau, E., Pozzi, S., Alexandre, P., Richardson, J., Merks, A., Parsons, M., Kashef, J., Linker, C., and Mayor, R. (2013). Par3 controls neural crest migration by promoting microtubule catastrophe during contact inhibition of locomotion. Development *140*, 4763-4775.
Morais-de-Sa, E., Mirouse, V., and St Johnston, D. (2010). aPKC phosphorylation of Bazooka defines the apical/lateral border in Drosophila epithelial cells. Cell *141*, 509-523.
Moreno-Bueno, G., Portillo, F., and Cano, A. (2008). Transcriptional regulation of cell polarity in EMT and cancer. Oncogene *27*, 6958-6969.
Munoz, W.A., and Trainor, P.A. (2015). Neural crest cell evolution: how and when did a neural crest cell become a neural crest cell. Current topics in developmental biology *111*, 3-26.
Nagafuchi, A., Ishihara, S., and Tsukita, S. (1994). The roles of catenins in the cadherin-mediated cell adhesion: functional analysis of E-cadherin-alpha catenin fusion molecules. The Journal of cell biology *127*, 235-245.

Nagafuchi, A., and Takeichi, M. (1988). Cell binding function of E-cadherin is regulated by the cytoplasmic domain. The EMBO journal *7*, 3679-3684.
Nakagawa, M., Fukata, M., Yamaga, M., Itoh, N., and Kaibuchi, K. (2001). Recruitment and activation of Rac1 by the formation of E-cadherin-mediated cell-cell adhesion sites. Journal of cell science *114*, 1829-1838.
Nakagawa, S., and Takeichi, M. (1995). Neural crest cell-cell adhesion controlled by sequential and subpopulation-specific expression of novel cadherins. Development *121*, 1321-1332.
Nandadasa, S., Tao, Q., Menon, N.R., Heasman, J., and Wylie, C. (2009). N- and E-cadherins in Xenopus are specifically required in the neural and non-neural ectoderm, respectively, for F-actin assembly and morphogenetic movements. Development *136*, 1327-1338.
Nanes, B.A., Chiasson-MacKenzie, C., Lowery, A.M., Ishiyama, N., Faundez, V., Ikura, M., Vincent, P.A., and Kowalczyk, A.P. (2012). p120-catenin binding masks an endocytic signal conserved in classical cadherins. The Journal of cell biology *199*, 365-380.
Nelson, W.J. (2008). Regulation of cell-cell adhesion by the cadherin-catenin complex. Biochemical Society transactions *36*, 149-155.
Nelson, W.J. (2009). Remodeling epithelial cell organization: transitions between front-rear and apical-basal polarity. Cold Spring Harbor perspectives in biology *1*, a000513.
Ng, M.R., Besser, A., Danuser, G., and Brugge, J.S. (2012). Substrate stiffness regulates cadherin-dependent collective migration through myosin-II contractility. The Journal of cell biology *199*, 545-563.
Nguyen, T.N., Uemura, A., Shih, W., and Yamada, S. (2010). Zyxin-mediated actin assembly is required for efficient wound closure. The Journal of biological chemistry *285*, 35439-35445.
Nichols, D.H. (1981). Neural crest formation in the head of the mouse embryo as observed using a new histological technique. Journal of embryology and experimental morphology *64*, 105-120.
Nichols, D.H. (1987). Ultrastructure of neural crest formation in the midbrain/rostral hindbrain and preotic hindbrain regions of the mouse embryo. The American journal of anatomy *179*, 143-154.
Nieman, M.T., Prudoff, R.S., Johnson, K.R., and Wheelock, M.J. (1999). N-cadherin promotes motility in human breast cancer cells regardless of their E-cadherin expression. The Journal of cell biology *147*, 631-644.
Nieto, M.A. (2011). The ins and outs of the epithelial to mesenchymal transition in health and disease. Annual review of cell and developmental biology *27*, 347-376.
Nieto, M.A., Sargent, M.G., Wilkinson, D.G., and Cooke, J. (1994). Control of cell behavior during vertebrate development by Slug, a zinc finger gene. Science *264*, 835-839.
Noren, N.K., Liu, B.P., Burridge, K., and Kreft, B. (2000). p120 catenin regulates the actin cytoskeleton via Rho family GTPases. The Journal of cell biology *150*, 567-580.
O'Brien, L.E., Jou, T.S., Pollack, A.L., Zhang, Q., Hansen, S.H., Yurchenco, P., and Mostov, K.E. (2001). Rac1 orientates epithelial apical polarity through effects on basolateral laminin assembly. Nature cell biology *3*, 831-838.

Oakes, P.W., Beckham, Y., Stricker, J., and Gardel, M.L. (2012). Tension is required but not sufficient for focal adhesion maturation without a stress fiber template. The Journal of cell biology *196*, 363-374.
Oas, R.G., Nanes, B.A., Esimai, C.C., Vincent, P.A., Garcia, A.J., and Kowalczyk, A.P. (2013). p120-catenin and beta-catenin differentially regulate cadherin adhesive function. Molecular biology of the cell *24*, 704-714.
Obata, S., Sago, H., Mori, N., Rochelle, J.M., Seldin, M.F., Davidson, M., St John, T., Taketani, S., and Suzuki, S.T. (1995). Protocadherin Pcdh2 shows properties similar to, but distinct from, those of classical cadherins. Journal of cell science *108 (Pt 12)*, 3765-3773.
Oda, H., Tsukita, S., and Takeichi, M. (1998). Dynamic behavior of the cadherin-based cell-cell adhesion system during Drosophila gastrulation. Developmental biology *203*, 435-450.
Ojakian, G.K., Ratcliffe, D.R., and Schwimmer, R. (2001). Integrin regulation of cell-cell adhesion during epithelial tubule formation. Journal of cell science *114*, 941-952.
Olesnicky Killian, E.C., Birkholz, D.A., and Artinger, K.B. (2009). A role for chemokine signaling in neural crest cell migration and craniofacial development. Developmental biology *333*, 161-172.
Ouyang, M., Lu, S., Kim, T., Chen, C.E., Seong, J., Leckband, D.E., Wang, F., Reynolds, A.B., Schwartz, M.A., and Wang, Y. (2013). N-cadherin regulates spatially polarized signals through distinct p120ctn and beta-catenin-dependent signalling pathways. Nature communications *4*, 1589.
Ozawa, M., Ringwald, M., and Kemler, R. (1990). Uvomorulin-catenin complex formation is regulated by a specific domain in the cytoplasmic region of the cell adhesion molecule. Proceedings of the National Academy of Sciences of the United States of America *87*, 4246-4250.
Ozdamar, B., Bose, R., Barrios-Rodiles, M., Wang, H.R., Zhang, Y., and Wrana, J.L. (2005). Regulation of the polarity protein Par6 by TGFbeta receptors controls epithelial cell plasticity. Science *307*, 1603-1609.
Palacios, F., Price, L., Schweitzer, J., Collard, J.G., and D'Souza-Schorey, C. (2001). An essential role for ARF6-regulated membrane traffic in adherens junction turnover and epithelial cell migration. The EMBO journal *20*, 4973-4986.
Parsons, J.T., Martin, K.H., Slack, J.K., Taylor, J.M., and Weed, S.A. (2000). Focal adhesion kinase: a regulator of focal adhesion dynamics and cell movement. Oncogene *19*, 5606-5613.
Patel, S.D., Ciatto, C., Chen, C.P., Bahna, F., Rajebhosale, M., Arkus, N., Schieren, I., Jessell, T.M., Honig, B., Price, S.R*., et al.* (2006). Type II cadherin ectodomain structures: implications for classical cadherin specificity. Cell *124*, 1255-1268.
Paterson, A.D., Parton, R.G., Ferguson, C., Stow, J.L., and Yap, A.S. (2003). Characterization of E-cadherin endocytosis in isolated MCF-7 and chinese hamster ovary cells: the initial fate of unbound E-cadherin. The Journal of biological chemistry *278*, 21050-21057.
Pegtel, D.M., Ellenbroek, S.I., Mertens, A.E., van der Kammen, R.A., de Rooij, J., and Collard, J.G. (2007). The Par-Tiam1 complex controls persistent migration by stabilizing microtubule-dependent front-rear polarity. Current biology : CB *17*, 1623-1634.

Peinado, H., Ballestar, E., Esteller, M., and Cano, A. (2004a). Snail mediates E-cadherin repression by the recruitment of the Sin3A/histone deacetylase 1 (HDAC1)/HDAC2 complex. Molecular and cellular biology *24*, 306-319.
Peinado, H., Marin, F., Cubillo, E., Stark, H.J., Fusenig, N., Nieto, M.A., and Cano, A. (2004b). Snail and E47 repressors of E-cadherin induce distinct invasive and angiogenic properties in vivo. Journal of cell science *117*, 2827-2839.
Pertz, O., Hodgson, L., Klemke, R.L., and Hahn, K.M. (2006). Spatiotemporal dynamics of RhoA activity in migrating cells. Nature *440*, 1069-1072.
Peyrieras, N., Hyafil, F., Louvard, D., Ploegh, H.L., and Jacob, F. (1983). Uvomorulin: a nonintegral membrane protein of early mouse embryo. Proceedings of the National Academy of Sciences of the United States of America *80*, 6274-6277.
Piloto, S., and Schilling, T.F. (2010). Ovo1 links Wnt signaling with N-cadherin localization during neural crest migration. Development *137*, 1981-1990.
Pokutta, S., Drees, F., Takai, Y., Nelson, W.J., and Weis, W.I. (2002). Biochemical and structural definition of the l-afadin- and actin-binding sites of alpha-catenin. The Journal of biological chemistry *277*, 18868-18874.
Pokutta, S., Drees, F., Yamada, S., Nelson, W.J., and Weis, W.I. (2008). Biochemical and structural analysis of alpha-catenin in cell-cell contacts. Biochemical Society transactions *36*, 141-147.
Pokutta, S., and Weis, W.I. (2000). Structure of the dimerization and beta-catenin-binding region of alpha-catenin. Molecular cell *5*, 533-543.
Pollard, T.D., and Borisy, G.G. (2003). Cellular motility driven by assembly and disassembly of actin filaments. Cell *112*, 453-465.
Polyak, K., and Weinberg, R.A. (2009). Transitions between epithelial and mesenchymal states: acquisition of malignant and stem cell traits. Nature reviews Cancer *9*, 265-273.
Ponti, A., Machacek, M., Gupton, S.L., Waterman-Storer, C.M., and Danuser, G. (2004). Two distinct actin networks drive the protrusion of migrating cells. Science *305*, 1782-1786.
Qin, Y., Meisen, W.H., Hao, Y., and Macara, I.G. (2010). Tuba, a Cdc42 GEF, is required for polarized spindle orientation during epithelial cyst formation. The Journal of cell biology *189*, 661-669.
Quinlan, M.P., and Hyatt, J.L. (1999). Establishment of the circumferential actin filament network is a prerequisite for localization of the cadherin-catenin complex in epithelial cells. Cell growth & differentiation : the molecular biology journal of the American Association for Cancer Research *10*, 839-854.
Ratheesh, A., Gomez, G.A., Priya, R., Verma, S., Kovacs, E.M., Jiang, K., Brown, N.H., Akhmanova, A., Stehbens, S.J., and Yap, A.S. (2012). Centralspindlin and alpha-catenin regulate Rho signalling at the epithelial zonula adherens. Nature cell biology *14*, 818-828.
Rauzi, M., Lenne, P.F., and Lecuit, T. (2010). Planar polarized actomyosin contractile flows control epithelial junction remodelling. Nature *468*, 1110-1114.
Reffay, M., Parrini, M.C., Cochet-Escartin, O., Ladoux, B., Buguin, A., Coscoy, S., Amblard, F., Camonis, J., and Silberzan, P. (2014). Interplay of RhoA and mechanical forces in collective cell migration driven by leader cells. Nature cell biology *16*, 217-223.

Reiss, K., Maretzky, T., Ludwig, A., Tousseyn, T., de Strooper, B., Hartmann, D., and Saftig, P. (2005). ADAM10 cleavage of N-cadherin and regulation of cell-cell adhesion and beta-catenin nuclear signalling. The EMBO journal *24*, 742-752.
Reynolds, A.B., Daniel, J., McCrea, P.D., Wheelock, M.J., Wu, J., and Zhang, Z. (1994). Identification of a new catenin: the tyrosine kinase substrate p120cas associates with E-cadherin complexes. Molecular and cellular biology *14*, 8333-8342.
Reynolds, A.B., Herbert, L., Cleveland, J.L., Berg, S.T., and Gaut, J.R. (1992). p120, a novel substrate of protein tyrosine kinase receptors and of p60v-src, is related to cadherin-binding factors beta-catenin, plakoglobin and armadillo. Oncogene *7*, 2439-2445.
Reynolds, A.B., Kanner, S.B., Bouton, A.H., Schaller, M.D., Weed, S.A., Flynn, D.C., and Parsons, J.T. (2014). SRChing for the substrates of Src. Oncogene *33*, 4537-4547.
Reynolds, A.B., Roesel, D.J., Kanner, S.B., and Parsons, J.T. (1989). Transformation-specific tyrosine phosphorylation of a novel cellular protein in chicken cells expressing oncogenic variants of the avian cellular src gene. Molecular and cellular biology *9*, 629-638.
Ridley, A.J. (2001). Rho GTPases and cell migration. Journal of cell science *114*, 2713-2722.
Ridley, A.J., Schwartz, M.A., Burridge, K., Firtel, R.A., Ginsberg, M.H., Borisy, G., Parsons, J.T., and Horwitz, A.R. (2003). Cell migration: integrating signals from front to back. Science *302*, 1704-1709.
Rimm, D.L., Koslov, E.R., Kebriaei, P., Cianci, C.D., and Morrow, J.S. (1995). Alpha 1(E)-catenin is an actin-binding and -bundling protein mediating the attachment of F-actin to the membrane adhesion complex. Proceedings of the National Academy of Sciences of the United States of America *92*, 8813-8817.
Riveline, D., Zamir, E., Balaban, N.Q., Schwarz, U.S., Ishizaki, T., Narumiya, S., Kam, Z., Geiger, B., and Bershadsky, A.D. (2001). Focal contacts as mechanosensors: externally applied local mechanical force induces growth of focal contacts by an mDia1-dependent and ROCK-independent mechanism. The Journal of cell biology *153*, 1175-1186.
Roca-Cusachs, P., Sunyer, R., and Trepat, X. (2013). Mechanical guidance of cell migration: lessons from chemotaxis. Current opinion in cell biology *25*, 543-549.
Rodriguez-Boulan, E., and Macara, I.G. (2014). Organization and execution of the epithelial polarity programme. Nature reviews Molecular cell biology *15*, 225-242.
Rooney, C., White, G., Nazgiewicz, A., Woodcock, S.A., Anderson, K.I., Ballestrem, C., and Malliri, A. (2010). The Rac activator STEF (Tiam2) regulates cell migration by microtubule-mediated focal adhesion disassembly. EMBO reports *11*, 292-298.
Roszik, J., Lisboa, D., Szollosi, J., and Vereb, G. (2009). Evaluation of intensity-based ratiometric FRET in image cytometry--approaches and a software solution. Cytometry Part A : the journal of the International Society for Analytical Cytology *75*, 761-767.
Sadaghiani, B., and Thiebaud, C.H. (1987). Neural crest development in the Xenopus laevis embryo, studied by interspecific transplantation and scanning electron microscopy. Developmental biology *124*, 91-110.

Saez, A., Buguin, A., Silberzan, P., and Ladoux, B. (2005). Is the mechanical activity of epithelial cells controlled by deformations or forces? Biophysical journal *89*, L52-54.
Sander, E.E., van Delft, S., ten Klooster, J.P., Reid, T., van der Kammen, R.A., Michiels, F., and Collard, J.G. (1998). Matrix-dependent Tiam1/Rac signaling in epithelial cells promotes either cell-cell adhesion or cell migration and is regulated by phosphatidylinositol 3-kinase. The Journal of cell biology *143*, 1385-1398.
Santiago, A., and Erickson, C.A. (2002). Ephrin-B ligands play a dual role in the control of neural crest cell migration. Development *129*, 3621-3632.
Sato, A., Scholl, A.M., Kuhn, E.N., Stadt, H.A., Decker, J.R., Pegram, K., Hutson, M.R., and Kirby, M.L. (2011). FGF8 signaling is chemotactic for cardiac neural crest cells. Developmental biology *354*, 18-30.
Sauka-Spengler, T., and Bronner-Fraser, M. (2008). A gene regulatory network orchestrates neural crest formation. Nature reviews Molecular cell biology *9*, 557-568.
Scarpa, E., Roycroft, A., Theveneau, E., Terriac, E., Piel, M., and Mayor, R. (2013). A novel method to study contact inhibition of locomotion using micropatterned substrates. Biology open *2*, 901-906.
Schatteman, G.C., Morrison-Graham, K., van Koppen, A., Weston, J.A., and Bowen-Pope, D.F. (1992). Regulation and role of PDGF receptor alpha-subunit expression during embryogenesis. Development *115*, 123-131.
Schwartz, M.A., and Shattil, S.J. (2000). Signaling networks linking integrins and rho family GTPases. Trends in biochemical sciences *25*, 388-391.
Sela-Donenfeld, D., and Kalcheim, C. (1999). Regulation of the onset of neural crest migration by coordinated activity of BMP4 and Noggin in the dorsal neural tube. Development *126*, 4749-4762.
Serres, M., Filhol, O., Lickert, H., Grangeasse, C., Chambaz, E.M., Stappert, J., Vincent, C., and Schmitt, D. (2000). The disruption of adherens junctions is associated with a decrease of E-cadherin phosphorylation by protein kinase CK2. Experimental cell research *257*, 255-264.
Shapiro, L., Fannon, A.M., Kwong, P.D., Thompson, A., Lehmann, M.S., Grubel, G., Legrand, J.F., Als-Nielsen, J., Colman, D.R., and Hendrickson, W.A. (1995). Structural basis of cell-cell adhesion by cadherins. Nature *374*, 327-337.
Sheehan, K.M., Gulmann, C., Eichler, G.S., Weinstein, J.N., Barrett, H.L., Kay, E.W., Conroy, R.M., Liotta, L.A., and Petricoin, E.F., 3rd (2008). Signal pathway profiling of epithelial and stromal compartments of colonic carcinoma reveals epithelial-mesenchymal transition. Oncogene *27*, 323-331.
Shin, K., Wang, Q., and Margolis, B. (2007). PATJ regulates directional migration of mammalian epithelial cells. EMBO reports *8*, 158-164.
Shoval, I., Ludwig, A., and Kalcheim, C. (2007). Antagonistic roles of full-length N-cadherin and its soluble BMP cleavage product in neural crest delamination. Development *134*, 491-501.
Simoes Sde, M., Blankenship, J.T., Weitz, O., Farrell, D.L., Tamada, M., Fernandez-Gonzalez, R., and Zallen, J.A. (2010). Rho-kinase directs Bazooka/Par-3 planar polarity during Drosophila axis elongation. Developmental cell *19*, 377-388.
Skaper, S.D., Kee, W.J., Facci, L., Macdonald, G., Doherty, P., and Walsh, F.S. (2000). The FGFR1 inhibitor PD 173074 selectively and potently antagonizes FGF-2 neurotrophic and neurotropic effects. Journal of neurochemistry *75*, 1520-1527.

Small, J.V., and Kaverina, I. (2003). Microtubules meet substrate adhesions to arrange cell polarity. Current opinion in cell biology *15*, 40-47.
Smith, A., Robinson, V., Patel, K., and Wilkinson, D.G. (1997). The EphA4 and EphB1 receptor tyrosine kinases and ephrin-B2 ligand regulate targeted migration of branchial neural crest cells. Current biology : CB *7*, 561-570.
Smith, A.L., Dohn, M.R., Brown, M.V., and Reynolds, A.B. (2012). Association of Rho-associated protein kinase 1 with E-cadherin complexes is mediated by p120-catenin. Molecular biology of the cell *23*, 99-110.
Smith, M.A., Blankman, E., Gardel, M.L., Luettjohann, L., Waterman, C.M., and Beckerle, M.C. (2010). A zyxin-mediated mechanism for actin stress fiber maintenance and repair. Developmental cell *19*, 365-376.
Smutny, M., Cox, H.L., Leerberg, J.M., Kovacs, E.M., Conti, M.A., Ferguson, C., Hamilton, N.A., Parton, R.G., Adelstein, R.S., and Yap, A.S. (2010). Myosin II isoforms identify distinct functional modules that support integrity of the epithelial zonula adherens. Nature cell biology *12*, 696-702.
Sperry, R.B., Bishop, N.H., Bramwell, J.J., Brodeur, M.N., Carter, M.J., Fowler, B.T., Lewis, Z.B., Maxfield, S.D., Staley, D.M., Vellinga, R.M.*, et al.* (2010). Zyxin controls migration in epithelial-mesenchymal transition by mediating actin-membrane linkages at cell-cell junctions. Journal of cellular physiology *222*, 612-624.
Sprague, B.L., Pego, R.L., Stavreva, D.A., and McNally, J.G. (2004). Analysis of binding reactions by fluorescence recovery after photobleaching. Biophysical journal *86*, 3473-3495.
Srinivasan, S., Wang, F., Glavas, S., Ott, A., Hofmann, F., Aktories, K., Kalman, D., and Bourne, H.R. (2003). Rac and Cdc42 play distinct roles in regulating PI(3,4,5)P3 and polarity during neutrophil chemotaxis. The Journal of cell biology *160*, 375-385.
St Johnston, D., and Ahringer, J. (2010). Cell polarity in eggs and epithelia: parallels and diversity. Cell *141*, 757-774.
Steventon, B., Araya, C., Linker, C., Kuriyama, S., and Mayor, R. (2009). Differential requirements of BMP and Wnt signalling during gastrulation and neurulation define two steps in neural crest induction. Development *136*, 771-779.
Stramer, B., Moreira, S., Millard, T., Evans, I., Huang, C.Y., Sabet, O., Milner, M., Dunn, G., Martin, P., and Wood, W. (2010a). Clasp-mediated microtubule bundling regulates persistent motility and contact repulsion in Drosophila macrophages in vivo. J Cell Biol *189*, 681-689.
Stramer, B., Moreira, S., Millard, T., Evans, I., Huang, C.Y., Sabet, O., Milner, M., Dunn, G., Martin, P., and Wood, W. (2010b). Clasp-mediated microtubule bundling regulates persistent motility and contact repulsion in Drosophila macrophages in vivo. The Journal of cell biology *189*, 681-689.
Svetic, V., Hollway, G.E., Elworthy, S., Chipperfield, T.R., Davison, C., Adams, R.J., Eisen, J.S., Ingham, P.W., Currie, P.D., and Kelsh, R.N. (2007). Sdf1a patterns zebrafish melanophores and links the somite and melanophore pattern defects in choker mutants. Development *134*, 1011-1022.
Taguchi, K., Ishiuchi, T., and Takeichi, M. (2011). Mechanosensitive EPLIN-dependent remodeling of adherens junctions regulates epithelial reshaping. The Journal of cell biology *194*, 643-656.
Taillard, E.D., Waelti, P., and Zuber, J. (2008). Few statistical tests for proportions comparison. Eur J Oper Res *185*, 1336-1350.

Takai, Y., and Nakanishi, H. (2003). Nectin and afadin: novel organizers of intercellular junctions. Journal of cell science *116*, 17-27.
Takaishi, K., Sasaki, T., Kotani, H., Nishioka, H., and Takai, Y. (1997). Regulation of cell-cell adhesion by rac and rho small G proteins in MDCK cells. The Journal of cell biology *139*, 1047-1059.
Tallquist, M.D., and Soriano, P. (2003). Cell autonomous requirement for PDGFRalpha in populations of cranial and cardiac neural crest cells. Development *130*, 507-518.
Tallquist, M.D., Weismann, K.E., Hellstrom, M., and Soriano, P. (2000). Early myotome specification regulates PDGFA expression and axial skeleton development. Development *127*, 5059-5070.
Tambe, D.T., Croutelle, U., Trepat, X., Park, C.Y., Kim, J.H., Millet, E., Butler, J.P., and Fredberg, J.J. (2013). Monolayer stress microscopy: limitations, artifacts, and accuracy of recovered intercellular stresses. PloS one *8*, e55172.
Tambe, D.T., Hardin, C.C., Angelini, T.E., Rajendran, K., Park, C.Y., Serra-Picamal, X., Zhou, E.H., Zaman, M.H., Butler, J.P., Weitz, D.A*., et al.* (2011). Collective cell guidance by cooperative intercellular forces. Nature materials *10*, 469-475.
Taneyhill, L.A., Coles, E.G., and Bronner-Fraser, M. (2007). Snail2 directly represses cadherin6B during epithelial-to-mesenchymal transitions of the neural crest. Development *134*, 1481-1490.
Tang, V.W., and Brieher, W.M. (2012). alpha-Actinin-4/FSGS1 is required for Arp2/3-dependent actin assembly at the adherens junction. The Journal of cell biology *196*, 115-130.
Tanoue, T., and Takeichi, M. (2004). Mammalian Fat1 cadherin regulates actin dynamics and cell-cell contact. The Journal of cell biology *165*, 517-528.
Taulet, N., Comunale, F., Favard, C., Charrasse, S., Bodin, S., and Gauthier-Rouviere, C. (2009). N-cadherin/p120 catenin association at cell-cell contacts occurs in cholesterol-rich membrane domains and is required for RhoA activation and myogenesis. The Journal of biological chemistry *284*, 23137-23145.
Taveau, J.C., Dubois, M., Le Bihan, O., Trepout, S., Almagro, S., Hewat, E., Durmort, C., Heyraud, S., Gulino-Debrac, D., and Lambert, O. (2008). Structure of artificial and natural VE-cadherin-based adherens junctions. Biochemical Society transactions *36*, 189-193.
Tepass, U. (2012). The apical polarity protein network in Drosophila epithelial cells: regulation of polarity, junctions, morphogenesis, cell growth, and survival. Annual review of cell and developmental biology *28*, 655-685.
Theveneau, E., Duband, J.L., and Altabef, M. (2007). Ets-1 confers cranial features on neural crest delamination. PloS one *2*, e1142.
Theveneau, E., Marchant, L., Kuriyama, S., Gull, M., Moepps, B., Parsons, M., and Mayor, R. (2010). Collective chemotaxis requires contact-dependent cell polarity. Developmental cell *19*, 39-53.
Theveneau, E., and Mayor, R. (2012a). Cadherins in collective cell migration of mesenchymal cells. Current opinion in cell biology *24*, 677-684.
Theveneau, E., and Mayor, R. (2012b). Neural crest delamination and migration: from epithelium-to-mesenchyme transition to collective cell migration. Developmental biology *366*, 34-54.

Theveneau, E., Steventon, B., Scarpa, E., Garcia, S., Trepat, X., Streit, A., and Mayor, R. (2013). Chase-and-run between adjacent cell populations promotes directional collective migration. Nature cell biology *15*, 763-772.
Thomas, W.A., Boscher, C., Chu, Y.S., Cuvelier, D., Martinez-Rico, C., Seddiki, R., Heysch, J., Ladoux, B., Thiery, J.P., Mege, R.M.*, et al.* (2013). alpha-Catenin and vinculin cooperate to promote high E-cadherin-based adhesion strength. The Journal of biological chemistry *288*, 4957-4969.
Thomason, H.A., Scothern, A., McHarg, S., and Garrod, D.R. (2010). Desmosomes: adhesive strength and signalling in health and disease. The Biochemical journal *429*, 419-433.
Thoreson, M.A., Anastasiadis, P.Z., Daniel, J.M., Ireton, R.C., Wheelock, M.J., Johnson, K.R., Hummingbird, D.K., and Reynolds, A.B. (2000). Selective uncoupling of p120(ctn) from E-cadherin disrupts strong adhesion. The Journal of cell biology *148*, 189-202.
Trelstad, R.L., Hay, E.D., and Revel, J.D. (1967). Cell contact during early morphogenesis in the chick embryo. Developmental biology *16*, 78-106.
Triana-Baltzer, G.B., and Blank, M. (2006). Cytoplasmic domain of protocadherin-alpha enhances homophilic interactions and recognizes cytoskeletal elements. Journal of neurobiology *66*, 393-407.
Tribulo, C., Aybar, M.J., Sanchez, S.S., and Mayor, R. (2004). A balance between the anti-apoptotic activity of Slug and the apoptotic activity of msx1 is required for the proper development of the neural crest. Developmental biology *275*, 325-342.
Trichet, L., Le Digabel, J., Hawkins, R.J., Vedula, S.R., Gupta, M., Ribrault, C., Hersen, P., Voituriez, R., and Ladoux, B. (2012). Evidence of a large-scale mechanosensing mechanism for cellular adaptation to substrate stiffness. Proceedings of the National Academy of Sciences of the United States of America *109*, 6933-6938.
Tsai, J., and Kam, L. (2009). Rigidity-dependent cross talk between integrin and cadherin signaling. Biophysical journal *96*, L39-41.
Tseng, Q., Duchemin-Pelletier, E., Deshiere, A., Balland, M., Guillou, H., Filhol, O., and Thery, M. (2012). Spatial organization of the extracellular matrix regulates cell-cell junction positioning. Proceedings of the National Academy of Sciences of the United States of America *109*, 1506-1511.
Utton, M.A., Eickholt, B., Howell, F.V., Wallis, J., and Doherty, P. (2001). Soluble N-cadherin stimulates fibroblast growth factor receptor dependent neurite outgrowth and N-cadherin and the fibroblast growth factor receptor co-cluster in cells. Journal of neurochemistry *76*, 1421-1430.
Valls, G., Codina, M., Miller, R.K., Del Valle-Perez, B., Vinyoles, M., Caelles, C., McCrea, P.D., Garcia de Herreros, A., and Dunach, M. (2012). Upon Wnt stimulation, Rac1 activation requires Rac1 and Vav2 binding to p120-catenin. Journal of cell science *125*, 5288-5301.
Vasioukhin, V., Bauer, C., Yin, M., and Fuchs, E. (2000). Directed actin polymerization is the driving force for epithelial cell-cell adhesion. Cell *100*, 209-219.
Vasioukhin, V., Bowers, E., Bauer, C., Degenstein, L., and Fuchs, E. (2001). Desmoplakin is essential in epidermal sheet formation. Nature cell biology *3*, 1076-1085.

Vega, S., Morales, A.V., Ocana, O.H., Valdes, F., Fabregat, I., and Nieto, M.A. (2004). Snail blocks the cell cycle and confers resistance to cell death. Genes & development *18*, 1131-1143.
Vendome, J., Posy, S., Jin, X., Bahna, F., Ahlsen, G., Shapiro, L., and Honig, B. (2011). Molecular design principles underlying beta-strand swapping in the adhesive dimerization of cadherins. Nature structural & molecular biology *18*, 693-700.
Villar-Cervino, V., Molano-Mazon, M., Catchpole, T., Valdeolmillos, M., Henkemeyer, M., Martinez, L.M., Borrell, V., and Marin, O. (2013). Contact repulsion controls the dispersion and final distribution of Cajal-Retzius cells. Neuron *77*, 457-471.
Vitorino, P., Hammer, M., Kim, J., and Meyer, T. (2011). A steering model of endothelial sheet migration recapitulates monolayer integrity and directed collective migration. Molecular and cellular biology *31*, 342-350.
von Schlippe, M., Marshall, J.F., Perry, P., Stone, M., Zhu, A.J., and Hart, I.R. (2000). Functional interaction between E-cadherin and alphav-containing integrins in carcinoma cells. Journal of cell science *113 (Pt 3)*, 425-437.
von Stein, W., Ramrath, A., Grimm, A., Muller-Borg, M., and Wodarz, A. (2005). Direct association of Bazooka/PAR-3 with the lipid phosphatase PTEN reveals a link between the PAR/aPKC complex and phosphoinositide signaling. Development *132*, 1675-1686.
Wahl, J.K., 3rd, Kim, Y.J., Cullen, J.M., Johnson, K.R., and Wheelock, M.J. (2003). N-cadherin-catenin complexes form prior to cleavage of the proregion and transport to the plasma membrane. The Journal of biological chemistry *278*, 17269-17276.
Wang, F., Herzmark, P., Weiner, O.D., Srinivasan, S., Servant, G., and Bourne, H.R. (2002). Lipid products of PI(3)Ks maintain persistent cell polarity and directed motility in neutrophils. Nature cell biology *4*, 513-518.
Wang, X., He, L., Wu, Y.I., Hahn, K.M., and Montell, D.J. (2010). Light-mediated activation reveals a key role for Rac in collective guidance of cell movement in vivo. Nature cell biology *12*, 591-597.
Wang, Y., Ku, C.J., Zhang, E.R., Artyukhin, A.B., Weiner, O.D., Wu, L.F., and Altschuler, S.J. (2013). Identifying network motifs that buffer front-to-back signaling in polarized neutrophils. Cell reports *3*, 1607-1616.
Watabe-Uchida, M., Uchida, N., Imamura, Y., Nagafuchi, A., Fujimoto, K., Uemura, T., Vermeulen, S., van Roy, F., Adamson, E.D., and Takeichi, M. (1998). alpha-Catenin-vinculin interaction functions to organize the apical junctional complex in epithelial cells. The Journal of cell biology *142*, 847-857.
Weber, G.F., Bjerke, M.A., and DeSimone, D.W. (2012). A mechanoresponsive cadherin-keratin complex directs polarized protrusive behavior and collective cell migration. Developmental cell *22*, 104-115.
Wegener, K.L., Partridge, A.W., Han, J., Pickford, A.R., Liddington, R.C., Ginsberg, M.H., and Campbell, I.D. (2007). Structural basis of integrin activation by talin. Cell *128*, 171-182.
Weston, J.A., Yoshida, H., Robinson, V., Nishikawa, S., Fraser, S.T., and Nishikawa, S. (2004). Neural crest and the origin of ectomesenchyme: neural fold heterogeneity suggests an alternative hypothesis. Developmental dynamics : an official publication of the American Association of Anatomists *229*, 118-130.
Wheelock, M.J., Shintani, Y., Maeda, M., Fukumoto, Y., and Johnson, K.R. (2008). Cadherin switching. Journal of cell science *121*, 727-735.

Whiteman, E.L., Liu, C.J., Fearon, E.R., and Margolis, B. (2008). The transcription factor snail represses Crumbs3 expression and disrupts apico-basal polarity complexes. Oncogene *27*, 3875-3879.
Wildenberg, G.A., Dohn, M.R., Carnahan, R.H., Davis, M.A., Lobdell, N.A., Settleman, J., and Reynolds, A.B. (2006). p120-catenin and p190RhoGAP regulate cell-cell adhesion by coordinating antagonism between Rac and Rho. Cell *127*, 1027-1039.
Williams, E.J., Williams, G., Howell, F.V., Skaper, S.D., Walsh, F.S., and Doherty, P. (2001). Identification of an N-cadherin motif that can interact with the fibroblast growth factor receptor and is required for axonal growth. The Journal of biological chemistry *276*, 43879-43886.
Williams, G., Williams, E.J., and Doherty, P. (2002). Dimeric versions of two short N-cadherin binding motifs (HAVDI and INPISG) function as N-cadherin agonists. The Journal of biological chemistry *277*, 4361-4367.
Winning, R.S., and Sargent, T.D. (1994). Pagliaccio, a member of the Eph family of receptor tyrosine kinase genes, has localized expression in a subset of neural crest and neural tissues in Xenopus laevis embryos. Mechanisms of development *46*, 219-229.
Woods, M.L., Carmona-Fontaine, C., Barnes, C.P., Couzin, I.D., Mayor, R., and Page, K.M. (2014). Directional collective cell migration emerges as a property of cell interactions. PloS one *9*, e104969.
Worthylake, R.A., and Burridge, K. (2003). RhoA and ROCK promote migration by limiting membrane protrusions. The Journal of biological chemistry *278*, 13578-13584.
Wu, Q., and Maniatis, T. (1999). A striking organization of a large family of human neural cadherin-like cell adhesion genes. Cell *97*, 779-790.
Wu, S.Y., Ferkowicz, M., and McClay, D.R. (2007). Ingression of primary mesenchyme cells of the sea urchin embryo: a precisely timed epithelial mesenchymal transition. Birth defects research Part C, Embryo today : reviews *81*, 241-252.
Wu, S.Y., Yang, Y.P., and McClay, D.R. (2008). Twist is an essential regulator of the skeletogenic gene regulatory network in the sea urchin embryo. Developmental biology *319*, 406-415.
Wu, Y.I., Frey, D., Lungu, O.I., Jaehrig, A., Schlichting, I., Kuhlman, B., and Hahn, K.M. (2009). A genetically encoded photoactivatable Rac controls the motility of living cells. Nature *461*, 104-108.
Xiao, K., Allison, D.F., Buckley, K.M., Kottke, M.D., Vincent, P.A., Faundez, V., and Kowalczyk, A.P. (2003). Cellular levels of p120 catenin function as a set point for cadherin expression levels in microvascular endothelial cells. The Journal of cell biology *163*, 535-545.
Xu, J., Wang, F., Van Keymeulen, A., Herzmark, P., Straight, A., Kelly, K., Takuwa, Y., Sugimoto, N., Mitchison, T., and Bourne, H.R. (2003). Divergent signals and cytoskeletal assemblies regulate self-organizing polarity in neutrophils. Cell *114*, 201-214.
Xu, Q., Mellitzer, G., Robinson, V., and Wilkinson, D.G. (1999). In vivo cell sorting in complementary segmental domains mediated by Eph receptors and ephrins. Nature *399*, 267-271.

Yamada, S., and Nelson, W.J. (2007). Localized zones of Rho and Rac activities drive initiation and expansion of epithelial cell-cell adhesion. The Journal of cell biology *178*, 517-527.
Yamada, S., Pokutta, S., Drees, F., Weis, W.I., and Nelson, W.J. (2005). Deconstructing the cadherin-catenin-actin complex. Cell *123*, 889-901.
Yanagisawa, M., and Anastasiadis, P.Z. (2006). p120 catenin is essential for mesenchymal cadherin-mediated regulation of cell motility and invasiveness. The Journal of cell biology *174*, 1087-1096.
Yanagisawa, M., Kaverina, I.N., Wang, A., Fujita, Y., Reynolds, A.B., and Anastasiadis, P.Z. (2004). A novel interaction between kinesin and p120 modulates p120 localization and function. The Journal of biological chemistry *279*, 9512-9521.
Yang, J., Mani, S.A., Donaher, J.L., Ramaswamy, S., Itzykson, R.A., Come, C., Savagner, P., Gitelman, I., Richardson, A., and Weinberg, R.A. (2004). Twist, a master regulator of morphogenesis, plays an essential role in tumor metastasis. Cell *117*, 927-939.
Yang, M.H., Hsu, D.S., Wang, H.W., Wang, H.J., Lan, H.Y., Yang, W.H., Huang, C.H., Kao, S.Y., Tzeng, C.H., Tai, S.K.*, et al.* (2010). Bmi1 is essential in Twist1-induced epithelial-mesenchymal transition. Nature cell biology *12*, 982-992.
Yap, A.S., Niessen, C.M., and Gumbiner, B.M. (1998). The juxtamembrane region of the cadherin cytoplasmic tail supports lateral clustering, adhesive strengthening, and interaction with p120ctn. The Journal of cell biology *141*, 779-789.
Yokoyama, K., Kamata, N., Fujimoto, R., Tsutsumi, S., Tomonari, M., Taki, M., Hosokawa, H., and Nagayama, M. (2003). Increased invasion and matrix metalloproteinase-2 expression by Snail-induced mesenchymal transition in squamous cell carcinomas. International journal of oncology *22*, 891-898.
Yonemura, S., Wada, Y., Watanabe, T., Nagafuchi, A., and Shibata, M. (2010). alpha-Catenin as a tension transducer that induces adherens junction development. Nature cell biology *12*, 533-542.
Yoo, S.K., Deng, Q., Cavnar, P.J., Wu, Y.I., Hahn, K.M., and Huttenlocher, A. (2010). Differential regulation of protrusion and polarity by PI3K during neutrophil motility in live zebrafish. Developmental cell *18*, 226-236.
Yoshida, C., and Takeichi, M. (1982). Teratocarcinoma cell adhesion: identification of a cell-surface protein involved in calcium-dependent cell aggregation. Cell *28*, 217-224.
Yu, C.H., Law, J.B., Suryana, M., Low, H.Y., and Sheetz, M.P. (2011). Early integrin binding to Arg-Gly-Asp peptide activates actin polymerization and contractile movement that stimulates outward translocation. Proceedings of the National Academy of Sciences of the United States of America *108*, 20585-20590.
Yu, H.H., and Moens, C.B. (2005). Semaphorin signaling guides cranial neural crest cell migration in zebrafish. Developmental biology *280*, 373-385.
Yu, M., Wang, J., Muller, D.J., and Helenius, J. (2015). In PC3 prostate cancer cells ephrin receptors crosstalk to beta1-integrins to strengthen adhesion to collagen type I. Scientific reports *5*, 8206.
Yue, J., Xie, M., Gou, X., Lee, P., Schneider, M.D., and Wu, X. (2014). Microtubules regulate focal adhesion dynamics through MAP4K4. Developmental cell *31*, 572-585.

Zaidel-Bar, R., Itzkovitz, S., Ma'ayan, A., Iyengar, R., and Geiger, B. (2007a). Functional atlas of the integrin adhesome. Nature cell biology *9*, 858-867.
Zaidel-Bar, R., Milo, R., Kam, Z., and Geiger, B. (2007b). A paxillin tyrosine phosphorylation switch regulates the assembly and form of cell-matrix adhesions. Journal of cell science *120*, 137-148.
Zhan, L., Rosenberg, A., Bergami, K.C., Yu, M., Xuan, Z., Jaffe, A.B., Allred, C., and Muthuswamy, S.K. (2008). Deregulation of scribble promotes mammary tumorigenesis and reveals a role for cell polarity in carcinoma. Cell *135*, 865-878.
Zihni, C., Munro, P.M., Elbediwy, A., Keep, N.H., Terry, S.J., Harris, J., Balda, M.S., and Matter, K. (2014). Dbl3 drives Cdc42 signaling at the apical margin to regulate junction position and apical differentiation. The Journal of cell biology *204*, 111-127.
Ziomek, C.A., and Johnson, M.H. (1980). Cell surface interaction induces polarization of mouse 8-cell blastomeres at compaction. Cell *21*, 935-942.
Zohn, I.E., Li, Y., Skolnik, E.Y., Anderson, K.V., Han, J., and Niswander, L. (2006). p38 and a p38-interacting protein are critical for downregulation of E-cadherin during mouse gastrulation. Cell *125*, 957-969.
Zumbrunn, J., Kinoshita, K., Hyman, A.A., and Nathke, I.S. (2001). Binding of the adenomatous polyposis coli protein to microtubules increases microtubule stability and is regulated by GSK3 beta phosphorylation. Current biology : CB *11*, 44-49.